The Design, Synthesis and Antiplasmodial Activity of a Series of Halogenated Fosmidomycin Analogues and Hybrid Drugs

A Thesis Submitted in Fulfilment of the Requirements for the degree of

Doctor of Philosophy (Pharmacy)

of

Rhodes University

By

Anthonia Folake Afolayan

MAY 2012

Abstract

Malaria continues to be a devastating disease and a major cause of death in sub-Saharan Africa. With resistance against most of the available antimalarial drugs, there is a need for ongoing research and development of antimalarial agents. Fosmidomycin and its acetyl analogue FR900098 have been identified as potent inhibitors of *Plasmodium falciparum*, the causative agent of the most deadly form of malaria. Clinical trials of these agents have revealed poor absorption due to their high hydrophilicity. In the present studies the effect of halogenation of the acyl chain as well as the biological effect of extending the acyl sidechain was explored. This provided the basis on which fosmidomycin hybrids were designed to investigate the feasibility of hybrid extending into NADPH binding pocket.

Synthesis of a series of halogenated FR900098 analogues was carried out in three stages. This included i) The introduction of the phosphonate group by reaction with 1,3-dibromopropane in an Arbuzov reaction, ii) The introduction of a hydroxamate group by reaction of the propyl phosphonate by means of a nucleophilic substitution reaction with BocNHOBn and iii) The introduction of a halogenated acyl side chain on a protected fosmidomycin backbone. The synthesis of fosmidomycin-hybrids for which chloroquine-fosmidomycin hybrids were used as the prototype, involved convergence of the two separately constructed moieties i.e. fosmidomycin and the quinoline moieties in a covalent linkage. The quinoline moiety was easily synthesized from the reaction of 4,7-dichloroquinoline with 1,2-diamino ethane. The aminoquinoline so formed resulted in chloroquine-fosmidomycin hybrids **3.8** and **3.9** when reacted with halogenated FR900098 analogues.

Antiplasmodial assays were conducted on the chloroquine-fosmidomycin hybrids and the halogenated fosmidomycin derivatives against the chloroquine resistant Gambian FCR-3 strain of *P. falciparum.* The most potent iodoacetyl fosmidomycin analogues **2.21** gave an IC_{50} value of 5.54 µM which is eight times more potent than the known antiplasmodial FR900098 which gave an IC_{50} value of 41.67 µM. All the halogenated FR900098 analogues showed better antiplasmodial activity than their non-halogenated derivatives. This indicated that the presence of halogens in the FR900098 analogues contributes to their biological

activity. The acetyl and propyl linked hybrids **3.8** and **3.9** showed potent antiplasmodial activity with IC_{50} values of 0.18 and 0.82 µM respectively. These were by far the most potent hybrids synthesized and provided leads for a new class of promising antimalarial agents.

Preliminary *E. coli* DXR enzyme inhibition assays were carried out on the halogenated fosmidomycin analogues. The results showed good inhibition of the enzyme by the phosphonic acids of the chloroacetyl and chloropropyl analogues **2.1** and **2.2** respectively. Molecular modelling of the compounds on *E. coli* (PDB code: 2EGH) and *P. falciparum* (PDB code: 3AUA) DXR showed strong binding of the halogenated fosmidomycin analogues while the hybrids in the absence of docked NADPH showed minimum binding to the enzymes.

Acknowledgements

A sincere thank you to my supervisor, Dr. Denzil Beukes for your unceasing guidance and support especially when going was tough. You truly are the best “BOSS”.
I would also like to extend my gratitude to

- Professor Peter Smith from the University of Cape Town for conducting the chloroquine sensitive antiplasmodial assays.
- Professor Robyn van Zyl Dr. from the University of Witwatersrand for conducting the chloroquine resistance antiplasmodial assays.
- Dr Kevin Lobb and Tope Olomola for helping with the molecular modeling .
- Dr. Nicodemus Mautsa for carrying out the antiplasmodial assay.
- Mr Morley and Prudence for technical support.
- Dr. Sandile Khamanga for proof reading my thesis and for your constant encouragement.
- The staff and post-graduate students at Rhodes University Faculty of Pharmacy for providing a great environment to work. Special thanks to my labmates Maynard, Tatenda, Jameel, Denzel and Mutenta. Pharmaceutical chemistry was a lot more exciting with you guys around.
- My chemistry department family especially “the Lunch group”, thank you for your support and encouragement.
- The Andrew Mellon Foundation Scholarship and the National Research Foundation for their financial support.

To my friends Vongani, Maynard (punchu), Lola, Segun and Tope, thank you for being my source of inspiration.
My deepest appreciation to David Oyedokun, you were a pillar of strength to me. Thank you for your moral and emotional support.
Finally to my parents Professor and Mrs Afolayan, thank you for your endless love, guidance, advice, encouragement and support. To my brother Sola and sister Lola for you always believing in me.

Contents

List of Figures

List of Schemes

List of Tables

List of Abbreviations

°C	Degrees Celsius
Arg	Arginine
Asn	Asparagine
Asp	Aspartic acid
bp	Basepair
BSA	Bovine serum albumin
$CDCl_3$	Deuterated chloroform
CH_2Cl_2	Dichloromethane
COSY	^1H-^1H Homonuclear Correlation Spectroscopy
Cys	Cysteine
d	Doublet
dd	Doublet of doublets
DEPT	Distortionless Enhancement of Polarisation Transfer
DOXP	1-deoxy-D-xylulose-5-phosphate
DXR	DOXP reductoisomerase
E. coli	*Escherichia coli*
*Ec*DXR	*E. coli* DOXP reductoisomerase
EIMS	Electron Impact Mass Spectrometry
EtOAc	Ethyl Acetate
eV	electron Volt
Glu	Glutamic acid
Gly	Glycine
His	Histidine
HMBC	Heteronuclear Multiple Bond Correlation
HPLC	High Performance Liquid Chromatography
HREIMS	High Resolution Electron Impact Mass Spectrometry
HRFABMS	High resolution fast atom bombardment
HSQC	Heteronuclear Single Bond Correlation
Hz	Hertz
IC_{50}	Inhibitory Concentration 50 %
IPTG	Isopropyl-β-D-galactopyranoside
IR	Infrared
J	Spin-Spin coupling constant (Hz)
Leu	Leucine
Lys	Lysine
m	Multiplet
m/*z*	Mass to charge ratio
MeOH	Methanol
MEP	2-C-methyl-D-erythritol 4-phosphate
Met	Methionine
MHz	Megahertz
multi	Multiplicity
MW	Molecular weight
NADPH	Nicotinamide adenine dinucleotide
NMR	Nuclear magnetic resonance
NMR	Nuclear Magnetic Resonance Specroscopy

NOESY	Nuclear Overhauser enhancement spectroscopy
P. falciparum	*Plasmodium falciparum*
*Pf*DXR	*P. falciparum* DOXP reductoisomerase
Phe	Phenylalanine
PMSF	Phenylmethylsulfonylfluoride
ppm	Parts per million
q	Quartet
s	Singlet
Ser	Serine
t	Triplet
THF	Tetrahydrofuran
TLC	Thin Layer Chromatography
Trp	Tryptophan
UV	Ultraviolet
δ	Chemical shift (ppm)

CHAPTER 1

1. LITERATURE REVIEW AND INTRODUCTION

In spite of our rapidly advancing knowledge about malaria, its causative agents, its mode of transmittance and the available preventative measures and treatment, it continues to be one of the most deadly infectious diseases in Africa. The World Health Organisation (WHO) reported 225 million cases of malaria and 781 000 deaths due to malaria in 2009.[1] About 91% of the mortality was reported in Africa, where expensive treatment cannot be afforded. About 30 000 travellers visiting malaria endemic regions from developed countries are reported to contract malaria annually. Given the increasing migration of people around the world from malaria endemic regions to non-endemic regions and *vice versa* malaria is fast becoming a major threat to humanity.[2] Scientists have an obligation to find solutions to the world's malaria problem by finding or developing effective and affordable drugs to combat the disease.

1.1 BRIEF OVERVIEW ON MALARIA ETIOLOGY AND TRANSMISSION OF THE CAUSATIVE AGENT

1.1.1 Causative organism and vector of malaria

Malaria symptoms have been recorded as far back as 2700 BC. However, it was not until 1889 that Alphonse Laveran discovered that malaria is caused by protozoa. Its transmission vector from human to human was later discovered in 1898 by Ronald Ross to be the female *Anopheles* mosquito.[1] Malaria is an infectious disease caused by species of the protozoan genus known as *Plasmodium*. *Plasmodium* belong to the apicomplexan strain and have a self-replicating plastid-like organelle known as the apicoplast, which is considered to have resulted from endosymbiosis of unicellular green algae in their evolution.[3] Five species are known to affect human beings and they include *Plasmodium falciparum*, *Plasmodium ovale*, *Plasmodium malariae*, *Plasmodium knowlesi*[4] and *Plasmodium vivax*. *P. falciparum* has been the cause of a large number of deaths, particularly in Africa.[5]

1.1.2 **Life cycle of the plasmodium parasite**

The life cycle of the plasmodium parasite begins when a female *Anopheles* mosquito bites and ingests blood from an infected host. The plasmodium gametocytes in the ingested blood reproduce sexually over 1 – 2 weeks in the gut of the mosquito (Figure 1.1) and are then introduced in the form of sporozoites when the mosquito bites another person. The sporozoites migrate into the hepatocytes where they multiply asexually.[6] The sporozoites enter the red blood cells as merozoites and continue to reproduce for another 1-3 days before rupturing the red blood cells for release at 48 hours interval.[5] Gametocytes form at the same time and are ingested by mosquitoes which starts the life cycle again.[6]

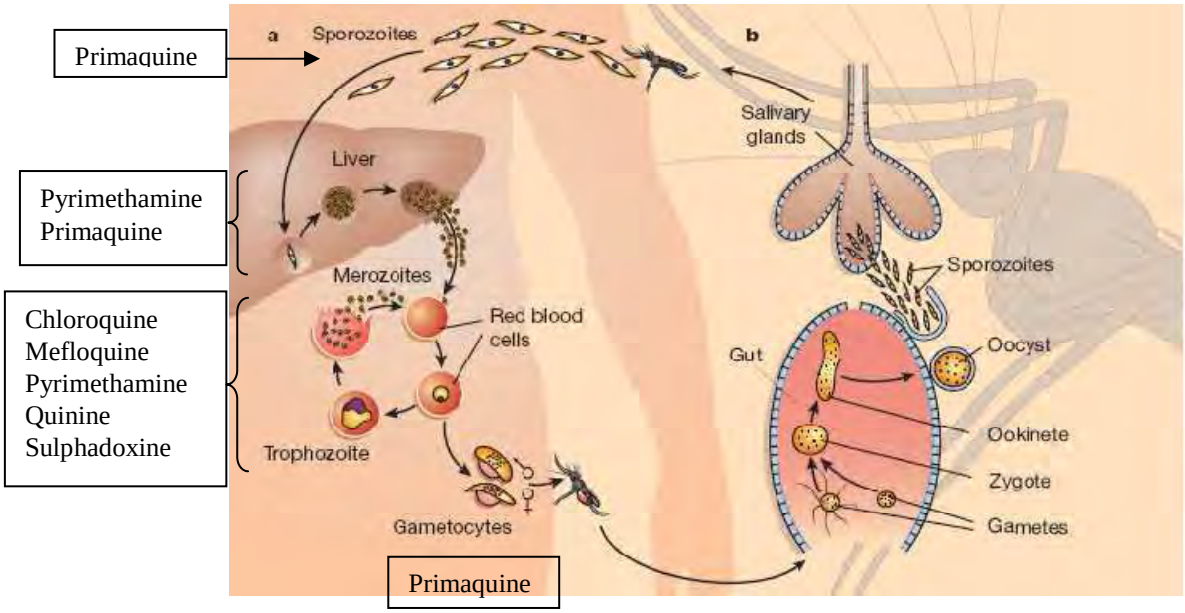

Figure 1.1. The life cycle of Plasmodium parasite[7]

1.1.3 **Signs and symptoms of malaria**

Although the severity of the disease caused by the five species of *Plasmodium* varies, they exhibit the same symptoms. The symptoms typically include: anaemia, splenomegally, jaundice, hepatomegally, and malaria paroxysm. The paroxysm corresponds with the rupturing of the red blood cells every 48 hours except for *P. malariae* which occurs every 72

hours.[8] Initially, the paroxysm is characterized by chills, rapid pulse, headache and nausea. These are then followed by profuse sweating and fever.[6]

1.2 CHEMO-THERAPEUTIC AGENTS USED FOR PREVENTION AND TREATMENT OF MALARIA

The life cycle of malaria parasites involves many stages. Thus far, no single drug has been able to eradicate all stages of the parasite in the human host. As such the antimalarial drugs are sometimes classified based on their antimalarial activity or the stages that they inhibit.[5, 9] These biological categories include:

1. Sporozoiticides: This group of drugs eradicates the sporozoites as soon as they enter the blood stream after a mosquito bite. This prevents the parasite from infecting the liver cells. Primaquine is known to have sporozoiticides activity.
2. Tissue schizonticides: These are drugs that destroy the exoerythrocytic liver-tissue stage of the parasite and thus prevent the parasites from entering the erythrocytes. This type of drugs is used as prophylaxis and one such example is pyrimethamine. Some tissue schizonticides are used to prevent relapse of *P. ovale* and *P. vivax* malaria e.g. primaquine.
3. Blood schizonticides: These drugs destroy the erythrocytic stage of the parasite which is responsible for the manifestation of malaria symptoms. This is the easiest phase to attack the parasite as the drugs are delivered directly into the blood stream. Many of the known antimalarial drugs are active at this stage and some examples include chloroquine, sulphadoxine and mefloquine.
4. Gametocides: This group of drugs destroy the sexual form of the parasite. This prevents transmission of parasite to the *Anopheles* mosquito and thus stops the lifecycle of the parasite. An example of a drug with gametocidal activity on four of the *Plasmodia* species that affects human is primaquine. No study has yet reported a full parasitological response of *P. knowlesi* to antimalarial drugs in human given its recent discovery to affect human.[10]

For the *Plasmodium* parasite to survive it obtains essential amino acids by digesting haemoglobin of the host red blood cells. This results in the production of haematin which is a

complex of ferriprotoporphyrin IX (Fe(III)PPIX) and is toxic to the parasite. The parasite then detoxifies haematin by converting it through biocrystallization to insoluble non-toxic haemozoin.[5]

On the basis of chemical or structural classification, the available chemotherapeutics for the prophylaxis and treatment of malaria can be categorized into three major groups. These include the aminoquinolines, antifolates and artemisinin derivatives. These groups of compounds have different targets and modes of action and as such are often used in combination as recommended by WHO. The aminoquinolines dates as far back as the 17th century with the use of quinine (Figure 1.2; **1.1**) while the antifolates have a fairly recent history (1950s). Although *Artemisia annua*, the plant from which artemisinin is derived, has been used by the Chinese for treatment of fever and other ailments for over two thousand years, the active compound was only isolated in 1972.[11] The evolution and mechanism of action of the different classes are discussed below.

1.2.1 **The Aminoquinolines**

This class of compounds are characterized by the presence of a quinoline nucleus in their chemical structure. Quinine (**1.1**) was first isolated from the bark of the cinchona tree in 1834 by Pelletier, a French chemist.[12] It is often extracted along with three other alkaloids: quinidine (**1.2**), cinchonine (**1.3**) and cinchonidine (**1.4**). Cinchonine (**1.3**) and cinchonidine (**1.4**) are optical isomers of each other lacking the methoxy group of quinine (**1.1**) while quinidine (**1.2**) is an optical isomer of quinine. Quinidine (**1.2**) has better antimalarial properties than quinine but unfortunately it is also highly cardiotoxic. The structure of quinine can be described as having three parts: the quinoline or 6-methoxyquinoline component, the quinuclidine component and the hydroxylated methylene group connecting the two rings (Figure 1.2). Different modifications to quinine failed to yield any compound with superior antimalarial activity and thus quinine was the sole drug used in the treatment of malaria for many years until after World War I. Quinine (**1.1**) acts as a blood schizonticide and also possesses some gametocidal activity against *P. vivax* and *P. malariae*. It is reserved for use in severe falciparum malaria especially in areas with known chloroquine resistance. Adverse effects to quinine include hypoglycaemia at therapeutic doses as well as a condition

known as cinchonism.[13] Cinchonism can develop from an overdose and sometimes standard doses of quinine. Mild cinchonism is characterized by a group of symptoms which include headache, blurred vision, vomiting, dizziness and confusion while severe symptoms include blindness, deafness, renal failure and death due to cardiotoxicity.

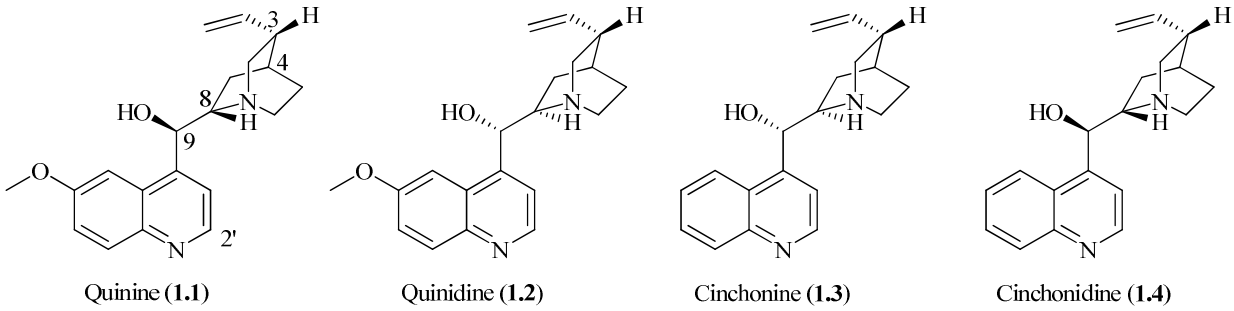

Figure 1.2. Alkaloids from the bark of the Cinchona tree

Both World War I and II played a significant role in the discovery and development of synthetic antimalarial agents. The shortage of quinine during World War I is believed to be the catalysing factor in the research to synthesize quinine (**1.1**) and the development of alternative agents to it. About 60 years before World War I, in an attempt to synthesize quinine, Perkin synthesized a dye that was later called Perkin's mauve.[14] Perkin's mauve encouraged research into using aniline derivatives as precursors in dye synthesis which then led to the synthesis of methylene blue (**1.5**). Koch and Ehrlich found that the dye stains cells selectively. They also noticed that methylene blue (**1.5**) could affect physiological functions of the cell, such as motility in the protozoa. This, in 1891, brought Guitmann and Ehrlich to the realization that they could use the dye as a chemotherapeutic agent to selectively target parasite cells in host tissues. They investigated its effect on two patients and successfully treated the patients for malaria with methylene blue.[14] Research on methylene blue was abandoned for 30 years due to its side effect of staining the subject's tissues and skin.

Erlich's student, Roehl, who at the time was working at I.G. Farben industries, continued to study the dye and developed a method for testing these compounds in canaries. Roehl modified the methyl side group of methylene blue (**1.5**) by incorporating basic aliphatic side chains.[14] The modifications significantly enhanced the antiplasmodial activity of the

compound but the compounds retain the properties of the dye that colours the patient's tissues. Schulemann from Elberfeld laboratories of Bayer which formed part of I.G. Farben industries in Germany applied the knowledge from this study and reasoned that the antimalarial activity of the quinoline nucleus of quinine (**1.1**) could be increased with this new basic side chain. This line of reasoning resulted in the synthesis of an 8-aminoquinoline, pamaquine (**1.6**, plasmoquine) in 1924 as the first synthetic antimalarial agent (Scheme1.1).[15]

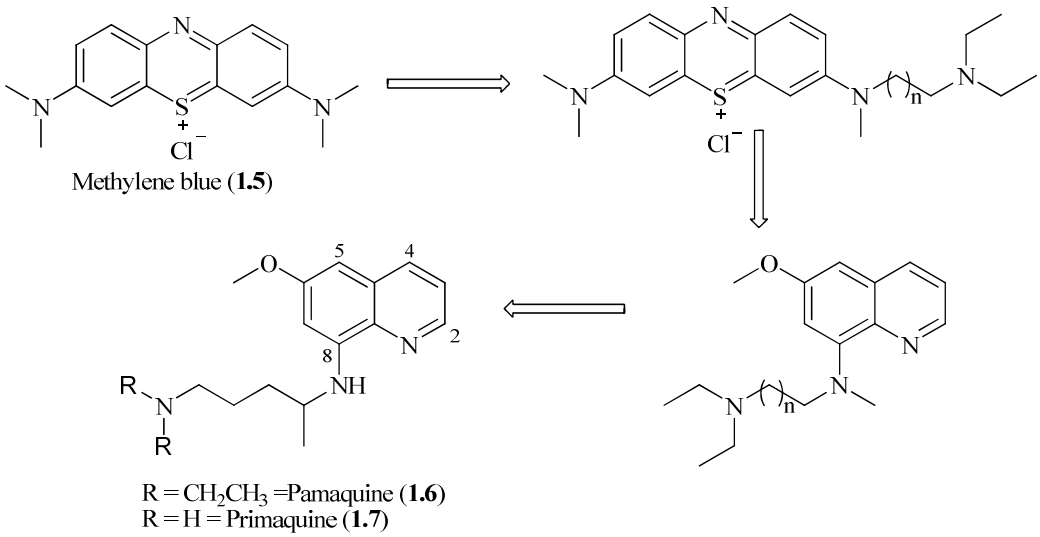

Scheme 1.1. Evolution of pamaquine (**1.6**) from methylene blue (**1.5**)

Pamaquine (**1.6**) had the advantage of being able to destroy plasmodium gametocytes and preventing relapse in *vivax* malaria. The 8-aminoquinolines were re-evaluated during and after World War II and this led to the synthesis of a series of derivatives from which primaquine (**1.7**) emerged as the most active and least toxic agent in 1946.[16] It differs from pamaquine (**1.6**) in that it lacks the diethyl groups from the side chains (Figure 1.3).[16, 17] Primaquine (**1.7**) is a tissue schizonticide used for the treatment of *P. vivax* and *P. ovale* infections and has virtually no effect on the blood stages of the parasite. Although the mechanism of action remains unclear, primaquine (**1.7)** is known to generate reactive oxygen species that results in the formation of superoxides and hydroxyl radicals which in turn destroy the parasite. As a side effect it causes haemolytic anaemia and is thus contraindicated in patients with glucose-6-phosphate dehydrogenase (G6PD) deficiency.[18] G6PD is an

enzyme important in red blood cell metabolism and often results in haemolytic anaemia in patients who are deficient especially during an infection.

A promising new development in the class of 8-aminoquinoline is tafenoquine (**1.8**), also known as WR238605, which is currently in phase IIb/III clinical trials for prevention and treatment of malaria. Tafenoquine (**1.8)** is a 5-phenoxy derivative of primaquine (**1.7**) developed by the Walter Reed Army Institute of Research (WRAIR) in the USA in an effort to find an alternative to primaquine which would be safer, longer acting and with a broader spectrum of activity.[19] Although its mode of action is unknown, it has been shown to have activity against the blood stages of malaria,[18, 20] has a longer half-life than primaquine and appears to be a good candidate for falciparum prophylaxis.[21] It also shows less toxicity as compared to primaquine[22] but retains the haemolytic property of the parent drug and thus is also not recommended for use in G6PD deficient patients.

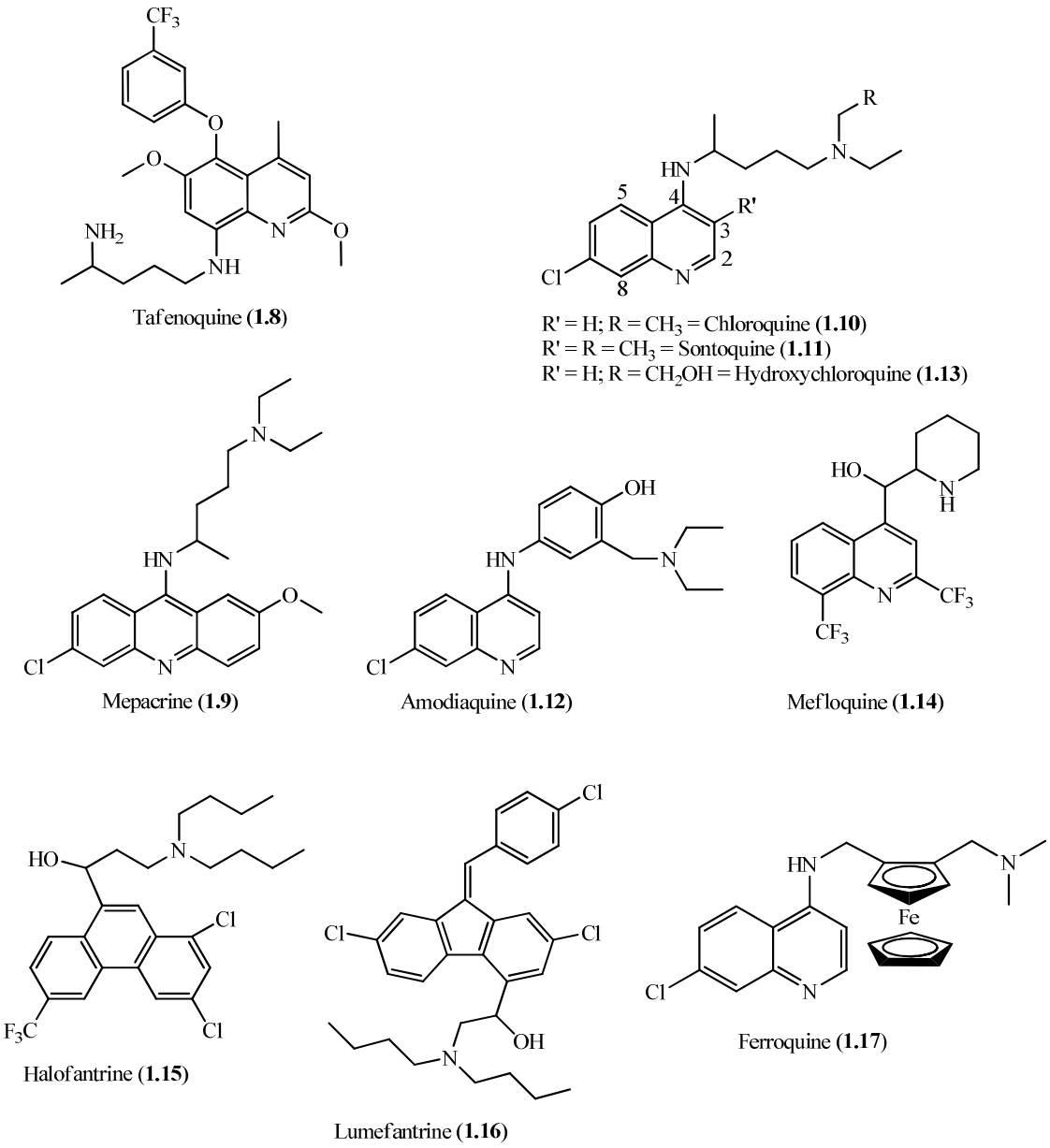

Figure 1.3. Structures of antimalaril aminoquinolines

After the discovery of pamaquine (**1.6**), a commercial research programme dedicated to discovering antimalarial drugs at Elberfeld laboratories was set up where researchers discovered mecaprine (**1.9**, quinacrine) in 1932. The compound evolved from the replacement of the quinoline ring of pamaquine with an acridine ring, introducing a chlorine atom and moving the side chain opposite to the ring nitrogen as it is in the quinine structure (Figure 1.3).[23] Mepacrine unfortunately was only fairly active as a cure or prophylaxis for

malaria while exhibiting toxicity over long-term administration and thus prompting the search for better antimalarial agents to continue. In an effort to better understand the structure activity relationship and improve its antimalarial activity, mepacrine was modified such that the methoxy-bearing ring was removed. This gave rise to chloroquine (**1.10**, resorchin) in 1934,[23] a representative of the 4-aminoquinolines. Chloroquine despite its good antimalarial activity was perceived to be too toxic and was abandoned. Its derivative sontoquine (**1.11**) which seemed less toxic was synthesized in 1936. Interest in chloroquine was rekindled in 1946 when allied scientists from the USA, Britain and Australia while working together obtained data from clinical studies conducted on sontoquine by a French physician. The US clinical trials showed that chloroquine was far superior to mepacrine.[24] Chloroquine became one of the most popular antimalarials known and was the drug of choice in many countries for the treatment of malaria.

Replacement of the alkylamino side chain of chloroquine (**1.10**) with an anilino group resulted in the development of amodiaquine (**1.12**) in 1950. Amodiaquine is a more active antimalarial drug than chloroquine but it is rapidly metabolized into its less active desethyl derivative.[25] It was used for treatment and prophylaxis of malaria but was stopped in the 1970s due to high toxicity which included hepatitis and agranulocytosis. Studies have however shown that these severe side effects are absent when used in doses required for malaria treatment.[26] Although the drug is still widely available in Africa its use remained discontinued in the USA.

The 4-aminoquinolines which include chloroquine (**1.10**), hydroxychloroquine (**1.13**) and amodiaquine (**1.12**) act as blood schizonticides.[1, 5] They are weak bases that accumulate in the red blood cells where they are able to attack parasites at the multiplying stage. Unlike the 8-aminoquinolines with unknown mode of action, 4-aminoquinolines are generally accepted to bind to haematin and as a result prevent the conversion of haematin to haemozoin. Haematin then accumulate in the digestive vacuole of the parasite where it destroys it.[27] 4-Aminoquinolines have a unique affinity for haematin that is higher than that of 8-aminoquinoline. The 7-chloro substituent of chloroquine is important to prevent the conversion of the toxic haematin to haemozoin and although it is necessary the chlorine substituent to be present it is not sufficient for a strong antiplasmodial activity.[28]

Other antimalarial agents that can be classified with the aminoquinolines include mefloquine (**1.14**), halofantrine (**1.15**) and lumefantrine (**1.16**). Although halofantrine and lumefantrine do not have the quinoline nucleus, they are structurally related to quinine. Mefloquine (WR 142490) and halofantrine were also discovered by WRAIR in the antimalarial drug development programme to address the problem of chloroquine resistant *P. falciparum* that was killing many of the American soldiers during the Vietnam War. During the programme WRAIR screened over 200 000 compounds coming up with mefloquine and halofantrine. Mefloquine was approved for marketing by the United States Food and Drug Administration (FDA) in 1989 while halofantrine was approved in 1992.[29]

The introduction of a 2-CF_3 group into the quinine (**1.1**) skeleton prevents metabolic 2'-hydroxylation and eventual deactivation of the drug. This gave rise to antimalarials such as mefloquine (**1.14**) which is a highly active blood schizonticide with a very long half-life (2 – 4 weeks). It is particularly effective against chloroquine-resistant strains of the plasmodium parasite but has a range of side effects that consists of neuropsychiatric, gastrointestinal and cardiovascular effects.[5] Resistance is easily developed to mefloquine due to its prolonged half-life and because of its relationship to quinine, cross-resistance between the two drugs have also been reported. Its use is therefore restricted to prophylaxis and to treatment of strains that are resistant to chloroquine or pyrimethamine and even then it is combined with another antimalarial drug to prevent development of resistance.

Halofantrine (**1.15**) is produced and used as a racemic mixture since the two enantiomers appear to have no significant difference in activity. It is a blood schizonticide active against chloroquine sensitive and chloroquine resistant strains of *P. falciparum*. Metabolic N-dealkylation of halofantrine produces an active metabolite, *N*-desbutylhalofantrine, which contributes to its overall antimalarial activity. Despite its high activity, it induces arrhythmias and is associated with prolonged depolarization and repolarization of the heart (QT intervals) which can lead to sudden death. High production cost, variable bioavailability and.[30] cross-resistance with mefloquine also limits its use.

The exact mechanism of action of quinine (**1.1**), mefloquine (**1.14**) and halofantrine (**1.15**) (classified as arylamino alcohols) against malaria is still unclear, it has been argued that

arylamino alcohols interfere with the dimerization of toxic haematin to haemozoin in a manner different to the mechanism of action of 4-aminoquinolines. In addition to interfering with the dimerization of haematin, quinine and mefloquine binds to phospholipids and inhibit the fusion of haemoglobin-laden vesicles to the digestive vacuole in the endolysosomal system. This is done either by directly impairing membrane function or by inhibiting calcium release from acidic stores. The arylamino alcohols also inhibit membrane recycling and as a result causes the death of the parasite.[31]

Lumefantrine (**1.16**) is a 2,4,7,9-substituted fluorene with schizonticidal activity. It is not used in monotherapy because it is slow acting. It is often used in combination with artemether (**1.32**) (co-artemether) to combine the rapid activity of the artemisinin derivative with lumefantrine's high cure rate. Although lumefantrine is structurally related to halofantrine it appears to have less cardiotoxic side effects than halofantrine.[21] Desbutyl-lumefantrine, is an active metabolite and has higher antimalarial activity and also shows synergistic effects with artemisinin.[32]

There is an on-going interest in the use of organometallic compounds in chemotherapy of diseases such as the use of platinum complexes for cancer treatment.[33] Biot *et al*. (1997) explored the incorporation of the organometallic ferrocenyl unit into the chloroquine molecule. It was postulated that addition of iron or a ferrocenyl group to the chloroquine molecule would abolish chloroquine resistance in chloroquine resistant *P. falciparum* since the parasite has a high affinity for iron. Several ferrocene-chloroquine compounds were synthesized with the ferrocenyl group covalently incorporated into the side chain of chloroquine.[34]

Ferroquine (Figure 1.3, **1.17**) emerged as the most active of the ferroquine-chloroquine series with better activity than chloroquine against both chloroquine sensitive and chloroquine resistant strains of *P. falciparum*.[35] Although the ferrocene group on its own does not possess antiplasmodial activity, it enhances the antiplasmodial property of chloroquine when enclosed inside the chloroquine structure and reverses chloroquine resistance by an unknown mechanism. Based on the similarities in their chemical structure ferroquine is postulated to

also bind to haematin to prevent haemozoin formation. Ferroquine is currently in phase IIb clinical trials under development as a promising antimalarial drug candidate.[36]

1.2.2 **Folate antagonists**

Research into new antimalarial agents resurged during World War II due to a lack of access to quinine (**1.1**). Drug development focused on pyrimidine derivatives as inhibitors of DNA synthesis.[37] This later led to the synthesis of proguanil (Figure 1.4, **1.18**) albeit with the replacement of the pyrimidine ring with a biguanide chain. Proguanil was found to be even more effective than mepacrine (**1.9**) and quinine (**1.1**) against avian malaria and it is able to cure relapse cases of *P. vivax* malaria. Proguanil is in fact a prodrug which is metabolized into the active metabolite, cycloguanil (**1.19**). Synthesis of proguanil analogues was encouraged by the observed activity of proguanil (**1.18**). It was found that chlorination of the phenyl ring and lengthening of the linker between the phenyl ring and the diaminopyrimidine ring of proguanil increases the potency of the drug. It is from this discovery that chlorproguanil (**1.20**) and clociguanil (**1.21**) emerged. Like proguanil, chlorproguanil is also a prodrug that is metabolized to the active metabolite chlorcycloguanil (**1.27**).[37]

Continuing with the pyrimidine work, Hitchings *et al*.[38] carried out tests on several substituted diaminopyrimidines with the aim to find an antagonist against the nucleic acids of fast-growing cells such as bacteria, protozoa and neoplasm. Since these parasites divide more rapidly than host cells an antagonist would affect the parasite more on the basis of differential growth rate.[38] Falco *et al*.[39] then observed that the structure of the diaminopyrimidines is similar to proguanil (**1.18**) which is a folic acid antagonist. He therefore hypothesized that 2,4-diaminopyrimidines would have antimalarial properties. Screening of this group of compounds led to the discovery of pyrimethamine (**1.22**) which closely resembles the active metabolite of proguanil and is 200 times more active than the latter in *P. berghei*.[23]

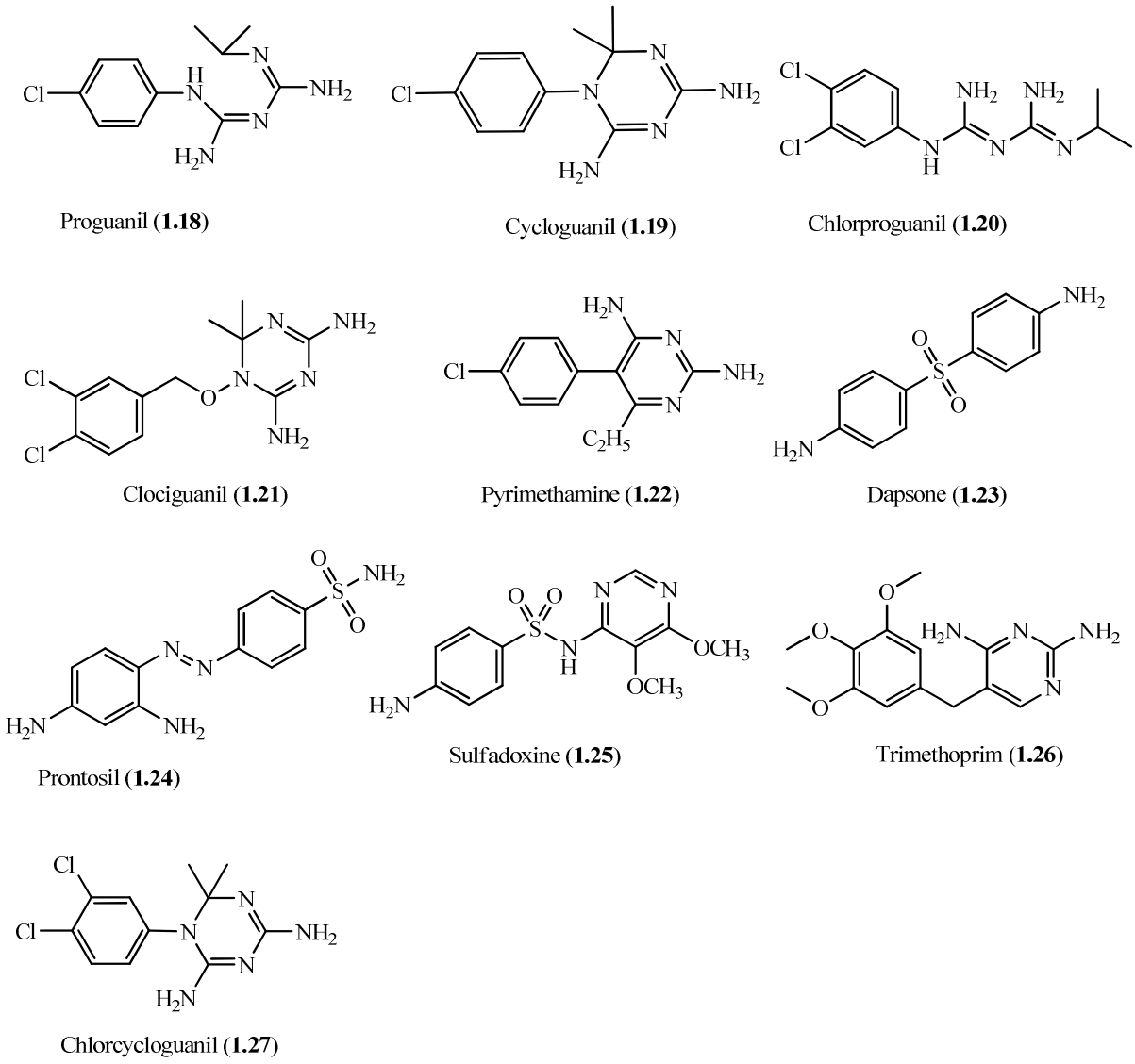

Figure 1.4. Folate inhibitors

Another class of antifolate drugs used in the treatment of malaria is the sulpha drugs. Dapsone (**1.23**) was first produced by Fromm and Wittmann in 1908 in an attempt to synthesize azo (-N=N-) dyes.[40] Its antimicrobial and antiplasmodial properties were however only discovered in the 1930s when research into sulpha drugs had surged due to the activity observed for Prontosil® (Figure 1.4, **1.24**). Prontosil®, also discovered in the 1930s, is a sulpha prodrug which is only activated biologically when metabolized to its active metabolite, sulphanilamide.

Proguanil (**1.18**), pyrimethamine (**1.22**) and the sulpha drugs (Figure 1.4) all inhibit plasmodia growth by interfering with folate biosynthesis in the malaria parasite. Folate is an important component in almost all living organisms. It is necessary for the biosynthesis of amino acids and DNA replication.[41] While humans cannot biosynthesize folate and rely on dietary intake, most bacteria and some protozoa such as *P. falciparum* are able to produce their own folate. *P. falciparum* can synthesize folate *de novo* and still make use of folate salvaged from the host cell.[41]

Two enzymes from the *Plasmodium* folate pathway have been the target of most antifolate drugs for malarial treatment. These enzymes are dihydrofolate reductase (DHFR) and dihydropteroate synthase (DHPS). DHFR has a homologue in humans with some differences while DHPS has no human homologue, making it a good target for antimalarial compounds. DPHS catalyses the condensation of 7,8-dihydro-6-hydroxymethylpterin pyrophosphate with *p*-aminobenzoic acid to form 7,8-dihydropteroate (Scheme 1). The dihydropteroate is later in the pathway converted to dihydrofolate which is reduced by DHFR in an NADPH-dependent reaction to tetrahydrofolate. The tetrahydrofolate are then converted into tetrahydrofolate cofactors which are necessary for nucleic and amino acids biosynthesis.[42]

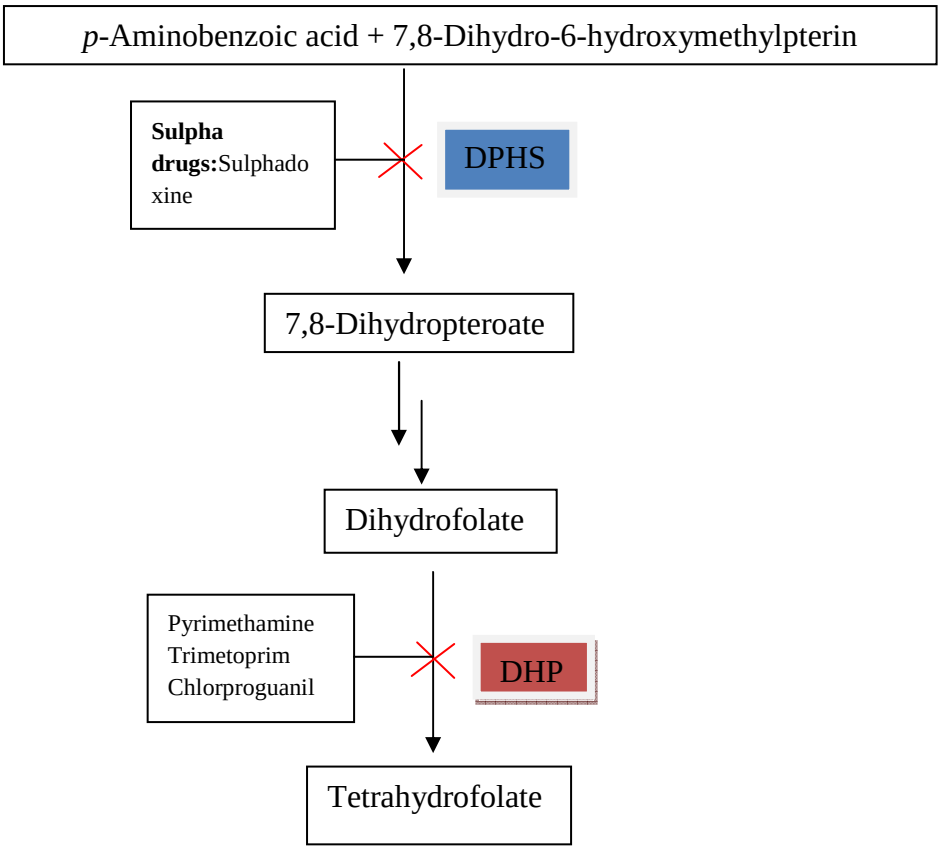

Scheme 1.2 Summarized pathway of folate biosynthesis and its inhibitors in *P. falciparum*

Antifolate drugs inhibit folate synthesis by blocking the enzymes of this pathway and as a result disrupt DNA replication in the parasite. These drugs are blood schizonticides although wide spread resistance has reduced their use. Sulpha-based drugs such as sulphadoxine (**1.25**) are structural inhibitors of DHPS. They inhibit the enzyme by competing with its substrate, *p*-aminobenzoic acid, for binding.[20]

Proguanil (**1.18**), chlorproguanil (**1.20**), Pyrimethamine (**1.22**) and trimethoprim (**1.26**) and are active against *Pf*DHFR.[42] and inhibit both the *de novo* synthesis of folates and the salvage of exogenous folate derivatives.[41] Combinations of DHFR inhibitors with DHPS inhibitors have synergistic effects. where one drug potentiates the effect of the other. An example of this is the combination of sulphadoxine with pyrimethamine (Fansidar®).

1.2.3 **Artemisinin derivatives**

The discovery of artemisinin emerged from "project 523" designed by Chinese researchers in 1967 to develop antimalarial therapies. A compound named Arteannuin B (Figure 1.5, **1.29**, qinghaosu II) was first isolated in 1972 from *Artemisia annua*, however this did not give the expected antimalarial effect and thus the search for the active compound in the plant continued. The crystalline form of artemisinin (**1.30**) was later isolated in 1973 from *A annua* which had been in use for over 2000 years in traditional Chinese medicine for the treatment of chills and fever.

Artemisinin (**1.30**) is a 1,2,4-trioxane, sesquiterpene lactone and its total synthesis was first reported in 1983.[43] Since then several groups have reported its synthesis and attempts have been made to genetically modify plant and microbes to produce the compound.[44, 45] Despite all these the main supply of the artemisinin still remains the plant *A. annua*. Even though its mode of action is still under debate, it is generally believed that the iron from haem attacks and breaks the endoperoxide linkage of the compound resulting in the formation of oxygen free radicals. The free radicals are then rearranged to carbon free radicals which alkylate and destroy the parasite proteins and eventually lead to the parasite's death.[46]

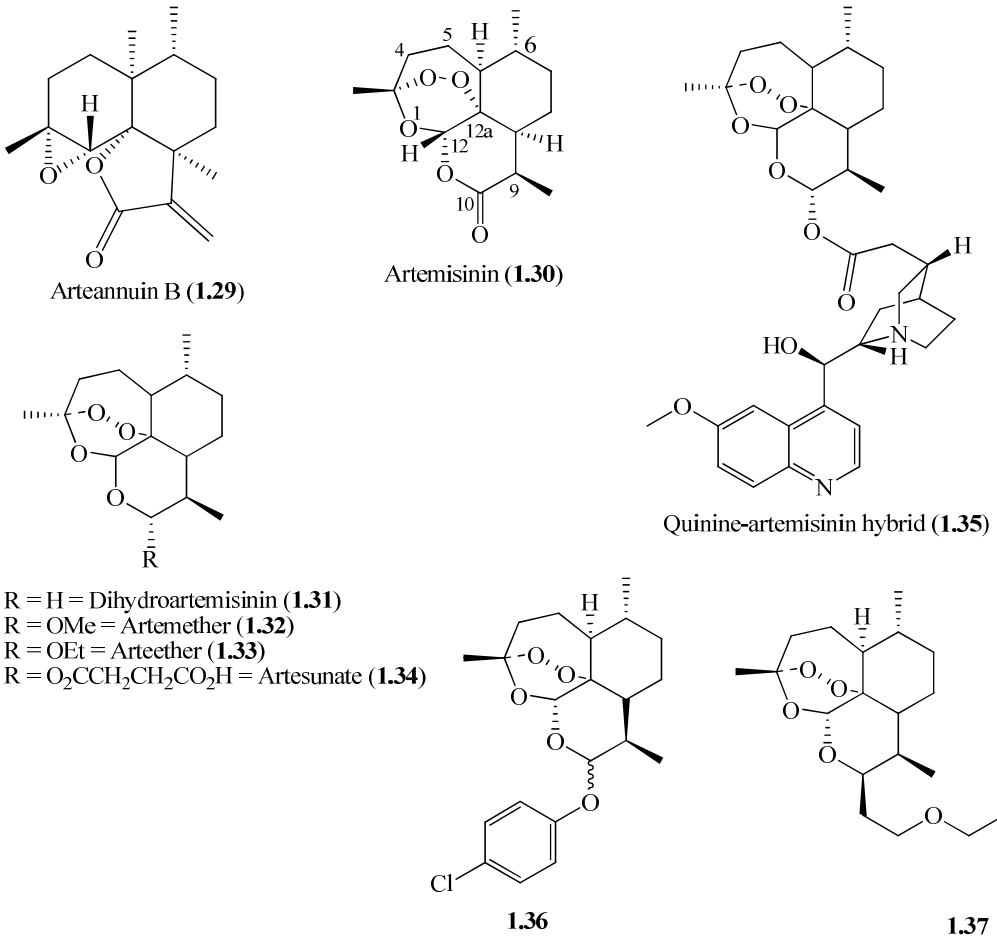

Figure 1.5. Artemisinin and its derivatives

Artemisinin derivatives are amongst the most potent antimalarial agents and are active against sexual and asexual stages of chloroquine sensitive and resistant strains of *P. falciparum*. The parent drug and its derivatives inhibit the trophozoite stage of the *Plasmodium* lifecycle, preventing the progression of the disease and making them the fastest acting antimalarial agents available. They also have gametocidal action thus preventing transmission of resistant strains.

Unfortunately the use of artemisinin has its limitations. It has poor oil and water solubility, a short plasma half-life of 3-5 hours and a high rate of recrudescence.[47] These preclude its use as monotherapy or prophylaxis. In order to improve its pharmacokinetic properties, derivatives of artemisinin were sought. Artemisinin is easily reduced to dihydroartemisinin (DHA, Figure 1.5, **1.31**) using sodium borohydride.[47] In an effort to increase artemisinin's oil

and water solubility, ether and ester derivatives of the compound were prepared from DHA. These first generation analogues included artemether (**1.32**) and arteether (**1.33**) which are oil soluble ether derivatives of artemisinin used for intramuscular administration. Artesunate (**1.34**) is a water soluble hemisuccinate ester of artemisinin used for intravenous treatment. These analogues are metabolized into the active metabolite DHA which still exhibit short plasma half-life and as a result the high rate of recrudescence persists.[47] In order to prevent recrudescence, the WHO has recommended that artemisinin derivatives be used with longer acting antimalarials as first line treatment for uncomplicated malaria. As such there are artemisinin combination therapies (ACTs) such as artesunate-mefloquine, artemether-lumefantrine (coartem®), artesunate-amodiaquine and DHA-piperaquine combinations.

Due to their fast rate of reducing parasitemia, it is envisaged that it will be difficult for the parasite to develop resistance to this class of drugs. However, low *Plasmodium* susceptibility to artesunate has been reported in some patients in Western Cambodia where artemisinin monotherapy is often used.[48] This raises concern about the development of resistance to artemisinin in the near future.

A comparison of the effect of artesunate (**1.34**) and quinine (**1.1**) on patients infected with the malaria parasite did not show any significant difference between the two drugs. Quinine however exhibited hypoglycaemia side effect when used as monotherapy.[49] A combination of these two drugs shows synergism in their antimalarial activity and prompted the synthesis of a quinine-artemisinin hybrid (**1.35**) which has since been shown to exert superior antimalarial activity to either of the two drugs alone or a 1:1 combination of the two. This hybrid also has a potent activity against 3D7 chloroquine resistant *P. falciparum*.[50]

Second generation artemisinin derivatives have been developed with the aim to increase the half-life and bioavailability of this group of compounds.[47, 51] This has resulted in some very potent derivatives such as **1.36** with excellent *in vitro* antimalarial activity and **1.37** which is 15 times more potent than artemisinin (**1.30**).[52] Medicine for Malaria Ventures (MMV), a non-profit organization focussed on developing antimalarial agents, has teamed up with various research groups to completely fully synthesize artemisinin derivatives that are active, have long half-lives, are safe and can be produced on a large scale. In this venture,

Vennerstrom and co-workers have designed and are developing completely synthetic ozonide antimalarial agents based on the 1,2,4-trioxolane moiety which is related to the artemisinin endoperoxide pharmacophore.[53] One such agent that has been selected for drug development is OZ277 (Figure 1.6, **1.38**), a secondary ozonide with a 5-membered 1,2,4-trioxolane ring. OZ277 is currently in phase III clinical trials and has been shown to have a rapid onset of action, is active against all asexual erythrocytic stages of *P. falciparum* but has low *in vivo* half-life of approximately two hours.[53] Although the exact mechanism of action of these peroxide agents is not clear, the ozonides are believed to act the same way as artemisinin and requires functional groups that are reactive with Fe(II) for antiplasmodial activity.

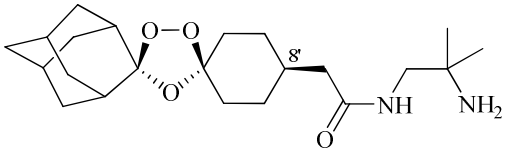

OZ277 (**1.38**)

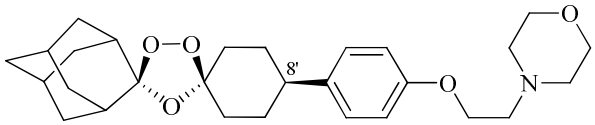

OZ439 (**1.39b**)

Figure 1.6. Structures of ozonides OZ277 (**1.38**) and OZ439 (**1.39**)

The same group has developed the next-generation ozonides with increased *in vivo* half-life.[54] This was achieved by replacing the *cis*-8'-alkyl group of the first generation ozonides such as in OZ277 (**1.38**) with *cis*-8'-phenyl group. The next-generation ozonides with the *cis*-8'-phenyl substituents were more than 50-fold more stable to Fe(II)-mediated degradation as compared to the first-generation ozonides. Nonetheless the next-generation ozonides reacts rapidly with haem to an extent that is comparable to the first-generation ozonides i.e. they are stable enough not to undergo haem-mediated degradation in blood yet react sufficiently with haem (Fe(II)-reactivity) to kill *Plasmodium* parasites. A candidate that has emerged superior from the next-generation ozonides and is currently in phase IIa clinical trials is OZ439 (Figure 1.7, **1.39**).[54] OZ439 has *in vitro* activity against *P. falciparum* and exhibit *in vivo* activity against *P. berghei*. It has a long half-life of more than 20 hours after oral administration to rats as compared to 0.5 hours for DHA (**1.31**) and one hour for OZ277. This is however still low as compared to mefloquine for example with half-life of two to four weeks and thus would still require combination with longer-acting antimalarial drugs to prevent rapid development of resistance.

1.3 PROBLEMS ASSOCIATED WITH KNOWN MALARIA TREATMENT: RESISTANCE

Treatment of malaria, especially in sub-Saharan countries where the disease is prevalent is inundated with many problems.[55] These include, access to treatment, safety of available treatment, tolerability, adherence and effectiveness of the treatment. Many of the countries where malaria is endemic are developing countries where many cannot afford $1 per treatment. The fact that malaria mostly affects these economically poor countries has not encouraged investment in the development of new antimalarial drugs.

The biggest problem by far in the treatment of malaria, is resistance. *P. falciparum* has shown resistance to virtually all known classes of antimalarial drugs on the market.[56] The development of widespread resistance to chloroquine, sulphadoxine and pyrimethamine individually and in combination has complicated the management of malaria. The WHO responded by recommending that combination therapies be used to reduce the rate at which resistance develops. The drugs are combined such that they have independent modes of action and different targets. Examples of these are non-artemisinin based combination such as Sulphadoxine-pyrimethamine + mefloquine and artemisinin-based combination such as artemether-lumefantrine. While these combinations have proved effective they are about 10 times more expensive than monotherapy treatment. In some cases resistance has developed to some combinations. This includes sulphadoxine-pyrimethamine + chloroquine in areas where *P. falciparum* resistance to chloroquine is high.[55]

1.3.1 **Chloroquine resistance mechanism**

Chloroquine (**1.10**) has been in use since the 1950s and was the first line treatment in many malaria endemic countries. Even now with widespread resistance, chloroquine (**1.10**) remains the treatment of choice in many economically poor countries because it is cheap. The mechanism of chloroquine resistance has been under investigation since the discovery that that the resistance can be reversed.

The mechanism of resistance of *P. falciparum* to chloroquine is still under investigation but it has been shown to be due to mutations in the chloroquine resistance transporter (PfCRT)

protein.[57] This protein transporter, found in the digestive vacuole of the parasite actively transports protonated chloroquine out of the digestive vacuole in exchange for proton. Although this happens in both chloroquine sensitive (CQS) and chloroquine resistant (CQR) strains of *P. falciparum*, it occurs at a much faster rate in the CQR parasites. The active transport of chloroquine out of the digestive vacuole of the CQR parasite is associated with substitution of positively charged lysine (K) at position 76 of the PfCRT polypeptide chain with uncharged threonine (T) i.e. K76T substitution.[58] The wild type PfCRT with its charged lysine creates an electrostatic environment which prevents access of charged chloroquine to PfCRT. Once mutated, the uncharged threonine makes PfCRT more accessible to the charged chloroquine which is then transported out of the digestive vacuole.[58, 59] Since resistance to chloroquine is due to its diminished accumulation within the digestive vacuole as opposed to chloroquine interaction with haematin, increase in the concentration of chloroquine within the vacuole should reverse the resistance.

Verapamil, a calcium channel blocker has been shown to reverse chloroquine resistance.[60] Verapamil is postulated to bind to the carrier protein and prevent the conformational change that allows the interconversion of the carrier from one state to another. Verapamil replaces the positively charged lysine which is absent in mutated parasite at position 76.[58] This restores the electrostatic charge of the protein and prevents charged chloroquine from binding to PfCRT and thus cannot be transported out of the digestive vacuole.

1.3.2 **Antifolate resistance**

P. falciparum resistance to folate inhibitors are due to single point mutations in the genes coding for the DHFR and DHPS enzymes. Resistance to pyrimethamine has been found to be due to accumulation of mutations on the *dhfr* domain of *P. falciparum* dihydrofolate reductase-thymidylate synthase (DHFR-TS). DHFR-TS of the parasite have 608 amino acids with the first 231 comprising of DHFR domain. Mutations at this domain on codons 51 (N51I), 59 (C59R) and 108 (S108N) lead to pyrimethamine resistance. S108N has been found to be a necessary first mutation in DHFR for resistance to any DHFR inhibitors to occur. It has also been established that the greater the number of mutations the greater the degree of resistance.[42]

WR99210 (Figure 1.7, **1.40**) is an active metabolite of PS-15 (**1.41**) that binds to and inhibit DHFR. WR99210 has the closest flexibility to DHFR substrate, dihydrofolate[61] and this is possibly why it is a very potent inhibitor and has low susceptibility to point mutations in DHFR. There is a possibility that mutations that are strong enough to disrupt the binding of WR99210 will also disrupt dihydrofolate from binding.[42]

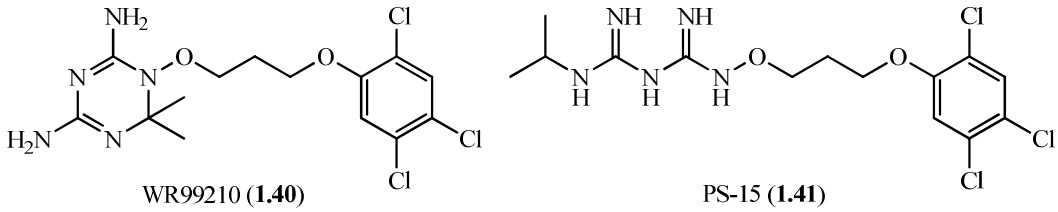

Figure 1.7. Chemical structures of WR99210 (**1.40**) and PS-15 (**1.41**)

Resistance to sulpha drugs occur also as a result of point mutations on DHPS and like DHFR, the more mutations on DPHS the greater the resistance to the sulpha drugs. Single mutations to A437G, K540E or S436A induce some degree of resistance. These mutations along with other multiple mutations are required for higher degrees of resistance to the sulpha drugs. The double mutant A437G/K540E is prevalent in Africa and when found with a triple mutant form of DHFR (N51I/C59R/S108N) results in a parasite that is highly resistant to sulphadoxine-pyrimethamine combination.[62]

The world currently relies heavily on artemisinin and its derivatives for the treatment of malaria. Though *in vitro* resistance has been reported[63] there has not been an unquestionable *in vivo* resistance to artemisinin. However, judging from the trend observed thus far, especially in western Cambodia where emergence of resistance to different antimalarials is not new and where there appears to be low susceptibility to artesunate, the plasmodium parasite might soon acquire resistance to artemisinin. This would be disastrous seeing that artemisinin class of drugs is currently one of the most effective treatment against the disease.

1.4 TARGETS FOR ANTIMALARIAL DRUGS

There has been cross resistance between many antimalarial drugs making it necessary to find new drugs and targets. These targets should preferably be specific to the parasite or with enough differences from homologous targets in the host in order that drug development could be directed toward more selective compounds for the parasite. The current approach to development of new antimalarial chemotherapy generally include: i) optimization of existing antimalarial agents e.g. combination therapies, ii) development of analogues of existing drugs, iii) use of compounds developed against other diseases, iv) development of drug resistance reversals, v) natural products and vi) development of active compounds against new targets.[64] The completion of *P. falciparum* genome sequencing has created a better understanding of the parasite biology, thus aiding the search for new drug targets. Table 1.1 shows some of these targets and their inhibitors.

Table 1.1. Identified targets for antimalarial agents[64-66]

Target Location	P/way or Process	Target Enzyme	Inhibitor
Parasite membrane	Phospholipid synthesis	Choline transporter	G-25
	Membrane transport	Unique channels	Dinucleoside dimmers
Apicoplast	DNA synthesis	DNA gyrase	Quinolones
	Transcription	RNA polymerase	Rifampicin
	Protein synthesis	Apicoplast ribosome	Doxycycline
	Type II fatty acid synthesis	FabH	Thiolactomycin
		FabI	Triclosan
	Isoprenoid synthesis	DXR	Fosmidomycin
	Protein farnesylation	Farnesyl transferase	Peptidomimetics
Mitochondrion	Electron transport	Cytochrome oxidoreductase	Atovaquone
Cytosol	Folate metabolism	DHFR	Pyrimethamine, proguanil, cycloproguanil
		DHPS	Sulphadoxine, dapsone
	Glycolysis	Lactate dehydrogenase	Gossypol derivatives
	Pyrimidine metabolism	Thymidylate synthase	5-fluoroorotate
		OPRT	5-substituted orotate analogues
	Shikimate pathway	EPSP synthase	Glyphosate
	Purine metabolism	HGPRT	Immucillin-H
	Calcium catabolism	SERCA	Artemisinin
Digestive vacuole	Haem polymerization	Haematin	Quinolines
	Hb degradation	Plasmepsins, falcipains	Leupeptin, pepstatin
	Reactive species generation	Unknown	Artemisinin
Nucleus	Cyclin-dependent protein kinases	pfnek-1, pfcrk-1, pfmrk	Isoquinolone sulphonamides, oxindole derivatives

1.5 THE APICOPLAST AS A DRUG TARGET FOR ANTIMALARIAL DRUG DEVELOPMENT

Plastids are organelles believed to originate from endosymbiotic bacteria or cyanobacteria. The endosymbiotic relationship is thought to have resulted from the engulfment of the cyanobacteria by a eukaryotic cell. The undigested bacterium then remained preserved as a plastid in the eukaryotic host cell. As such the plastids are semi-autonomous and serve as a site for many metabolic processes that the host cell has come to depend upon.[67] An example of such a plastid is the chloroplast found in plants and some algae. Chloroplast serves a number of functions in these organisms the most significant of which is photosynthesis.

An important non-photosynthetic plastid found in apicomplexan parasites is the apicoplast. Apicoplast originated as a result of a secondary endosymbiosis of a red-alga which already contained a plastid.[68] The apocoplast in *P. falciparum* (Figure 1.8) is believed to perform a number of housekeeping functions necessary for the survival of the parasite. While these functions have not been conclusively defined, the apicoplast is thought to be the site of fatty acid synthesis, is implicated in haem and amino acid synthesis and has been proven to be the site of non-mevalonate isoprenoid biosynthesis in the parasite.

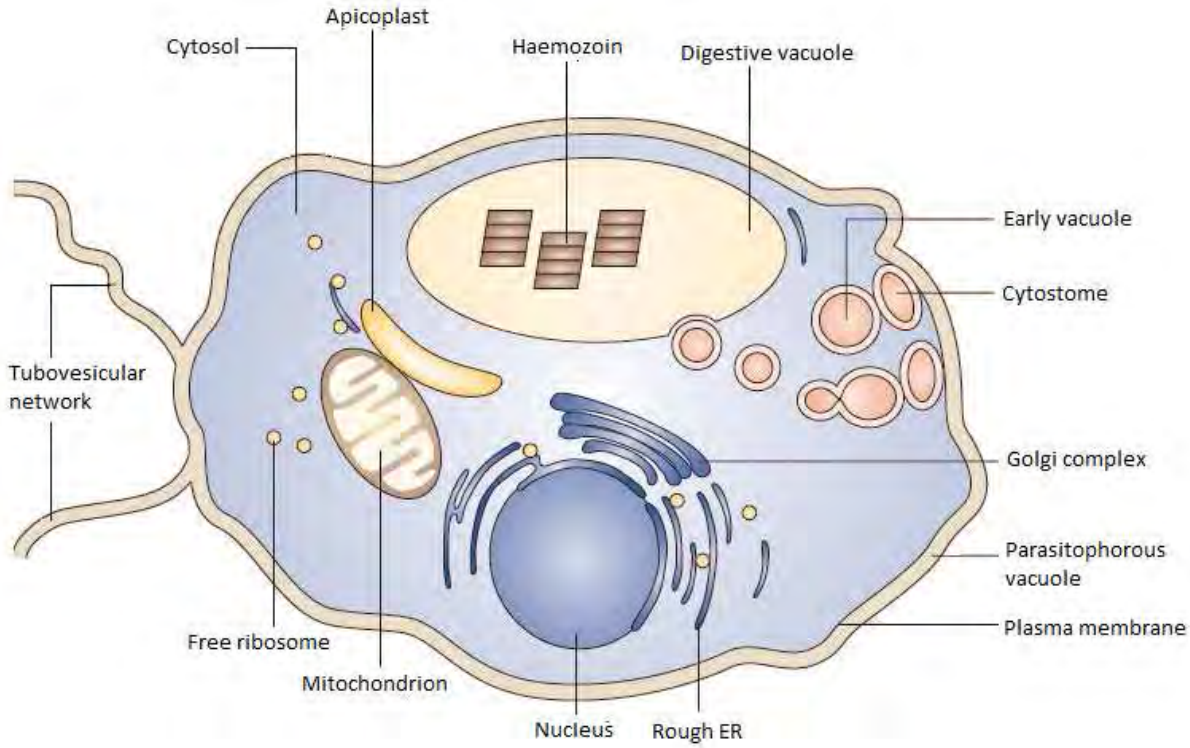

Figure 1.8. Cellular structure of *P. falciparum* trophozoite showing the apicoplast[69]

Due to their prokaryotic origin from the primary endosymbiosis, the metabolic processes that take place in the apicoplast are significantly different to that of their eukaryotic host and can thus be selectively targeted for drug development. Being semi-autonomous the apicoplast replicates its own DNA, transcribe and translate its RNA into proteins. Coupled with fatty acid and isoprenoid biosynthesis,[67] the apicoplast has been deemed indispensible to the malarial parasite.[68] Identifying the functions of the apicoplast has prompted drug development research to inhibit the *P. falciparum* growth by inhibiting the processes that take place in the organelle.

1.5.1 **DNA replication, transcription and translation**

Based on their prokaryotic origin, antibiotics have been found to effectively inhibit plasmodial growth. To this end ciprofloxacin has been shown to directly inhibit apicoplast

DNA replication in *P. falciparum*.[70] Rifampicin inhibits bacterial RNA polymerase, preventing transcription in bacteria. This explanation is used to rationalise its antiplasmodial activity, although direct evidence of this has not been observed in the apicoplast.[68] Several antibiotics have been suggested to inhibit plasmodial growth through inhibition of protein translation in the parasite at the apicoplast level. These antibiotics include thiostrepton, micrococcin, clindamycin, doxycycline, tetracycline and amythiamycin.[67]

1.5.2 **Fatty acid biosynthesis**

Biosynthesis of fatty acid in humans is catalyzed by a multifunctional protein classified as a type I fatty acid synthase. Until recently, it was believed that plasmodium species are unable to produce their own fatty acids but rely on the host cell for their needs. Plants, bacteria and plasmodium biosynthesize their fatty acids in a pathway that requires separate enzymes at different stages, known as type II synthases. Some of the type II synthases include acyl carrier proteins (ACP) FabB, FabH, FabZ and FabI which take part in a series of condensation and dehydration reactions. Identification of genes that codes for these ACP in association with the apicoplast of *P. falciparum* confirms the occurrence of a type II fatty acid biosynthetic pathway in the parasite. This provides new targets to which new antiplasmodial drugs can be developed.[71] Triclosan, a known antibacterial, has been shown to inhibit the growth of *P. falciparum*. It binds and inhibits the enoyl-ACP reductase (FabI), the enzyme that elongates the fatty acids at the rate-limiting final step of the synthesis.[72]

1.5.3 **Isoprenoid biosynthesis**

Isoprenoid biosynthesis is one of the functions observed in the apicoplast of *P. falciparum*. This process is inhibited by fosmidomycin, an antibiotic which binds to 1-deoxy-D-xylulose 5-phosphate reductoisomerase (DXR), one of the enzymes of the isoprenoid synthetic pathway.[73] Yeh *et al*.[74] recently discovered that fosmidomycin inhibition can be rescued by externally supplying isopentenyl pyrophosphate (IPP) to the parasite. Parasite survival was also observed in those plasmodial cells which had lost their apicoplast when externally supplemented with IPP during the blood stage growth of *P. falciparum*. This indicated that

isoprenoid biosynthesis is the only essential function of the plasmodial apicoplast at the blood stage, validating this pathway as a target for development of antimalarial drugs.

1.6 TARGETING THE MEVALONATE-INDEPENDENT PATHWAY

1.6.1 **The mevalonate and mevalonate-independent pathways**

For many years, the mevalonate pathway was believed to be the only route for the biosynthesis of isoprene units. Isoprene units include the 5-carbon isomers isopentenyl pyrophosphate (IPP) and dimethylallyl pyrophosphate (DMAPP) which are added head-to-tail in different chain lengths to make different isoprenoids. Isoprenoids are a very diverse family of natural compounds comprising over 35 000 compounds such as steroids, bile salts and carotenoids that play important roles in all organisms. They are involved in signal transduction, membrane structure, electron transport and growth regulations.[75] The mevalonate pathway involves the condensation of three molecules of acetyl-coenzyme A (acetyl-CoA) to give 3-hydroxy-3-methylglutaryl CoA (HMG-CoA). HMG-CoA is reduced to mevalonic acid (MVA) by HMG-CoA reductase and subsequent phosphorylation of the MVA by kinases result in mevalonate-5-diphosphate. Mevalonate diphosphate decarboxylase in a decarboxylation reaction converts mevalonate-5-diphosphate to IPP. DMAPP is then formed from the action of IPP isomerase on IPP (Scheme 1.3).

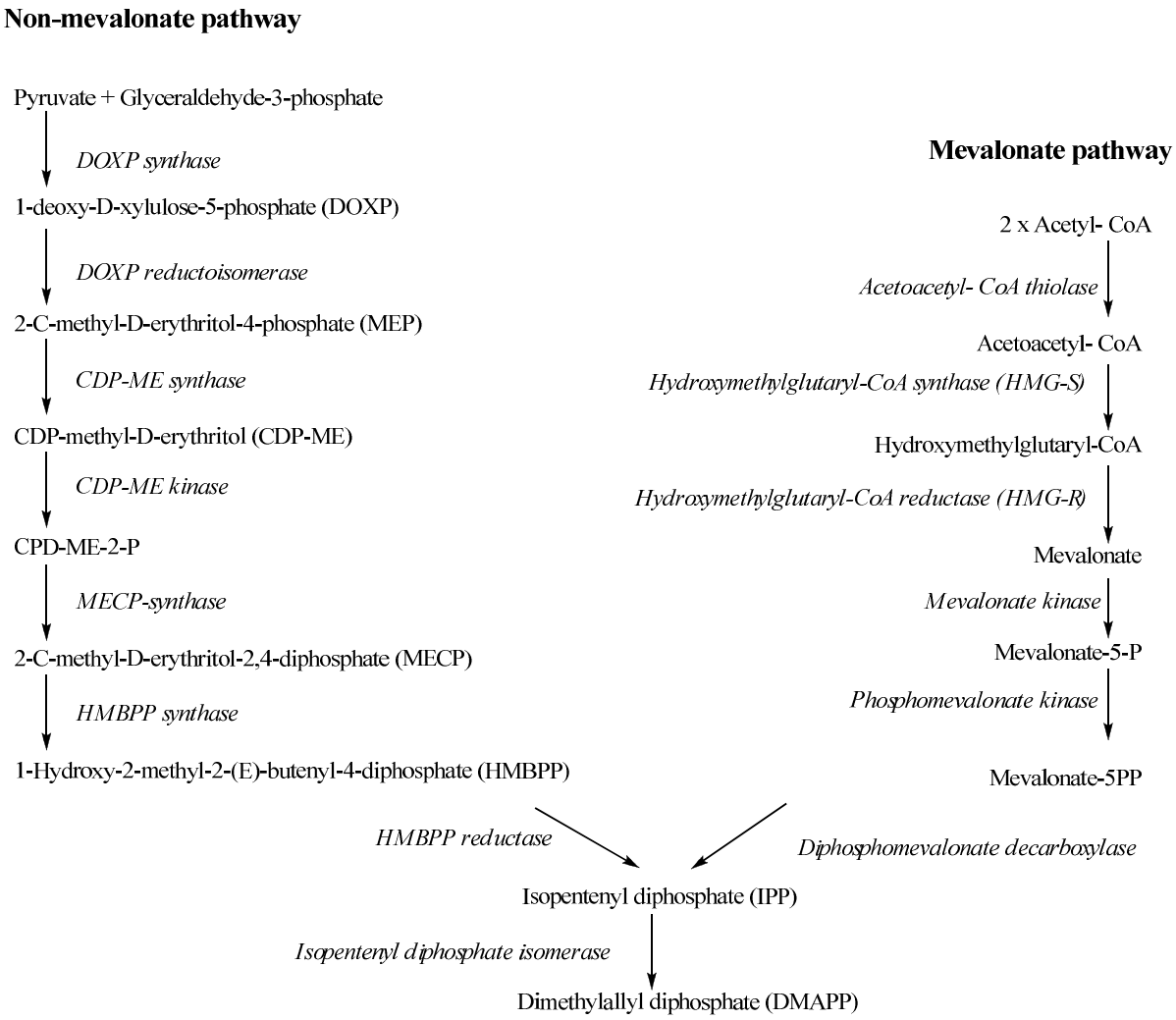

Scheme 1.3. The Mevalonate and Non-mevalonate pathways of terpenoid synthesis

In the early 1990s, Rohmer *et al.* (1993) discovered an alternative pathway to the synthesis of isoprene units in bacteria.[76] This mevalonate-independent pathway (also known as non-mevalonate pathway, DOXP pathway or MEP pathway) has since been identified in green algae, higher plants[77] and in the apicoplast of *P. falciparum*.[73] The pathway consists of seven steps that begin with the condensation of glyceraldehyde-3-phosphate and pyruvate by 1-deoxy-D-xylulose 5-phosphate (DOXP) synthase (DXS) to form DOXP. The second step constitutes the first step that is specific to this pathway and involves the intramolecular rearrangement and reduction of DOXP in an NADPH dependent reaction to form 2-C-methyl-D-erythritol (MEP) by DOXP reductoisomerase (DXR or IspC). 4-Diphosphocytidyl-2-C-methyl-D-erythritol (CDP-ME) synthase (IspD) cytidilates MEP to CDP-ME releasing pyrophosphate in the process. In an ATP dependent reaction, the 2-hydroxy group on CDP-

ME is phosphorylated by CDP-ME kinase (CMK or IspE) to form CDP-ME-2-phosphate. 2-C-methyl-D-erythritol-2,4-cyclodiphosphate (MECDP) synthase (IspF) cyclises CDP-ME-2-phosphate to MECDP. Ring opening reduction of MECDP by 1-hydroxy-2-methyl-2-buten-4-yl diphosphate (HMBPP) synthase (GcpE or IspG) gives rise to HMBPP. In the final step HMBPP is again reduced followed by removal of a hydroxyl group to form a mixture of IPP and DMAPP in a reaction catalysed by IPP/DMAPP synthase (LytB or IspH).[78]

1.6.2 **DXR as a validated target**

The formation of DOXP, catalysed by DXS in the first step of the mevalonate-independent pathway, is also involved in thiamine and pyridoxol biosynthesis in *Escherichia coli*.[79] This makes the second step i.e. the DXR catalyzed conversion of DOXP to MEP the first committed step of the mevalonate-independent pathway. The fact that the pathway and its enzymes are absent in humans make them even more desirable as drug targets. Each enzyme of the pathway is thus a potential target for the development of antibacterial, herbicidal and antiplasmodial agents.

Soon after the discovery of the non-mevalonate pathway, the antibacterial fosmidomycin (**1.46**) was identified as an inhibitor of the pathway, specifically inhibiting the DXR enzyme.[80] The phase II clinical trial of fosmidomycin in combination with clindamycin revealed a good tolerability and safety profile for the drug.[81] Fosmidomycin has been shown to inhibit recombinant DXR from *E. coli*,[80] *P. falciparum*[73] and *M. tuberculosis*[82] in *in vitro* assays. Yet, compounds downstream from the DXR reaction in the pathway, most notably MEP, have also been detected after fosmidomycin treatment in three studies.[83-85] This is unexpected since the pathway should end when DXR is inhibited by fosmidomycin. This raised questions as to whether fosmidomycin inhibits DXR or another enzyme in the plasmodium parasite to give its antimalarial effect, and if it does, is DXR really necessary for parasite survival? In an attempt to find answers to these questions, a study was conducted with parasites from which the *dxr* gene had been removed. The study showed no parasite growth when the *dxr* gene is absent, confirming that DXR is essential for *P. falciparum* growth.[86] This nevertheless still did not explain the presence of MEP after addition of fosmidomycin to the DXR assays.

It is important to functionally validate potential therapeutic targets. Although fosmidomycin inhibits recombinant *Pf*DXR, *in vitro*, and has antiplasmodial and antimalarial activity, *in vivo*, it is still not a proof that fosmidomycin binds only to DXR, *in vivo*. Zhang *et al*.[87] found that fosmidomycin exclusively blocks an enzyme/s of the DOXP pathway. This was shown by the rescuing of fosmidomycin-mediated growth inhibition when the growth medium was supplemented with isoprenol. Had fosmidomycin been attacking any other function outside the DOXP pathway, addition of the isoprenol should not rescue the growth inhibition. Enzymes of this pathway were thus validated as targets for drug development. In the same study, the intermediate 2-C-methylerythrose 4-phosphate formed during the conversion of DOXP to MEP was found to increase upon fosmidomycin addition which means that fosmidomycin probably blocks the conversion of the intermediate to MEP. All the other metabolites isolated downstream of MEP decreases. Metabolic profiling of the fosmidomycin-treated *Plasmodium* thus identifies IspD as the second target in the parasite. There was weak inhibition of purified IspD when treated with fosmidomycin suggesting that inhibition of this pathway by fosmidomycin might be more complicated than initially anticipated. Computational docking of IspD with fosmidomycin and 2-C-methylerythrose 4-phosphate showed that the intermediate binds better to the enzyme than fosmidomycin. Zhang and co-workers speculated that it is the accumulated intermediate upon treatment with fosmidomycin that binds to and inhibit IspD as opposed to fosmidomycin itself binding to the enzyme.[87] This explains why MEP was present even after addition of fosmidomycin to the assay. Given that DXR inhibition by fosmidomycin led to all the effect that was observed and which inhibited the parasite growth, DXR was as a result functionally validated as target for antiplasmodial agents.

1.6.3 **General features and characteristics of the DXR enzyme**

DXR is a homodimer (Figure 1.9 A) in which each monomer is divided into 3 subunits that form a V-shape. While the crystal structure of *P. falciparum* DXR (*Pf*DXR) has only recently been reported,[88] *E. coli* DXR (*Ec*DXR) has been extensively studied.[89-94] Each monomer of *Ec*DXR has a molecular mass of 43.5 kDa and consists of 398 residues. The monomer is divided into (i) the N- or amino-terminal dinucleotide binding domain which forms one arm of the V-shape, (ii) the carboxyl-terminal which forms the other arm of the "V" and (iii) the

connecting domain which links the N- and the C-terminals (Figure 1.9 B). The N-terminal is made up of residues 1-150 and is the site of NADPH binding which is necessary for the activity of the enzyme. The carboxyl-terminal is a four-helix bundle comprising of residues 312-398 and is reported to play a structural role in supporting the catalytic domain. The connecting domain houses the catalytic site of the enzyme where substrate, metal ion and inhibitors bind and is involved in the dimerization of the enzyme.[89, 90] The connective domain comprises of residues 160 – 270 and also integrates residues 206 – 216 which make up the flexible "lid" that closes over the active site upon substrate or inhibitor binding to shield the active site from solvent.

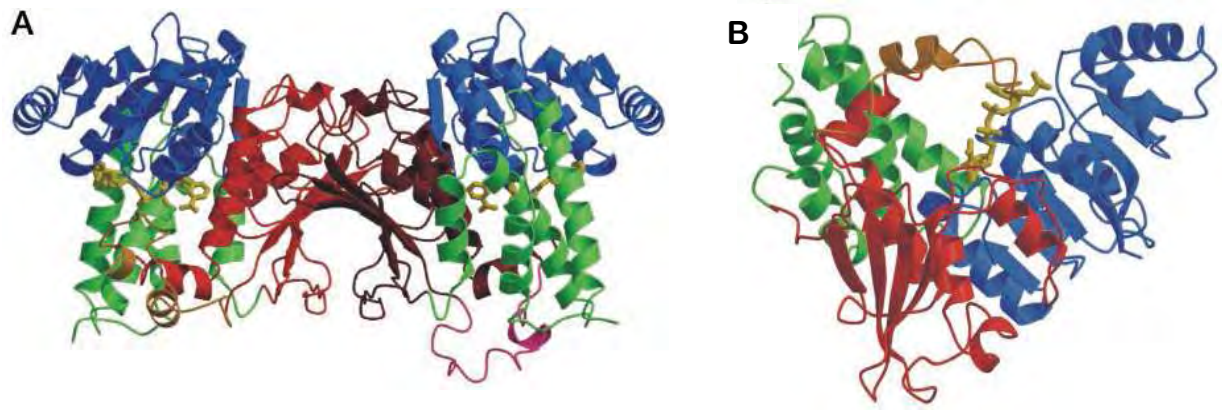

Figure 1.9. Crystal structure of EcDXR[90]

Ribbon representation of DXR dimer (A) and monomer (B) showing the three domains: amino-terminal (blue), connective domain (red) and carboxyl terminal (green) modelled with NADPH (yellow) and showing the flexible loop (ochre)

1.6.4 **The 1-deoxy-D-xylulose 5-phosphate reductoisomerase catalyzed reaction**

It was established over the years that the transformation of DOXP (Scheme 1.4, **1.42)** to MEP (**1.44**) happens in two steps, a rearrangement step followed by a NADPH and divalent metal ion-dependent reduction step. NADPH is required for the initial rearrangement of DOXP to 2-C-methylerythrose-4-phosphate intermediate (**1.43**) but no reduction occurs until the next stage when the intermediate is converted to MEP (Scheme 1.4).[95]

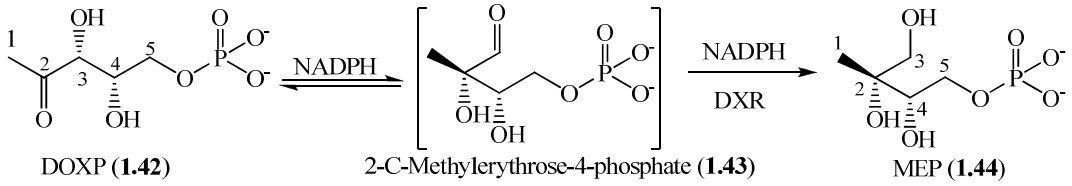

Scheme 1.4. DXR catalyzed conversion of DOXP to MEP[95, 96]

Two mechanisms were proposed for the rearrangement of DOXP to 2-C-methylerythrose-4-phosphate, the α-ketol rearrangement and the retroaldol-aldol rearrangement. The α-ketol rearrangement involves the deprotonation of the C-3 hydroxyl followed by C-4 shift to C-2 to give the 2-C-methylerythrose-4-phosphate intermediate (Scheme 1.5 A, **1.43**).

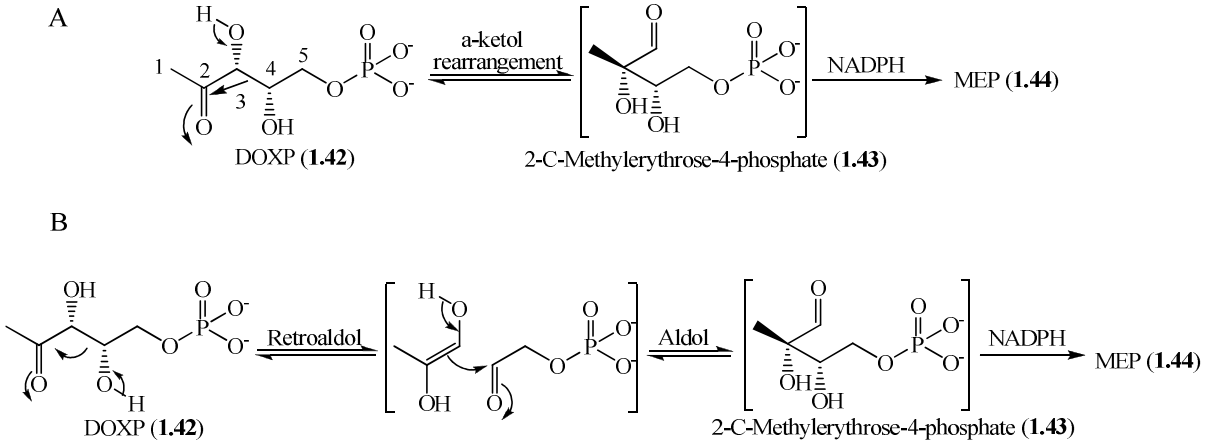

Scheme 1.5. The α-ketol rearrangement (A) and retroaldol-aldol rearrangement (B) mechanism[96]

The retroaldol-aldol reaction involves the breakage of the C3-C4 bond, followed by an aldol condensation of the two segments with a resulting shift of C-4 to C-2 (Scheme 1.5 B). Determining the correct mechanism for the conversion of DOXP to MEP has been an ongoing project for researchers. Munos *et al.*[97] and Wong and Cox[96] found more evidence favouring the retroaldol-aldol mechanism. The two groups incorporated ^{2}H selectively at C-3 and C-4, synthesizing 3-^{2}H DOXP and 4-^{2}H DOXP, respectively. A competitive secondary kinetic isotope effect (KIE) study of the DXR reaction was then carried out separately with both deuterated substrates. KIE can be used to observe hybridization changes of a carbon atom. The study was used to distinguish between the α-ketol and retroaldol-aldol mechanisms

by observing the re-hybridization pattern of the substrates to 2-C-methylerythrose-4-phosphate. Hybridization changes would be expected at C-2 and C-3 and no change at C-4 if the α-ketol reaction occurred i.e. KIE will be expected for the 3-^{2}H DOXP and no KIE for the 4-^{2}H DOXP. The studies reported sp^3 to sp^2 hybridization for both 3-^{2}H DOXP and 4-^{2}H DOXP and re-hybridization back to sp^3 for 4-^{2}H substrate. This is consistent with the retroaldol-aldol mechanism and confirms the presence of this mechanism in the DOXP pathway.[96, 97] The rearrangement step was confirmed to be the rate-limiting step of the reaction.[98]

The stereochemistry of the reduction step of the DXR reaction was established based on the delivery of pro-*S* hydride from NADPH to the *re* face of the intermediate aldehyde. This earned DXR a class B dehydrogenase classification.[99]

1.6.5 **FR-900098 and fosmidomycin as inhibitors of DXR**

FR900098 (Figure 1.10, **1.45**) was originally isolated from *Streptomyces rubellomurinus* sp. nov ATCC31215[100] and later synthesized.[101] Fosmidomycin (**1.46**) was also isolated from *S. lavendulae* and exhibited superior antimicrobial activity to FR900098.[102] The activity of fosmidomycin was narrowed down to inhibition of isoprenoid biosynthesis in those organisms that produce isoprene units exclusively *via* the DOXP pathway. This was identified by fosmidomycin's inhibition of menaquinone and carotenoid biosynthesis in *Micrococcus luteus*.[103]

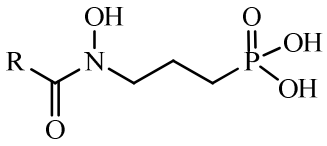

R = CH_3 = FR900098 (**1.45**)
R = H = Fosmidomycin (**1.46**)

Figure 1.10. Structures of FR900098 (**1.45**) and fosmidomycin (**1.46**)

Fosmidomycin (**1.46**) and its derivative FR900098 (**1.45**) are structurally simple compounds consisting of phosphonic acid and a retro-hydroxamate groups which are necessary for their

inhibitory activity. Fosmidomycin was found to be a specific inhibitor of DXR preventing conversion of DOXP to MEP (**1.44**).[80] Jomaa and co-workers[73] identified the DOXP (**1.42**) pathway in *P. falciparum* and found that both fosmidomycin and FR900098 inhibit the pathway. Interestingly, FR-900098 showed better antiplasmodial activity than fosmidomycin both *in vivo* and *in vitro*.

1.6.6 **Binding of substrate and inhibitors to DXR enzyme**

The first piece of evidence that the inhibitor (fosmidomycin, **1.46**), binds in a similar mode as the substrate (DOXP) to DXR was the molecular docking of the crystal structure complex of *Ec*DXR with fosmidomycin and Mn^{2+} (pdb code: 1ONP).[91] This was only later confirmed when the ternary complex structure of *Ec*DXR with the substrate was solved by Sweeney *et al*.[89] The binding of substrate or inhibitor to the enzyme in the presence of NADPH induces a considerable conformational change. This flexibility of DXR is important for substrate binding and catalysis and also results in the formation of a catalytic pocket over which the flexible 'lid' closes. The catalytic pocket or the substrate binding cavity so formed is divided into three regions: i) the positively charged pocket into which the phosphonate end of the inhibitor binds, ii) the hydrophobic region which accommodates the propyl backbone and iii) the amphipatic region where the hydroxamate binds.[89] The phosphate moiety of DOXP forms a network of hydrogen bonds with Ser186, Asn227, Lys228 and His209. The C-2 carbonyl also forms hydrogen bonds with Glu152 and Ser151, C-3 hydroxyl with Lys125 and Glu231 and C-4 hydroxyl group with Glu152, Asn227 and Lys228. Similarly, the phosphonate moiety of fosmidomycin forms hydrogen bonds with Ser186, Ser222, Asn227 and Lys228 while the *N*-formyl-*N*-hydroxyl group of the hydroxamate component forms an octahedral coordination with a divalent metal ion as well as the carbonic acids Asp150, Glu152 and Glu231 and one water molecule.[91, 94]

The binding site of fosmidomycin in *Pf*DXR as resolved by Umeda *et al*.[88] also consists of three regions which include a binding pocket for the phosphonate, a hydrophobic patch for the propyl backbone and a binding pocket for the hydroxamate group. The phosphonate binding pocket houses residues Ser270, Asn311, His293 and two water molecules to which the phosphonate forms tight hydrogen bonds. The coordination of the hydroxamate group of

fosmidomycin with Mg^{2+} to residues Asp231, Glu233 and Glu315 is such that it forms a distorted trigonal bipyramidal geometry where the two oxygen atoms of the inhibitor adopt a *cis*-arrangement.[88] FR900098 (**1.45**) interact with the DXR enzyme in a similar mode to fosmidomycin (**1.46**). Its methyl group has a Van der Waals interaction with the indole group of Trp296 and is suggested to be the reason for its higher antiplasmodial activity as compared to fosmidomycin. It is also possible that the interaction is needed for the *cis* arrangement of the two hydroxamate oxygen atoms such that there are six atoms in the same plane (Figure 1.11), allowing for the binding of the metal ion at the active site. The complex of FR900098 when compared with fosmidomycin showed an induced fit movement of the active site residues of the *Pf*DXR to accommodate the methyl group of the compound.

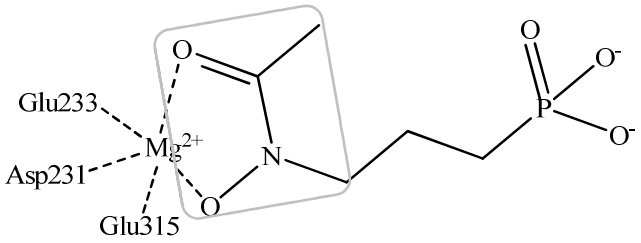

Figure 1.11. Metal coordination of FR900098 **(**1.45**)** with *Pf*DXR[88]

1.6.7 **The pharmacokinetics and toxicological properties of fosmidomycin**

The oral absorption of fosmidomycin (**1.46**) is about 30%. At 0.25 h after dosing a healthy volunteer's serum concentration was 157 µg/ml for an intravenous (i.v.) dose of fosmidomycin at 30 mg/kg, 12.3 µg/ml for an intramuscular (i.m.) dose of 7.5 mg/kg and 2.45 µg/ml for a 500 mg oral dose.[104] In rats, fosmidomycin (**1.46**) is rapidly distributed into tissues with high concentrations in kidney, liver and bones. The serum level after i.v. injection fitted a 3-compartment open model with first order kinetics.[105] Fosmidomycin is not metabolized, it is excreted unchanged in urine. Urine recovery of the drug over 24 hours after dosing was 85% of the i.v. dose, 66% of the i.m. dose and 26% of the oral dose. Fosmidomycin has a half-life of 1.8 hours after i.v. dose and shows no accumulation in the serum or urine after repeated oral or parenteral dosing.[20, 104]

Fosmidomycin is well tolerated even when given in repeated doses of 8 g/day i.v for seven days, 4 g/day i.m for five days and 4 g/day orally for 7 days. No abnormalities or changes were observed in physical, haematological, biochemical or urine examination.[106] In some cases at the highest dose level, nausea, vomiting and loose stools were observed.[20]

1.7 FOSMIDOMYCIN AND FR900098 AS LEAD COMPOUNDS IN DRUG DESIGN

1.7.1 Structure activity relationship of fosmidomycin and FR900098

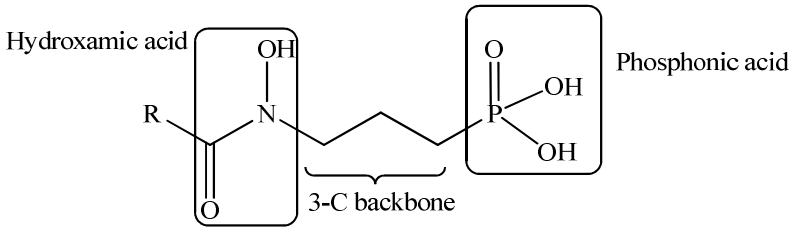

R = CH_3 = FR900098 (**1.45**)
R = H = Fosmidomycin (**1.46**)

Fosmidomycin (**1.46**) and FR900098 (**1.45**) interact at the active site of the DXR enzyme with the phosphonate group, the 3-carbon backbone and the hydroxamate group of the compounds (Figure 1.12). The phosphonate moiety forms tight hydrogen bonds with the active site of the enzyme at the phosphonate binding pocket. The hydroxamate group of the lead compounds is essential for the binding of the inhibitors to the divalent metal ion found at the active site of the enzyme.

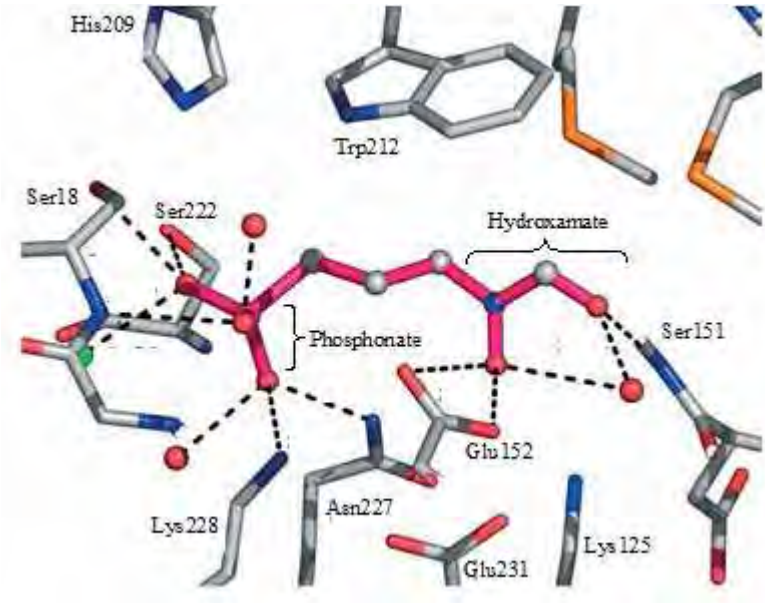

Figure 1.12. Hydrogen bond interaction of Fosmidomycin (**1.46**, pink) with DXR active site[89]

The latest study of *Pf*DXR in complex with inhibitors[88] revealed that a *cis* arrangement of the two oxygen atoms of the hydroxamate moiety is necessary for the metal chelation. It has been suggested that any functional group with *cis* arrangement of two oxygen atom might also exhibit comparable metal coordination. The 3-carbon spacer in these lead compounds appears to be optimum for the hydrophobic binding of the backbone to the hydrophobic pocket of the enzyme at the active site. Compounds with shorter spacers would be unable to occupy both the phosphonate and the hydroxamate binding site and longer spacers would not be able to efficiently bind to the site.

The problems associated with fosmidomycin pharmacokinetics i.e. low oral absorption, short plasma half-life, high rate of recrudescence and the need for a long duration of treatment when used as mono-therapy have prompted research into developing compounds with better pharmacokinetic profiles. Several analogues of fosmidomycin (**1.46**) have been synthesized, focusing on different parts of the compound.[104, 107-109]

1.7.2 **Phosphonate esters of fosmidomycin and FR900098**

Given that the oral bioavailability of fosmidomycin is only 30% due to its high polarity and the ease of ionization of the phosphonate group at physiological pH,[105] masking this property of the phosphonate group was expected to improve bioavailability. Ester prodrugs of fosmidomycin and FR900098 were synthesized to mask the polar properties and improve the oral bioavailability of the drugs. The esters are expected to be more lipophilic and therefore cross the membranes through diffusion after which esterases will cleave off the ester group and release the active drug.[110] Substituted and un-substituted diaryl esters of FR900098 such as **1.47** and **1.48** (Figure 1.13) were synthesized and although these compounds showed improved oral activity in infected mice,[109] there were concerns about the toxicity of the envisaged phenol derivative that will be generated upon cleavage of the esters.

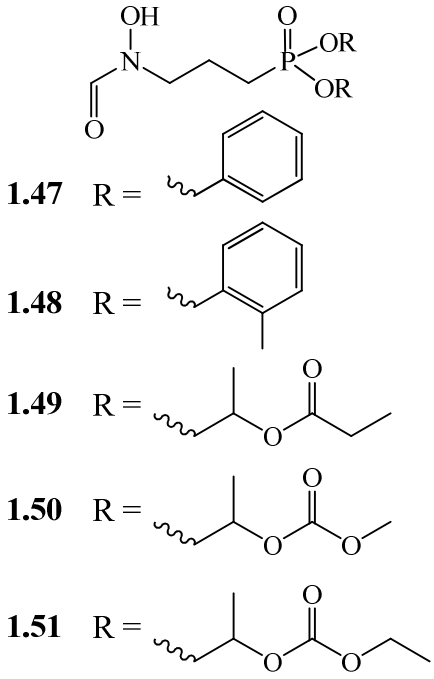

Figure 1.13. Diaryl and acyloxylalkyl esters of FR900098

Masking the phosphonate group to form acyloxyalkyl esters resulted in prodrugs with significantly higher antiplasmodial activity than FR900098 (**1.45**). Ortmann and co-workers[108] synthesized series a of acyloxyalkyl esters (Figure 1.13) of which the pivaloyloxymethyl ester **1.49** emerges with better activity than the parent drug in reducing paracetaemia in untreated control mice. Acetyloxyethyl **1.50** and propionyloxyethyl **1.51** as well as compounds **1.52** and **1.53** also showed higher activity than FR900098. Double ester

prodrug **1.50** showed the best antiplasmodial activity *in vivo* which was 2-fold that of FR900098 against *P. vinckei* and 5-fold more active against *P. falciparum in vitro*. These compounds showed no effect on recombinant *E. coli* DXR, confirming that the antiplasmodial activity of the compounds is due to the release of free FR900098 in the parasite. The masking of the phosphonate moiety thus increases the oral bioavailability of FR900098 and also increases the intrinsic activity of the drug probably due to the increased concentration of the drug at the active site.[110] The half-life of the compounds will probably remain the same as that of FR900098 since the active drug is still the same.

1.7.3 **Isosteric replacement of the phosphonate group**

The replacement of the phosphonate group of fosmidomycin (**1.46)** or FR900098 (**1.45**) with carboxylate (**1.54**) or sulphonamide (Figure 1.14, **1.55**) groups resulted in drastically reduced activity against *Synechocystis* sp. PCC6803 DXR. This was ascribed to the presence of two ionizable groups on the phosphonate, one ionizable groups on the carboxylate and sulphamate which is neutral depending on the pH.[111] Another explanation could be the structural difference where the phosphonate has a pyramidal structure and the carboxylate a planar structure.[88] The non-*N*-methylated retro-hydroxamate analogues **1.56** and **1.57** with carboxylate and sulphonate groups instead of phosphonate group showed 4000 – 6000-fold reduced activity against *E. coli* DXR than **1.58** with the phosphonate group. The *N*-methylated derivatives were generally more active than the non-*N*-methylated analogues, but ultimately the phosphonated analogues were more active than the carboxylate or sulphonate analogues such as **1.59** and **1.60** which were 500 – 1000 folds less active than the phosphonated analogue **1.61** (Table 1.2). Unfortunately the activity of these compounds against *P. falciparum* DXR was not tested for better comparison of their antiplasmodial potential.

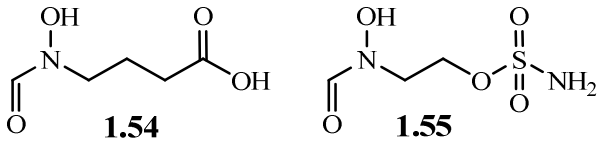

Figure 1.14. Analogues with modified phosphonate groups

Table 1.2. Analogues with reverse hydroxamate and modified phosphonate groups

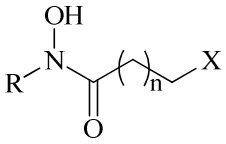

Compound	X	R	N	*E. coli* DXR: IC_{50} (µM)
1.56	COOH	H	2	720
1.57	SO_3H	H	2	1000
1.58	$PO(OH)_2$	H	2	0.17
1.59	COOH	Me	2	25
1.60	SO_3H	Me	2	48
1.61	$PO(OH)_2$	Me	2	0.049
FR900098 (1.45)				0.032

1.7.4 **Modifications of the hydroxamate group**

The *N*-formyl/*N*-acetyl and *N*-hydroxyl groups of fosmidomycin and FR900098 are important for the inhibitory effect of these compounds. These groups ensure the anchorage of the inhibitors through metal chelation to the divalent ion at the site of action. Replacement of the *N*-hydroxyl with a *N*-methyl group resulted in very weak inhibitors of *Synechocystis* sp. PCC6803 DXR.[111] Reverse hydroxamate analogues **1.62** and **1.63** (Figure 1.15) have been synthesized[111, 112] and both show some activity against *E. coli* DXR,[112] since they are still able to chelate metals. The features of the analogues are the same as those of the parent drugs but arranged differently. This rearrangement however results in lower antimicrobial activity than fosmidomycin. Interestingly, **1.63** remains active against fosmidomycin resistant *E. coli* strains. Courtois *et al.*[113] synthesized and investigated the inhibition of fosmidomycin analogues containing benzoxazolone or oxazolopyridinone moieties against ajmalicine production in *Catharanthus roseus* plant cell culture. Inhibition of ajmalicine production was used as a marker for monoterpenoid indole alkaloids inhibition. Surprisingly, the series gave rise to four diethyl esters that inhibited ajmalicine accumulation. Two of these esters **1.64** and **1.65** lost their inhibitory effect when converted to their corresponding phosphonic acid **1.66** and **1.67** respectively (Figure 1.13). More diethyl esters of fosmidomycin-oxazolopyridinones derivatives were later synthesized by Mincheva *et al.*[114] and compounds **1.68** and **1.69**

respectively inhibited alkaloid production by 91% and 87% as compared with 69% inhibition exhibited by fosmidomycin in *Catharantus roseus* cells.

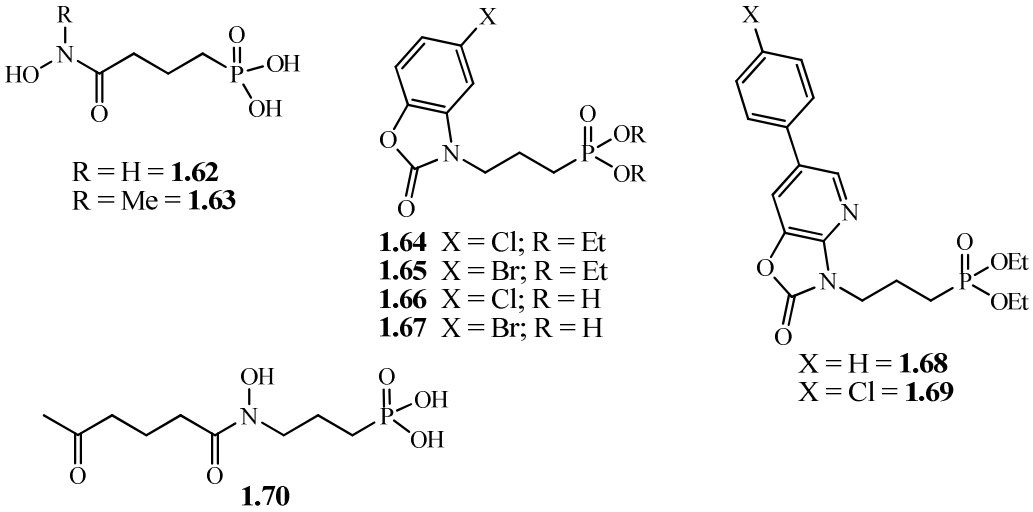

Figure 1.15. Fosmidomycin analogues with hydroxamate modifications

Replacement of the formyl residue of fosmidomycin with spacious acyl residues resulted in analogues which were active against recombinant *E. coli* DXR in the micromolar range. The most active analogue of the synthesized series, **1.70** (Figure 1.15) was significantly less active (IC_{50} 5.4 µM) than fosmidomycin (IC_{50} 0.035 µM).[115]

1.7.5 **Modifications of the propyl chain backbone**

Decreasing the length of the propyl carbon chain separating the phosphonate and the hydroxamate groups of fosmidomycin or FR90098 has been shown to diminish the antimicrobial effect of these compounds.[116]Although antimicrobial or antiplasmodial effects of a lengthened carbon spacer analogue of the compounds have not been reported, retro-hydroxamate analogues of FR900098 and fosmidomycin have been tested (compound **1.62** and **1.63**, section. 1.7.4). Reversing the arrangement of the hydroxamate group of fosmidomycin and FR900098 increases the carbon spacer between the phosphonate and the hydroxamate. While these compounds remain potent against *E. coli*, their activity is reduced. Shortening the length of the compounds or decreasing the number of methylene as in

compounds **1.71** and **1.72** (Table 1.3) severely decreases the affinity of the compounds for *E. coli* DXR (IC_{50} 1000 and 77 µM, respectively) as compared to **1.62** and **1.63** (IC_{50} 1 and 0.5 µM, respectively). This is possibly because the compounds were too short to occupy the space between the phosphonate and hydroxamate binding sites on the enzyme. Conversely, lengthening the compounds as in **1.73** and **1.74** with an additional methylene group gave better activity (0.27 and 0.11 µM, respectively) albeit less than the activity of **1.62** and **1.63**.[117]

Table 1.3. Analogues with varying chain length between the hydroxamate and the phosphonate groups[117]

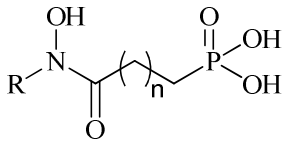

Compound	**R**	**N**	***E. coli* DXR IC_{50} (µM)**
1.71	H	1	1000
1.72	Me	1	19
1.73	H	3	0.27
1.74	Me	3	0.11
FR900098 (1.45)			0.032

Introducing electronegative atoms to the carbon backbone of fosmidomycin and FR900098 has given rise to some potent antiplasmodial compounds. The β-oxaisosteres of fosmidomycin and FR90009, compounds **1.75** and **1.76** (Figure 1.16) showed high growth inhibition against the *P. falciparum* 3D7 strain with **1.76** being more active than both fosmidomycin and FR90098. The retro-hydroxamate β-oxaisostere **1.77** was even more potent against the parasite than **1.76**. Although the antiplasmodial activity of γ-oxa retro hydroxamate compounds **1.78** and **1.79** were not reported, the activity against *E. coli* DXR were much less than the parent drugs and their β-oxa analogues.[104]

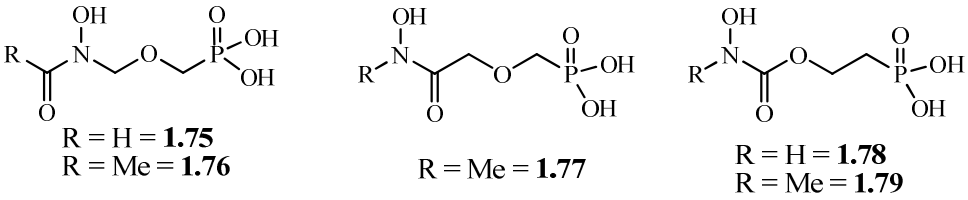

Figure 1.16. β-Iso-oxasteres of fosmidomycin and FR900098

Fosmidomycin analogues with α-aryl substitution have generally shown improved antiplasmodial activity compared to fosmidomycin (compounds **1.80– 1.86**, Table 1.4).[107] Of the series reported, the most active of the compounds are those with halogens substituents on the α-aryl group. The most potent, halogen substituted analogue of the series, **1.80**, showed a higher activity against *P. falciparum* Dd2 and 3D7 strains with IC_{50} values of 0.028 and 0.090 µM compared to FR900098 with 0.18 and 0.32 µM, respectively.

Table 1.4. Substituted α-aryl analogues of fosmidomycin (**1.46**) and FR900098 (**1.45**)[107]

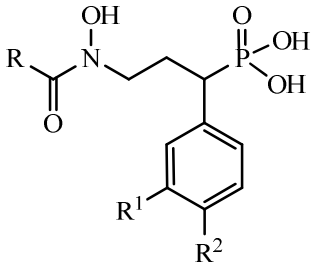

Compound	R	R^1	R^2	Dd2: IC_{50} (µM)	3D7: IC_{50} (µM)
1.80	H	Cl	Cl	0.028	0.090
1.81	Me	Cl	Cl	0.090	0.25
1.82	Me	H	H	0.35	0.55
1.83	Me	Me	H	0.22	0.95
1.84	H	OMe	H	0.20	0.36
1.85	Me	OMe	H	0.27	0.85
1.86	Me	Cl	H	0.095	0.35
FR900098 (1.45)	CH_3	-	-	0.18	0.32

1.8 AIM, RATIONALE AND OBJECTIVES

With the high number of annual mortalities due to malaria and the failing battle against resistance, it is imperative that research towards the development of new antimalarial compounds continue. Fosmidomycin and its derivatives have advantages such as target selectivity and activity against both CQS and CQR strains of *P. falciparum*. This offers a basis on which further development can be carried out to improve on the activity and the disadvantages of the compounds as antiplasmodial or antimalarial agents. Thus, the aim of this project was to design and synthesize new fosmidomycin analogues with potential antiplasmodial activity. More specifically, we wished to address two specific research questions. Firstly, we wished to explore the effect of halogenation in the acyl chain on the biological activity of FR900098 analogues. Secondly, we wanted to explore the feasibility of extending the acyl chain of FR90098 into the NADPH binding site and still producing DXR inhibition. The latter provide the added advantage of opening up possibilities of fosmidomycin-hybrid design (Scheme 1.6).

Therefore the specific objectives of this project were:

1. To synthesise a series of halogenated fosmidomycin analogues of varying chain length.
2. To synthesise analogues of FR900098 by extending the acyl side chain into the NADPH binding pocket (using chloroquine-fosmidomycin as a model compound)
3. To assess the antiplasmodial and DXR inhibitory activity of synthesized compounds
4. To explore the binding interactions of the synthesized compounds using molecular docking studies

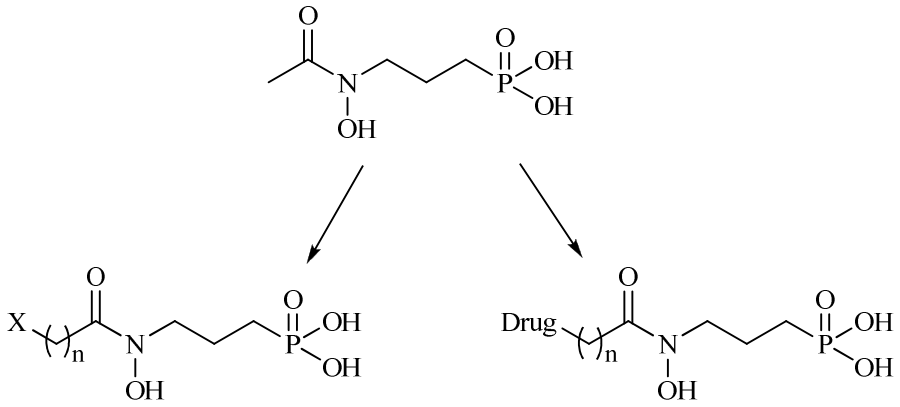

Scheme 1.6. Summary scheme of the aims of the research.

CHAPTER 2

2. DESIGN AND SYNTHESIS OF HALOGENATED FOSMIDOMYCIN ANALOGUES

2.1 INTRODUCTION

Several analogues of fosmidomycin (**1.46**) and FR900098 (**1.45**) have been synthesized in an effort to either improve the oral bioavailability or increase the potency of the drugs as antiplasmodial or antibacterial agents (Chapter 1).[107, 118-120] Three main strategies have been utilized to improve the activity of these compounds. These include (i) esterification of the phosphonate group, (ii) extending the acyl side chain and (iii) introducing an aromatic ring alpha to the phosphonate group. In this chapter we explore the effect of halogenation as well as lengthening of the acyl side chain on the activity of fosmidomycin analogs. This was inspired by the promising antiplasmodial activity of fosmidomycin intermediates produced in the process of synthesizing the chloroquine- and pyrazinoic acid-fosmidomycin hybrids discussed in chapter 3.

2.1.1 **Rationale for the synthesis of halogenated fosmidomycin analogues**

The synthesis of halogenated analogues and their antiplasmodial activity carried out in this study was supported firstly by the findings that analogues of fosmidomycin and FR900098 containing halogen substituents have in many cases shown better activity against DXR than the analogues without the halogens.[107, 121] Silber and co-workers have also predicted, using adaptation of fields for molecular comparison (AFMoC), that compounds with halogens are more active against DXR than fosmidomycin or FR900098,[122] thus making this aspect worth investigating. Another rationale behind the study was that fosmidomycin and FR900098 are highly hydrophilic and thus have low oral bioavailability or absorption into the parasite. Halogens are known to increase lipophilicity with the exception of fluorine which can either increase or decrease the lipophilicity of compounds.[123] Increasing the length of the acyl side chain is also expected to increase lipophilicity of the compounds. We therefore reasoned that the halogenated FR900098 analogues proposed in this study would increase both the activity and the lipophilicity of the compounds and therefore make it easier for the compounds to pass

through the membranes of the parasites. The calculated LogP (cLogP) of the chlorinated FR900098 analogues **2.1** in comparison with FR900098 and fosmidomycin (Table 2.1) clearly shows the effect of the addition of a chlorine substituent on the lipophilicity of the compounds. The lipophilicity increased from -1.600 for FR900098 to -1.035 for the chlorinated analogue **2.1**. Increasing the acyl chain length also showed significant increase in the LogP and hence lipophilicity of the compounds as is observed for compounds **2.2** and **2.3** at -0.764 and -0.494, respectively.

Table 2.1. cLogP of fosmidomycin, FR900098 and the proposed chlorinated analogues

Compound	**Structure**	**cLogP***
Fosmidomycin (**1.46**)	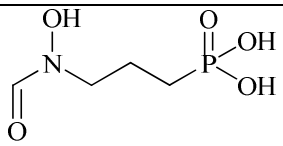	-1.578
FR900098 (**1.45**)	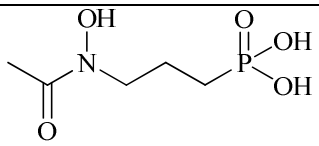	-1.600
2.1	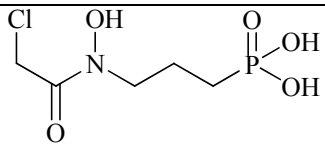	-1.035
2.2	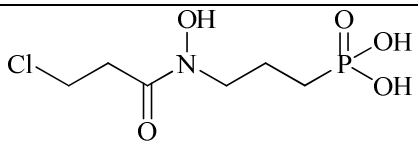	-0.764
2.3	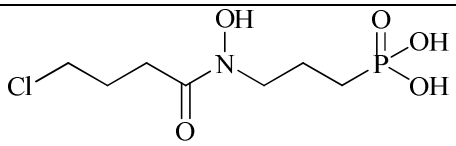	-0.494

*Calculated on molinspiration (http://www.molinspiration.com/cgi-bin/properties)

2.1.1 **Synthetic approaches to fosmidomycin and related compounds**

The synthesis of fosmidomycin analogues can be divided into three main stages which include: (i) introduction of the phosphonate moiety into a three carbon backbone, (ii) introduction of the hydroxylamine moiety and (iii) *N*-acylation of the latter.

Introduction of the phosphonate group

Introduction of the phosphonate group, or C-P bond formation, is an essential key step in the synthesis of the fosmidomycin analogues as this group is essential for tight binding to the DXR active site. The most common synthetic methods used to introduce the phosphonate moiety in fosmidomycin analogues are the Michaelis-Arbuzov reaction (also known as the Arbuzov reaction) and the Michaelis-Becker reaction. The reaction was originally discovered by Michaelis[124] and later explored by Arbuzov.[125, 126] The Arbuzov reaction involves heating a trialkylphosphite with an alkyl halide at a temperature of between 120^{o}C and 160^{o}C to form a dialkyl phosphonate ester (Scheme 2.1). The reaction proceeds through nucleophilic attack on the alkyl halide by the lone pair electrons of the phosphorus atom to form a phosphonium intermediate. A second nucleophilic attack by the halide anion on the phosphonium intermediate gives the dialkylphosphonate ester and a new alkyl halide (Scheme 2.1 A). This method has been successfully employed in the synthesis of phosphonated *N*-heteroarylcarboxamides[118] and diaryl ester prodrugs of FR900098.[109]

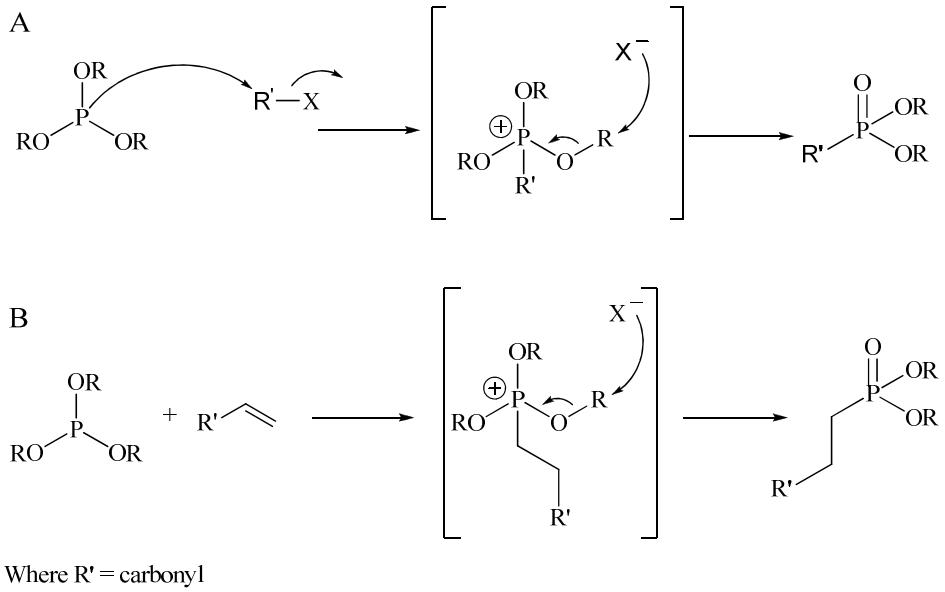

Scheme 2.1. TheMichaelis-Arbuzov reaction[127]

A scheme showing alkylation of the phosphonate through a nucleophilic reaction with an alkyl halide (A) and with an activated alkene (B)

Fosmidomycin (**1.46**) and FR00098 (**1.45**) were first synthesized in 1980 using the Michaelis-Becker reaction to introduce the phosphonate moiety of the compounds.[101] The reaction occurs through a nucleophilic attack of the mesomeric anions of the salt on the alkyl halide to give a dialkyl phosphonate ester.[127] Another method that has been used to phosphorylate fosmidomycin analogues is the addition of an alkyl phosphonate to an activated double bond.[107] This involves the addition of a nucleophilic phosphorus such as trialkyl phosphite to an alkene or alkyne that is substituted with an acceptor such as an α,β-unsaturated aldehyde or ketone in order to obtain the dialkyl phosphonic ester (Scheme 2.1 B).

A method that makes use of cesium carbonate (Cs_2CO_3) was recently described by Cohen *et al.*[128] The reaction involves the use of Cs_2CO_3 as a base and tetrabutylammonium iodide (TBAI) as a phase transfer catalyst in the formation of the C-P bond. The high efficiency of the reaction has been attributed to the Cs effect. The Cs ion has a very large ionic radius and low charge density. It also has a low degree of solvation and ion pairing as compared to other alkali salts.[129] In an aprotic solvent such as DMF with high dielectric constant, Cs is “naked” and this property makes it highly reactive. The mild reaction described by Cohen progress at

room temperature, where Cs_2CO_3 together with the phase transfer catalyst are added to the dialkyl phosphite followed by the alkyl halide to give phosphonate esters in good yields.

Scheme 2.2 shows a summary of the methods that have been employed in the introduction of the phosphonate moiety to fosmidomycin analogues as described above.

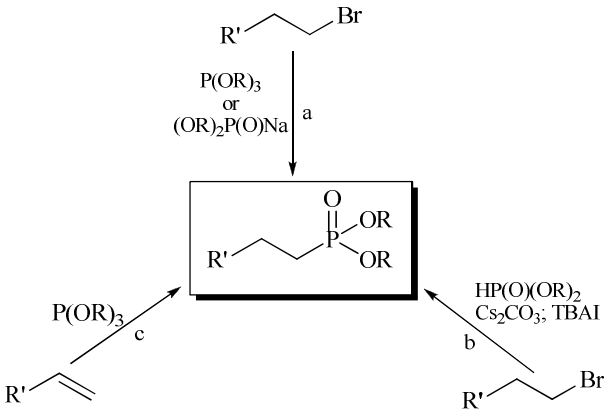

Scheme 2.2. Schematic review of phosphonate introduction in the synthesis of fosmidomycin analogues.
a[20, 101, 109, 118]; b [128]; c[107]

The synthesis of halogenated fosmidomycin analogues as described in this chapter employed two of the methods discussed above, the Arbuzov reaction and the Cs_2CO_3 reaction. This was based on ease of the reactions and the availability of the starting materials.

Introduction of the hydroxylamine group

Introduction of the hydroxylamine group into the fosmidomycin analogues have mostly been through similar approaches but using different sources of hydroxylamine reagents. This includes masked amines such as BocNHOBn,[120, 130] BocNHOBoc,[109] TsNHOBn[20, 111, 131] in a base catalyzed reaction with an alkyl halide (Scheme 2.3). The base deprotonates the amine, allowing it to initiate a nucleophilic attack on the alkyl halide. Other methods of incorporating hydroxylamine have involved the conversion of an aldehyde by treatment with *O*-protected hydroxylamine to yield an oxime which is then reduced with sodium cyanoborohydride.[107, 132, 133] In another approach by Schlüter *et al*,[134] dioxolane was used as

the starting material, which gave the *O*-protected hydroxylamine after acid hydrolysis followed by oxime formation and subsequent reduction by sodium cyanoborohydride in an acidic medium.

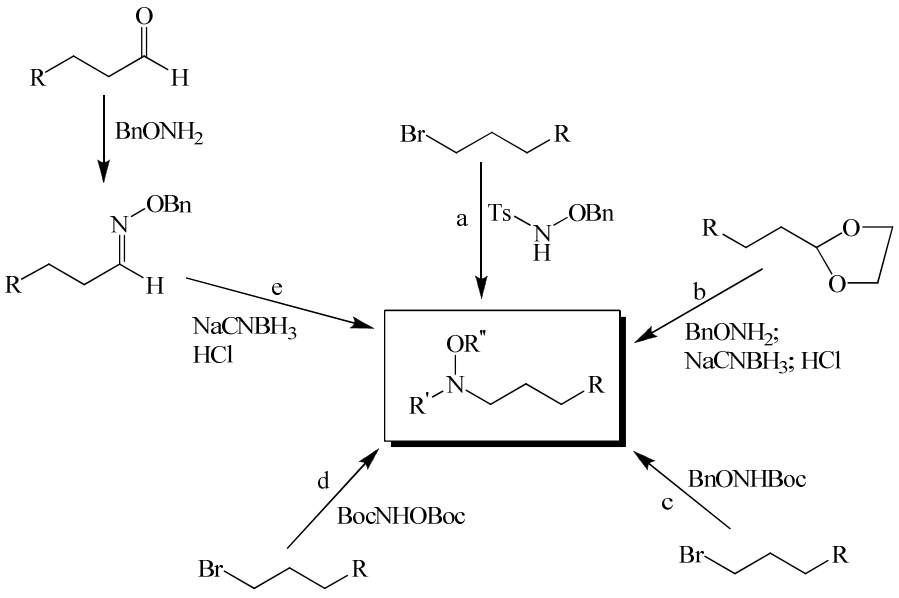

Where R = Phosphonate or phosphate ester

R′ = Boc; Ts; H

R″= Bn; Boc

Scheme 2.3. Schematic review of hydroxylamine introduction to fosmidomycin analogues a[20, 111, 131]; b[134]; c[120, 130]; d[109]; e[107, 132, 133]

The retrohydroxamate functionality is introduced into fosmidomycin analogues by acylation with an appropriate acid chloride. Different halogenated acyl chlorides were used in the synthesis of the halogenated fosmidomycin analogues discussed in this chapter. The reaction generally involves the treatment of the *O*-protected amine with the required acyl chloride to obtain the desired retrohydroxamate compound.

Both the *N*-oxime and the phosphonic acid moieties of fosmidomycin and its analogues are sensitive to harsh reaction conditions and is therefore protected during the course of the synthesis. As such these groups are mostly incorporated in their protected form. The final stage of a series of reactions involving these protected forms of *N*-oximes or phosphonates is

therefore the removal of these protective groups. Typically, the *N*-oxime is protected by a benzyl group and will usually be removed or hydrolyzed by hydrogenation using a suitable catalyst such as Pd/C or $Pd(OH)_2/C$. In some instances a Boc group is used and is easily removed by treatment with TFA.

The phosphonate is also sometimes protected with a benzyl or phenol group. However the most common protective group for the phosphonates of fosmidomycin analogues is the ethyl ester and sometimes the methyl ester. The esters are generally easily hydrolyzed to free phosphonic acid by transesterification with TMSBr (trimethylsilyl bromide) or TMSI (trimethylsilyl iodide) and subsequent hydrolysis with H_2O. In some instances the TMSX are not effective and harsher conditions have to be employed. This could involve refluxing the esters under very acidic conditions which in turn could be incompatible with other sensitive groups in the compound.

2.1.2 **Synthetic objectives**

The initial motivation for this study came from the observed antiplasmodial activity of selected halogenated fosmidomycin analogues or the reactive α-bromoketone intermediates in the process of synthesizing chloroquine-fosmidomycin hybrids (Chapter 3). While many investigations around fosmidomycin have been directed at improving the activity of the drug, most have focussed on increasing the lipophilicity of the compound. These have mainly been achieved through substitution at the α-carbon and by synthesizing phosphonate esters, respectively. Few studies have attempted improving these properties from the hydroxamate end of the compound. In view of the fact that several derivatives with one or more chlorine atoms at the α-position have consistently proved to be more active than their non-halogenated analogues[107, 121] , this study focused on modifications to FR900098 by incorporating halogens at the side chain.

Having established that extending the hydroxamate side chain of fosmidomycin by 5 to 19 carbons significantly decreases the activity of the compound,[115] this project also focused on synthesizing compounds with a side chain of two to four carbons with a terminal chlorine

atom. This is expected to increase the lipophilicity of the compounds and thus increase its absorption.

Therefore, the aim of this part of the study was to synthesize halogenated analogues of FR900098 (**1.45**) and extended chlorinated acyl chain derivatives of FR900098 with potential activity against *P. falciparum*. As such the specific objective of this chapter was to describe the synthesis of halogenated derivatives of FR900098. This research will contribute to determining if the fosmidomycin side chain can be extended beyond the acetyl side chain (FR900098) without decreasing its activity and also if halogens at the side chains will have any effect on the activity of the compounds.

2.2 RESULTS AND DISCUSSION

2.2.1 Synthetic strategy

Ultimately, the phosphonic acids of the halogenated derivatives were required in order to compare their antiplasmodial activity and DXR inhibition activity with the parent drug FR900098. To this end, a retrosynthetic route showing the development of the analogues from 1,3-dibromopropane (**2.6**) to the free phosphonic acids was generated as shown in Scheme 3.4. This was a combination of the approaches used by Kurz and co-workers[120] as well as Reichenberg and co-workers[109] to synthesize ester protected prodrugs of fosmidomycin (**1.46**) and FR900098 (**1.45**). The reaction begins by the introduction of the protected phosphonate group on to 1,3-dibromopropane (**2.6**) by an Arbuzov reaction. This is followed by incorporation of the protected amine to give the fosmidomycin backbone. Partial deprotection of the amine followed by acylation of the backbone with different chloroacyl chlorides should yield the desired extended chlorinated acyl side chain analogues. The final stage involves the deprotection of the hydroxamate and phosphonate groups to release the free phosphonic acids.

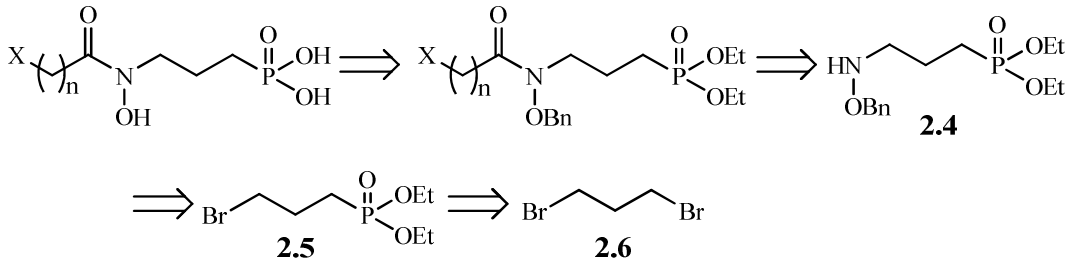

Scheme 2.4. Retrosynthetic route toward halogenated fosmidomycin analogues

2.2.2 **Synthesis of the fosmidomycin backbone (2.4)**

As established previously, it is important to conserve the fosmidomycin backbone structure, which includes the phosphonate moiety, the hydroxamate moiety and the propyl linker between the two functional groups. Since the modifications envisaged in this project were to occur at the side chain, synthesis of the fosmidomycin backbone (**2.4**) was carried out before modifications to the side chain. This has the advantage of being able to synthesize large quantities of **2.4** from which all the other analogues could be derived.

Scheme 2.5 shows the synthesis of the fosmidomycin backbone **(2.4)** which began with the Arbuzov reaction of triethylphosphite ($P(OEt)_3$) with **2.6** to afford the bromophosphonate **2.5** in 54% yield. The hydroxamate component of the analogues was then introduced by reacting **2.5** with *tert*-butyl benzyloxycarbamate(BnONHBoc) in the presence of NaH. Using a method adapted from Gebhardt and coworker,[135] the reaction was initially carried out in dry DMF at room temperature. This however only gave a 25% yield of the desired protected FR900098 backbone **2.7**. As this compound was to serve as the basis for the synthesis of most of the FR900098 analogues intended, optimizing the yield of this reaction was desired. Changing the reaction solvent to freshly distilled THF ensured a 100% yield (Scheme 2.5).

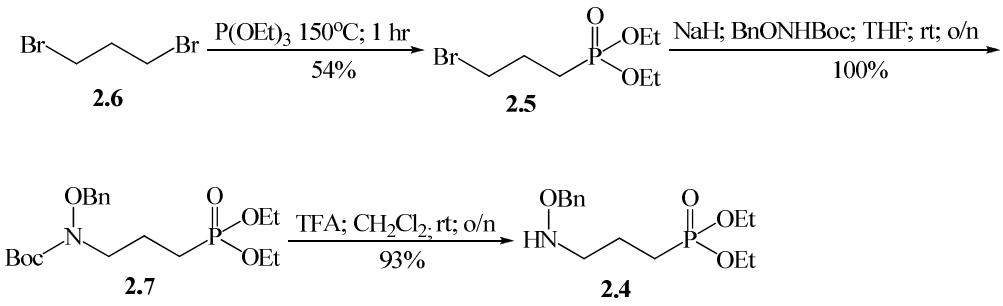

Scheme 2.5. Synthesis of protected hydroxyamino-propylphosphonate backbone (**2.4**) of FR900098 analogues

Selective deprotection of the hydroxamate moiety by the removal of the Boc group was achieved by stirring **2.7** in equivalent volumes of TFA and CH_2Cl_2 at room temperature overnight to yield **2.4** in 93%. This compound thus served as a precursor from which the analogues discussed in this thesis were synthesized.

The ^{1}H and ^{13}C NMR spectra of fosmidomycin analogues in $CDCl_3$ and D_2O are characterized by broad signals and complex splitting patterns. A combination of one- and two-dimensional NMR techniques is therefore required to confirm and assign the spectra of all synthesized compounds. For this reason, it might be useful to briefly discuss the spectroscopic characteristics of compound **2.4**, which is the simplest analogue in this series. This would then facilitate discussion of some of the more complex analogues.

The ^{1}H NMR spectrum of **2.4** (Figure 2.1) in combination with its ^{1}H-^{1}H COSY NMR spectrum (Figure 2.2) allowed the identification of three isolated spin systems. The three carbon fosmidomycin backbone is represented by ^{1}H NMR signals at δ 2.92 (2H, t, J = 6.0 Hz, H-3) and two overlapping methylenes at δ1.72 (4H, m, H-1 and H2). Signals at δ 4.0 (4H, m, H-1') and δ 1.27 (6H, t, J = 7.0 Hz, H-2') can be assigned to the ethyl protecting group on the phosphonate ester while the benzyloxy-protecting group is represented by signals at δ 7.26 (5H, m, Ar) and 4.64 (2H, s, H-1").

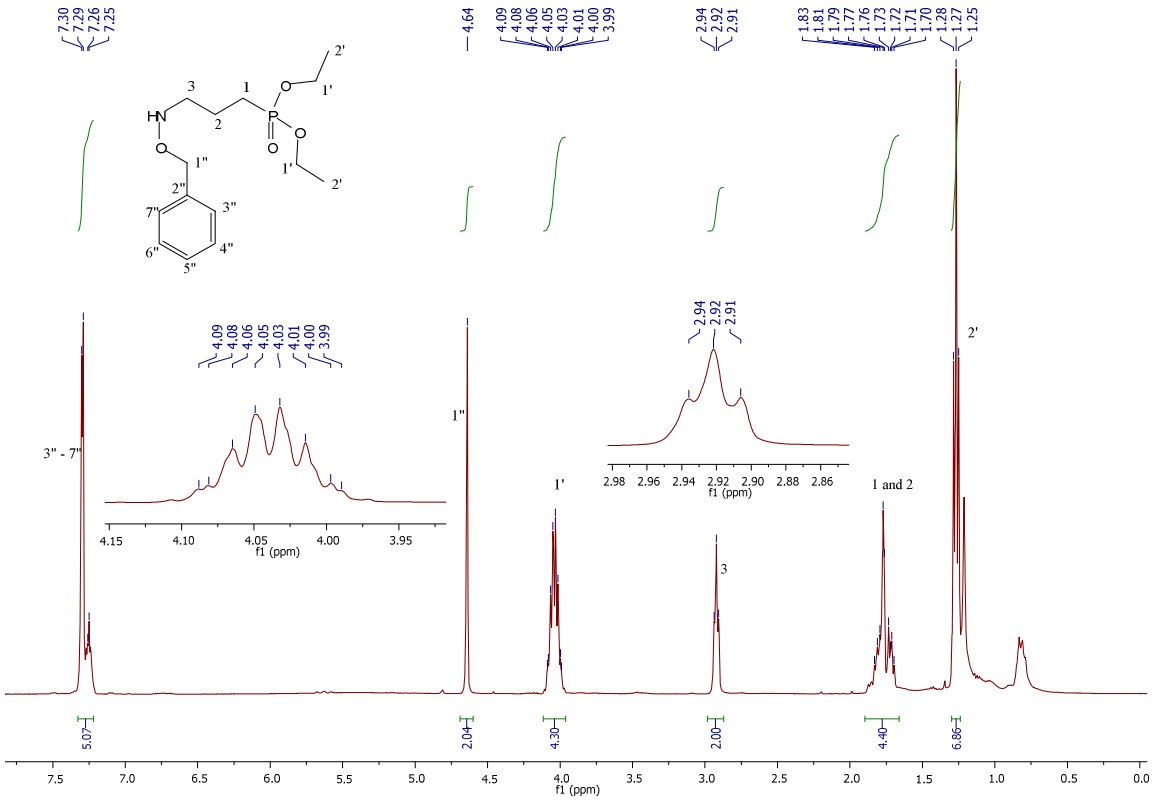

Figure 2.1 ^{1}H NMR spectrum of **2.4** ($CDCl_3$, 400 MHz)

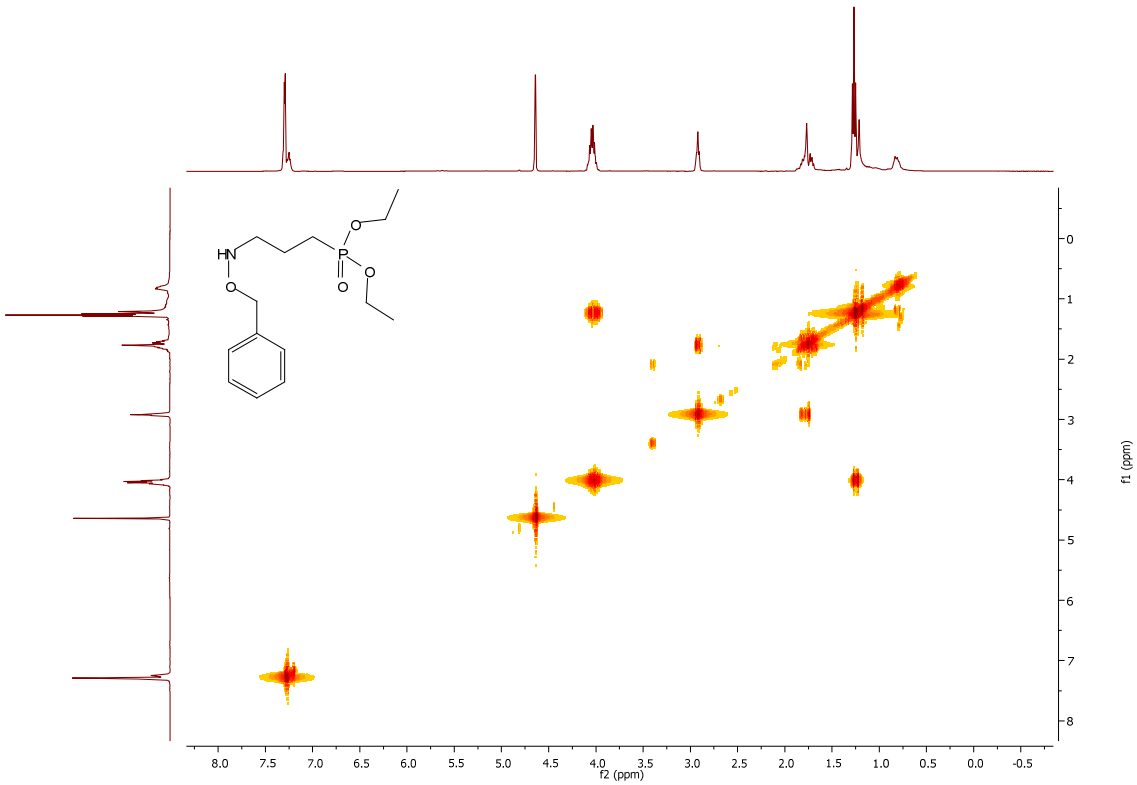

Figure 2.2 ^{1}H – ^{1}H COSY NMR spectrum of **2.4** ($CDCl_3$, 400 MHz)

The assignment of the carbons was also done by analysing both one and two dimensional NMR spectra (HSQC and HMBC). The carbons (Figure 2.3) of the fosmidomycin backbone appear at δ 52.0 (d, $^{3}J_{C,P}$ = 16.6 Hz, C-3), 23.1 (d, $^{1}J_{C,P}$ = 142.1 Hz, C-1) and 20.4 (d, $^{2}J_{C,P}$ = 4.9 Hz, C-2) while the ethyl protecting group exhibit carbon signals at δ 61.5 (d, $^{2}J_{C,P}$ = 6.5 Hz, C-1') and 16.4 (d, $^{3}J_{C,P}$ = 6.0 Hz, C-2'). The benzyloxy-protecting group shows signals at δ 76.3 (C-1"), 137.7 (C-2"), 128.4 (C-4" and C-6"), 128.3 (C-3" and C-7") and 127.8 (C-5"). The ^{13}C NMR spectra described throughout this study were proton decoupled but the effect of phosphorus coupling could be observed. Coupling to phosphorus could be observed for one to three bonds between the phosphorus and the C- nuclei but any coupling greater than three bonds was not observed. The ^{13}C NMR spectrum of **2.4** (Figure 2.3) showed doublets of the methylene and methyl carbons of the ethyl esters δ 61.5 (d, C-2', $^{2}J_{C\text{-}P}$ = 6.5 Hz) and 16.4 (d, C-1', $^{3}J_{C\text{-}P}$ = 6.0 Hz) respectively. These chemical shifts and coupling constants are typical of diethyl alkyl phosphonate esters.[118] Another observation typical of the diethyl alkyl phosphonate is the large coupling constant of one bond coupling of carbon to phosphorus ($^{1}J_{C\text{-}P}$), which was 142.1 Hz for the shift at δ 23.1 (C-1) of **2.4**. $^{2}J_{C\text{-}P}$ and $^{3}J_{C\text{-}P}$ coupling are significantly smaller than $^{1}J_{C\text{-}P}$ coupling in these types of compounds. This was observed for compound **2.4** which had a $^{2}J_{C\text{-}P}$constant of 4.9 Hz for the chemical shift at δ 20.5 (d; C-2) and a $^{3}J_{C\text{-}P}$ constant of 16.6 Hz for the doublet at δ 52.0 (d; C-3) as compared to $^{1}J_{C\text{-}P}$ of 142.1 Hz for C-1 at δ 23.1. $^{2}J_{C\text{-}P}$ is influenced by the hybridized state of the C-2 and would increase from a sp^3 carbon to a sp^2 carbon. $^{3}J_{C\text{-}P}$ of phosphorus to C-3 coupling follows the Karplus relationship which is dependent on the dihedral angle between the affected nuclei.[136, 137] Since the backbone **2.4** is mostly conserved in fosmidomycin analogues and the halogenated FR900098 analogues synthesized in the present study, NMR properties of **2.4** was expected and found to carry through in ^{13}C NMR spectra of the compounds.

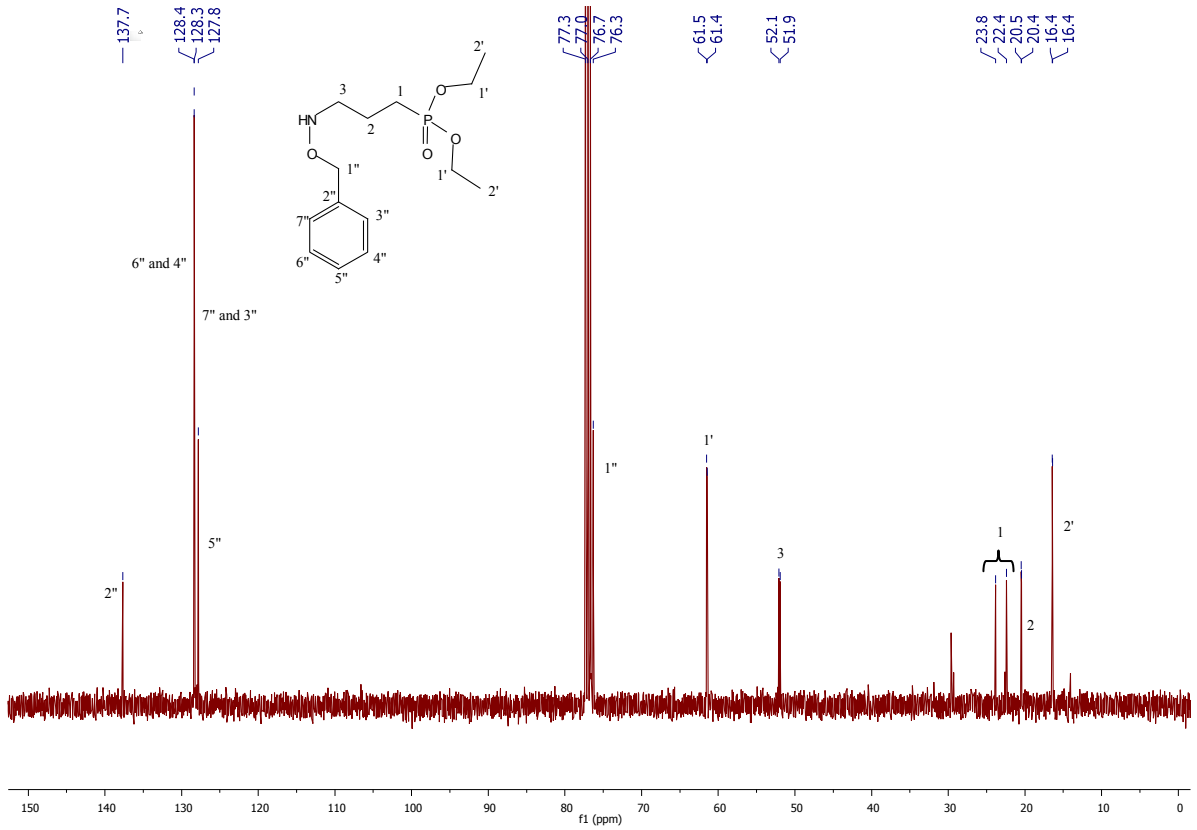

Figure 2.3. ^{13}C NMR spectrum of **2.4** ($CDCl_3$, 100 MHz)

2.2.3 **Synthesis of fosmidomycin analogues with chlorinated acyl side chains**

Following the successful synthesis of the partially deprotected hydroxyamino propylphosphonate (**2.4**) we now turned our attention to the preparation of various chlorinated fosmidomycin/FR900098 analogues with two, three and four carbon side chains, **2.8**, **2.9** and **2.11** respectively (Table 2.2). The compounds were synthesized to investigate the effect of increased lipophilicity by short side chains and the presence of the chlorine atom on antiplasmodial activity. The non-halogenated analogues **2.10** and **2.12** were also synthesized in order to compare and determine if the presence of the chlorine atom, the extended side chain or a combination of both have any effect on the antiplasmodial activity of the compounds.

Table 2.2. Synthesis of chlorinated acetyl, propionyl and butyryl analogues of fosmidomycin

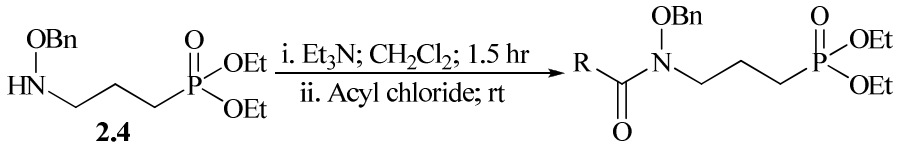

Acyl chloride	R	Time (hr)	Product	Yield (%)
Chloroacetyl chloride	$-CH_2Cl$	2.5	**2.8**	60
3-chloropropionyl chloride	$-CH_2CH_2Cl$	2.5	**2.9**	33
	$-CH=CH_2$		**2.10**	11
4-Chlorobutyryl chloride	$CH_2CH_2CH_2Cl$	3.5	**2.11**	53
Acetyl Chloride	$-CH_3$	2.5	**2.12**	89

Synthesis of the chlorinated analogues of fosmidomycin commenced with acylation of **2.4** with an appropriate acyl chloride using triethylamine as base to give the acetyl, chloroacetyl, chloropropionyl and chlorobutyryl derivatives (Table 2.2; **2.8 – 2.12**). Not, surprisingly, the reaction of with chloropropionyl chloride also gave the derivative **2.10**. This occurred *via* base-catalyzed elimination of HCl due to the increased acidity of the α-protons (Scheme 2.6). This was an advantage as the derivative was also required for comparison of the effect of the chlorine atom on the activity of the compounds on the DXR enzyme and plasmodium growth. Loss of the terminal chlorine was not observed with the chloroacetyl and chlorobutyryl derivatives.

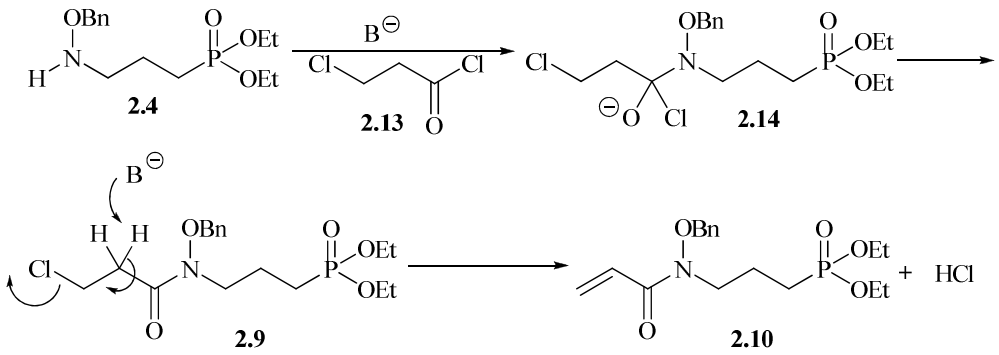

Scheme 2.6. Proposed mechanism of chloride elimination to form **2.10**

2.2.4 **Structural assignment of chlorinated acyl fosmidomycin analogues**

As expected the NMR spectra of the precursor **2.4** and analogues **2.8 – 2.12** were very similar to each other. The major difference being the number of signals observed for the hydroxamic acid side chains. The structures of the analogues were confirmed by extensive one and two dimensional NMR experiments. Here we will focus our attention on compound **2.11** and will then highlight key spectroscopic features of the other synthesized compounds.

HRESI-MS provided a molecular ion peak at m/z 406.1544 which is consistent with a molecular formula of $C_{18}H_{29}ClNO_5P$ $[M + H]^+$ for compound **2.11**. The ^1H NMR spectrum of **2.11** (Figure 2.4) showed a number of complex, overlapping signals. Two key spin systems were identified from the ^1H NMR and ^1H-^1H COSY (Figure 2.5) spectra of **2.11**, and were confirmed by analysis of ^{13}C (Figure 2.6), HSQC and HMBC NMR data. These consisted of the fosmidomycin propyl backbone at δ 1.69 (2H, m, H-1), 1.92 (2H, m, H-2) and 3.68 (2H; t; 6.5 Hz; H-3) and the chloroacyl side chain at 2.55 (2H; t; 6.8 Hz; H-5), 2.02 (2H; m; H-6) and 3.55 (2H; t; 5.9 Hz; H-7). In addition, ^1H NMR signals corresponding to the phosphonate ester protecting group were observed at δ1.27 (6H; t; 6.9 Hz; H-2') and 4.04 (4H; m; H-1') while signals at δ7.35 (5H; s; H-2" – H-7") were assigned to the benzyl protecting group of the hydroxylamine.

The ^{13}C NMR spectrum showed the characteristic phosphorus-carbon splitting as observed for the fosmidomycin backbone **2.4**. The ethyl ester doublets were observed at δ 61.5 (d, 6.0 Hz, C-1') and 16.3 (d, 6.0Hz, C-2'). The propyl carbons were observed at δ 45.8 (s, C-3), 23.0 (d, 142.0 Hz, C-1) and 20.2 (d, 5.0 Hz, C-2) while the aromatic carbons of the benzyl protecting group resonated between 134.1 – 128.7 ppm. The deshielded signal at 173.6 was assigned to the carbonyl carbon C-4 and the chemical shifts at 45.5 (s, C-7), 29.2 (s, C-5) and 27.1 (s, C-6) accounted for the remaining carbons of the butyryl side chain of compound **2.11**.

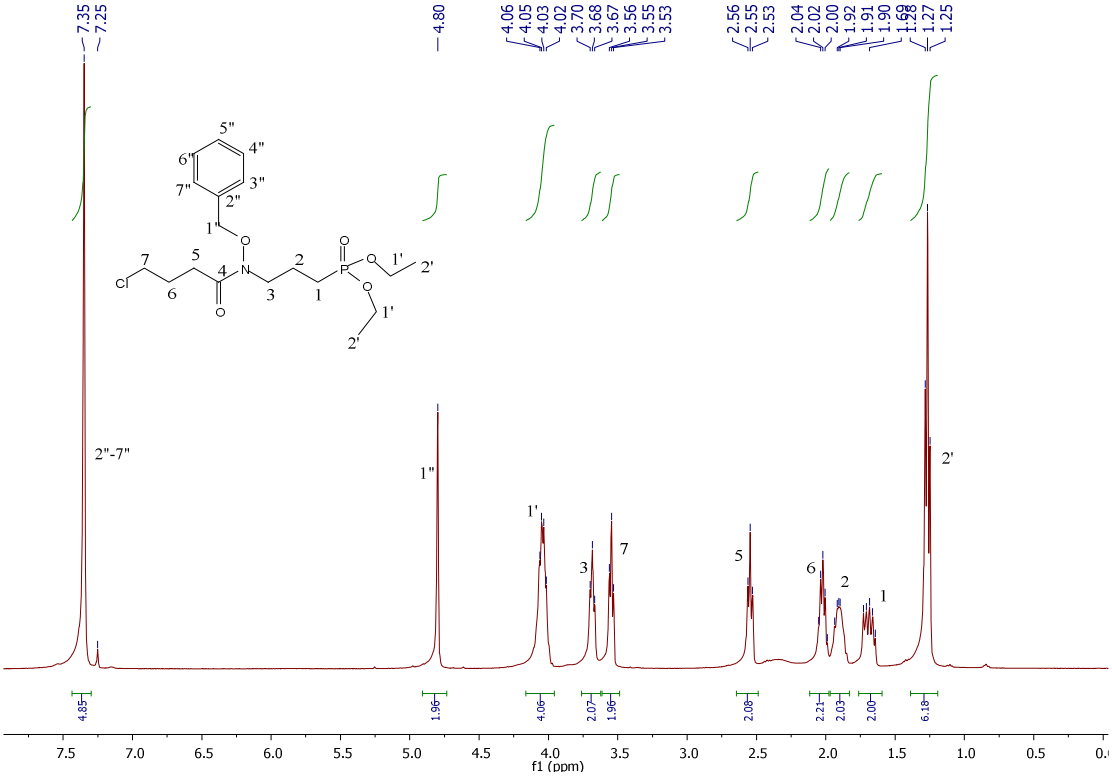

Figure 2.4. ^{1}H NMR spectrum of **2.11** ($CDCl_3$, 400 MHz)

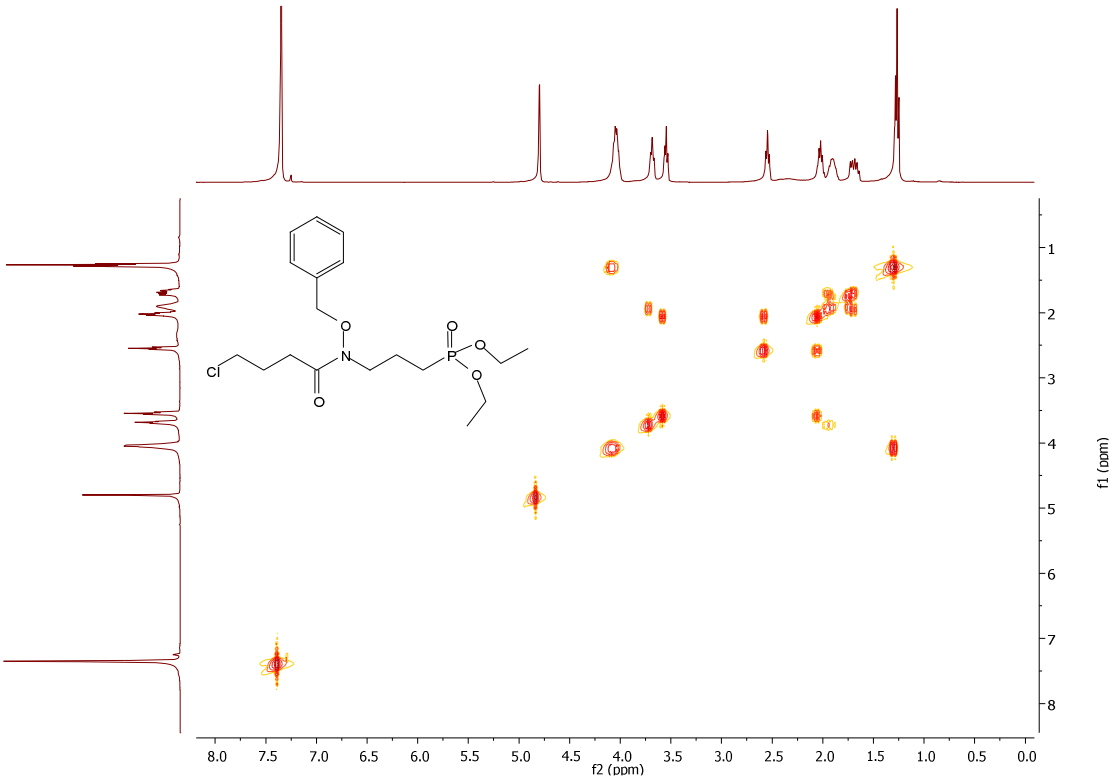

Figure 2.5. ^{1}H – ^{1}H COSY NMR spectrum of **2.11** ($CDCl_3$, 400 MHz)

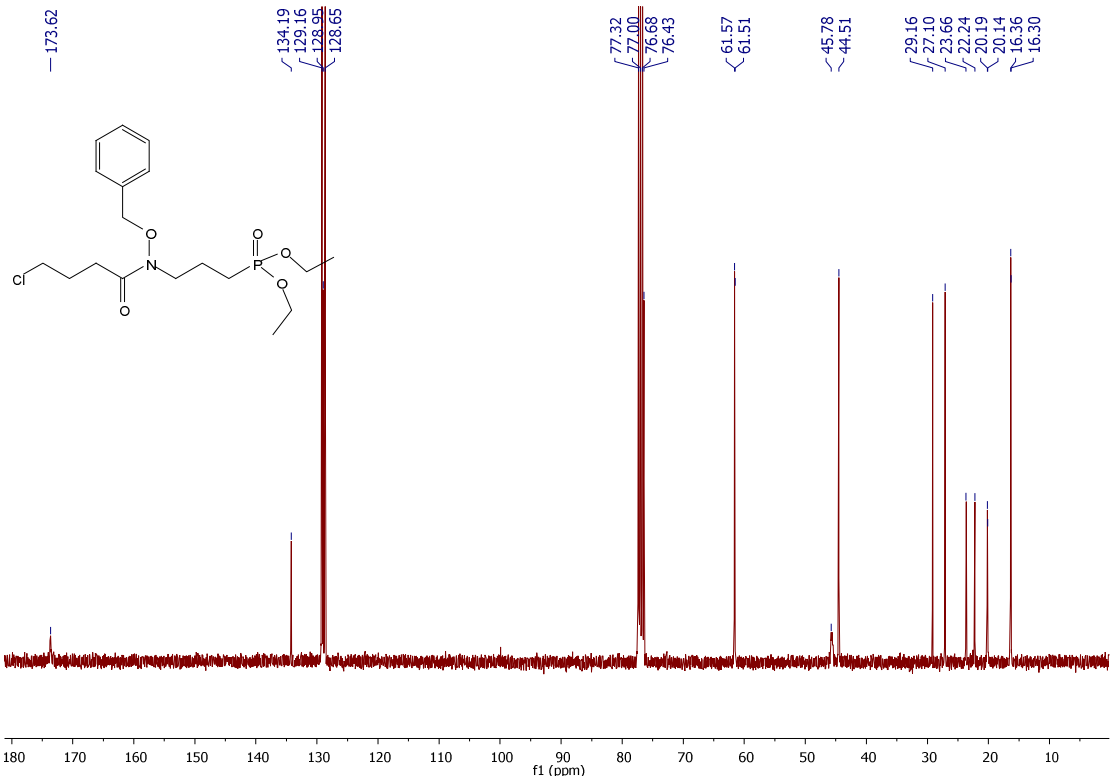

Figure 2.6. ^{13}C NMR spectrum of **2.11** ($CDCl_3$, 100 MHz)

All other spectroscopic data confirmed the structure of **2.11** as diethyl 3-(*N*-(benzyloxy)-4-chlorobutanamido)propylphosphonate.

The molecular formula $C_{16}H_{25}ClNO_5P$ $[M + H]^+$was deduced from the ESI-MS analysis of chloroacetyl analogue **2.8** which gave the molecular ion at m/z 378.1226. It showed very similar 1D NMR spectra to that of the chlorobutyryl analogue **2.11**. Where compound **2.11** showed three methylene signals, compound **2.8** showed only one chloromethylene proton shift at δ 4.10 (s, H-5) which showed an HSQC correlation to the carbon signal at 40.99 (s, C-5). The proton also showed an HMBC correlation to the carbonyl carbon at δ 168.0 (s, C-4). This data together with all other spectroscopic data obtained for **2.8** established it as diethyl 3-(*N*-(benzyloxy)-2-chloroacetamido)propylphosphonate.

The chloropropyl analogue **2.9** also displayed similar NMR spectra to **2.11**. The two methylene protons of the acyl side chain were observed at δ 2.83 (t, 6.6 Hz, H-5) and 3.74 (s, H-6) which overlaps with H-3 triplet also at 3.74 ppm. The corresponding carbons were observed at δ 35.4 (s, C-5) and 39.3 (s, C-6), respectively. The ESI-MS of compound **2.9**

gave molecular ion peak at *m/z* 392.1394 which correlates with the molecular formula $C_{17}H_{27}ClNO_5P$ $[M + H]^+$. All other spectroscopic data further confirm **2.9** as diethyl 3-(*N*-(benzyloxy)-3-chloropropanamido)propylphosphonate.

Compound **2.12** is the protected analogue of FR900098. It also exhibits similar spectroscopic backbone data to **2.8**, **2.9** and **2.11**. However, where all the other analogues had methylene groups at the acyl side chain, **2.12** has only one isolated methyl group which is observed at δ 2.04 (s, H-5) in the ^{1}H NMR spectrum and δ 20.3 (s, C-5) in the ^{13}C NMR spectrum. The NMR data corresponds with the literature data reported for the compound diethyl 3-(*N*-(benzyloxy)acetamido)propylphosphonate.[108]

As was observed with the chlorinated analogues, the ^{1}H NMR spectrum of the acrylate-fosmidomycin derivative **2.10** (Figure 2.7) showed the presence of fosmidomycin backbone methylene protons at δ 1.75 (H-1), 1.95 (H-2) and 3.76 (H-3). The methyl triplet and methylene multiplets of the ethyl ester were also observed at δ 1.28 and 4.06 respectively. The interesting part of the ^{1}H NMR spectrum showing differences to the chlorinated analogues were the two doublets observed at δ 5.71 (1H; J = 10.4 Hz; H-6_A) and 6.39 (1H; J = 17.1 Hz; H-6_B) and a double doublet observed at δ 6.71 (1H; J = 10.4, 17.1 Hz). The fact that both doublets showed HSQC correlations to the same carbon at δ 129.3 (C-6) and are both coupled to the methine double doublet showed that each proton of the methylene groups are enantiotropic. This is characteristic of a monosubstituted alkene. The ESI-MS of compound **2.10** showed its molecular ion at m/z 356.1621 which is consistent with the molecular formula $C_{17}H_{26}NO_5P$ $[M + H]^+$ and along with UV and IR confirmed compound **2.10** as diethyl 3-(N-(benzyloxy)acrylamido)propylphosphonate.

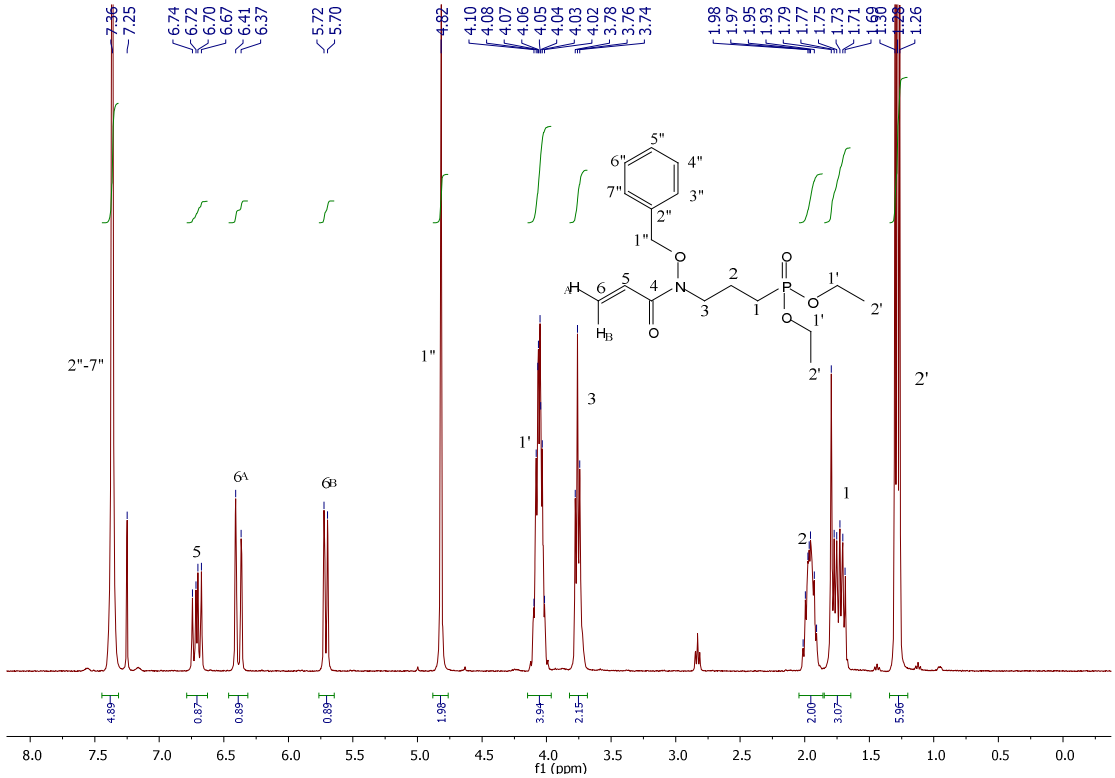

Figure 2.7. ^{1}H NMR spectrum of **2.10**

2.2.5 **Antiplasmodial activity of the extended chlorinated acyl side chain analogues**

The main aim of this part of the study was to obtain potential antiplasmodial compounds from the lead compounds fosmidomycin (**1.46**) and FR900098 (**1.45**). As a result the synthetic progress of the research was guided by antiplasmodial assays. Given that a series of extended chlorinated acyl side chain analogues of FR900098 had been synthesized, compounds **2.8 – 2.12** were tested for antiplasmodial activity to guide the project forward.

This initial *in vitro* antiplasmodial test of the analogues was conducted on a chloroquine sensitive D10 strain of *P. falciparum.* The test was carried out on continuous *in vitro* cultures of asexual erythrocyte stages of the parasite which were maintained using a modified method of Trager and Jensen.[138] Table 2.3 shows the results obtained from the antiplasmodial assay.

Table 2.3. Antiplasmodial activity of compounds **2.8 – 2.12**

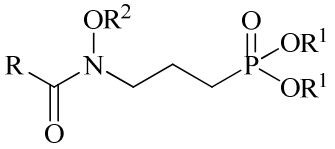

Compound	R	R^1	R^2	D10:IC_{50} (µM)
FR900098 (1.45)	$-CH_3$	H	H	43.4
2.8	$-CH_2Cl$	Et	Bn	7.5
2.9	$-CH_2CH_2Cl$	Et	Bn	> 100
2.10	$-CH=CH_2$	Et	Bn	47.5*
2.11	$-CH_2CH_2CH_2Cl$	Et	Bn	> 100
2.12	$-CH_3$	Et	Bn	> 100
chloroquine				0.07

*Estimated from percentage parasite survival

The antiplasmodial assay revealed the chloroacetyl analogue **2.8** to be the most active of the synthesized series (IC_{50} = 7.5 µM), even more active than FR900098 (IC_{50} =43.4 µM) used as the positive control. To a lesser extent **2.10** also showed some activity (IC_{50} = 47.5 µM) while **2.9** and **2.11** – **2.12** were considered inactive (IC_{50} > 100 µM). From these results it was clear that the presence of a chlorine atom was responsible for the activity of **2.8** since the acetyl analogue, **2.12**, was not active. This gave rise to questions regarding the binding site of these protected analogues of FR900098. The possibility exists that the medium in which the plasmodium parasite was cultured, which included human blood, might contain esterases which could hydrolyse the compounds prior to uptake by the parasite. This is not expected to show superior activity over FR900098 (**1.45**) since it would still be difficult for the resulting phosphonic acid to be absorbed through the membranes of the parasite. Should the protected compounds however be absorbed into the parasite, it was expected that non-specific esterases would hydrolyse the compounds to release the free phosphonic acid to bind to the target enzyme DXR. This means that **2.12** should be hydrolyzed to FR900098 (**1.45**) and should thus be active against the parasite. As this was not the case the next question arose as to whether the compounds got to the site of action without being deprotected and the chlorine atom is solely responsible for the activity observed for **2.8**. Alternatively, **2.8** might have a different target other than DXR. In order to answer these questions, synthesis and testing of unprotected halogenated FR900098 was thus required.

The loss of activity observed with **2.9** as compared to **2.8** and the inactivity of **2.11** shows that increasing the length of the acyl side chain decreases the antiplasmodial activity of the compounds. Due to the lack of the terminal chlorine atom in **2.10**, its antiplasmodial activity was expected to be even less than that of **2.9** but was not the case. This is attributed to the terminal double bond of the compound which could be attacked by a nucleophile or which could alkylate DXR or another target in the plasmodium parasite.

2.2.6 **Synthesis of bromo- and iodo analogues of FR900098**

The promising antiplasmodial activity demonstrated by **2.8** established that the presence of chlorine group on the acyl side chain was important in improving antiplasmodial activity. This guided the synthesis of the FR900098 analogues into the next stage which was to investigate the effect of other halogens other than chlorine on antiplasmodial activity. To this end, compounds **2.15 – 2.17** were synthesized (Figure 2.8).

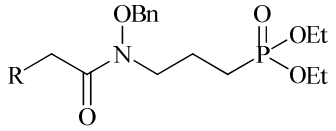

2.15 R = I
2.16 R = CH_2I
2.17 R = Br

Figure 2.8. Target bromo- and iodo-analogues of FR900098

The brominated analogue **2.17** was synthesized using the same procedure used to synthesize the chlorinated analogues and acylating hydroxaminopropyl phosphonate (**2.4**) with bromoacetyl chloride (Scheme 2.7 A). Column chromatography of the crude product gave **2.17** in 87% yield. Due to unavailability of iodoacetyl chloride the same procedure could not be used to synthesize the iodide analogue. In a Finkelstein reaction, **2.8** was stirred with NaI at room temperature overnight to obtain the iodinated **2.15** in 79% yield without requiring further purification (Scheme 2.7 B). Finkelstein reaction of **2.9** to **2.16** required more aggressive conditions. Stirring of **2.9** with NaI in acetone for 24 hours gave no product. However, heating the reaction mixture at reflux for four hours followed by stirring at room temperature for three days gave **2.16** in 54% yield after purification (Scheme 2.7 C).

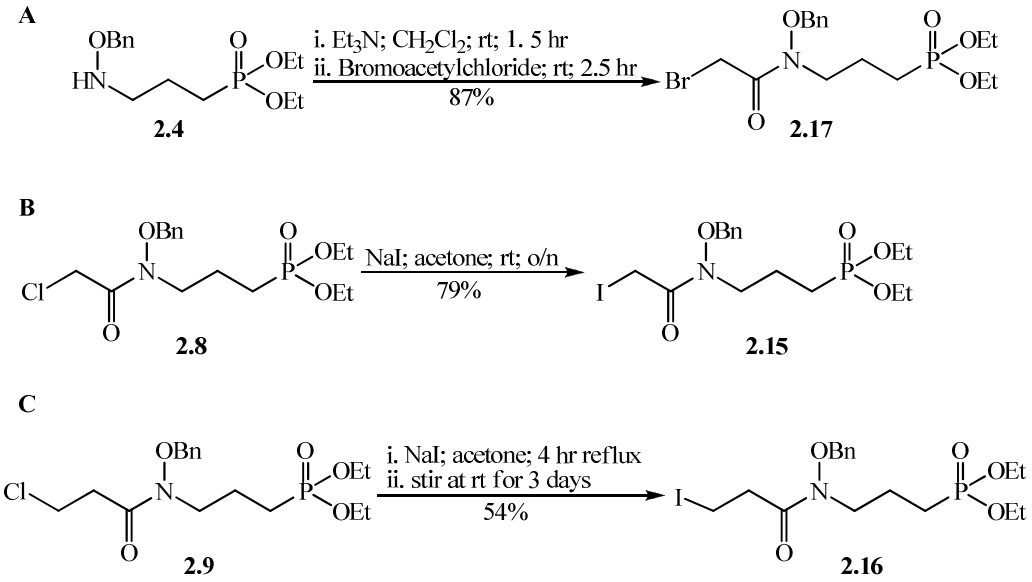

Scheme 2.7. Synthesis of bromo- and iodo-FR900098 analogues

The NMR spectra of **2.15 – 2.17** shared the same characteristics as described for the chlorinated fosmidomycin analogues **2.8 – 2.12**. Compounds **2.15** and **2.17** gave NMR spectra which were similar to that of **2.8**, the major difference observed being the upfield shift of the halomethylene group at the side chain for each compound. Where the ^{1}H NMR spectrum of **2.8** showed the chlorinated methylene protons (H-5) at δ 4.10, the iodinated (**2.16**) and brominated (**2.17**) derivatives were less deshielded at δ 3.73 and 3.87, respectively (Table 2.4). The ^{13}C NMR spectra particularly highlighted the difference in the chemical shift of the iodomethylene carbon of **2.15** at a characteristic δ -5.11 (C-5) as compared to 40.99 and 41.02 for **2.8** and **2.17**, respectively (Table 2.4).

Table 2.4. Comparison of ^{1}H (400MHz) and ^{13}C NMR (100 MHz) dataof compounds **2.8**, **2.15** and **2.17** in $CDCl_3$

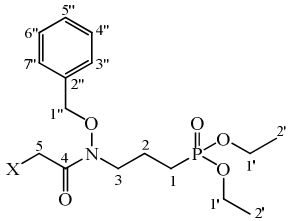

	2.8 (X = Cl)		**2.15 (X = I)**		**2.17 (X = Br)**	
Position	**δ ^{1}H (#; mult; J_{HZ})**	**δ ^{13}C (#; mult; J_{C-P})**	**δ ^{1}H (#; mult; J_{HZ})**	**δ ^{13}C (#; mult; J_{C-P})**	**δ ^{1}H (#; mult; J_{HZ})**	**δ ^{13}C (#; mult; J_{C-P})**
2’	1.29 (6H; t; 7.1)	16.4 (2 x CH_3; 5.9)	1.28 (6H; t; 7.0)	16.4 (2 x CH_3; d; 6.0)	1.29 (6H; t; 7.0)	16.4 (2 x CH_3; d; 6.0)
1’	4.07 (4H; m) *	61.7 (2 x CH_2; 6.5)	4.06 (4H; m)	61.6 (2 x CH_2; d; 7.0)	4.07 (4H; m)	61.6 (2 x CH_2; d; 7.0)
1	1.72 (2H; m)	22.9 (CH_2; d; 142.8)	1.75 (2H; m)	22.8 (CH_2; d; 142)	1.73 (2H; m)	22.8 (CH_2; d; 142)
2	1.95 (2H; m)	20.1 (CH_2; d; 4.7)	1.94 (2H; m)	19.7 (CH_2; d; 4.0)	1.94 (2H; m)	20.0 (CH_2; d; 5.0)
3	3.75 (2H; t; 6.9)	46.1 (CH_2; s)	3.72 (2H; t; 6.7) #	45.8 (CH_2; s)	3.75 (2H; t; 6.0)	45.9 (CH_2; s)
4	-	168.0 (C=O; s)	-	169.8 (C=O; s)	-	168.1 (C=O; br s)
5	4.10 (2H; s) *	40.99 (CH_2; s)	3.73 (2H; s) #	-5.1 (CH_2; s)	3.87 (2H; s)	41.02 (CH_2; s)
1”	4.86 (2H; s)	76.7 (CH_2; s)	4.92 (2H; s)	76.3 (CH_2; s)	4.90 (2H; s)	76.6 (CH_2;s)
2”-7” (Ar-H)	7.38 (5H; s)		7.38 (5H; s)		7.38 (5H, s)	
2”		133.7 (C; s),		133.9 (C; s)		133.7 (C; s)
4” and 6”		129.3 (2 x CH)*		129.2 (2 x CH; s)		129.3(2 x CH; s)
5”		129.3 (CH; s)*		129.2 (CH; s)		129.3(CH; s)
3” and 7”		128.9 (2 x CH; s)		128.8 (2 x CH; s)		128.8 (2 x CH; s)

*/# overlapping chemical shifts

2.2.7 **Debenzylation of halogenated FR900098 analogues**

Based on the initial antiplasmodial results of compounds **2.8 – 2.12** (Table 2.3), it was necessary to synthesize the deprotected derivatives of the halogenated analogues. This would help to determine the effect of the protective groups on the absorption of the compounds and hence their antiplasmodial effect. The removal of benzyl and ester protective groups was carried out in stages such that the benzyl groups were hydrolysed first to release the free hydroxamic acid esters. These compounds were tested for antiplasmodial activity to determine the effect of the benzyl group since the esters have been shown to promote absorption of this group of compounds.

Debenzylation of compounds is often successfully achieved by hydrogenolysis. This reaction was initially explored for the synthesis of the halogenated hydroxamic acids **2.18** – **2.24** (Figure 2.9).

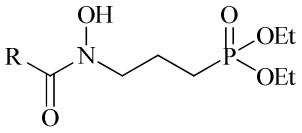

2.18 R = CH_3
2.19 R = CH_2Cl
2.20 R = CH_2Br
2.21 R = CH_2I
2.22 R = CH_2CH_2Cl
2.23 R = CH_2CH_3
2.24 R = $CH_2CH_2CH_2Cl$

Figure 2.9. Targeted debenzylated halogenated-FR900098 analogues

Compound **2.18** was obtained by hydrogenation of **2.12** in methanol, using Pd/C as a catalyst (Scheme 2.8 A). The same procedure when carried out on **2.8** however resulted in debenzylation as well as dechlorination of the compound to **2.18** (Scheme 2.8 B). Changing Pd/C to Pearlman's catalyst ($Pd(OH)_2/C$) rendered the reaction more benign and was used to successfully debenzylate **2.8** – **2.11** to give **2.19** and **2.22 – 2.24** respectively without loss of the chloride atom. Attempts to debenzylate **2.15** and **2.17** with Pearlman's catalyst resulted in the loss of iodine and bromine atoms respectively from the starting compounds. While there was the possibility of debenzylating the halogenated analogues under harsh conditions, for example acid hydrolysis, it was thought that the compounds would be more liable to degradation. For this reason Finkelstein reaction was adopted to substitute chlorine for the

desired halogen after debenzylation of **2.19**. Stirring **2.19** with NaI in acetone for two days at room temperature gave 100% conversion to **2.21** (Scheme 2.8 C). Finkelstein reaction with LiBr proved more difficult as only 50% conversion was achieved after three days of stirring at room temperature. LiBr salt, **2.19** and the brominated product **2.20** are soluble in aqueous solvents, which made separation of the product difficult. The progress of the reaction was monitored with TLC and ^{1}H NMR. When no further progress was observed after three days, the reaction was halted and worked up by concentrating it under reduced pressure, redissolving it in EtOAc and washing with brine. The crude product obtained was again treated with fresh LiBr and stirred for three days. The reaction with work up was repeated three times at the end of which most of the **2.19** had been converted to **2.20**.

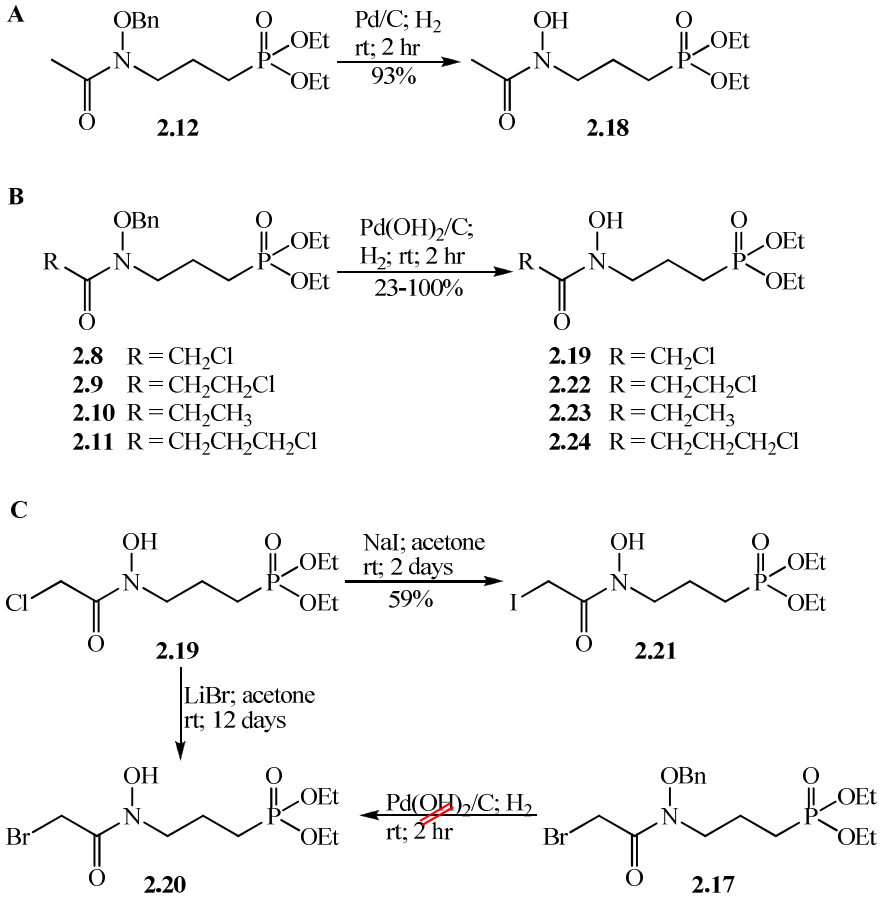

Scheme 2.8. Debenzylation of halogenated FR900098 analogues

2.2.8 Antiplasmodial activity of protected halogenated acetyl analogues and debenzylated analogues of FR900098

The antiplasmodial activity of the deprotected halogenated fosmidomycin analogues was carried out on the CQR Gambian FCR-3 Strain of *P. falciparum*.[I] The culture of plasmodium was maintained by the method described by Trager and Jenson[138] and modified by Van Zyl and Viljoen.[139] Antiplasmodial activity was assessed using the [^{3}H]-hypoxanthine method against one cycle of plasmodial growth (48 hours). The tests were conducted in triplicate and the IC_{50} of the compounds were calculated based on the *in vitro* uptake of [^{3}H]-hypoxanthine. Table 2.5 shows the antiplasmodial activity of the debenzylated analogues of FR900098 in comparison with bis(pivaloyloxymethyl) ester prodrugs of fosmidomycin (**2.25**) and FR900098 (**2.26**).

[I]Due to an outbreak of a significant contamination of cultures the antiplasmodial assays could not be done in the same lab where CQS *P. falciparum* strain was initially used.

Table 2.5. Antiplasmodial activity of protected and partially protected halogenated FR900098 analogues

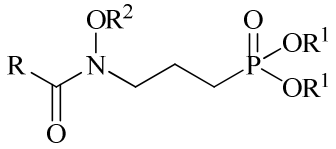

	R	R^1	R^2	FCR-3: IC_{50} (µM)	SD (µM)	D10:IC_{50} (µM)
FR900098 (1.45)	$-CH_3$	H	H	41.67	7.24	> 43.4
2.8	$-CH_2Cl$	Et	Bn	9.06	0.38	7.5
2.12	$-CH_3$	Et	Bn	>100	29.84	>100
2.15	$-CH_2I$	Et	Bn	8.08	0.91	-
2.16	$-CH_2CH_2I$	Et	Bn	> 100	13.32	-
2.17	$-CH_2Br$	Et	Bn	11.11	2.43	-
2.18	$-CH_3$	Et	H	> 100	20.58	
2.19	$-CH_2Cl$	Et	H	18.06	4.04	> 100
2.20	$-CH_2Br$	Et	H	9.44	2.00	-
2.21	$-CH_2I$	Et	H	5.54	0.72	-
2.22	$-CH_2CH_2Cl$	Et	H	> 100	7.78	-
2.23	$-CH_2CH_3$	Et	H	> 100	27.76	-
2.24	$-CH_2CH_2CH_2Cl$	Et	H	> 100	9.21	-
2.25[134]	-H	$C(CH_3)_3$-C(O)-O-CH_2	H	2.1[#]	-	-
2.26[134]	$-CH_3$	$C(CH_3)_3$-C(O)-O-CH_2	H	0.4[#]	-	-
Chloroquine (1.10)				0.07		

[#] Tested on *P. falciparum* 3D7 strain

For comparison between CQS D10 strain used earlier in the study and the CQR FCR-3 strain, compound **2.8** was again tested on FCR-3. The different strains of *P. falciparum* responded to the halogenated FR900098 analogue equally as there was no major difference in the activity of **2.8** on CQS D10 with IC_{50} = 7.5 µM and CQR FCR-3 with IC_{50} = 9.06 µM (Table 2.5). As fosmidomycin and its analogues have a different target to CQ this result was not surprising.

From the initial antiplasmodial activity of the protected chlorinated FR900098 analogue **2.8** compared with the unchlorinated **2.12** it was concluded that introduction of chlorine to the compound improved its activity. This trend was also observed with the debenzylated

FR900098 analogue **2.18** which showed no activity on FCR-3 (IC_{50} > 100 µM) while analogues **2.19 – 2.21** showed good activity with IC_{50} values of 18.06, 9.44 and 5.54 µM respectively. The benzyl-protected and unprotected acetyl halogenated FR900098 analogues **2.8**, **2.15**, **2.17** and **2.19 – 2.21** were all more active against the parasite than FR900098 (**1.45**), indicating that the increased lipophilicity helps improve the activity of the compounds possibly by improving their absorption into the plasmodium. An alternative explanation may be that the haloacetyl analogues react non-selectively with various biological targets and may not affect DXR at all. This can only be confirmed by assessing the cytotoxicity of these compounds and evaluating their activity against DXR.

The halogenated analogues with propyl and butyryl side chain did not affect the survival of the plasmodium parasite, demonstrating that acetyl side chain is optimum for antiplasmodial activity and any increase in length will decrease or result in loss of activity.

It remains unclear if the halogenated analogues are de-esterified in the plasmodium before reaching the site of action on DXR. The debenzylated acetyl derivative **2.18** was inactive as was the fully protected acetyl analogue **2.12**, both of which were expected to have been hydrolyzed to FR900098 within the parasite. The effect of the protective group at the site of action would only be clarified by testing the compounds directly on DXR enzyme (chapter 4). Umeda *et al*. [88] discovered that the phosphonate binding pocket of *P. falciparum* DXR has space for small functional groups on the phosphonate end. This could mean that the ethyl ester protection on the phosphonate is able to fit into the active site such that the analogues are still able to inhibit the enzyme.

The presence of the benzyl group on the halogenated analogues has no significant effect on the antiplasmodial activity of the compounds. This was clearly demonstrated by the most active iodoacetyl derivative **2.21** with no benzyl group and an IC_{50} value of 5.54 µM as compared to its benzylated iodoacetyl analogue **2.15** with IC_{50} value of 8.08 µM. The analogues also compared well with the bis(pivaloyloxymethyl) ester prodrug of fosmidomycin (**2.25**, IC_{50} = 2.1 µM) though significantly less active than the FR900098 ester prodrug (**2.26**) with an IC_{50} of 0.4 µM.[134] A combination of the halogenated analogue with a

bis(pivaloyloxymethyl) ester as opposed to diethyl ester might be worth exploring in order to improve the antiplasmodial activity of the compounds.

2.2.9 **Attempted deprotection of the phosphonate ester group**

Once the benzyl group had been removed from the halogenated FR900098 analogues, the next stage was to hydrolyze the phosphonate esters into free phosphonic acids. Hydrolysis of fosmidomycin phosphonate esters analogues in many literature procedures have often been achieved by transesterification with TMSBr or TMSI. This mild reaction was attempted on the synthesized halogenated compounds and this proved to be a challenge.

Following a modified microwave method described by Kumar and co-worker[140] the debenzylated acetyl analogue **2.18** dissolved in dry CH_3CN was treated with TMSBr for 10 minutes in a microwave powered at 50 W and 40^oC temperature. The resulting product showed degradation of the starting material. Attempting the reaction on the chloroacetyl derivative **2.19** also resulted in degradation while no reaction occurred with the protected propyl analogues **2.9** and **2.10** (Scheme 2.9 A). In order to validate the method, the same procedure was carried out on diethyl 3-bromopropylphosphonate and it successfully gave the required pure white crystals of **2.27** (Scheme 2.9 B). This showed that although the reaction could be adopted for hydrolysis of phosphonate esters, it is not compatible with the synthesized halogenated fosmidomycin analogues.

After the unsuccessful attempt to hydrolyse the phosphonate ester using the microwave, the more conventional method of stirring the ester with TMSBr in a dry solvent was employed. The acetyl hydroxamic acid derivative **2.18** was treated with 5 molar equivalents of TMSBr at 0^oC. The temperature was allowed to rise to room temperature and stirred for four days. After working up the reaction FR900098 was obtained as a pure compound (Scheme 2.9 C). Unfortunately, attempts to hydrolyse the esters of fully protected **2.9** and **2.10** and the partially deprotected **2.19 – 2.21** using the same method resulted in degradation of the starting esters and none of the desired phosphonic acids. Consequently, the more reactive TMSI was used in place of TMSBr, stirring the reaction for two hours at room temperature. The ^1H NMR spectrum of the crude product did not show the usual ethyl shift. As promising

as the product was, all attempts to purify it using a C-18 Sep-Pak cartridge and reversed phase HPLC was unsuccessful.

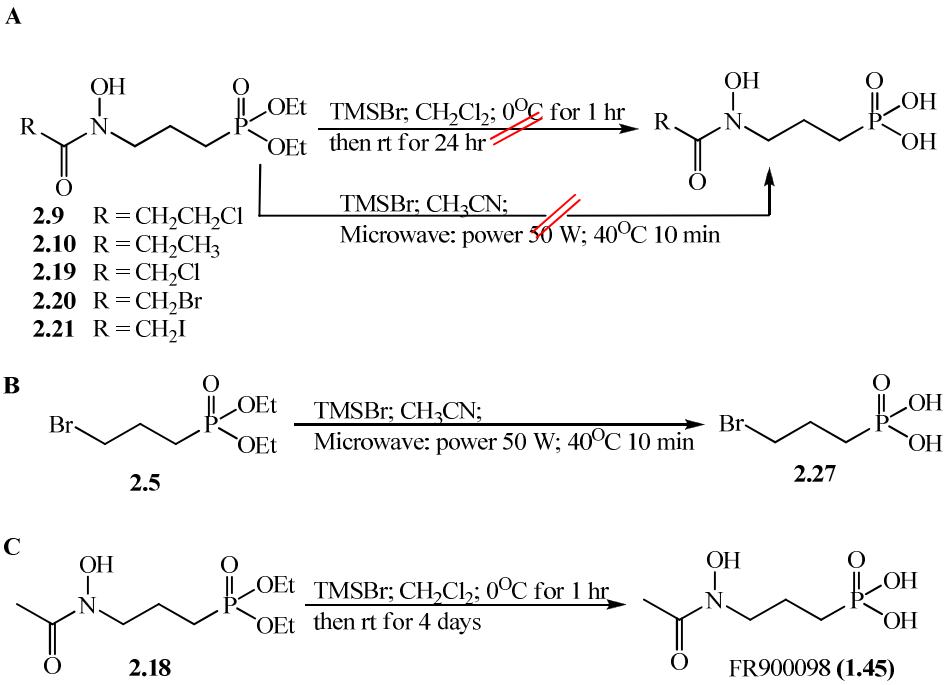

Scheme 2.9. Attempted ester hydrolysis of halogenated FR900098 analogues

An attempt to synthesize the phosphonic acid analogues without protecting the phosphonate throughout the synthetic steps was also unsuccessful. Acid hydrolysis of **2.4** prior to the reaction with acyl chloride was attempted. ^{1}H NMR spectroscopy again revealed degradation of the starting **2.4** (Scheme 2.10). All these failed attempts necessitated looking for alternative methods to obtain the free phosphonic acid analogues.

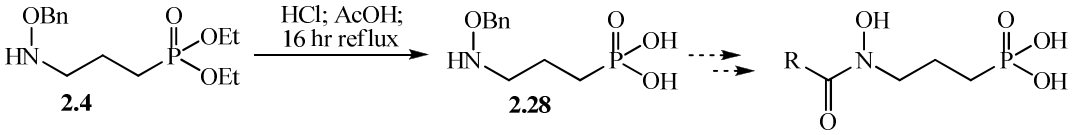

Scheme 2.10. Attempted ester hydrolysis of **2.4**

2.2.10 Synthesis of benzyl-protected analogues of FR900098

All attempts to hydrolyze the diethyl phosphonate ester analogues described in the previous section were unsuccessful hence a protective group that is easy to remove was required. Since it was possible to remove the benzyl group from the hydroxamate end it was reasoned that protecting the phosphonate with the same group might be easier to remove and this can be done at the same time as the removal of the protection from the O-protected hydroxylamine. This meant that the whole series of reactions previously described for the diethyl ester phosphonate would be carried out on the benzyl-protected phosphonate i.e. the *de novo* synthesis of the compounds was required. Attempts to substitute the ethyl group of **2.4** with a benzyl group by treatment of the ester with TMSBr followed by $COCl_2$, pyridine and BuOH (Scheme 2.11) gave rise to a crude product with an inconclusive ^{1}H NMR spectrum. It was difficult to determine if the desired substitution had taken place and if it had, it was clear from the NMR spectrum that it would require optimizing the reaction to obtain enough of the product to proceed with the remaining steps of the reaction. The effort to introduce dibenzyl phosphite onto 1,3-dibromopropane (**2.6**) in the presence of NaH as a base was also to no avail as no reaction occurred between the two compounds.

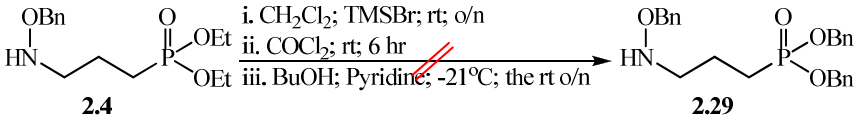

Scheme 2.11. Attempted substitution of ethyl with benzyl protective group

Following on from this, 1,3-dibromopropane (**2.6**) was reacted with dibenzylphosphite (**2.30**, $(BnO)_2P(O)H$) using the method described by Cohen *et al.*[128] Cs_2CO_3 and tetramethyl ammonium iodide $(CH_3)_4NI$) were added to a solution of $(BnO)_2P(O)H$ in anhydrous DMF. The suspension was stirred for an hour before introducing 1,3-dibromopropane (**2.6)** and thereafter stirred for 64 hours at room temperature (Scheme 2.12). Working up the reaction by extraction into EtOAc and purification by column chromatography afforded the benzyl-protected bromopropylphosphonate **2.31** in 63% yield. The hydroxamic moiety was introduced by reaction with BocNHOBn. Unlike the reaction of BocNHOBn with bromophosphonate **2.5** which gave 100% yield of the protected fosmidomycin backbone **2.7**,

BocNHOBn reacted with benzyl protected **2.31** to give the benzyl protected fosmidomycin backbone **2.32** in 56% yield (Scheme 2.12). Treatment of **2.32** with 1:1 (v/v) ratio of TFA and CH_2Cl_2 resulted in 15% yield of the partially deprotected backbone **2.33**. The low yield was unexpected as the same reaction on **2.7** had afforded **2.4** in 93% yield. The conditions of the reaction were thus modified such that TFA was only 50 molar equivalent of the starting material (**2.32**) and CH_2Cl_2 was twice the volume of TFA. The reaction temperature was reduced to 0^oC and stirred for 45 minutes[141] to yield a satisfying 97% product of **2.33** requiring no further purification. Treatment of **2.33** with appropriate acyl chlorides generated a series of benzyl-protected protected FR900098 analogues. Hydrogenolysis of these analogues using $Pd(OH)_2/C$ as catalyst gave the desired phosphonic acids in quantitative yields (Scheme 2.12).

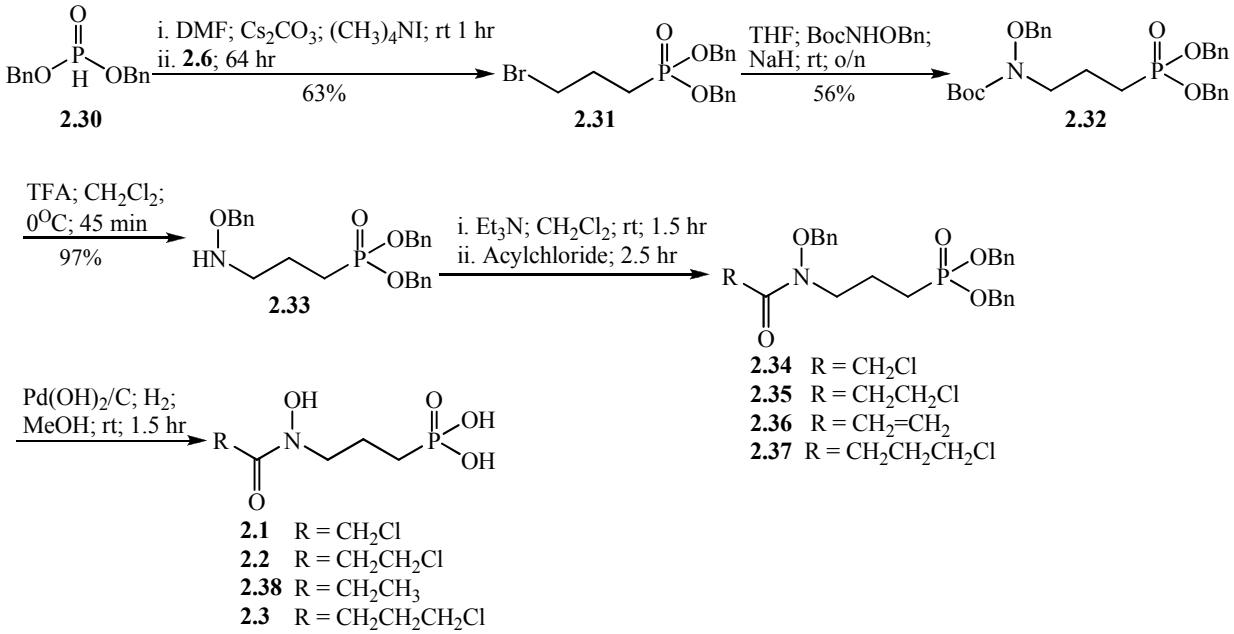

Scheme 2.12. Synthesis of chlorinated phosphonic acid analogues of FR900098

Finkelstein reaction of **2.34** with NaI gave **2.39** but hydrogenation of this compound led to loss of iodine (Scheme 2.13). Attempts to substitute the chlorine atom of **2.1** with iodine were unsuccessful as the phosphonic acid was insoluble in the reaction solvent, acetone. Compound **2.1** was soluble in H_2O and MeOH both of which cannot be used for the Finkelstein reaction due to the solubility of NaI and the expected NaCl salt in these solvent.

Finkelstein reaction is a reversible reaction and thus its strength relies on the relative solubility of the salts in the reaction solvent. NaI is soluble in acetone while NaCl is insoluble and will precipitate out of the solution once formed, this drives the reaction forward. In water or MeOH, all the salt as well as the compounds are soluble and the chances of forming equilibrium between the chloride and iodine analogues of FR900098 is very high. Separation and purification of these salt and highly polar compounds will be almost impossible.

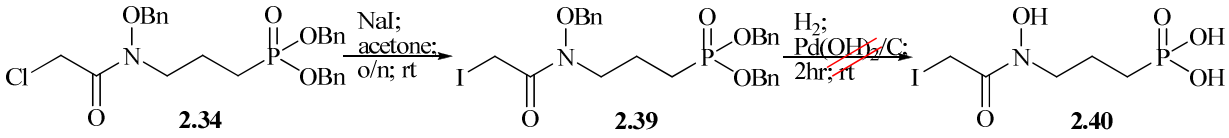

Scheme 2.13. Attempted synthesis of iodinated analogue **2.40**

2.2.11 **Analysis of degradation product of 2.3**

An observation was made during an attempt to obtain 2D NMR data for **2.3**, which showed that the compound was degrading in D_2O as early as nine hours after synthesis. This prevented ^{13}C NMR and 2D NMR data of pure **2.3** from being obtained as the compound was degrading during the course of acquiring the spectra. The progress of the degradation was monitored by ^{1}H NMR and by day 25 no further degradation was observed (Figure 2.10), although some of the original **2.3** was still present.

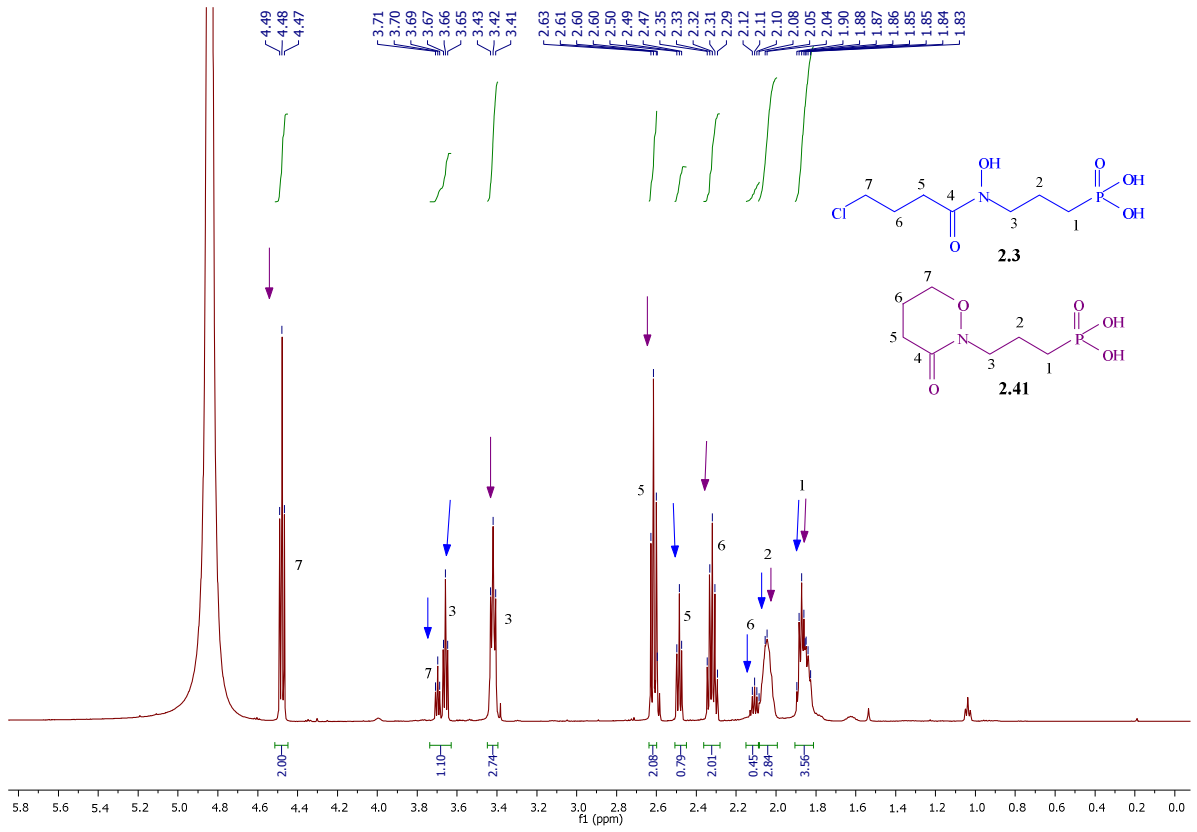

Figure 2.10. ^{1}H NMR spectrum (D_2O; 600 MHz) of the degradation mixture of **2.3** after 25 days

The cleanliness of the ^{1}H NMR spectrum after degradation and the better resolution of the chemical shifts as compared to the spectrum of **2.3** (Figure 2.10) which showed broad chemical shifts were intriguing. It suggested a systematic degradation or conversion of the original compound to form a more stable water soluble product. Analysis of the NMR spectra showed diminishing methylene shifts at δ 3.70 and 3.75 in the ^{1}H NMR spectrum of **2.3** giving rise to the new peaks at δ 4.48 and 3.42 (Figure 2.11) respectively in the degradation mixture.

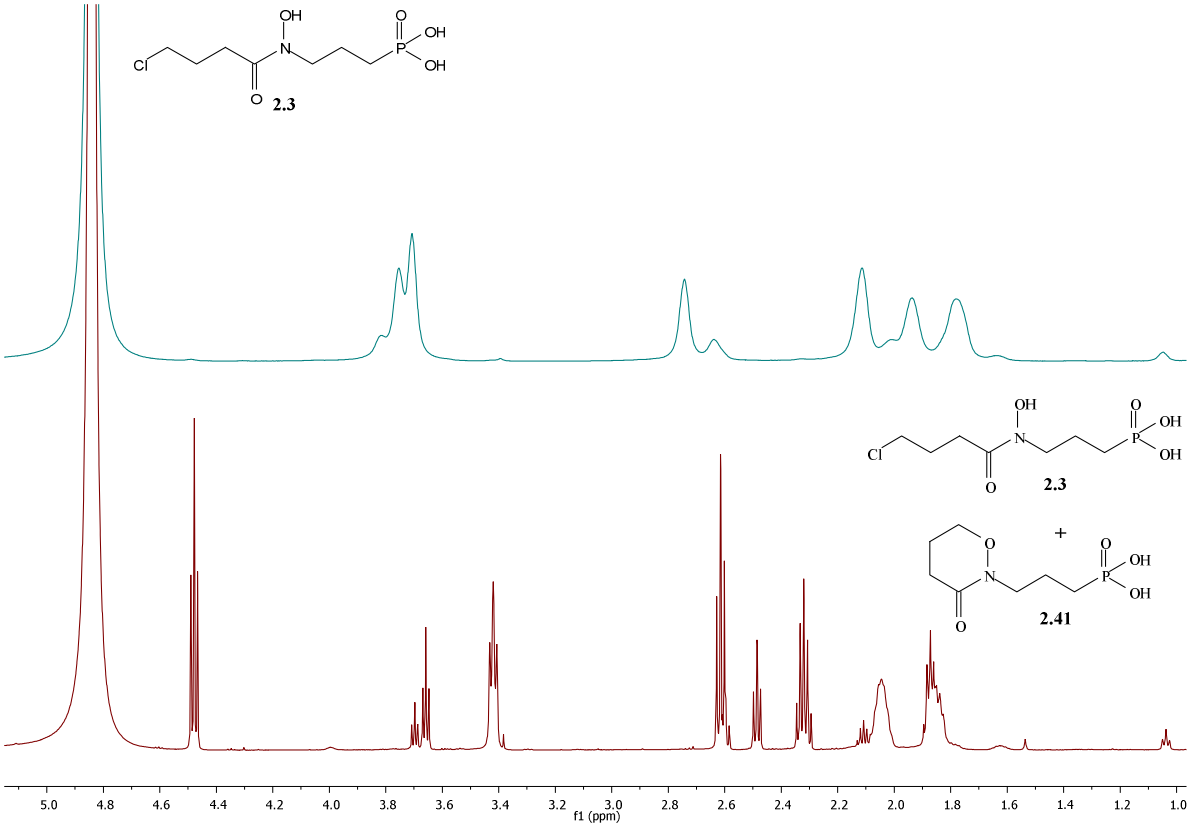

Figure 2.11. Comparison of ^{1}H NMR spectra of pure **2.3** (D_2O; 600 MHz) and the degradation mixture after 25 days in D_2O

The new methylene triplet at δ 3.42 (H-3) showed a ^{1}H-^{1}H COSY NMR correlation to the multiplet at δ 2.05 (H-2) which in turn showed another correlation to 1.86 (H-1). This is the same pattern observed for the methylene protons of the propyl linker between the hydroxamate and the phosphonate of all the synthesized FR900098 analogues, confirming that this part of the molecule is present and intact. The triplet at δ 4.48 (2H; *J* = 7.2 Hz) showed a COSY relationship to the multiplet at δ 2.36 (2H; H-6) which in turn also showed a correlation to the triplet at δ 2.61 (2H; *J* = 8.23 Hz). All of these shifts integrated to two protons each. The correlation of δ 2.32, 2.61 and 4.48 to the carbonyl carbon at δ 183.2 indicated their positions as the side chain to the retrohydroxamate group. The fact that the methylene triplet at δ 3.70 of the **2.3** was deshielded to 4.48 in the degradation product suggests a more electronegative atom than chlorine was now attached to the carbon carrying the protons at δ 70.7. This analysis corresponded with the expected result of the product which would form when the lone pair of electrons of the N-oxime oxygen attacks the

chlorinated carbon of the side chain of **2.3**. This would result in the removal of the chlorine as a good leaving group and intramolecular cyclization of the side chain to afford **2.41** (Scheme 2.14). The structure could not be confirmed however, because samples could not be separated and pure samples were not obtained for further analysis.

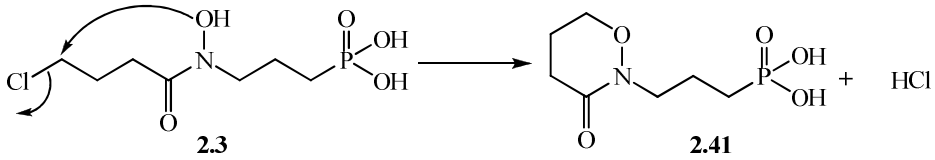

Scheme 2.14. Proposed mechanism of intramolecular cyclization of **2.3** to **2.41**

2.2.12 **Antiplasmodial activity of deprotected Fosmidomycin analogues**

The antiplasmodial assay of the phosphonic acid analogues of FR900098 **2.1 – 2.3** and **2.38** was carried out on the CQR FCR-3 strain of *P. falciparum*. As expected, none of the phosphonic acids (Table 2.6) was as active as their ester analogues (Table 3.5). This confirmed that the increased lipophilicity of the ester compounds enhanced their absorption into the parasite and as a result more concentration of the drugs was delivered to the site of action. It was however not anticipated that FR900098 would show better activity (IC_{50} = 41.67 µM) against the plasmodium than the chlorinated **2.1** (IC_{50} = 64.07 µM) considering that the protected chlorinated analogue **2.8** and the debenzylated chlorinated analogue **2.19** showed better activity than the unchlorinated protected analogues of FR900098 **2.12** and **2.18** respectively (Table 2.5).What was important however was that while the hydroxamic acid of FR900098 (**2.18**) was inactive, the hydroxamic acid of **321** (**2.19**) was active even more so than FR900098 and as such is a promising antimalarial agent.

Table 2.6. Antiplasmodial activity of deprotected halogenated Fosmidomycin analogues

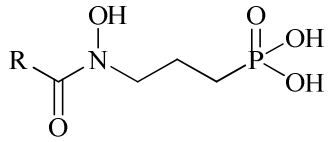

Compound	R	FCR-3: IC_{50} (µM)	SD (µM)
FR900098 (1.45)	$-CH_3$	41.67	7.24
2.1	$-CH_2Cl$	64.07	2.87
2.2	$-CH_2CH_2Cl$	> 100	11.63
2.38	$-CH_2CH_3$	> 100	14.16
2.3	$-CH_2CH_2CH_2Cl$	> 100	12.99

2.2.13 Synthesis and antiplasmodial activity of Boc-substituted halogenated FR900098 analogues

In an effort to retain the lipophilic properties of **2.8** and determine if varying the protective group on hydroxamate group would affect the antiplasmodial activity of the FR900098 analogues, a substitution of the protecting benzyl was sought. The *N*-oxime can be protected with different protecting groups however the Boc group was selected due to the ease with which it is removed and the high yield following the removal. Boc protected analogues **2.42** and **2.43** were synthesized from **2.19** since it showed the best antiplasmodial activity.

The Boc group was introduced to the chlorinated **2.19** by reacting with Boc anhydride yielding the Boc-protected chloroacetyl analogue **2.42**. Finkelstein reaction of NaI and **2.42** produced the iodinated derivative **2.43** (Scheme 2.15)

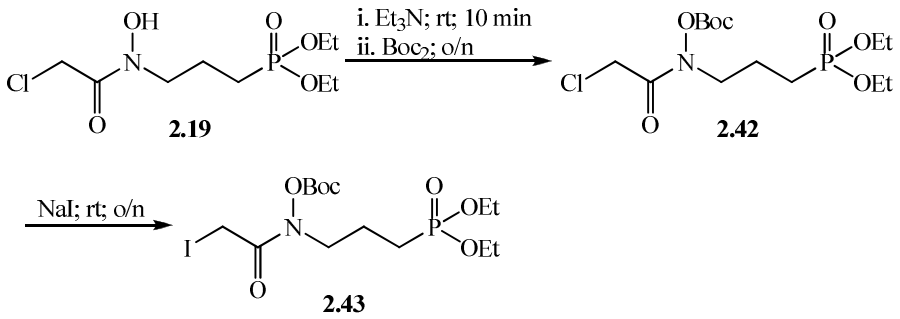

Scheme 2.15. Synthesis of Boc-protected halogenated derivatives of FR900098

Compounds **2.42** and **2.43** were tested against CQR Gambian FCR-3 strain of *P. falciparum*. Both compounds exhibited good activity against the parasite with **2.42** having an IC_{50} of 14.98 ± 0.31 µM and **2.43** an IC_{50} of 6.12 ± 0.59 µM. Their activity is comparable with those observed for **2.8** (IC_{50}9.09 ± 0.38 µM) and **2.15** (IC_{50} 8.08 ± 0.91 µM) which are the chloride and iodide analogues respectively. The result clearly shows no significant difference in the antiplasmodial activity of the compounds when the benzyl protecting group is substituted with a Boc group. The choice of which protecting group is better might come down to the cytotoxicity profile of different analogues containing both protecting groups.

2.3 SUMMARY OF ANTIPLASMODIAL ACTIVITY

The fully protected halogenated acetyl analogues of FR900098 (**2.8**, **2.5** and **2.17**) as well as the hydroxamic acid phosphonate esters **2.19 – 2.21** have demonstrated superior antiplasmodial activity to FR900098 (**1.45**) against CQR FCR-3 *P. falciparum*. This activity is attributed to the increased lipophilicity of compounds, as compared to FR900098 as well as the presence of halogens at the acetyl side chain. Extending the acyl side chain with halogenated and non-halogenated propyl or butyryl group results in loss of antiplasmodial activity.

Substitution of the *O*-benzyl protecting group with Boc did not show any appreciable difference in antiplasmodial activity of the halogenated FR900098 derivatives. However, having a lipophilic protective group on the hydroxamate seem unnecessary since the free hydroxamic acid **2.19 – 2.21** maintained their antiplasmodial activity even without the benzyl

group. It is worth mentioning that based on the reactive nature of halogens the halogenated FR900098 analogues could exhibit non-specific interaction within a host cell. Cytotoxic property of these compounds would have to be determined in order to establish their selectivity for the malaria parasite.

2.4 EXPERIMENTAL

2.4.1 Antiplasmodial assay for chloroquine resistance Gambian FCR-3 strain of *P. falciparum*

The antiplasmodial assay for the chloroquine resistant Gambian FCR-3 strain was carried out by Prof. van Zyl at the Department of Pharmacy and Pharmacology, University of Witwatersrand.

Parasite cultivation

The chloroquine-resistant Gambian FCR-3 strain of the malaria parasite *Plasmodium falciparum* was cultured *in vitro* in human erythrocytes according to the methods described by Jensen and Trager,[138] and modified by van Zyl and Viljoen.[139] In brief, parasitized erythrocytes were suspended at a 5% haematocrit in RPMI-1640, supplemented with 10 mM D-glucose, 0.32 mM hypoxanthine, 50 mg/L gentamicin, 10% (v/v) heat inactivated human plasma. The culture was buffered with 25 mM HEPES and 25 mM $NaHCO_3$. Cultures were maintained daily and incubated at 37°C with a gas mixture of 5% CO_2, 3% O_2 and the balance with N_2. For experimental purposes, cultures were synchronized with 5% D-sorbitol when the parasites were in the ring stage.[142] The percentage parasitaemia and stages were assessed daily by microscopic examination of thin blood smears stained with Giemsa.

Antiplasmodial screening

The antimalarial activity of the various extracts was determined using the tritiated hypoxanthine incorporation assay.[143] The parasite suspension, consisted predominately the ring stage and was adjusted to a 0.5% parasitaemia and 1% haematocrit. The suspension was

then exposed to the different compounds at 50µM concentration (plated in triplicate) for a single cycle of parasite growth. All assays were carried out using untreated parasites and uninfected red blood cells as controls. Labelled ^{3}H-hypoxanthine (0.5 µCi/ well, Amersham) was added after 24 h and the parasitic DNA was harvested on a Wallac® GFB-filtermat with a Titertek® cell harvester. The filtermats were dried and counted in the Wallac®beta counter. The counts per minute (cpm) were generated and the parasite survival rate calculated. The IC_{50} value for each compound was determined from the log sigmoid dose response curve generated by the Enzfitter®and Prism® software. Chloroquine was used as the reference antimalarial agents. Each experiment was repeated, at least, in triplicate.

2.4.2 **Antiplasmodial assay for chloroquine sensitive D10 strain of *P. falciparum***

Antiplasmodial assay was conducted by Prof. Peter J. Smith at the Division of Pharmacology, University of Cape Town.

All the samples were tested in duplicates against the D10 strain of chloroquine sensitive *P. falciparum*. The continuous *in vitro* culture of the asexual erythrocytic stage used in the experiment was maintained using a modified method of Trager and Jensen.[138] The result was quantitatively assessed to determine the *in vitro* antiplasmodial activity through the lactate dehydrogenase assay according to a modified method of Makler.[144]

A 2mg/ml stock solution of the test samples were prepared in 10% methanol and sonicated to enhance solubility. Samples not completely dissolved were tested as suspension. Stock solutions were stored at -20ºC and further dilutions were prepared on the day of the experiment. A full dose-response was performed for all compounds to determine the IC50 value. Chloroquine was used as the reference drug and was tested at concentrations of 30, 15 and 7.5 ng/ml. The full dose response experiment of the test samples was started at a concentration of 100 µg/ml and was serially diluted 2-folds to give 10 concentrations with a minimum of 0.2 µg/ml. Chloroquine was tested at a starting concentration of 100 ng/ml. The highest concentration of solvent used did not have any measurable effect on the parasites.

2.4.3 **General experimental, equipment, chemicals and reagents**

The following general procedures were used unless stated otherwise. All solvents used for column chromatography and HPLC were HPLC grade obtained from Sigma- Aldrich (EtOAc) and BDH laboratory supplies. Normal phase TLC was performed on TLC silica gel 60 F_{254}.The plates were viewed under UV light (254 nm) and developed in iodine vapour or phosphomolybdic acid solution. Purification by column chromatography was carried out using Merck Kieselgel 60 (0.040-0.063).

HPLC was conducted on a Waters 1525 Binary HPLC pump equipped with Waters 2487 dual wavelength absorbance detector. The UV absorbance was read at wavelengths of 254 and 234 nm and a range of 2.0 in AUFs. Normal Phase chromatography was performed using Whatman Partisil 10 column with a 40 cm X 10 mm i.d.

IR spectra were recorded on Perkin-Elmer Spectrum 100 FT-IR spectrometer with neat compounds placed on diamond window. UV was conducted on Lambda 25 Perkin Elmer UV-Vis spectrometer.

Electrospray ionization mass spectrometry (ESI-MS) was obtained using Waters Synapt G2 with direct injection (1 µl) into a stream of 50% acetonitrile, 0.1% formic acid using a Waters UPLC at flow rate of 0.2 ml/min.

The NMR spectra were recorded on a Bruker Avance 400 or 600 NMR spectrometer using standard pulse sequences. Chemical shifts were recorded in parts per million (ppm). NMR solvents used included $CDCl_3$, MeOD and D_2O and were referenced to residual undeuterated solvent signals ($CDCl_3$: δ_H = 7.25 ppm, δ_C = 77.0 ppm; MeOD: δ_H = 4.84 ppm; δ_C = 49.0 ppm; D_2O: δ_H = 4.84 ppm).

All reactions requiring anhydrous conditions were conducted in flame-dried apparatus. Under N_2, THF was dried over sodium wire and benzophenone as described in literature.[145]

2.4.4 **Synthetic procedures and spectroscopic data**

Diethyl (3-bromopropyl)phosphonate (2.8)

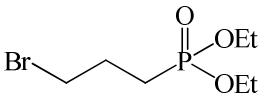

In a 50ml round bottom flask equipped with a stirrer bar and condenser, triethyl phosphate ($P(OEt)_3$;1.5 ml; 8.74 mmol) was heated at 150^0C with 1,3-dibromopropane (**2.6**, 1.33 ml; 13.12 mmol). The reaction was monitored by TLC and stopped after one hour when all the $P(OEt)_3$ had reacted. Column chromatography (Et_2O/CH_2Cl_2, 1:1) of the crude product afforded the desired pure product as a colourless oil (1.21g; 54%). **^{1}H NMR** (400 MHz; $CDCl_3$): δ = 4.02 (m, 4H, P-O-C$\underline{H_2}$-CH_3); 3.40 (t, *J* = 6.5 Hz, 2H, P-CH_2-CH_2-C$\underline{H_2}$); 2.07 (m, 2H, P-CH_2C$\underline{H_2}$); 1.82 (m, 2H, P-C$\underline{H_2}$); 1.25 (t, *J* = 7.1 Hz, 6H, P-O-CH_2-C$\underline{H_3}$) ppm. **^{13}C NMR** (100 MHz; $CDCl_3$): δ = 61.5 (d, *J* = 6.5 Hz, 2 x CH_2, P-O-$\underline{C}H_2$-CH_3); 33.4 (d, *J* = 18.6 Hz, P-CH_2-CH_2-$\underline{C}H_2$); 25.8 (d, *J* = 4.3 Hz, P-CH_2-$\underline{C}H_2$); 24.2 (d, *J* = 142.6 Hz, P-$\underline{C}H_2$); 16.3 (d, *J* = 6.0 Hz, 2 x CH_3, P-O-CH_2-$\underline{C}H_3$) ppm.

***Tert*-butyl benzyloxy(3-(diethoxyphosphoryl)propyl)carbamate (2.7)**

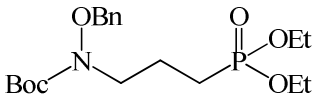

Under dry conditions, *tert*-butyl benzyloxycarbamate (1.16 g; 5.2 mmol) was dissolved in 20 ml freshly distilled THF at room temperature. NaH (0.25 g; 10.4 mmol) was added to the carbamate solution in portions over 15 minutes. After stirring the mixture for 30 minutes, **2.8** (1.35 g; 5.2 mmol) was added dropwise and left to stir overnight. The cloudy white mixture was concentrated under reduced pressure and 10 ml of H_2O was added. The resulting crude mixture was extracted with EtOAc (20ml x 3). The combined EtOAc extracts was washed with saturated brine solution (10 ml) and dried over anhydrous Na_2SO_4 before concentrating *in vacuo* to give the desired pure compound (2.08 g; 100%) as a colourless oil without further purification. **^{1}H NMR** (400 MHz; $CDCl_3$): δ = 7.34 (m, 5H, N-O-CH_2-Ph-$\underline{H}$); 4.81 (s, 2H, N-O-C$\underline{H_2}$-Ph); 4.05 (m, 4H, P-O-C$\underline{H_2}$-CH_3); 3.45 (t, *J* = 6.8 Hz, 2H, P-$CH_2CH_2C\underline{H_2}$); 1.88(m, 2H, P-CH_2-C$\underline{H_2}$); 1.71(m, 2H, P-C$\underline{H_2}$); 1.48 (s, 9H, N-C(O)-O-C(C$\underline{H_3}$)$_3$); 1.27 (t, *J* = 7.0 Hz, 6H, P-O-CH_2-C$\underline{H_3}$). **^{13}C NMR** (100 MHz; $CDCl_3$): δ = 156.4 (s, N-$\underline{C}$(O)-O-C(CH_3)$_3$); 135.4 (s, N-O-CH_2-$\underline{C}$=CH-); 129.3 (s, 2 x CH,N-O-CH_2-C=CH-$\underline{C}$H=); 128.5 (s, N-O-CH_2-C=CH-

CH=CH); 128.4 (s, 2 xCH, N-O-CH_2-C=CH-); 81.4 (s; N-C(O)-O-C(CH_3)$_3$); 77.0 (s, N-O-CH_2-Ph); 61.5 (d, *J* = 6.5 Hz,2 x CH_2, P-O-CH_2-CH_3); 49.8 (d, *J* = 19.2 Hz, P-CH_2-CH_2-CH_2); 28.2 (s,3 x CH_3,N-C(O)-O-C(CH_3)$_3$); 23.0 (d, *J* = 142.6 Hz, P-CH_2); 20.4 (d, *J*= 4.7 Hz, P-CH_2CH_2); 16.4 (d, *J* = 6.0 Hz, 2 x CH_3, P-O-CH_2-CH_3).

Diethyl 3-(benzyloxyamino)propylphosphonate (2.4)[146]

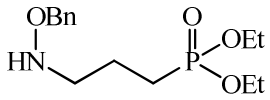

Compound **2.7** (0.3 g; 0.75 mmol) was dissolved in CH_2Cl_2 (3 ml). TFA (3 ml) was added at room temperature and stirred overnight and the solvent was removed under reduced pressure. The resulting residue was washed with a saturated solution of $NaHCO_3$ (10 ml) and extracted with EtOAc (3x 10 ml). The combined organic phase was washed with saturated brine, dried over anhydrous Na_2SO_4 and concentrated under reduced pressure. The concentrated product (0.21 g; 93%) was used in the next reaction without further purification.

^{1}H NMR (400 MHz; $CDCl_3$): δ = 7.31 (m, 5H, N-O-CH_2-Ph-H); 4.68 (s, 2H, N-O-CH_2-Ph); 4.04 (m, 4H, P-O-CH_2-CH_3); 2.96 (t, *J* = 6.3 Hz, 2H, P-CH_2-CH_2-CH_2); 1.79 (m, 2H, P-CH_2-CH_2); 1.73 (m, 2H, P-CH_2) 1.29 (t, *J* = 7.0 Hz, 6H, P-O-CH_2-CH_3) ppm. **^{13}C NMR** (100 MHz; $CDCl_3$): δ = 137.7 (s,N-O-CH_2-C=CH-); 128.4 (s, 2 x CH,N-O-CH_2-C=CH-CH=); 128.3 (s, 2 x CH,N-O-CH_2-C=CH-); 127.8 (s, N-O-CH_2-C=CH-CH=CH); 76.3 (s, N-O-CH_2-Ph); 61.5 (d, *J* = 6.5 Hz; 2 x CH_2, P-O-CH_2-CH_3); 52.0 (d, *J* = 16.6 Hz, P-CH_2-CH_2-CH_2); 23.1 (d, *J* = 142.1 Hz, P-CH_2); 20.5 (d, *J* = 4.9 Hz, P-CH_2CH_2); 16.4 (d, *J* = 6.0 Hz, 2 x CH_3,P-O-CH_2-CH_3) ppm.

General procedure for the synthesis of Diethyl 3-(*N*-(benzyloxy)-chloroalkyl)propylphosphonate (2.8 – 2.12 and 2.17)

A solution of **2.4** (0.25 g; 0.83 mmol) in CH_2Cl_2(20 ml) was treated with Et_3N (0.14 ml; 1.05 mmol) at room temperature. The mixture was stirred for 1.5 h, and the respective acyl chloride (1.05 mmol) was added dropwise and stirred for another 2.5 h (except for **2.11** which was stirred for 3.5 h). The mixture was diluted with CH_2Cl_2 (10 ml) and washed with water (20 ml), saturated $NaHCO_3$ solution (20 ml), and finally with saturated brine solution (5 ml).

The organic layer was dried over anhydrous $MgSO_4$. The concentrated product was purified by silica gel (10 g) column chromatography first eluting with EtOAc (50 ml), then MeOH/EtOAc (1:9, 50 ml) to give the pure products as clear, yellow oils.

Diethyl 3-(*N*-(benzyloxy)-2-chloroacetamido)propylphosphonate (2.8)

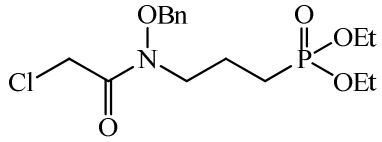

Yield: 0.25 g; 79%. See Tables 2.1 and 2.2 for **^{1}H NMR** (400 MHz, $CDCl_3$) and **^{13}C NMR** (100 MHz, $CDCl_3$) assignments.

Mass (HRESI-MS): Calculated for $C_{16}H_{25}ClNO_5P$ $[M + H]^+$: 378.1237, Found: 378.1226

IR: ν_{max} 3458, 2982, 1672 (C=O), 1238 (P=O), 1023; **UV**: λ_{max} 209.07 nm

Diethyl 3-(N-(benzyloxy)-3-chloropropanamido)propylphosphonate (2.9)

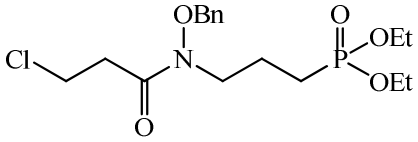

Yield: 0.11 g; 33%. **NMR** (400 MHz, $CDCl_3$) δ 7.37 (s, 5H, Ar-H); 4.82 (s, 2H,N-O-CH_2-Ar); 4.06 (m, 4H,P-O-CH_2-CH_3); 3.74 (overlapped t, J = 5.87 Hz, 4H, P-$CH_2CH_2CH_2$ and CH_2-Cl); 2.83 (t, J = 6.6 Hz, 2H, C(O)-CH_2);1.94 (m, 2H,P-CH_2CH_2); 1.71 (m, 2H, P-CH_2); 1.29 (t, J = 7.0 Hz, 6H, P-O-CH_2-CH_3) ppm. **^{13}C NMR** (100 MHz, $CDCl_3$) δ 171.9 (s, C=O); 134. 1 (s, N-O-CH_2-C=CH-); 129.3 (s, 2 x CH, N-O-CH_2-C=CH-CH=); 129.1 (s, N-O-CH_2-C=CH-CH=CH); 128.8 (s, 2 x CH, N-O-CH_2-C=CH-); 76.6 (s, N-O-CH_2-Ph); 61.6 (d, J = 6.5 Hz, 2 x CH_2,P-O-CH_2); 45.5 (s, P-$CH_2CH_2CH_2$); 39.3 (s, CH_2-Cl);35.4 (s, C(O)-CH_2); 23.0 (d, J = 142.7 Hz, P-CH_2); 20.2 (d,J = 4.7 Hz,P-CH_2-CH_2); 16.4 (d, J = 5.9 Hz, 2 x CH_3, P-O-CH_2-CH_3) ppm.

Mass (HRESI-MS): Calculated for $C_{17}H_{27}ClNO_5P$ $[M + H]^+$: 392.1394, Found: 392.1394

IR: ν_{max} 3459, 2981, 1657 (C=O), 1238 (P=O), 1022; **UV**: λ_{max} 206.23 nm

Diethyl 3-(*N*-(benzyloxy)acrylamido)propylphosphonate (2.10)

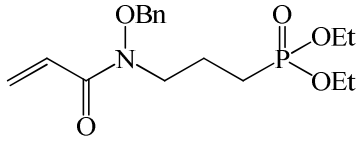

Yield: 0.03 g; 11%. **NMR** (400 MHz, $CDCl_3$) δ 7.36 (s, 5H, Ar-H);6.71 (dd, *J* = 10.4 and 17.1 Hz, 1H, C(O)-CH); 6.39 (d, *J* = 17.1 Hz, 1H, C(O)-CH-CH_{2A}); 5.71 (d, *J* = 10.4 Hz, 1H, C(O)-CH-CH_{2B}); 4.82 (s, 2H,N-O-CH_2-Ph); 4.06(m, 4H,P-O-CH_2-CH_3); 3.76 (t, *J* = 6.9 Hz, 2H, P-$CH_2CH_2CH_2$); 1.96 (m, 2H,P-CH_2CH_2); 1.74 (m, 2H, P-CH_2); 1.28 (t, *J* = 7.0 Hz, 6H, P-O-CH_2-CH_3) ppm. **^{13}C NMR** (100 MHz, $CDCl_3$) δ 167.0 (s, C=O); 134. 1 (s, N-O-CH_2-C=CH-.); 129.3 (s, C(O)-CH-CH_2); 129.2 (s, 2 x CH, N-O-CH_2-C=CH-CH=); 129.0 (s, N-O-CH_2-C=CH-CH=CH); 128.7 (s, 2 x CH, N-O-CH_2-C=CH-); 126.1 (s, C(O)-CH)77.1 (s, N-O-CH_2-Ph); 61.6 (d, *J* = 7.0 Hz, 2 x CH_2, P-O-CH_2); 45.7 (br s, P-$CH_2CH_2CH_2$); 23.0 (d, *J* = 142.0 Hz, P-CH_2); 20.3 (d, *J* = 5.0 Hz, P-CH_2-CH_2); 16.4 (d, *J* = 6.0 Hz, 2 x CH_3, P-O-CH_2-CH_3) ppm.

Mass (ESI-MS): Calculated for $C_{17}H_{26}NO_5P$ $[M + H]^+$: 356.1627, Found: 356.1621

IR: ν_{max} 3461, 2982, 1655 (C=O), 1237 (P=O), 1020; **UV**: λ_{max} 204.98 nm

Diethyl 3-(*N*-(benzyloxy)-4-chlorobutanamido)propylphosphonate (2.11)

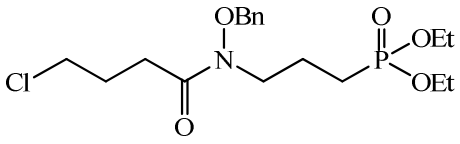

Yield: 0.17 g; 53.4%. **NMR** (400 MHz, $CDCl_3$) δ 7.35 (s, 5H, Ar-H); 4.80 (s, 2H,N-O-CH_2-Ar); 4.04(m, 4H,P-O-CH_2-CH_3); 3.68 (t, *J* = 6.5 Hz, 2H, P-$CH_2CH_2CH_2$) 3.55 (t,*J* = 5.9 Hz, 2H,CH_2-Cl); 2.55(t, *J* = 6.8 Hz, 2H, C(O)-CH_2);2.02 (m, 2H, C(O)-CH_2-CH_2);1.91 (m, 2H,P-CH_2CH_2); 1.69 (m, 2H, P-CH_2); 1.27 (t, *J* = 6.9 Hz, 6H, P-O-CH_2-CH_3) ppm. **^{13}C NMR** (100 MHz, $CDCl_3$) δ 173.6 (s, C=O); 134.2 (s, N-O-CH_2-C=CH-.); 129.2 (s, 2 x CH, N-O-CH_2-

C=CH-CH=); 128.9 (s, N-O-CH_2-C=CH-CH=CH); 128.7 (s, 2 x CH, N-O-CH_2-C=CH-); 76.4 (s, N-O-CH_2-Ph); 61.5 (d, *J* = 6.0 Hz, 2 x CH_2, P-O-CH_2); 45.8 (br s, P-$CH_2CH_2CH_2$); 44.5 (s, CH_2-Cl); 29.2 (s, C(O)-CH_2); 27.1 (s, C(O)-CH_2-CH_2); 23.0 (d, *J* = 142.0 Hz, P-CH_2); 20.2 (d, *J* = 5.0 Hz, P-CH_2-CH_2); 16.3 (d, *J* = 6.0 Hz, 2 x CH_3, P-O-CH_2-CH_3) ppm.

Mass (ESI-MS): Calculated for $C_{18}H_{29}ClNO_5P$ $[M + H]^+$: 406.1550, Found: 406.1544

IR: ν_{max} 3462, 2981, 1659 (C=O), 1239 (P=O), 1025 **UV**: λ_{max} 209.12nm

Diethyl 3-(*N*-(benzyloxy)acetamido)propylphosphonate (2.12)[108]

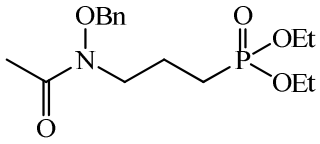

Yield: 0.25 g; 89%. **NMR** (400 MHz, $CDCl_3$) δ 7.33 (s, 5H, Ar-H); 4.77 (s, 2H,N-O-CH_2-Ar); 4.03(m, 4H,P-O-CH_2-CH_3); 3.66 (t, *J* = 6.6 Hz, 2H, P-$CH_2CH_2CH_2$); 2.04 (s, 3H,C(O)-CH_3); 1.91 (m, 2H,P-CH_2CH_2); 1.68 (m, 2H, P-CH_2); 1.25 (t, *J* = 7.0 Hz, 6H, P-O-CH_2-CH_3) ppm. **^{13}C NMR** (100 MHz, $CDCl_3$) δ 166.2 (s, C=O); 134.3 (s, N-O-CH_2-C=CH-.); 129.0 (s, 2 x CH, N-O-CH_2-C=CH-CH=); 128.9 (s, N-O-CH_2-C=CH-CH=CH); 128.6 (s, 2 x CH, N-O-CH_2-C=CH-); 76.3 (s, N-O-CH_2-Ph); 61.4 (d, *J* = 6.5 Hz, 2 x CH_2, P-O-CH_2); 45.4 (s, P-$CH_2CH_2CH_2$); 22.9 (d, *J* = 142.7 Hz, P-CH_2);20.3 (s, C(O)-CH_3); 20.2 (d, *J* = 4.7 Hz, P-CH_2-CH_2); 16.3 (d, *J* = 5.9 Hz, 2 x CH_3, P-O-CH_2-CH_3) ppm.

Diethyl 3-(*N*-(benzyloxy)-2-bromoacetamido)propylphosphonate (2.17)

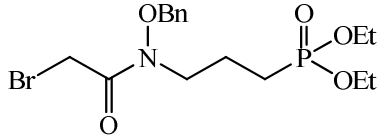

Yield: 0.30 g; 87%. See Tables 2.3 and 2.4 for ^{1}H NMR (400 MHz, $CDCl_3$) and ^{13}C NMR (100 MHz, $CDCl_3$) assignments.

Mass (ESI-MS): Calculated for $C_{16}H_{25}BrNO_5P$ $[M]^+$: 422.0732, Found: 422.0735

IR: ν_{max} 3430, 2983, 1664 (C=O), 1210, 1018; **UV**: λ_{max} 209.01 nm

Diethyl 3-(*N*-(benzyloxy)-2-iodoacetamido)propylphosphonate (2.15).

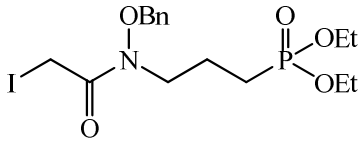

Compound **2.8** (0.26 g; 0.68 mmol) and NaI (0.31 g; 2.03 mmol) were dissolved in 10 ml acetone and stirred at room temperature overnight. The white precipitate was filtered off and the filtrate was concentrated under reduced pressure. The crude product was re-dissolved in 20 ml CH_2Cl_2 and washed with 10 ml of water and then with 5 ml of brine. The organic layer was dried over $MgSO_4$ and concentrated *in-vacuo* to yield the pure yellow oil (0.25 g; 78.5%).

See Tables 2.3 and 2.4 for ^{1}H NMR (400 MHz, $CDCl_3$) and ^{13}C NMR (100 MHz, $CDCl_3$) assignments.

Mass (ESI-MS): Calculated for $C_{16}H_{25}INO_5P$ $[M + H]^+$: 470.0593, Found: 470.0590

IR: ν_{max} 3453, 2981, 1654 (C=O), 1238 (P=O), 1020; **UV**: λ_{max} 209.35 nm

Diethyl 3-(*N*-(benzyloxy)-3-iodopropanamido)propylphosphonate (2.16)

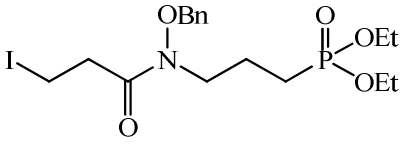

Compound **2.9** (0.14 g; 0.37 mmol) and NaI (0.17 g; 1.10 mmol) were dissolved in 10 ml acetone and stirred at room temperature for 24 h. The solution was then refluxed for 4 h and thereafter allowed to cool to room temperature and stirred another three days. The white precipitate was filtered off and the filtrate was concentrated under reduced pressure. The crude product was re-dissolved in CH_2Cl_2 and washed with water and brine. The organic

layer was dried over $MgSO_4$ and concentrated *in vacuo*. The crude product was purified with reverse phase HPLC using 20:80 H_2O: MeOH to yield pure clear colourless oil (0.10 g; 56%).

^{1}H NMR (400 MHz, $CDCl_3$) δ 7.38 (s, 5H, Ar-H); 4.82 (s, 2H,N-O-CH_2-Ar); 4.07 (m, 4H,P-O-CH_2-CH_3); 3.72 (t, *J* = 6.7 Hz, 2H, P-$CH_2CH_2CH_2$); 3.30 (t, *J* = 7.0 Hz, 2H, CH_2-I); 3.00 (t, *J* = 7.0 Hz, 2H, C(O)-CH_2); 1.94 (m, 2H,P-CH_2CH_2); 1.72 (m, 2H, P-CH_2); 1.29 (t, *J* = 7.0 Hz, 6H, P-O-CH_2-CH_3) ppm. **^{13}C NMR** (100 MHz, $CDCl_3$) δ 172.2 (s, C=O); 134.1 (s, N-O-CH_2-C=CH-.); 129.3 (s, 2 x CH, N-O-CH_2-C=CH-CH=); 129.2 (s, N-O-CH_2-C=CH-CH=CH); 128.8 (s, 2 x CH, N-O-CH_2-C=CH-); 76.6 (s, N-O-CH_2-Ph); 61.6 (d, *J* = 6.5 Hz, 2 x CH_2, P-O-CH_2); 45.8 (s, N-CH_2); 36.6 (s, C(O)-CH_2); 23.1 (d, *J* = 142.7 Hz, P-CH_2); 20.2 (br s, P-CH_2-CH_2); 16.4 (d, *J* = 5.9 Hz, 2 x CH_3, P-O-CH_2-CH_3); -2.8 (s, CH_2-I) ppm.

Mass (ESI-MS): Calculated for $C_{17}H_{27}INO_5P$ $[M + H]^+$: 484.0750, Found: 484.0748

IR: ν_{max} 3460, 2980, 1655 (C=O), 1237 (P=O), 1021; **UV**: λ_{max} 217.01 nm

General procedure for the preparation of diethyl 3-(*N*-hydroxamido)propylphosphonate compounds 2.18, 2.19 and 2.22 – 2.24

The O-protected hydroxamic acids **2.8 – 2.12** (0.20 g) were dissolved in 20 ml MeOH. $Pd(OH)_2$/C (0.04 g) was added to the solution (except for **2.12** where Pd/C was used) and hydrogen gas was introduced to the mixture by means of an inflated a balloon to generate a positive pressure. The suspension was stirred for two hours at room temperature after which it was filtered through celite. The filtrate was concentrated under reduced pressure to give violet coloured oils **2.18**, **2.19** and **2.22 – 2.24** respectively.

Diethyl 3-(*N*-hydroxyacetamido)propylphosphonate (2.18)[147]

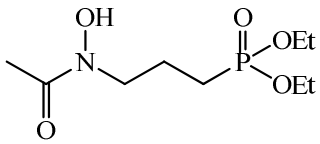

Yield: 0.14 g; 93%. **^{1}H NMR** (400 MHz, MeOD) δ 4.13 (m, 4H, P(O)-CH_2); 3.71 (t, *J* = 6.2 Hz, 2H, P-CH_2-CH_2-CH_2); 2.14 (s, 3H, C(O)-CH_3); 1.89 (m, 4H; P-CH_2-CH_2); 1.36 (t, *J* = 7.0 Hz, 6H, P(O)-CH_2-CH_3) ppm. **^{13}C NMR** (100 MHz, MeOD) δ173.9 (s, C=O); 63.3 (d, *J*

= 7.0 Hz, 2 x CH_2, P(O)-$\underline{C}H_2$); 49.1 (d, *J* = 18.9 Hz,P-CH_2-CH_2-$\underline{C}H_2$); 23.2 (d, *J* = 141.0 Hz, P-$\underline{C}H_2$); 21.0 (d, *J* = 4.0 Hz, P-CH_2-$\underline{C}H_2$); 20.2 (s, C(O)CH_3); 16.7 (d, *J* = 6.0 Hz, 2 x CH_3, P(O)-CH_2-$\underline{C}H_3$) ppm.

Diethyl 3-(2-chloro-*N*-hydroxyacetamido)propylphosphonate (2.19)

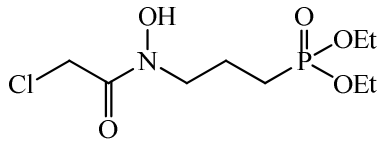

Yield: 0.15 g; 100%.**^{1}H NMR** (400 MHz, MeOD) δ 4.36 (s, 2H, $C\underline{H_2}$-Cl); 4.06 (br s, 4H, P(O)-$C\underline{H_2}$); 3.70 (br t, *J* = 6.1 Hz, 2H, P-CH_2-CH_2-$C\underline{H_2}$); 1.83 (m, 4H; P-$C\underline{H_2}$-$C\underline{H_2}$); 1.31 (t, *J* = 6.6 Hz, 6H, P(O)-CH_2-$C\underline{H_3}$) ppm. **^{13}C NMR** (100 MHz, MeOD) δ169.4 (s, $\underline{C}$=O); 63.32 (d, *J* = 6.0 Hz, 2 x CH_2, P(O)-$\underline{C}H_2$); 49.9 (d, *J* = 20.0 Hz,P-CH_2-CH_2-$\underline{C}H_2$); 42.0 (s, $\underline{C}H_2$-Cl); 23.1 (d, *J* = 142.0 Hz, P-$\underline{C}H_2$); 20.8 (s, P-CH_2-$\underline{C}H_2$); 16.7 (d, *J* = 6.0 Hz, 2 x CH_3, P(O)-CH_2-$\underline{C}H_3$ ppm.

Mass (ESI-MS): Calculated for $C_9H_{19}ClNO_5P$ $[M + H]^+$: 288.0768, Found: 288.0768

IR: ν_{max} 3137, 2983, 2909, 1651 (C=O), 1018; **UV**: λ_{max} 211.34 nm

Diethyl 3-(3-chloro-*N*-hydroxypropanamido)propylphosphonate (2.22)

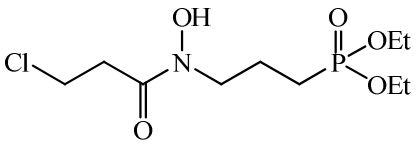

Yield: 0.12 g; 76%. **^{1}H NMR** (400 MHz, MeOD) δ 4.06 (m, 4H, P(O)-C$\underline{H_2}$); 3.75 (t, *J* = 6.4 Hz, 2H, C$\underline{H_2}$-Cl); 3.66 (t, *J* = 6.3 Hz, 2H, P-CH$_2$-CH$_2$-C$\underline{H_2}$); 2.93 (t, *J* = 6.2 Hz, 2H, C(O)-C$\underline{H_2}$); 1.81(m, 4H; P-C$\underline{H_2}$-C$\underline{H_2}$); 1.29 (t, *J* = 7.0 Hz, 6H, P(O)-CH$_2$-C$\underline{H_3}$) ppm. **^{13}C NMR** (100 MHz, MeOD) δ172.6 (s, $\underline{C}$=O); 63.3 (d, *J* = 6.4 Hz, 2 x CH$_2$, P(O)-$\underline{C}$H$_2$); 49.9 (s,P-CH$_2$-CH$_2$-$\underline{C}$H$_2$); 40.3 (s, $\underline{C}$H$_2$-Cl); 36.4 (s, C(O)-$\underline{C}$H$_2$); 23.2 (d, *J* = 142.0 Hz, P-$\underline{C}$H$_2$); 20.9 (d, *J* = 5.0 Hz, P-CH$_2$-$\underline{C}$H$_2$); 16.7 (d, *J* = 6.0 Hz, 2 x CH$_3$, P(O)-CH$_2$-$\underline{C}$H$_3$) ppm.

Mass (ESI-MS): Calculated for $C_{10}H_{21}ClNO_5P$ $[M + Na]^+$: 324.0744, Found: 324.0745

IR: ν_{max} 3150, 2983, 2909,1647 (C=O), 1238 (P=O), 1025; **UV**: λ_{max} 206.57 nm

Diethyl 3-(*N*-hydroxyacrylamido)propylphosphonate (2.23)

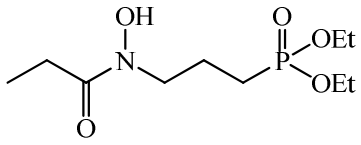

Yield: 0.15 g; 100%. **^{1}H NMR** (400 MHz, MeOD) δ 4.06 (m, 4H, P(O)-C$\underline{H_2}$); 3.63 (t, *J* = 6.3 Hz, 2H, P-CH$_2$-CH$_2$-C$\underline{H_2}$); 2.45 (br d, *J* = 7.2 Hz, 2H, C(O)-C$\underline{H_2}$); 1.78 (m, 4H; P-C$\underline{H_2}$-C$\underline{H_2}$); 1.29 (t, *J* = 7.0 Hz, 6H, P(O)-CH$_2$-C$\underline{H_3}$); 1.06 (t, *J* = 7.5 Hz, 3H, C(O)-CH$_2$-C$\underline{H_3}$) ppm. **^{13}C NMR** (100MHz, MeOD) δ177.2 (s, $\underline{C}$=O); 63.3 (d, *J* = 6.0 Hz, 2 x CH$_2$, P(O)-$\underline{C}$H$_2$); 49.9 (s,P-CH$_2$-CH$_2$-$\underline{C}$H$_2$); 26.5 (s, C(O)-$\underline{C}$H$_2$); 23.2 (d, *J* = 141.0 Hz, P-$\underline{C}$H$_2$); 21.0 (br s, P-CH$_2$-$\underline{C}$H$_2$); 16.7 (d, *J* = 6.0 Hz, 2 x CH$_3$, P(O)-CH$_2$-$\underline{C}$H$_3$); 9.3 (s, C(O)-CH$_2$-$\underline{C}$H$_3$) ppm.

Mass (ESI-MS): Calculated for $C_{10}H_{22}NO_5P$ $[M + H]^+$: 268.1314, Found: 268.1315

IR: ν_{max} 3160, 2981, 2937, 1627 (C=O), 1023; **UV**: λ_{max} 205.66 nm

Diethyl 3-(4-chloro-*N*-hydroxybutanamido)propylphosphonate (2.24)

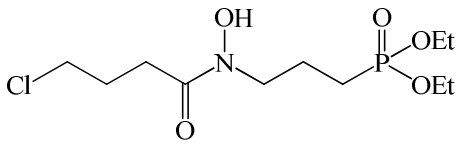

Yield: 0.04 g; 23%.**^{1}H NMR** (600 MHz, MeOD) δ 4.05 (m, 4H, P(O)-C$\underline{H_2}$); 3.60 (t, *J* = 6.5 Hz, 2H, C$\underline{H_2}$-Cl); 3.76 (t, *J* = 5.6 Hz, 2H, P-CH_2-CH_2-C$\underline{H_2}$); 2.68 (t, *J* = 7.2 Hz, 2H, C(O)-C$\underline{H_2}$); 2.08 (m, 2H, (CO)-CH_2-C$\underline{H_2}$); 1.95 (m, 2H, P-C$\underline{H_2}$-C$\underline{H_2}$); 1.82 (m, 2H; P-C$\underline{H_2}$); 1.31(t, *J* = 7.0 Hz, 6H, P(O)CH_2C$\underline{H_3}$) ppm. **^{13}C NMR** (150 MHz, MeOD) δ173.9 (s, $\underline{C}$=O); 62.30 (d, *J* = 6.6 Hz, 2 x CH_2, P(O)-$\underline{C}H_2$); 47.6 (s,P-CH_2-CH_2-$\underline{C}H_2$); 44.8 (s, $\underline{C}H_2$Cl); 29.6 (s, C(O)-$\underline{C}H_2$); 27.5 (s, C(O)-CH_2-$\underline{C}H_2$) 22.1 (d, *J* = 140.3 Hz, P-$\underline{C}H_2$); 18.7 (d, *J* = 5.1 Hz, P-CH_2-$\underline{C}H_2$); 16.3(d, *J* = 5.7 Hz, 2 x CH_3, P(O)-CH_2-$\underline{C}H_3$) ppm.

Mass (ESI-MS): Calculated for $C_{11}H_{23}ClNO_5P$ $[M + H]^+$: 316.1081, Found: 316.1082

IR: ν_{max} 3169, 2982, 2932, 1645 (C=O), 1213; **UV**: λ_{max} 203.41 nm

Diethyl 3-(2-bromo-*N*-hydroxyacetamido)propylphosphonate (2.20)

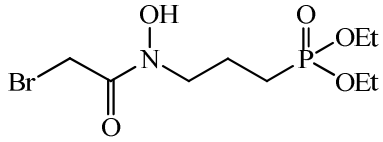

Part 1: Compound **2.19** (0.11 g; 0.39 mmol) was dissolved in 15 ml acetone and LiBr (0.42 g; 4.9 mmol) was added and stirred for 48 hours a room temperature. More LiBr (0.16 g; 1.84 mmol) and acetone (5 ml) were added to the reaction mixture and refluxed for four hours before stirring at room temperature for another 24 hours. The cloudy solution was filtered and concentrated under reduced pressure. The crude product was re-dissolved in 30ml EtOAc and washed with brine (5ml). **Part 2**: The organic phase was concentrated *in vacuo* and re-dissolved in 15 ml acetone with fresh LiBr (0.42g). The solution was stirred for 72 hours and worked up as before. Part 2 was repeated twice to obtain an orange crude product that was purified over 10 g silica gel column eluting with MeOH:EtOAc (1:9) to afford **2.20** (0.28 g; 58%).

^{1}H NMR (600 MHz, $CDCl_3$) δ 4.12 (s, 2H, C(O)-C<u>H</u>$_2$-Br); 4.05 (m, 4H, P-O-C<u>H</u>$_2$); 3.74 (t, *J* = 6.07 Hz, 2H, P-CH_2-CH_2-C<u>H</u>$_2$); 1.95 (m, 2H, P-CH_2-C<u>H</u>$_2$); 1.80 (m, 2H, P-C<u>H</u>$_2$); 1.30 (t, *J* = 7.06 Hz, 6H, P-O-CH_2-C<u>H</u>$_3$) ppm.**^{13}C NMR** (150 MHz, $CDCl_3$) δ 167.9 (s, <u>C</u>=O); 62.34 (d, *J* = 6.72 Hz, 2 x CH_2, P-O-<u>C</u>H_2); 48.4 (d, *J* = 8.48 Hz, P-CH_2-CH_2<u>C</u>H_2); 27.2 (s, <u>C</u>H_2-Br), 22.0 (d, *J* = 140.74 Hz, P-<u>C</u>H_2); 19.0 (d, *J* = 5.18 Hz, P-CH_2-<u>C</u>H_2); 16.3 (d, *J* = 6.01 Hz, 2 x CH_3, P-O-CH_2-<u>C</u>H_3) ppm.

Mass (ESI-MS): Calculated for $C_9H_{19}BrNO_5P$ $[M + H]^+$: 332.0262, Found: 332.0258

Diethyl 3-(*N*-hydroxy-2-iodoacetamido)propylphosphonate (2.21)

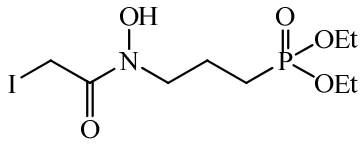

Compound **2.19** (0.11 g; 0.40 mmol) and NaI (0.18 g; 1.21 mmol) were dissolved in 10 ml acetone and stirred for two days at room temperature. The product was filtered and the filtrate was concentrated under reduced pressure. The crude product was dissolved in water (5 ml) and 1.5 g NaI was added. The solution was then extracted with 10 ml EtOAc. The solution was concentrated *in vacuo* to afford 0.09 g (59%) of pure yellow oil.

^{1}H NMR (400 MHz, D_2O) δ 4.23 (m, 4H, P(O)-C<u>H</u>$_2$); 4.05 (s, 2H, C<u>H</u>$_2$-I); 3.79 (br s, 2H, P-CH_2-CH_2-C<u>H</u>$_2$); 2.03 (m, 4H; P-C<u>H</u>$_2$-C<u>H</u>$_2$); 1.41 (t, *J* = 7.0 Hz, 6H, P(O)-CH_2-C<u>H</u>$_3$) ppm. **^{13}C NMR** (100 MHz, D_2O) δ172.4 (s, <u>C</u>=O);64.0 (d, *J* = 6.0 Hz, 2 x CH_2, P(O)-<u>C</u>H_2); 49.0 (d, *J* = 19.0 Hz,P-CH_2-CH_2-<u>C</u>H2); 21.6 (d, *J* = 139.0 Hz, P<u>C</u>H_2); 19.3 (d, *J* = 5.0 Hz,P-CH_2-<u>C</u>H_2); 16.2 (d, *J* = 6.0 Hz, 2 x CH_3, P(O)-CH_2-<u>C</u>H_3); -5.2 (s, <u>C</u>H_2-I) ppm.

Mass (ESI-MS): Calculated for $C_9H_{19}INO_5P$ $[M + H]^+$: 380.0124, Found: 380.0124

IR: ν_{max} 3134, 2981, 2908, 1634 (C=O), 1204, 1017; **UV**: λ_{max} 220.73 nm

Dibenzyl 3-bromopropylphosphonate (2.31)

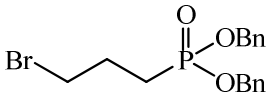

Dibenzyl phosphite (**2.30**, 1.50 ml; 6.79 mmol) was dissolved in 90 ml of anhydrous DMF under N_2 gas. Cs_2CO_3 (6.64 g; 20.39 mmol) and tetramethylammonium iodide $(CH_3)_4NI$; 4.10 g; 20.39 mmol) were added sequentially at room temperature and stirred for 1 h. 1,3-Dibromopropane (2.08 ml; 20.39 mmol) was added and the suspension was stirred for 66 hrs. The suspension was poured into 110 ml of H_2O and extracted three times with EtOAc. The combined organic layer was washed with water (100 ml) three times and then with brine (50 ml). The organic solution was then dried over anhydrous Na_2SO_4 and concentrated *in vaccuo*. SiO_2 gel column chromatography using gradient EtOAc:Hexane from 20% EtOAc to 50% EtOAc gave 1.76 g (67%) of pure product as a colourless oil.

^{1}H NMR (600 MHz, $CDCl_3$) δ 7.34 (m, 10H, P-(O)CH_2-Ph-H); 5.05 (dd, *J* = 9.00, 11.81 Hz, 2H, P-(O)CH_2-Ph-H); 4.96 (dd, *J* = 8.34, 11.83 Hz, 2H, P-(O)CH_2-Ph-H); 3.37 (t, *J* = 6.49 Hz, 2H, P-CH_2-CH_2-CH_2); 2.08(m, 2H, P-CH_2-CH_2); 1.89 (m, 2H, P-CH_2) ppm. **^{13}C NMR** (150 MHz, $CDCl_3$) δ 136.3 (d, *J* = 5.91 Hz, 2 x C, P-O-CH_2-C=CH-); 128.7 (s, 4 x CH, P-O-CH_2-C=CH-CH=); 128.6 (s, 2 x CH, P-O-CH_2-C=CH-CH=CH-); 128.1 (s, 4 x CH, P-O-CH_2-C=CH-); 67.4 (d, *J* = 6.44 Hz, 2 x CH_2, P(O)-CH_2-Ph); 33.5 (d, *J* = 19.04 Hz, P-CH_2-CH_2-CH_2); 25.9 (d, *J* = 4.28 Hz, P-CH_2-CH_2); 24.9(d, *J* = 142.21 Hz,P-CH_2) ppm.

***Tert*-butyl benzyloxy(3-(bis(benzyloxy)phosphoryl)propyl)carbamate (2.32)**

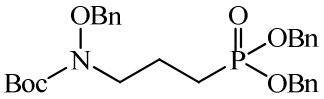

Under dry conditions BocNHOBn (0.80 g; 3.58 mmol) was dissolved in 25 ml freshly dried THF. NaH (0.17 g; 7.09 mmol) was added in portions to the BocNHOBn solution at room temperature and stirred for 30 min. Compound **2.31** (1.38 g; 3.60 mmol) was added dropwise and the reaction mixture was stirred overnight. The suspension was concentrated under reduced pressure and re-suspended in H_2O (30 ml). The aqueous solution was extracted three times with EtOAc (25 ml) and the combined organic phase was washed with brine (20 ml).

The EtOAc solution was then dried over anhydrous Na_2SO_4 and concentrated under reduced pressure. The crude product was purified over silica gel column chromatography eluting with 20:80 EtOAc:Hexane (400ml) then 50:50 EtOAc:Hexane (600 ml) to give the pure compound **2.32** (0.71g; 56%) as a colourless oil in the later fraction.

^{1}H NMR (600 MHz, $CDCl_3$) δ 7.32(m, 15H, P-O-CH_2-Ph-H and N-O-CH_2-Ph-H); 5.02 (m, 2H,P-O-CH_2-Ph-H)4.94 (dd, *J* = 8.26, 11.59 Hz, 2H, P-O-CH_2-Ph-H); 4.77 (s, 2H, N-O-CH_2-Ph-H)); 3.42 (t, *J* = 6.75 Hz, 2H, P-CH_2-CH_2-CH_2); 1.87 (m, 2H, P-CH_2-CH_2); 1.75 (m, 2H, P-CH_2); 1.47 (s, 9H, N-C-(O)-O-C(CH_3)) ppm. **^{13}C NMR** (150 MHz, $CDCl_3$) δ 156.5 (s, N-C-(O)-O-C(CH_3); 136.4 (d, *J* = 5.96 Hz, 2 x C, P-O-CH_2-C=); 135.4 (s, N-O-CH_2-C=); 129.4 (s, 2 x CH, N-O-CH_2-C=CH-CH); 128.6 (s, 4 x CH, P-O-CH_2-C=CH-CH=); 128.5 (s, N- O-CH_2-C=CH-CH=CH); 128.4 (s, 2 x CH, P-O-CH_2-C=CH-CH=CH-); 128.3 (s, 2 x CH, N-O-CH_2-C=CH-); 127.9 (s, 4 x CH, P-O-CH_2-C=CH-); 81.5 (s, N-C-(O)-O-C(CH_3)); 77.0 (s, N-O-CH_2-Ph-H); 67.1 (d, *J* = 6.40 Hz, 2 x CH_2, P-O-CH_2-Ph-H); 49.9 (d, *J* = 19.60 Hz, P-CH_2-CH_2-CH_2); 28.3 (s, 3 x CH_3, N-C-(O)-O-C(CH_3)); 23.5 (d, *J* = 142.29 Hz, P-CH_2); 20.4 (d, *J* = 4.77 Hz, P-CH_2-CH_2) ppm.

Dibenzyl 3-(benzyloxyamino)propylphosphonate (2.33)[115]

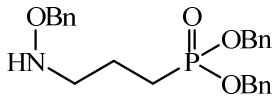

Compound **2.32** (0.38 g; 0.72 mmol) was dissolved in CH_2Cl_2 (10 ml) and cooled to 0^{O}C. TFA (2.77 ml; 36.17) mmol) was added dropwise while the solution was stirred at 0^{O}C for 45 minutes. Volatile components were removed from the solution and the resulting product re-dissolved in saturated solution of $NaHCO_3$ (30 ml). The solution was extracted three times with EtOAc (25 ml) and the combined organic phase was washed with brine (20 ml) and dried over anhydrous Na_2SO_4. The product was concentrated to give **2.33** as pure clear yellow oil (0.30 g; 97 %).

^{1}H NMR (600 MHz, $CDCl_3$) δ 7.31 (m, 15H, P-O-CH_2-Ph-H and N-O-CH_2-Ph-H); 5.04 (dd, *J* = 8.9, 11.7 Hz, 2H, P-O-CH_2-Ph-H); 4.95 (dd, *J* = 8.1, 11.8 Hz, 2H, P-O-CH_2-Ph-H); 4.63 (s, 2H, N-O-CH_2-Ph-H); 2.91 (t, *J* = 6.0 Hz, 2H, P-CH_2-CH_2-CH_2); 1.82 (m, 2H, P-CH_2-CH_2); 1.81 (m, 2H, P-CH_2) ppm. **^{13}C NMR** (150 MHz, $CDCl_3$) δ 137.8 (s, N-O-CH_2-

C=);136.4 (d, *J* = 6.0 Hz, 2 x C, P-O-CH_2-C=); 128.6 (s, Ar-C), 128.4 (s, Ar-C), 128.4 (s, Ar-C), 127.9 (s, Ar-C), 127.8 (s, Ar-C); 76.3 (s, N-O-CH_2-Ph-H); 67.1 (d, *J* = 6.4Hz, 2 x CH_2, P-O-CH_2-Ph-H); 53.0 (d, *J* = 16.8 Hz, P-CH_2-CH_2-CH_2); 23.6 (d, *J* = 141.6 Hz, P-CH_2); 20.5 (d, *J* = 4.9 Hz, P-CH_2-CH_2) ppm.

Dibenzyl 3-(*N*-(benzyloxy)-2-chloroacetamido)propylphosphonate (2.34)

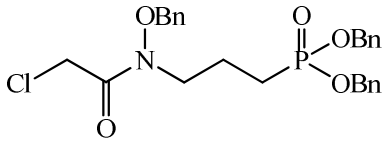

A solution of **2.33** (0.20g; 0.47 mmol) and Et_3N (0.08 ml; 0.56 mmol) in CH_2Cl_2 (30 ml) was stirred at room temperature for 1.5 hr. Chloroacetyl chloride (0.05 ml; 0.56 mmol) was added dropwise and the solution was stirred for a further 2.5 hr. CH_2Cl_2 (30 ml) was added and the solution was washed three times with H_2O (50 ml), twice with a saturated solution of $NaHCO_3$ (50 ml) and once with brine (20 ml). The combined organic phase was dried over $MgSO_4$ and concentrated under reduced pressure. The crude product was purified over SiO_2 gel column chromatography using a gradient solvent system of EtOAc:Hexane. The pure, transparent, light yellow oil of **2.34** was collected in the 10:0 EtOAc fraction (0.11 g; 46%).

^{1}H NMR (600 MHz, $CDCl_3$) δ 7.34(m, 15H, P-O-CH_2-Ph-H and N-O-CH_2-Ph-H); 5.03 (dd, *J* = 9.1, 11.8 Hz, 2H, P-O-CH_2-Ph-H); 4.94 (dd, *J* = 8.4, 11.8 Hz, 2H, P-O-CH_2-Ph-H); 4.78 (s, 2H, N-O-CH_2-Ph-H)); 4.06 (s, 2H, CH_2-Cl); 3.69 (t, *J* = 6.5 Hz, 2H, P-CH_2-CH_2-CH_2); 1.91 (m, 2H, P-CH_2-CH_2); 1.74 (m, 2H, P-CH_2) ppm.**^{13}C NMR** (150 MHz, $CDCl_3$) δ 167.8 (s, C=O); 136.2 (d, *J* = 5.7 Hz, 2 x C, P-O-CH_2-C=); 133.6 (s, N-O-CH_2-C=); 129.2 (s, 3 x N-O-CH_2-C=CH-CH=CH); 128.8 (s, 2 x CH, P-O-CH_2-C=CH-CH=CH-); 128.5 (s, 4 x CH, P-O-CH_2-C=CH-CH=); 128.4 (s, 2 x CH, N-O-CH_2-C=CH-); 127.9 (s, 4 x CH, P-O-CH_2-C=CH-); 76.6 (s, N-O-CH_2-Ph-H); 67.2 (d, *J* = 6.4 Hz, 2 x CH_2, P-O-CH_2-Ph-H); 45.8 (s, P-CH_2-CH_2-CH_2); 41.0 (s, CH_2-Cl) 23.2 (d, *J* = 142.2 Hz, P-CH_2); 19.9 (d, *J* = 4.5 Hz, P-CH_2-CH_2) ppm.

Mass (ESI-MS): Calculated for $C_{26}H_{29}ClNO_5P$ $[M + H]^+$: 502.1550, Found: 502.1548

IR: ν_{max} 3463, 2949, 1669 (C=O), 1238 (P=O), 990; **UV**: λ_{max} 208.52 nm

Dibenzyl 3-(*N*-(benzyloxy)-3-chloropropanamido)propylphosphonate (2.35)

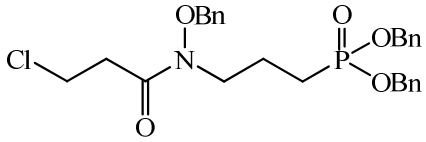

A solution of **2.33** (0.18g; 0.43 mmol) and Et_3N (0.05 ml; 0.35 mmol) in CH_2Cl_2 (30 ml) was stirred at room temperature for 1.5 hr. Chloropropionyl chloride (0.05 ml; 0.51 mmol) was added dropwise and the solution was stirred for a further 2.5 hr. CH_2Cl_2 (30 ml) was added and the solution was washed three times with H_2O (50 ml), twice with a saturated solution of $NaHCO_3$ (50 ml) and once with brine (20 ml). The combined organic phase was dried over $MgSO_4$ and concentrated under reduced pressure. Flash column chromatography (EtOAc/CH_2Cl_2 1:3) of the crude product afforded pure yellow oil of **2.35** (0.05 g; 23%).

^{1}H NMR (600 MHz, $CDCl_3$) δ 7.34 (m, 15H, P-O-CH_2-Ph-H and N-O-CH_2-Ph-H); 5.02 (dd, *J* = 8.9, 11.8 Hz, 2H, P-O-CH_2-Ph-H); 4.94 (dd, *J* = 8.2, 11.8 Hz, 2H, P-O-CH_2-Ph-H); 4.76 (s, 2H, N-O-CH_2-Ph-H)); 3.72 (t, *J* = 6.7 HZ, 2H, CH_2-Cl); 3.67 (t, *J* = 6.0 Hz, 2H, P-CH_2-CH_2-CH_2); 2.79 (t, *J* = 6.5 Hz, 2H, C(O)-CH_2); 1.90 (m, 2H, P-CH_2-CH_2); 1.75 (m, 2H, P-CH_2) ppm. **^{13}C NMR** (150 MHz, $CDCl_3$) δ 171.3 (s, C=O); 136.3 (d, *J* = 5.9 Hz, 2 x C, P-O-CH_2-C=); 134.0 (s, N-O-CH_2-C=); 129.2 (s, 2 x CH, N-O-CH_2-C=CH-CH); 129.1 (s,N- O-CH_2-C=CH-CH=CH); 128.8 (s, 2 x CH, P-O-CH_2-C=CH-CH=CH-); 128.6 (s, 4 x CH, P-O-CH_2-C=CH-CH=); 128.4 (s, 2 x CH, N-O-CH_2-C=CH-); 127.9 (s, 4 x CH, P-O-CH_2-C=CH-); 76.5 (s, N-O-CH_2-Ph-H); 67.2 (d, *J* = 6.5 Hz, 2 x CH_2, P-O-CH_2-Ph-H); 45.4 (s, P-CH_2-CH_2-CH_2); 39.2 (s, CH_2-Cl); 35.4 (s, C(O)-CH_2) 23.3 (d, *J* = 142.2 Hz, P-CH_2); 20.1 (s, P-CH_2-CH_2) ppm.

Mass (ESI-MS): Calculated for $C_{27}H_{31}ClNO_5P$ $[M + H]^+$: 516.1707, Found: 516.1713

IR: ν_{max} 3457, 2954, 1658 (C=O), 1242 (P=O), 991; **UV**: λ_{max} 208.73 nm

Dibenzyl 3-(*N*-(benzyloxy)acrylamido)propylphosphonate (2.36)

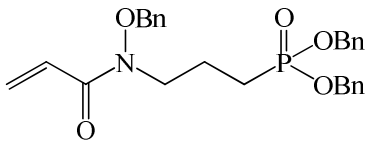

A solution of **2.33** (0.20 g; 0.47 mmol) and Et_3N (0.08 ml; 0.56 mmol) in CH_2Cl_2 (30 ml) was stirred at room temperature for 1.5 hr. Chloropropionyl chloride (0.05 ml; 0.55 mmol) was added dropwise and the solution was stirred for a further 2.5 hr. CH_2Cl_2 (30 ml) was added and the solution was washed three times with H_2O (50 ml), twice with a saturated solution of $NaHCO_3$ (50 ml) and once with brine (20 ml). The combined organic phase was dried over $MgSO_4$ and concentrated under reduced pressure. The crude product was purified over SiO_2 gel column chromatography using a gradient solvent system of EtOAc:Hexane. The pure, transparent, colourless oil of **2.36** collected in the 10:0 EtOAc fraction (0.6 g; 27%).

^{1}H NMR (600 MHz, $CDCl_3$) δ 7.37 – 7.27 (m, 15H, P-O-CH_2-Ph-H and N-O-CH_2-Ph-H); 6.68 (dd, *J* = 10.4, 16.9 Hz, 1H, C(O)-CH); 6.38 (d, *J* = 17.0 Hz, 1H, C(O)-CH-CH_{2A}); 5.71 (d, *J* = 10.6 Hz, 1H, C(O)-CH-CH_{2B}); 5.02 (dd, *J* = 9.0, 11.8 Hz, 2H, P-O-CH_2-Ph-H); 4.94 (dd, *J* = 8.2, 11.8 Hz, 2H, P-O-CH_2-Ph-H); 4.76 (s, 2H, N-O-CH_2-Ph-H); 3.71 (t, *J* = 6.8 HZ, 2H, P-CH_2-CH_2-CH_2); 1.94 (m, 2H, P-CH_2-CH_2); 1.76 (m, 2H, P-CH_2) ppm. **^{13}C NMR** (150 MHz, $CDCl_3$) δ 166.6 (s, C=O); 136.3 (d, *J* = 5.9 Hz, 2 x C, P-O-CH_2-C=); 134.0 (s, N-O-CH_2-C=); 129.2 (s, C(O)-CH-CH_2); 129.1 (s, 2 x CH, N-O-CH_2-C=CH-CH); 129.0 (s, N- O-CH_2-C=CH-CH=CH); 128.7 (s, 2 x CH, P-O-CH_2-C=CH-CH=CH-); 128.5 (s, 4 x CH, P-O-CH_2-C=CH-CH=); 128.3 (s, 2 x CH, N-O-CH_2-C=CH-); 127.9 (s, 4 x CH, P-O-CH_2-C=CH-); 126.1 (s, C(O)-CH); 77.1 (s, N-O-CH_2-Ph-H); 67.1 (d, *J* = 6.4 Hz, 2 x CH_2, P-O-CH_2-Ph-H); 45.7 (s, P-CH_2-CH_2-CH_2); 23.3 (d, *J* = 142.1 Hz, P-CH_2); 20.3 (d, *J* = 4.6 Hz, P-CH_2-CH_2) ppm.

Mass (ESI-MS): Calculated for $C_{27}H_{30}NO_5P$ $[M + H]^+$: 480.1940, Found: 480.1943

IR: ν_{max} 3477, 2947, 1653 (C=O), 1238 (P=O), 986; **UV**: λ_{max} 208.35 nm

Dibenzyl 3-(*N*-(benzyloxy)-4-chlorobutanamido)propylphosphonate (2.37)

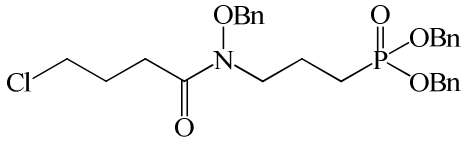

A solution of **2.33** (0.20 g; 0.47 mmol) and Et_3N (0.08 ml; 0.56 mmol) in CH_2Cl_2 (30 ml) was stirred at room temperature for 1.5 hr. Chlorobutryryl chloride (0.06 ml; 0.56 mmol) was added dropwise and the solution was stirred for a further 3.5 hr. CH_2Cl_2 (30 ml) was added and the solution was washed three times with H_2O (50 ml), twice with a saturated solution of $NaHCO_3$ (50 ml) and once with brine (20 ml). The combined organic phase was dried over $MgSO_4$ and concentrated under reduced pressure. The crude product was purified over SiO_2 gel column chromatography eluting first with 100ml EtOAc/Hexane 2:8 then 5:5. The pure oil of **2.37** was collected in the later fraction (0.06 g; 24%).

^{1}H NMR (600 MHz, $CDCl_3$) δ 7.33 (m, 15H, P-O-CH_2-Ph-H and N-O-CH_2-Ph-H); 5.02 (m, Hz, 2H, P-O-CH_2-Ph-H); 4.94 (dd, *J* = 8.5, 11.5 Hz, 2H, P-O-CH_2-Ph-H); 4.76 (s, 2H, N-O-CH_2-Ph-H); 3.65 (br s, 2H, P-CH_2-CH_2-CH_2); 3.56 (t, *J* = 6.1 Hz, 2H, CH_2-Cl); 2.54 (t, *J* = 6.3 Hz, 2H, C(O)-CH_2); 2.03 (m, 2H, C(O)-CH_2-CH_2); 1.90 (m, 2H, P-CH_2-CH_2); 1.74 (m, 2H, P-CH_2) ppm. **^{13}C NMR** (150 MHz, $CDCl_3$) δ 173.9 (s, C=O); 136.3 (d, *J* = 5.9 Hz, 2 x C, P-O-CH_2-C=); 134.2 (s, N-O-CH_2-C=); 129.2 (s, 2 x CH, N-O-CH_2-C=CH-CH); 129.0 (s, N-O-CH_2-C=CH-CH=CH); 128.7 (s, 2 x CH, P-O-CH_2-C=CH-CH=CH-); 128.6 (s, 4 x CH, P-O-CH_2-C=CH-CH=); 128.4 (s, 2 x CH, N-O-CH_2-C=CH-); 127.9 (s, 4 x CH, P-O-CH_2-C=CH-); 76.8 (s, N-O-CH_2-Ph-H); 67.2 (d, *J* = 6.4 Hz, 2 x CH_2, P-O-CH_2-Ph-H); 45.5 (s, P-CH_2-CH_2-CH_2); 44.6 (s, CH_2-Cl); 29.2 (s, C(O)-CH_2); 27.1 (s, C(O)-CH_2-CH_2); 23.4 (d, *J* = 142.1 Hz, P-CH_2); 20.2 (br s, P-CH_2-CH_2) ppm.

Mass (ESI-MS): Calculated for $C_{28}H_{33}ClNO_5P$ $[M + H]^+$: 530.1863, Found: 530.1865

IR: ν_{max} 3465, 2950, 1657 (C=O), 1238 (P=O), 990; **UV**: λ_{max} 210.89 nm

General procedure for the preparation of 3-(*N*-hydroxyamido)propylphosphonic acids 2.1 – 2.3 and 2.38

The benzyl-protected hydroxamic acids **2.34 – 2.37** (0.10 g) were dissolved in 20 ml MeOH. $Pd(OH)_2/C$ (0.02 g) was added to the solution and hydrogen gas was introduced to the mixture by means of a balloon to generate a positive pressure. The suspension was stirred for 1hr 45 minutes at room temperature then filtered over celite. The filtrate was concentrated under reduced pressure to give violet coloured oils **2.1 – 2.3** and **2.38**.

3-(2-chloro-*N*-hydroxyacetamido)propylphosphonic acid (2.1)

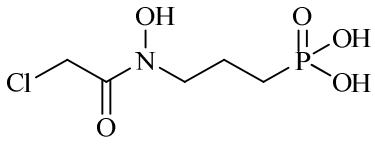

Yield: 0.046 g; 100%. **^{1}H NMR** (600 MHz; D_2O): δ 4.46 (s, 2H, C$\underline{H_2}$-Cl); 3.73 (br s, 2H, P-$CH_2CH_2C\underline{H_2}$); 1.90 (br s, P-CH_2-C$\underline{H_2}$); 1.77 (br s, 2H, P-C$\underline{H_2}$). **^{13}C NMR** (150 MHz; D_2O): δ 169.3 (s, $\underline{C}$=O); 49.3 (br s, P-CH_2-CH_2-$\underline{C}H_2$); 41.6 (s, $\underline{C}H_2$-Cl); 23.8 (d, *J* = 140.9 Hz, P-$\underline{C}H_2$); 19.8 (s,P-$CH_2\underline{C}H_2$) ppm.

Mass (ESI-MS): Calculated for $C_5H_{11}ClNO_5P$ $[M + H]^+$: 232.0142, Found: 232.0139

IR: ν_{max} 3146, 2868, 1619 (C=O), 1220 (P=O), 1128; **UV**: λ_{max} 211.38 nm

3-(3-chloro-*N*-hydroxypropanamido)propylphosphonic acid (2.2)

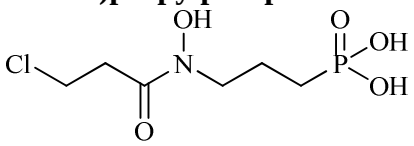

Yield: 0.046 g; 96%. **^{1}H NMR** (600 MHz, D_2O) δ 3.90 (t, *J* = 5.9 HZ, 2H, C$\underline{H_2}$-Cl); 3.79 (t, *J* = 6.4 Hz, 2H, P-CH_2-CH_2-C$\underline{H_2}$); 3.11 (t, *J* = 6.0 Hz, 2H, C(O)-C$\underline{H_2}$); 1.95 (m, 2H, P-CH_2-C$\underline{H_2}$); 1.73 (m, 2H, P-C$\underline{H_2}$) ppm. **^{13}C NMR** (150 MHz, D_2O) δ 172.7 (s, C=O); 48.8 (s, P-CH_2-CH_2-$\underline{C}H_2$); 39.7 (s, $\underline{C}H_2$-Cl); 34.8 (s, C(O)-$\underline{C}H_2$) 24.5 (d, *J* = 136.6 Hz, P-$\underline{C}H_2$); 20.3 (s, P-CH_2-$\underline{C}H_2$) ppm.

Mass (ESI-MS): Calculated for $C_6H_{13}ClNO_5P$ $[M + H]^+$: 246.0298, Found: 246.0300

IR: ν_{max} 3153, 2924, 1615 (C=O), 1054; **UV**: λ_{max} 208.29 nm

3-(N-hydroxypropionamido)propylphosphonic acid (2.38)

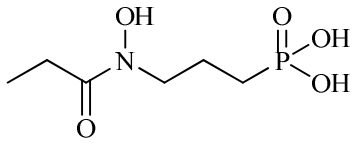

Yield: 0.044 g; 100%. **^{1}H NMR** (600 MHz, D_2O) δ 3.77 (s, 2H, P-CH_2-CH_2-C$\underline{H_2}$); 2.59 (br s, 2H, C$\underline{H_2}$-CH3); 1.95 (br s, 2H, P-CH_2-C$\underline{H_2}$); 1.80 (br s, 2H, P-C$\underline{H_2}$); 1.15 (br s, 3H, CH_2C$\underline{H_3}$) ppm.**^{13}C NMR** (150 MHz, D_2O) δ 177.6 (s, C=O); 48.6 (s, P-CH_2-CH_2-$\underline{C}H_2$); 25.4 (s, $\underline{C}H_2$-CH_3); 23.6 (s, P-$\underline{C}H_2$); 20.1 (s, P-CH_2-$\underline{C}H_2$); 8.6 (s, CH_2-$\underline{C}H_3$).

Mass (ESI-MS): Calculated for $C_6H_{14}NO_5P$ $[M + H]^+$: 212.0688, Found: 212.0694

IR: ν_{max}3164, 2876, 1598, 1217, 925; **UV**: λ_{max} 207.89 nm

3-(4-chloro-N-hydroxybutanamido)propylphosphonic acid (2.3)

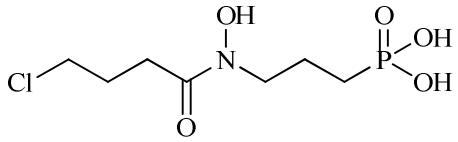

Yield: 0.015 g; 30%. **^{1}H NMR** (600 MHz, D_2O) δ 3.70 (t, *J* = 6.4 Hz, 2H, C$\underline{H_2}$-Cl); 3.66 (t, *J* = 6.5 Hz, 2H, P-CH_2-CH_2-C$\underline{H_2}$); 2.49 (t, *J* = 7.5 Hz, 2H, C(O)-C$\underline{H_2}$); 2.11 (m, 2H, C(O)-CH_2-C$\underline{H_2}$); 2.06 (m, 2H, P-CH_2-C$\underline{H_2}$); 1.86 (m, 2H, P-C$\underline{H_2}$) ppm. **^{13}C NMR**: Could not be obtained due to fast degradation.

Mass (ESI-MS): Was not obtained as product was mixed

IR: ν_{max} 3135, 2873, 1616 (C=O), 1240 (P=O); **UV**: λ_{max} 206.88 nm

Dibenzyl 3-(*N*-(benzyloxy)-2-iodoacetamido)propylphosphonate (2.39)

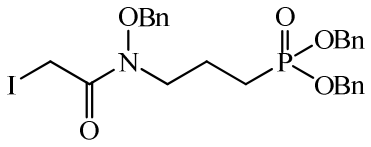

Compound **2.34** (0.16 g; 0.32 mmol) and NaI (0.15 g; 0.97 mmol) were dissolved in 20 ml acetone at room temperature and stirred overnight. The resulting suspension was filtered and the filtrate was concentrated under reduced pressure. The crude product was re-dissolved in 20 ml EtOAc and washed with 10 ml of water and then with 5 ml of brine. The organic layer was dried over Na_2SO_4 and concentrated *in vacuo* to yield **2.39** as a yellow oil (0.18 g; 97%).

^{1}H NMR (600 MHz, $CDCl_3$) δ 7.33 (m, 15H, P-O-CH_2-Ph-H and N-O-CH_2-Ph-H); 5.03 (dd, *J* = 9.1, 11.6 Hz, 2H, P-O-CH_2-Ph-H); 4.94 (dd, *J* = 8.2, 11.8 Hz, 2H, P-O-CH_2-Ph-H); 4.85 (s, 2H, N-O-CH_2-Ph-H)); 3.70 (s, 2H, CH_2-I); 3.69 (br s, 2H, P-CH_2-CH_2-CH_2); 1.93 (m, 2H, P-CH_2-CH_2); 1.79 (m, 2H, P-CH_2) ppm.**^{13}C NMR** (150 MHz, $CDCl_3$) δ 169.7 (s, C=O); 136.3 (d, *J* = 5.7 Hz, 2 x C, P-O-CH_2-C=); 133.8 (s, N-O-CH_2-C=); 129.19 (s, 2 x CH, N-O-CH_2-C=CH-CH); 129.16 (s, N- O-CH_2-C=CH-CH=CH); 128.8 (s, 2 x CH, P-O-CH_2-C=CH-CH=CH-); 128.6 (s, 4 x CH, P-O-CH_2-C=CH-CH=); 128.4 (s, 2 x CH, N-O-CH_2-C=CH-); 127.9 (s, 4 x CH, P-O-CH_2-C=CH-); 76.3 (s, N-O-CH_2-Ph-H); 67.2 (d, *J* = 6.4 Hz, 2 x CH_2, P-O-CH_2-Ph-H); 45.4 (s, P-CH_2-CH_2-CH_2); 23.2 (d, *J* = 141.8 Hz, P-CH_2); 19.6 (s, P-CH_2-CH_2);-5.1 (s, CH_2-I) ppm.

Diethyl 3-(*N*-(*tert*-butyloxycarbonyl)-2-chloroacetamido)propylphosphonate (2.42)

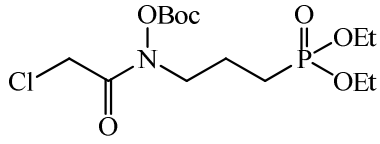

Et_3N (0.08 ml; 0.54 mmol) was added to a solution of compound **2.19** (0.16 g; 0.54 mmol) in 15 ml dry THF, was added at room temperature and the mixture was stirred for 10 minutes. Di-*tert*-butyl dicarbonate (Boc_2O; 0.12 g; 0.54 mmol) was pre-dissolved in 5 ml THF and added dropwise at room temperature to the solution of **2.19**. The reaction was stirred overnight then concentrated under reduced pressure. The crude product was re-dissolved in

20 ml CH_2Cl_2 and washed consecutively with 10 ml saturated solution of $NaHCO_3$, H_2O and brine. The organic phase was dried over anhydrous $MgSO_4$ and concentrated *in vacuo*. The concentrated organic fraction was purified over SiO_2 gel chromatography eluting with 50 ml consecutively with 100% CH_2Cl_2, 50:50 CH_2Cl_2: EtOAc, 100% EtOAc and 100% MeOH. The pure **2.42** was obtained from the 100% EtOAc fraction as a clear colourless oil (0.08g, 38%).

^{1}H NMR (400 MHz; $CDCl_3$): δ 4.06 (s, 2H, C$\underline{H_2}$-Cl); 4.04 (m, 4H, P-O-C$\underline{H_2}$-CH_3); 3.78 (t, *J* = 6.5 Hz, 2H, P-$CH_2CH_2C\underline{H_2}$); 1.89 (m, 2H, P-CH_2-C$\underline{H_2}$); 1.73 (m, 2H, P-C$\underline{H_2}$); 1.50 (s, 9H, N-O-C(O)-O-C(C$\underline{H_3}$)$_3$); 1.27 (t, *J* = 7.0 Hz, 6H, P-O-CH_2-C$\underline{H_3}$). **^{13}C NMR** (100 MHz; $CDCl_3$): δ 166.7 (s, $\underline{C}$=O); 151.4 (s, N-O-$\underline{C}$(O)-O-C$(CH_3)_3$); 86.9 (s; N-C(O)-O-$\underline{C}(CH_3)_3$); 61.6 (d, *J* = 6.5 Hz, 2 x CH_2, P-O-$\underline{C}H_2$-CH_3); 49.0 (s, P-CH_2-CH_2-$\underline{C}H_2$); 40.6 (s, $\underline{C}H_2$-Cl); 27.4 (s, 3 x CH_3, N-C(O)-O-C($\underline{C}H_3$)$_3$); 22.7 (d, *J* = 143.2 Hz, P-$\underline{C}H_2$); 20.0 (d, *J*= 4.0 Hz, P-$CH_2\underline{C}H_2$); 16.3 (d, *J* = 6.0 Hz, 2 x CH_3, P-O-CH_2-$\underline{C}H_3$).

Mass (ESI-MS): Calculated for $C_{14}H_{27}ClNO_7P$ $[M + H]^+$: 388.1290, Found: 388.1289

IR: ν_{max}3154, 2983, 1663 (C=O), 1259 (P=O), 1027

Diethyl 3-(*N*-(*tert*-butoxycarbonyloxy)-2-iodoacetamido)propylphosphonate (2.43)

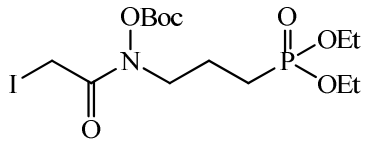

Compound **2.42** (0.08 g; 0.20 mmol) and NaI (0.92 g; 0.62 mmol) were dissolved in 15 ml acetone at room temperature and stirred overnight. The resulting suspension was filtered and filtrate was concentrated under reduced pressure. The crude product was re-dissolved in 20 ml EtOAc and washed with 10 ml of water and then with 5 ml of brine. The organic layer was dried over Na_2SO_4 and concentrated *in vacuo* to yield **2.43** as yellow oil (0.07 g; 67%).

^{1}H NMR (400 MHz; $CDCl_3$): δ 4.07 (m, 4H, P-O-C$\underline{H_2}$-CH_3); 3.78 (t, *J* = 6.6 Hz, 2H, P-$CH_2CH_2C\underline{H_2}$); 3.72 (s, 2H, C$\underline{H_2}$-I); 1.91 (m, 2H, P-CH_2-C$\underline{H_2}$); 1.77 (m, 2H, P-C$\underline{H_2}$); 1.53 (s, 9H, N-O-C(O)-O-C(C$\underline{H_3}$)$_3$); 1.29 (t, *J* = 6.4 Hz, 6H, P-O-CH_2-C$\underline{H_3}$). **^{13}C NMR** (100 MHz;

$CDCl_3$): δ 171.1 (s, C=O); 151.3 (s, N-O-C(O)-O-C(CH_3)$_3$); 86.8 (s; N-C(O)-O-C(CH_3)$_3$); 61.6 (d, *J* = 6.5 Hz, 2 x CH_2, P-O-CH_2-CH_3); 48.4 (s, P-CH_2-CH_2-CH_2); 27.5 (s, 3 x CH_3, N-C(O)-O-C(CH_3)$_3$); 22.7 (d, *J* = 143.9 Hz, P-CH_2); 19.9 (br s, P-CH_2CH_2); 16.4 (d, *J* = 6.0 Hz, 2 x CH_3, P-O-CH_2-CH_3); -6.3(s, CH_2-I).

Mass (ESI-MS): Calculated for $C_{14}H_{27}INO_7P$ $[M + H]^+$: 480.0650, Found: 480.0657

CHAPTER 3

3. SYNTHESIS OF CHLOROQUINE-FOSMIDOMYCIN HYBRIDS

3.1 INTRODUCTION

Hybridization of drugs has been employed as an effective strategy to overcome drug resistance in different areas of medicinal chemistry. Drug hybridization involves linking two or more individual drugs or pharmacophores by a covalent bond to make one drug compound.[148] It has become common practice to use a combination of drugs to treat infectious diseases in order to prevent emergence of resistance to the individual drugs and improve efficacy due to synergistic effects of the individual drugs. Hybrid drugs while sharing the advantages of drug combinations also offer a simpler way of delivering the drugs. Other advantages of hybrid drugs may include better patient compliance and more predictable pharmacokinetic-pharmacodynamic relationship as compared to two separately dosed drugs.

There has been an increased interest in development of hybrid drugs for the treatment of malaria in recent years. Many of these hybrids involve hybridization of two known antimalarial drugs e.g. artemisinin-quinine hybrid (Figure 3.1, **1.35**)[50] or two known drugs with different biological activity such as chloroquine-imipramine hybrid (Figure 3.1, **3.1**).[149] The artemisinin-quinine hybrid (**1.35**) combines the fast-acting property of artemisinin with the slower and longer acting quinine such that the hybrid has the advantage of a longer half-life than artemisinin and has a quick onset of action when compared to quinine alone. The chloroquine-imipramine hybrid (**3.1**) was designed to reverse chloroquine resistance even though imipramine is not a known antimalarial agent. Since the discovery that chloroquine resistance can be reversed, several diverse molecules, termed reversal agents, have been identified to reverse chloroquine resistance. Some of the reversal agents have been studied to have two aromatic rings usually with an aliphatic nitrogen a few atoms away from the aromatic rings. They are postulated to bind and prevent the chloroquine transporter protein PfCRT from actively removing chloroquine from the digestive vacuole of the parasite (section 1.3.1).[58] Examples of identified reversal agents include the calcium channel blocker verapamil,[150] antipsychotics such as imipramine[151] and antihistamines such as

chlorpheniramine.[152] In this study we investigated hybridized chloroquinoline compound with fosmidomycin derivatives.

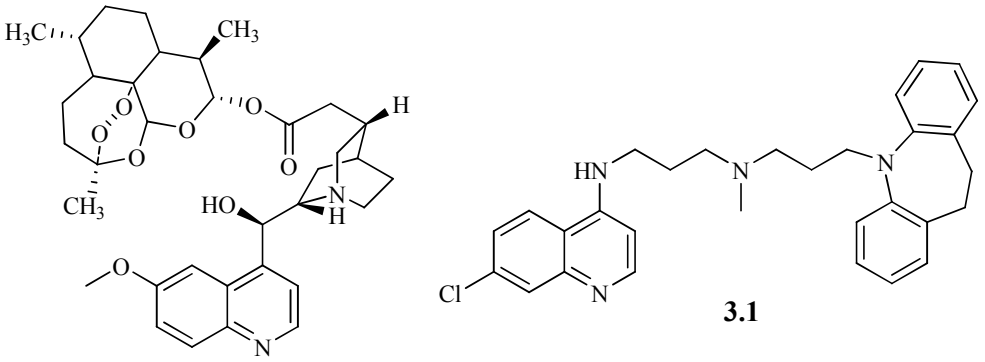

Figure 3.1. Antimalarial hybrids

Fosmidomycin (**1.46**) and its acetyl analogue FR900098 (**1.45**) as discussed in chapter 1 are inhibitors of DXR in organisms such as *E. coli*, *P. falciparum*, and *M. tuberculosis*. Many organisms possessing this enzyme require an active uptake of fosmidomycin and FR900098 in order to inhibit the enzyme because the compounds are highly hydrophilic and cannot pass through membranes unaided. It thus follows that provided these compound could be absorbed into the bacteria or plasmodium species, there is a chance that they could inhibit DXR and hence the growth of the parasites. Increasing their lipophilic property through ester prodrugs has been shown to increase their oral absorption as well as absorption into the parasite. We postulated that increasing the lipophilicity of the DXR inhibitors through hybridization with a known antimalarial compound would not only increase the absorption of the compounds into the parasite but could also provide a dual mode of action for such a hybrid. This is true especially if both drugs have different targets within the plasmodium parasite, which is a desired property for malaria chemotherapy.

Chloroquine (**1.10**) was considered for hybridization with fosmidomycin due to its low side effect profile, affordability as well as the history of its antiplasmodial success when hybridized with other compounds such as shown in Figure 3.1. Chloroquine (CQ) resistance (section 1.3.1) is due to mutations in the chloroquine resistance transporter (PfCRT) protein and not the ability of the drug to inhibit its target. Hybridizing a CQ-like molecule with

fosmidomycin analogues to form a single compound could help overcome the limitations of individual compounds. Of particular interest to us was whether we could produce a hybrid compound containing an active fosmidomycin component with improved pharmacokinetic profile. Although we focus on using chloroquine as hybrid component, in this study, it may be possible to use other antimalarial drugs in a similar way. A chloroquine-fosmidomycin hybrid may accumulate in the digestive vacuole which would mean that it's likely not going to reach sufficient concentrations in the apicoplast. In this case it will act as a chloroquine analogue targeting haem detoxification. However, of it is actively transported out of the digestive vacuole it will then likely reach the required concentrations to target the apicoplast. Furthermore, the most important aspect of this study is to explore the feasibility of extending the acyl chain in fosmidomycin into the NADPH binding pocket to give rise to a completely novel series of DXR inhibitors.

The hybrid of CQ and fosmidomycin was designed such that chloroquine and fosmidomycin retain their functional groups which are necessary for antiplasmodial activity. This meant that the CQ moiety would consist of its chloroquinoline core for activity as well as two basic nitrogen atoms for concentration within the acidic digestive vacuole of the parasite. The fosmidomycin moiety would also retain the phosphonate group and the retrohydroxamate group which is necessary for metal chelation at the active site of the DXR enzyme where it exhibit its inhibitory property.

3.1.1 **Approach to the design and synthesis of chloroquine-fosmidomycin hybrids**

It has been established that the binding pocket at the active site of DXR into which fosmidomycin binds requires a free phosphonic acid in order to bind and inhibit the enzyme.[88] Hybridization of fosmidomycin to chloroquine derivative was considered at the phosphonate end, the hydroxamate end and at the α-position to the phosphorus. Due to the fact that the enzyme is flexible, it has been suggested that the phosphonate binding pocket within the DXR active site might also be able to accommodate a very small functional group but not a group as big as a chloroquinoline derivative. This left the options of hybridizing the fosmidomycin analogue with the quinoline derivative on the carbon at α-position to the phosphorus atom or at the hydroxamate side chain. This resulted in the two proposed hybrid

structures **3.2** and **33** respectively (Figure 3.2). While substitution of fosmidomycin (**1.46**) and FR900098 (**1.45**) at these two sites often show reduced inhibitory activity of the compounds, some successes have been reported such as the α-substituted compound **1.80** (section 1.7.5) and the extended side chain analogue **1.70** (section 1.6.4) discussed in Chapter 1. Recent research in DXR inhibitor design has focused on exploring the binding pocket alpha to the phosphonate.[104, 107, 121, 130] Relatively little attention has been paid to the possibility of exploring the NADPH binding pocket of DXR. Support for this idea was obtained from docking studies of the fosmidomycin-chloroquine hybrids **3.3** and **3.4** (Figure 3.2) on DXR in the absence of NADPH, which gave promising inhibition results on *E. coli* DXR (Chapter 4).

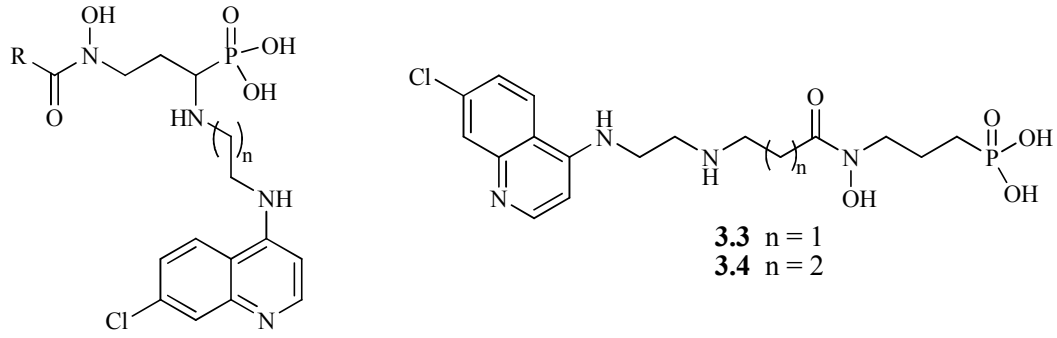

Figure 3.2. Proposed structures of chloroquine-fosmidomycin hybrids

Our synthetic strategy employed a convergent synthesis of the hybrid by first constructing the fosmidomycin and the chloroquine moieties separately (Scheme 3.1). While the aminoquinoline moiety can be easily synthesized by reactions of appropriate diaminoalkane with 4,7-dichloroquinoline (**2.6**), the synthesis of the fosmidomycin component is somewhat more complicated as described in Chapter 2. A retrosynthetic method for the synthesis of chloroquine-fosmidomycin hybrids **3.3** and **3.4** was developed (Scheme 3.4). Implementing the synthetic method then gave rise to some of the halogenated fosmidomycin which was explored in the previous chapter. Aminoquinoline (**3.5**) is easily synthesised from the reaction of 4,7-dichloroquinoline (**3.6**) and diaminoethane (**3.7**). Reaction of the quinoline with the halogenated analogues was expected to result in chloroquine-fosmidomycin hybrids.

The antiplasmodial results of the halogenated fosmidomycin analogues had shown the derivatives with acetyl side chain to be the most potent and to a lesser extent the propyl

analogues. It was unknown if the length of the side chain, which was to be a linker between the hybridized compounds, would have any effect on the antiplasmodial activity of the hybrids. Thus the effect of varying the length of the carbon chain between the fosmidomycin and the aminoquinoline group was investigated by synthesizing hybrids with acetyl and propyl linkers (**3.3** and **3.4** respectively).

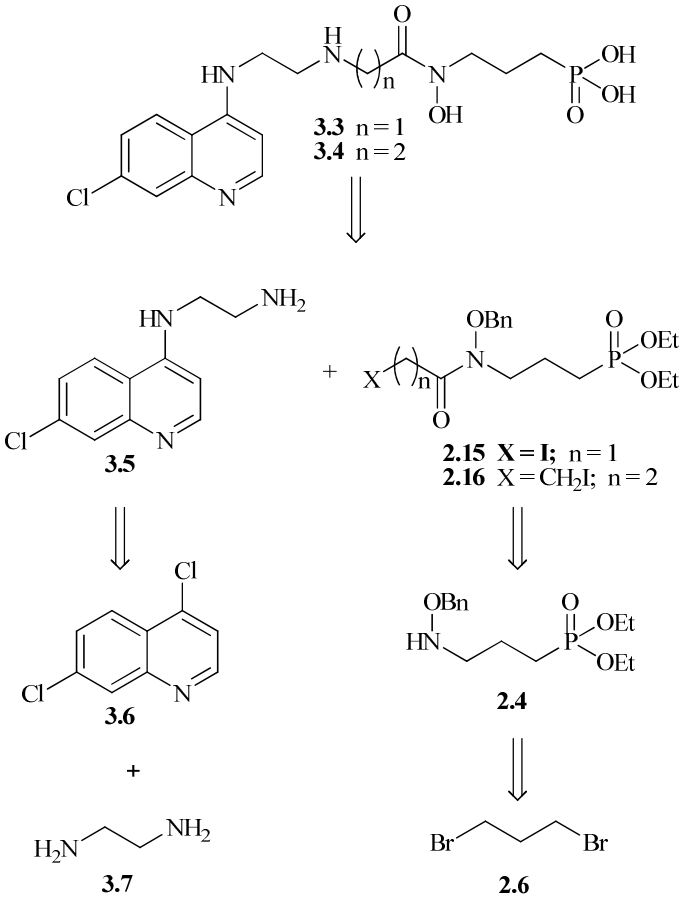

Scheme 3.1. Retrosynthetic analysis of the chloroquine-fosmidomycin hybrids

3.2 RESULTS AND DISCUSSION

3.2.1 **Synthesis of chloroquine-fosmidomycin hybrids**

A detailed discussion of the synthesis of a number of halogenated FR900098 analogues is presented in Chapter 2. The synthesis of the chloroquine part of the hybrid involve the

reaction of 4,7-dichloroquinoline (**3.6**) with 1,2-diaminoethane (**3.7**) by heating at 110°C for six hours to obtain **3.5**.[153] Compound **3.5** possesses the chloroquinoline core and two basic nitrogen atoms required for the compound to be active against plasmodium species. The fosmidomycin components of the hybrid included the iodoacetyl derivative **2.15** and the iodopropionyl derivatives **2.16**. In two separate reactions **2.15** and **2.16** were stirred with **3.5** at room temperature overnight to obtain **3.8** and **3.9** respectively (Scheme 3.2). The primary amine of **3.5** was able to displace iodine from the fosmidomycin components to covalently link the two parts of the hybrids, giving **3.8** in 48% yield and **3.9** in 79% yield.

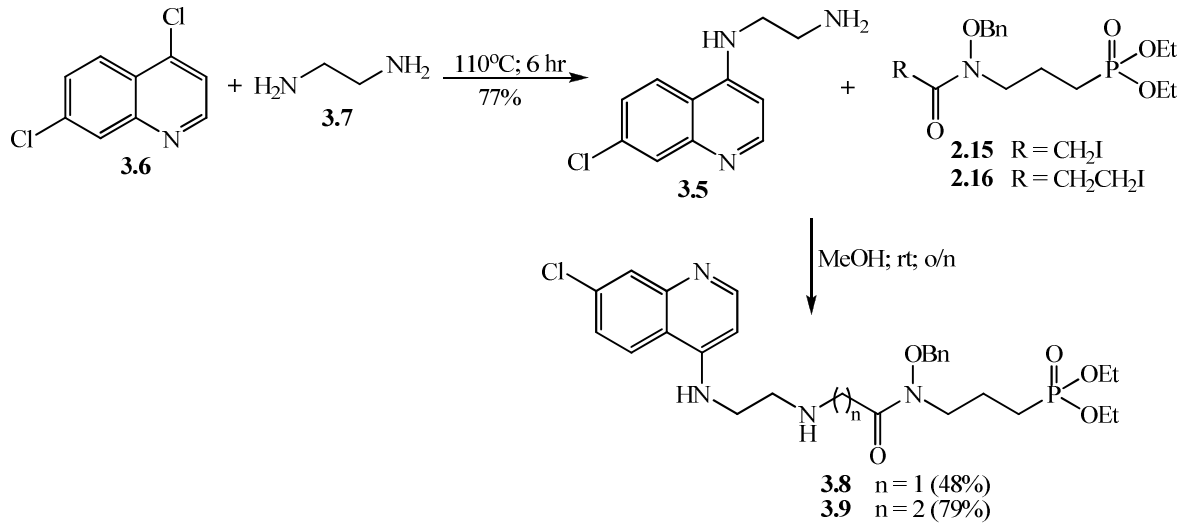

Scheme 3.2. Synthesis of chloroquine-fosmidomycin hybrids **3.8** and **3.9**

3.2.2 **Structure analysis of chloroquine-fosmidomycin hybrids**

High resolution mass spectroscopy of **3.9** showed a molecular ion peak at *m/z* 577.2339. This is consistent with the molecular formula $C_{28}H_{38}ClN_4O_5P$ expected for the hybrid. Due to the fact that the hybrid was synthesized by combining the completely synthesized quinoline and fosmidomycin analogue segments it was not surprising to see that the NMR spectra of the hybrid was similar in part to the NMR spectra of the individual components with characteristic phosphonate splitting as described in Chapter 2.

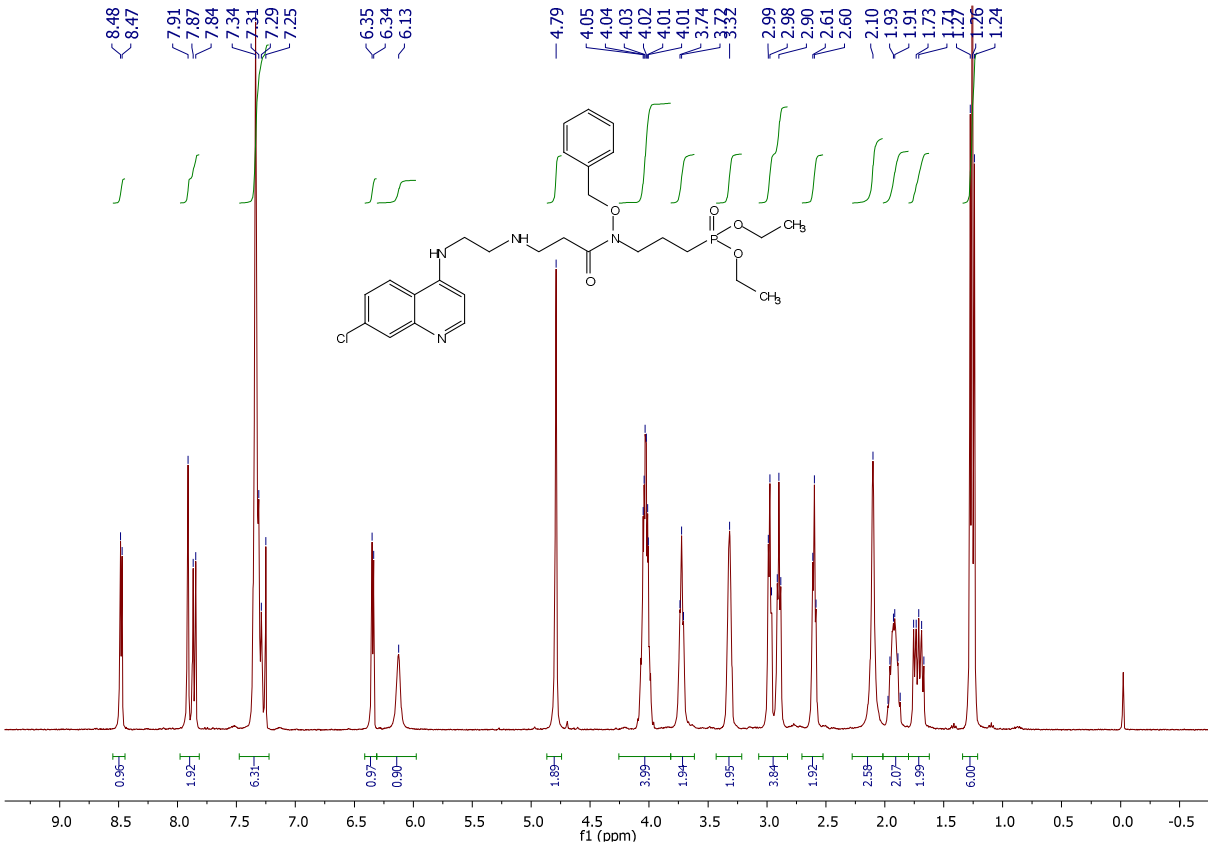

Figure 3.3. ^{1}H NMR spectrum ($CDCl_3$, 400 MHz) of **3.9**

Two dimensional and one dimensional NMR analysis of the hybrids were conducted to ensure that the two segments making up the hybrids were linked and were not present as individual components of a mixture. The ^{1}H NMR spectrum of **3.9** showed eight methylene protons (Figure 3.3 and Table 3.1) with characteristic overlapping of the phosphorus coupled signals. The methylene at δ 4.04 was coupled to the methyl triplet at δ 1.26, confirming the ethyl ester group of the compound. The methylene shift at δ 1.93 (H-2) showed ^{1}H-^{1}H COSY correlations to δ1.73 (H-1) and 3.37 (H-3), which is the same pattern observed for H-1, H-2 and H-3 for compound **2.16**. The more deshielded signals at δ 2.60 (H-5) and 2.90 (H-6) showed COSY correlations to each other and an HMBC correlations to the carbonyl carbon at δ 173.97 (C-4). The most important relationship was the HMBC correlations of the methylene protons at δ 2.90 (H-6) and 2.97 (H-7) to the carbons at δ 46.99 (C-7) and 43.93 (C-6) respectively (Table 3.1). This confirmed that the two components i.e. the quinoline and the fosmidomycin analogue components making up the hybrid were linked. The structure of

3.8 was similarly elucidated and all other spectroscopic data obtained for **3.8** and **3.9** confirmed the structures of the hybrids.

Table 3.1. ^{1}Dand ^{2}D NMR (400 MHz) data of **3.9** in $CDCl_3$

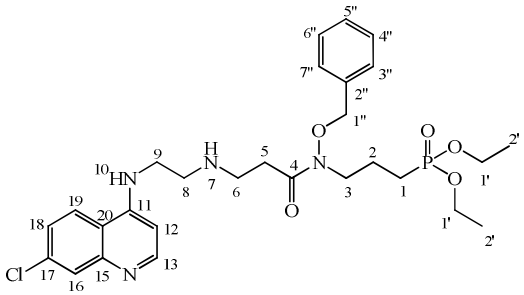

Position[II]	δ **^{1}H (#; mult; J_{HZ})**	**^{13}C (#; mult; J_{HZ})**	**^{1}H-^{1}H COSY**	**^{1}H-^{13}C HMBC**
2’	1.26 (6H; t; 7.0)	16.39 (2 x CH_3; d; 5.9)	H-1’	C-1’
1’	4.11 – 3.96 (4H; m)	61.61 (2 x CH_2; d; 6.5)	H-2’	C-2’
1	1,79 – 1.66 (2H; m)	22.97 (CH_2; d; 142.7)	H-2	C-2
2	2.01 – 1.85 (2H; m)	20.20 (CH_2; br s)	H-1; H-3	C-1
3	3.72 (2H; t; 6.2)	45.37 (CH_2; s)	H-2	C-2
4		173.97 (C=O; s)		
5	2.60 (2H; t; 5.6)	32.41 (CH_2; s)	H-6	C-4; C-6
6	2.90 (2H; t; 5.7)	43.93 (CH_2; s)	H-5	C-4; C-7; C-8
8	2.97 (2H; t; 5.4)	46.99 (CH_2; s)	H-9	C-6
9	3.32 (2H; s)	41.93 (CH_2; s)	H-8; H-10	
10	6.13 (1H; br s)		H-9	
11		150.08 (C; s)		
12	6.34 (1H; d; 5.4)	98.97 (CH; s)	H-13	C-13
13	8.48 (1H; d; 5.3)	151.90 (CH; s)	H-12	C-11
15		140.03 (C; s)		
16	7.91 (1H; s)	128.43 (CH; s)		C-18
17		134.72 (C; s)		
18	7.37 – 7.26 (1H; m)*	125.00 (CH; s)	H-19	C-20
19	7.86 (1H; d; 8.9)	121.88 (CH; s)	H-18	C-11
20		117. 47 (C; s)		
1”	4.79 (2H; s)	76.38 (CH_2; s)		
2” – 7”	7.37 – 7.26 (5H; m)*			
2”		134. 10 (CH; s)		
4” and 6”		129.13 (2 x CH; s)		
5”		129.06 (CH; s)		
3” and 7”		128.73 (2 x CH; s)		

*overlapping chemical shifts

[II]Atoms are numbered for easier comparison and are not the standard numbering system

3.2.3 **Attempted Deprotection of the Chloroquine-fosmidomycin hybrids**

Deprotection of the hybrid was desired to compare the effect of the free phosphonic acid on absorption and antiplasmodial activity of the compounds. This was attempted in stages i.e. debenzylation of the hybrids followed by ester hydrolysis. Initial attempts to remove the benzyl protecting group of **3.8** by hydrogenation using Pd/C resulted in degradation of the sample. The catalyst was then changed to $Pd(OH)_2/C$, also to no avail. It was suspected that the presence of the aliphatic amines was hindering hydrogenolysis of the hybrid as they have been known to cause problems during debenzylation.[154] To investigate this hypothesis 1,2-diaminoethane (**3.7**) was reacted with the alkene analogue **2.10** of **2.16** to produce **3.10** and thereafter hydrogenolysis of the product was conducted with Pd/C. The reaction was successful and the benzyl protecting group was hydrolysed from the N-oxime to afford **3.11** (Scheme 3.3). This disproved the hypothesis that the aliphatic amines were responsible for the prevention of hydrolysis of the benzyl group from the hybrid. Unfortunately no reaction was observed between 4,7-dichloroquinoline (**3.6**) and **3.11** when stirred together overnight to try and obtain the desired benzyl deprotected hybrid **3.12**.

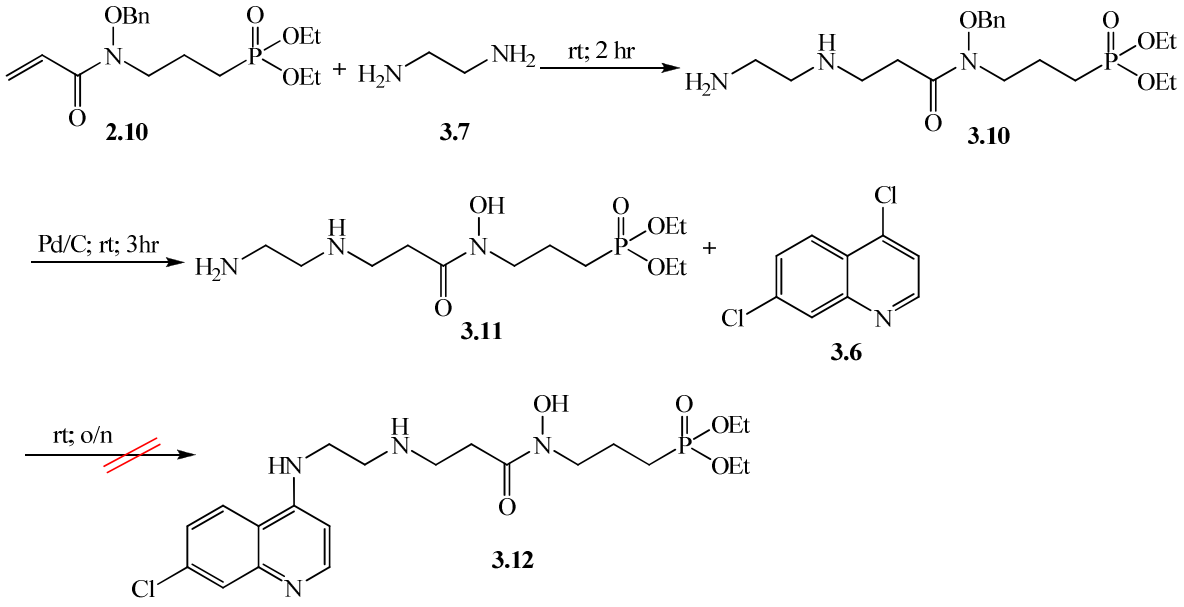

Scheme 3.3. Attempted preparation of deprotected hybrid **3.12**

The hydrogenolysis method was modified to attempt debenzylating **3.9**. The reaction was carried out under inert atmosphere, which involved degassing a hot mixture of **3.9** with Pd/C in MeOH and introducing N_2 gas. Cyclohexene was added to the system as the hydrogen donor and stirred overnight at room temperature. The crude product after workup did not show the desired semi-deprotected hybrid **3.12**.

After all attempts to use a mild hydrogenation method failed, a harsher method of debenzylation using BCl_3 was employed. Due to the small amount of hybrid available, the method was carried out on the fully protected fosmidomycin backbone **2.7** in order to determine if the method will be successful in the production of **3.13** before applying it to the hybrids. A 1 M solution of BCl_3 in CH_2Cl_2 was introduced into the reaction vessel containing **2.7** in dry CH_2Cl_2 at -78^{o}C. The temperature was kept at -60^{o}C for three hours and thereafter allowed to heat up to room temperature and stirred overnight (Scheme 3.4). ^{1}H NMR of the crude product after work up did not indicate presence of the Boc group and an attempt to purify this crude product mixture did not yield the desired compound.

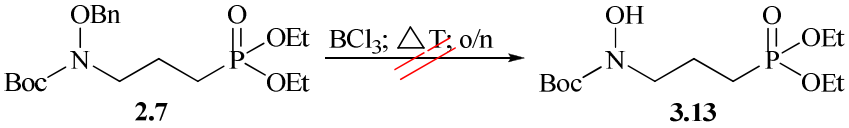

2.7 **3.13**

Scheme 3.4. Attempted debenzylation of fosmidomycin backbone **2.7**

In a last attempt to deprotect the hybrid, the ethyl group of the phosphate ester of **3.9** was substituted with benzyl group. The benzyl protected hybrid **3.14** was synthesized by reacting **3.5** with **2.363**, a benzyl protected analogue of **2.10**. The hybrid was then hydrogenated at atmospheric pressure using Pearlman's catalyst and AcOH (Scheme 2.5). Analysis of the ^{1}H NMR of the product showed broad peaks that were inconclusive in determining the presence of starting material or product. However, the benzyl group still appeared in the spectrum indicating that the reaction had again been ineffective at yielding the desired unprotected hybrid **3.4**.

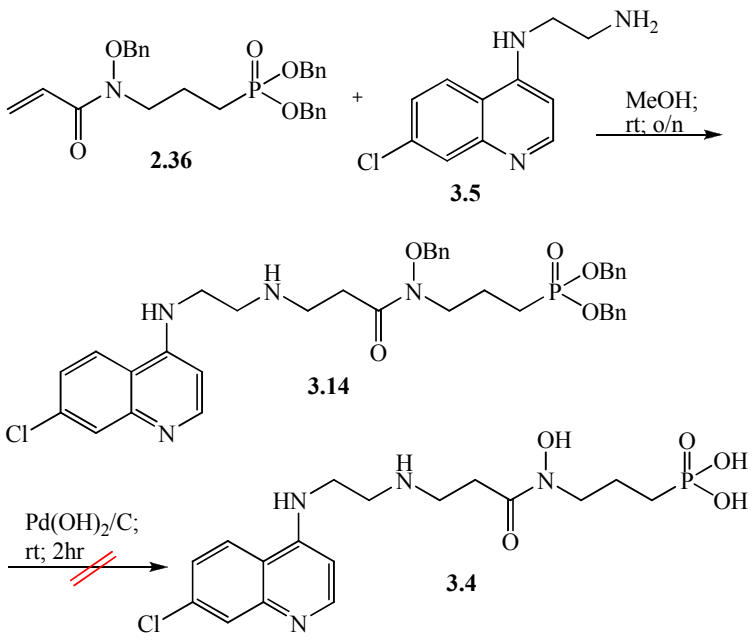

Scheme 3.5. Attempted synthesis of deprotected hybrid **3.4**

Having unsuccessfully attempted various methods of benzyl deprotection to synthesize the free hybrid, it was decide that the protected hybrid alone would be tested for antiplasmodial activity. Whilst it would have been useful to compare the effectiveness of the protected hybrid versus the unprotected hybrid, the antiplasmodial activity of the protected hybrid was expected to be higher against the *Plasmodium* parasite. This is because the protective groups would increase the lipophilicity of the compounds. This in turn would increase the absorption of the compound into the parasite where *in vivo* deprotection might occur to release the free hybrid for activity.

3.2.1 **Antiplasmodial activity of fosmidomycin hybrids**

Antiplasmodial activity of the hybrids and their intermediates were determined against CQR Gambian FCR-3 strain of *P. falciparum*. The chloroquinoline group of compounds showed the best antiplasmodial activity against the parasite even when compared with the active halogenated fosmidomycin analogues (Table 3.2), exhibiting $IC_{50} < 5\mu M$.

Table 3.2 Antiplasmodial activity of Chloroquine-fosmidomycin and their intermediates against CQS D10 and CQR FCR-3 strains of *P. falciparum*

		% parasite survival (CQS D10)				CQR FCR-3	
Comp		**20 (µg/ml)**	**10 (µg/ml)**	**5 (µg/ml)**	***IC_{50} (µM)**	**IC_{50} (µM)**	**SD**
3.5	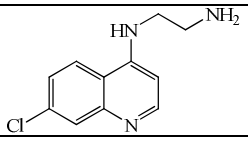	6.5	3.3	8.7	15.2	0.02	0.01
2.15	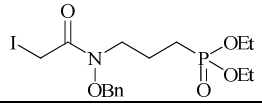	0.02	2.4	2.0	6.0	8.08	0.91
2.16	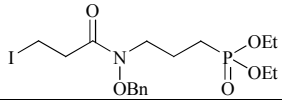	26.6	59.7	75.0	26.9	ND	ND
2.4	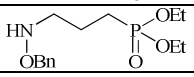	100	98	95	2133.9	ND	ND
3.8	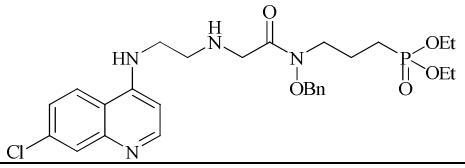	ND	ND	ND	ND	0.18	0.05
3.9	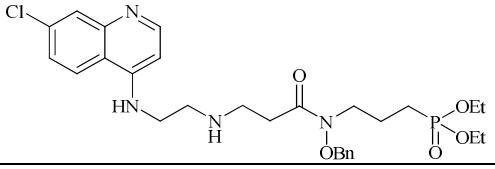	10.6	9.0	10.3	6.7	0.82	0.12
2.10	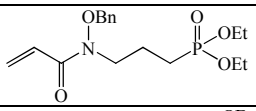	12.8	28.7	66.7	25.9	ND	ND
3.10	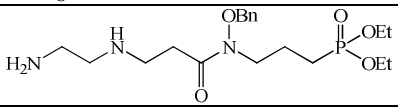	36.1	72.2	66.0	36.7	ND	ND
3.11	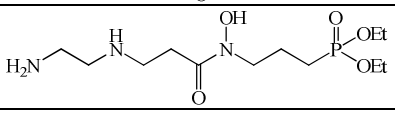	73.7	73.2	73.4	115.0	ND	ND
2.7	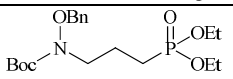	14	21	66	21.9	ND	ND
1.10	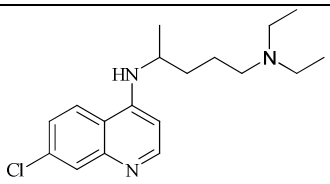 Chloroquine	0.03	0.052	0.089	0.062	0.07	0.01

ND =Not determined; * = Estimated IC_{50} values

The CQR FCR-3 *P. falciparum* showed borderline resistance to chloroquine (**1.10**) at 0.07 µM (70 nM) seeing that the threshold defining resistance to this strain is 70 – 120 nM. The antiplasmodial test of the chloroquine-fosmidomycin hybrids as well as the fosmidomycin analogue intermediates provided promising antiplasmodial results. Not surprisingly chloroaminoquinoline **3.5** showed the most potent activity against CQR FCR-3 strain of *P. falciparum* with an IC_{50} of 0.02 µM (Table 3.2). This is even more potent than the literature reported IC_{50} values of 231.1[155] and 92 nM[27] against CQS D10 *P. falciparum*.

The acetyl linked chloroquine-fosmidomycin hybrid **3.8** with an IC_{50} value of 0.18 µM against FCR-3 showed four times more antiplasmodial activity than the propyl linked hybrid **3.9** with an IC_{50} value of 0.82 µM. This indicates that the length of the linker between the hybrid components is important for the antiplasmodial activity of the hybrids. For the reason that these hybrids are fully protected and are unlikely to fit into the DXR active site, coupled with the fact that the chloroaminoquinoline **3.5** showed better antiplasmodial activity than these hybrids, it is most likely that the mechanism of action of the hybrids is related to the mechanism of action of aminoquinolines. In order to get a better understanding of the relationship between the compounds and the DXR enzyme *in silico* studies of the hybrids docked into the active site of DXR was conducted. The study, explored in chapter 4, was also expected to provide more information on the role of the different chain linker between the two moieties making up the hybrids.

3.2.2 **Synthesis of pyrazinoic acid-FR90098 hybrid (3.15)**

Having observed high antiplasmodial activity for the chloroquine-fosmidomycin hybrids **3.8** and **3.9**, the motivation to hybridize fosmidomycin with another class of drug developed. The new hybrid was designed such that only the fosmidomycin component would possess antimalarial property. This was expected to shed more light on whether both components of hybrids **3.8** and **3.9** were responsible for the activity of the compounds or only one of the two moieties was responsible.

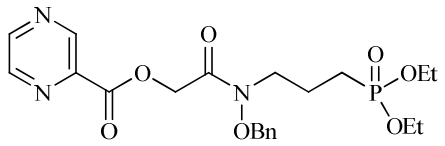

3.15

Figure 3.4. Pyrazinoic acid-FR90098 hybrid

Pyrazinoic acid (Scheme 3.6, POA, **3.16**), the active metabolite of pyrazinamide used in the treatment of tuberculosis was selected for hybridization with fosmidomycin analogues. POA (**3.16**) was selected on the basis that it has a simple structure which is bulky enough and could fit into the DXR active site of fosmidomycin and NADPH as predicted for the chloroquine-fosmidomycin hybrid. The compound was also favoured because its hybrid with fosmidomycin could provide a drug that is not only active against malaria but also against tuberculosis which is another major cause of death by infectious diseases in Africa. At the very least if inactive against *P. falciparum*, the hybrid could create a lead compound from which other antimycobacterial agents can be developed since *Mycobacterium tuberculosis*, the causative agent of tuberculosis, also requires DXR for survival.[156] Pyrazinamide resistance by *M. tuberculosis* has been reported and is attributed to mutation in the pyrazinamidase gene which codes for the pyrazinamidase enzyme that hydrolyse pyrazinamide to POA.[157] It is therefore envisaged that a hybrid of this drug with fosmidomycin might provide reversal for its resistance in the mycobacterium while promoting the uptake of fosmidomycin component by the bacterium although this was not the focus of this study.

POA-FR900098 hybrid **3.15** emerged from the esterification reaction of POA (**3.16**) with the protected bromine analogue of FR900098, **2.17** (Scheme 3.6). The two components were refluxed for six hours to afford hybrid **3.15** at a very good yield of 97%. Attempt to debenzylate **3.15** did not yield the desired hydroxamic acid **3.17**.

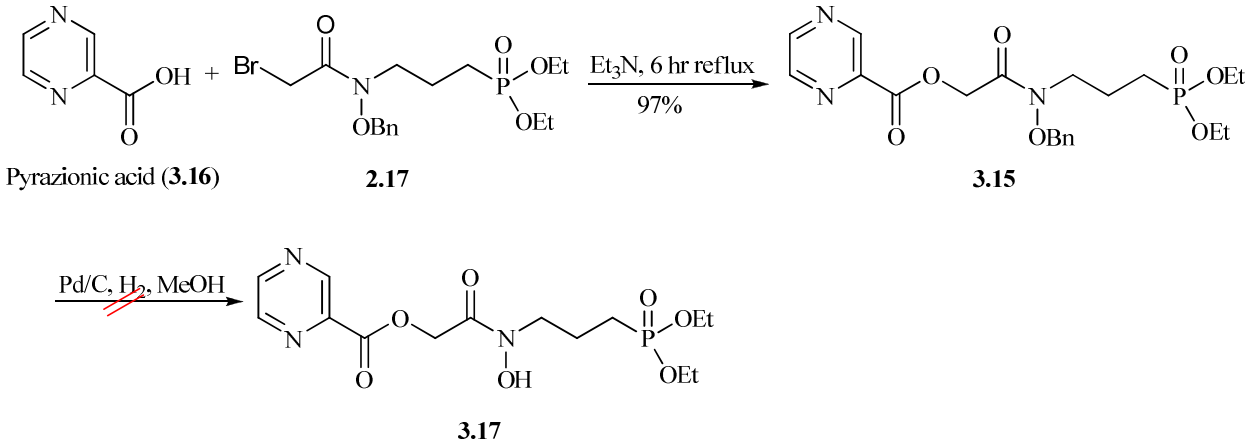

Scheme 3.6. Synthesis of Pyrazinoic acid-fosmidomycin hybrid

The structure of the POA-FR900098 was confirmed with 1D and 2D NMR, UV, IR and mass spectroscopy. The proton spectrum of the hybrid (Figure 3.5) showed similar spin systems as observed for the fosmidomycin moiety of the chloroquine-fosmidomycin hybrids. Signals for the ethyl ester were be observed at δ 1.29 (t; 7.0 Hz; 6H; H-2') and 4.05 (m; 4H; H-1') while the methylene protons of the propyl backbone resonated δ 1.72 (m, 2H; H-1), 1.95 (m, 2H; H-2) and 3.74 (t; 6.8 Hz; 2H; H-3). The methylene linking the POA to the FR900098 derivative was observed as a singlet at δ 5.01. While the benzyl protons could be observed at 7.39, the POA aromatic protons were more deshieled at δ 9.32 (s; H-9), 8.75 (s; H-11) and 8.71 (s, H-12). The carbon data showed the ester and amide carbonyl carbons at δ 167.6 and 163.5 respectively (Table 3.3). An HMBC correlation between δ 5.01 and 167.6 confirmed the ester linkage between the POA component and the FR900098 derivative.

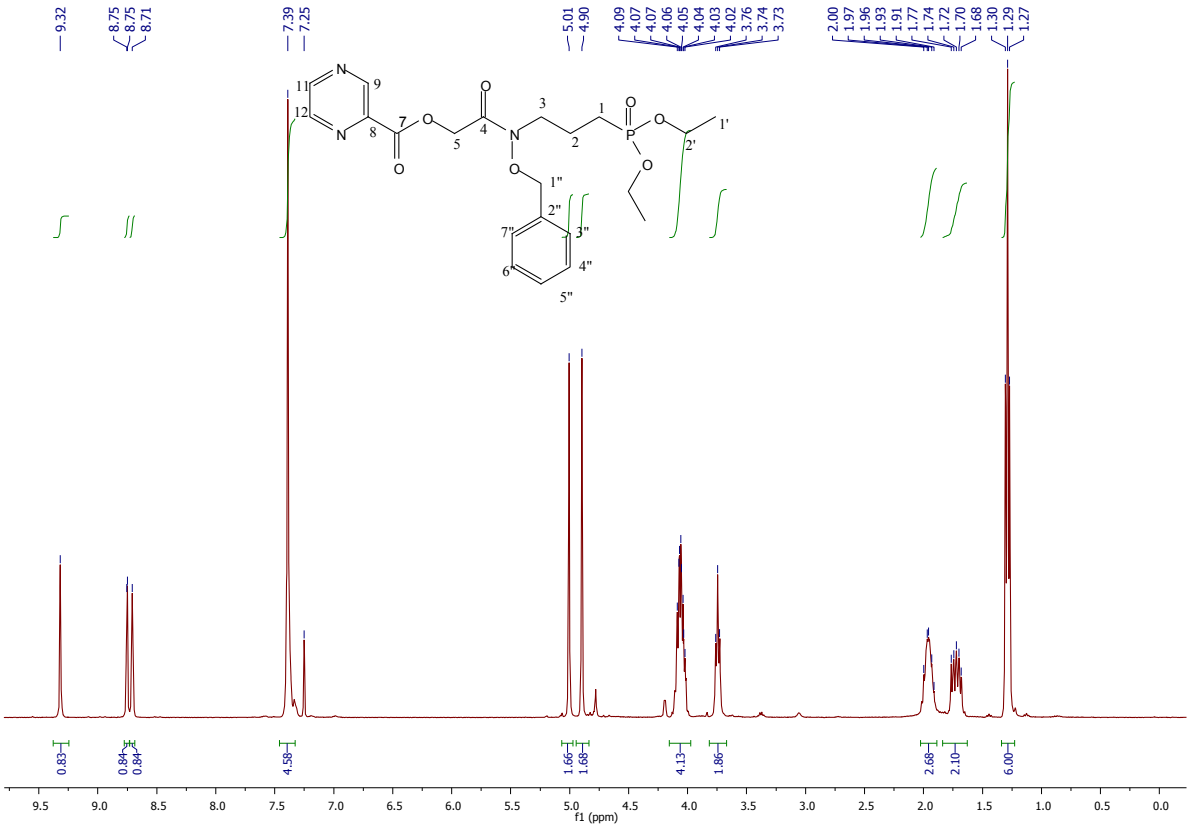

Figure 3.5. ^{1}H NMR spectrum ($CDCl_3$; 400 MHz) of POA-fosmidomycin hybrid **3.15**

Table 3.3 ^{1}D and ^{2}D NMR (400 MHz) data of **3.15** in $CDCl_3$

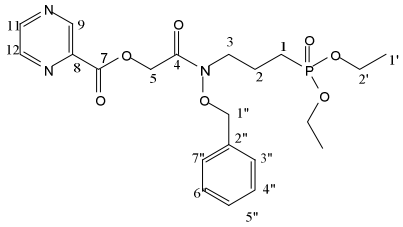

Position[III]	δ **^{1}H (#; mult; J_{HZ})**	**^{13}C (#; mult; J_{HZ})**	**^{1}H-^{1}H COSY**	**^{1}H-^{13}C HMBC**
1’	1.29 (6H; t; 7.0)	16.4 (2 x CH_3; d; 6.0)	H-2’	C-2’
2’	4.05 (4H; m)	61.6 (2 x CH_2; d; 6.5)	H-1’	C-1’
1	1,72 (2H; m)	22.8 (CH_2; d; 142.7)	H-2	C-2
2	1.95 (2H; m)	20.0 (CH_2; d; 4.7)	H-1; H-3	C-1; C-3
3	3.74 (2H; t; 6.8)	46.0 (CH_2; d; 19.1)	H-2	C-1; C-2
4		163.5 (C=O; s)		
5	5.01 (2H; s)	62.6 (CH_2; s)		C-4; C-6
7		167.6 (C=O; s)		
8		142.8 (C; s)		
9	9.32 (1H; s)	146.5 (CH; s)		C-11; C-8
11	8.75 (1H; s)	147.9 (CH; s)		C-9; C-12
12	8.71 (1H; s)	144.4 (CH; s)		C-8; C-11;
1”	4.90 (2H; s)	76.38 (CH_2; s)	2”	
3” – 7”	7.39 (5H; m)			
2”		133.7 (CH; s)		
4” and 6”		129.4 (2 x CH; s)		
5”		129.4 (CH; s)		
3” and 7”		128.9 (2 x CH; s)		

As was the case with the chloroquine-fosmidomycin hybrids **3.8** and **3.9**, attempts to deprotect the POA-fosmidomycin hybrid **3.15** through hydrogenation using Pd/C as catalyst or by treatment with BCl_3 were ineffective. At this point it was suspected that the aromatic nitrogens might be responsible for the resistance of the hybrids to debenzylation. To investigate this, benzoyl chloride (Scheme 3.7, **3.18**) was reacted with the fosmidomycin backbone **2.4** to afford the protected benzyl fosmidomycin derivative **3.19** (Scheme 3.7). The benzyl group of compound **3.19** was easily hydrolysed through hydrogenation with Pd/C to give **3.20**. This further reiterate that the presence of aromatic nitrogen is responsible for the

[III]Atoms are numbered for easier comparison and are not the standard numbering system

resistance to debenzylation observed for both the chloroquine-fosmidomycin hybrids **3.8** and **3.9** as well as the POA -fosmidomycin hybrid **3.15**. While it was desirable to have the free hydroxamic acids for comparison with fosmidomycin (**1.46**) and FR900098 (**1.45**), it was expected that the presence of the protective groups on the hybrids would increase the lipophilicity of the compounds and thus render them more absorbable through the parasite membrane than the free acid derivatives.

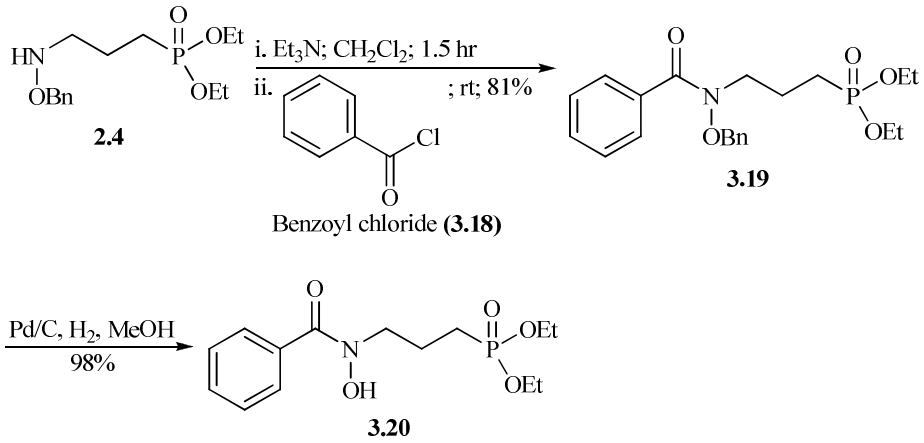

Scheme 3.7. Synthesis and debenzylation of benzyl substituted fosmidomycin analogue

3.2.3 **Antiplasmodial activity of pyrazinoic acid-FR90098 hybrid (3.15) and benzyl substituted fosmidomycin analogue**

The antiplasmodial activity of the POA-fosmidomycin hybrid **3.15** as well the benzyl substituted fosmidomycin analogues **3.19** and **3.20** were tested against CQS *P. falciparum* D10 strain. The brominated fosmidomycin intermediate **2.17** was also tested for comparison.

The POA-FR900098 hybrid **3.15** and the benzyl fosmidomycin analogues **3.19** and **3.20** had no significant activity on the plasmodium parasite (Table 3.4). This also promotes the fact that the antiplasmodial activity observed for chloroquine-fosmidomycin hybrids was most probably due to the aminoquinoline moiety of the compounds.

Table 3.4. Antiplasmodial activity of POA-FR900098 hybrid and fosmidomycin derivatives

		D10: % parasite survival				
Comp	**Structure**	**20 µg/ml**	**10 µg/ml**	**5 µg/ml**	**Cal. IC_{50} (µM)**	**cLogP**
3.15	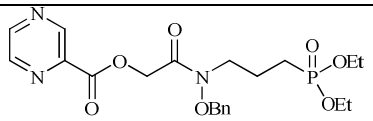	78.7	91.7	87.4	110.4	1.524
2.17	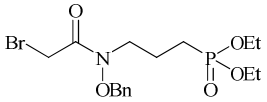	0.00	3.04	26.1	11.1	2.271
3.19	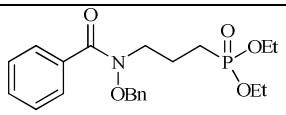	62.7	71.2	73.7	62.2	3.246
3.20	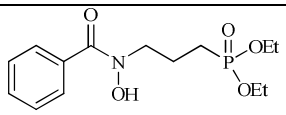	88.4	87.5	79.8	412.3	1.327

In conclusion the fosmidomycin derivatives were successfully hybridized with a quinoline derivative, POA and benzoyl chloride. Only the hybrid with quinoline derivatives were however active against *P. falciparum* indicating that the activity is most probably due to the quinoline moiety than the fosmidomycin constituent. It would be useful to obtain the free or deprotected form of the hybrid in order to determine if the lack of apparent fosmidomycin activity is as a result of the protection or if the size of the molecule is perhaps preventing the binding of the hybrid to the DXR enzyme

3.3 EXPERIMENTAL

3.3.1 **Antiplasmodial assays**

The Antiplasmodial assays were carried out as described in sections 2. 4.1 and 2.4.2.

3.3.2 **General experimental, equipment, chemicals and reagents**

The details of the general experimental, equipment, chemicals and reagent used were as described in section 2.4.3

3.3.3 **Synthetic procedures and spectroscopic data**

N^1-(7-chloroquinolin-4-yl)ethane-1,2-diamine (3.5)

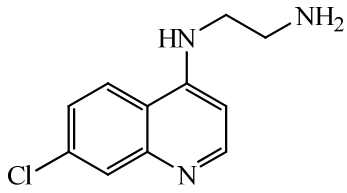

1,2-Diaminoethane (**3.7**, 1.7 ml; 25.43 mmol) was stirred with 4,7-dichloroquinoline (**3.6**, 1.03 g; 5.18 mmol) at 110^0C for 6 hours under N_2 gas. The reaction mixture was cooled to room temperature and 25 ml 1.0 M NaOH solution was added and the mixture extracted three times with CH_2Cl_2. The combined organic layers was washed with water and brine and dried over anhydrous Na_2SO_4. CH_2Cl_2 was removed under reduced pressure to obtain pure pale yellow crystals (0.89 g; 77%).

^{1}H NMR (400 MHz, $CDCl_3$) δ 8.50 (d, *J* = 5.3 Hz, 1H, -N-C=CH-C<u>H</u>=); 7.93 (br s,1H, =N-C=C<u>H</u>-C-Cl); 7.71 (d, *J* = 8.9 Hz, 1H, Cl-C=CH-C<u>H</u>=); 7.33 (br d, *J* = 8.9 Hz, 1H, Cl-C=C<u>H</u>-CH=); 6.38 (d, *J* = 5.35 Hz, 1H, -N-C=C<u>H</u>-CH=); 5.27 (s, 2H, N<u>H</u>$_2$), 3.31 (m, 2H, -NH-C<u>H</u>$_2$), 3.10 (m, 2H, C<u>H</u>$_2$-NH$_2$) ppm.**^{13}C NMR** (101 MHz, $CDCl_3$) δ 152.1(s, -NH-C=CH-C<u>H</u>=); 149.9 (s, -NH-<u>C</u>=); 149.2 (s, =N-<u>C</u>=C-); 134.81 (s, Cl-<u>C</u>=C-); 128.8(s, =N-C=<u>C</u>H-C-Cl);

125.2 (s, Cl-C=CH-CH); 121.2 (s, Cl-C=CH-CH=); 117.4 (s, Cl-C=CH-CH=C-); 99.2 (s, -NH-C=CH-CH=); 44.8 (s, -NH-CH_2-); 40.2 (s, CH_2-NH_2) ppm. mp 43-45 ^oC.[158]

Diethyl 3-(N-(benzyloxy)-2-(2-(7-chloroquinolin-4-ylamino)ethylamino)acetamido)propylphosphonate (3.8)

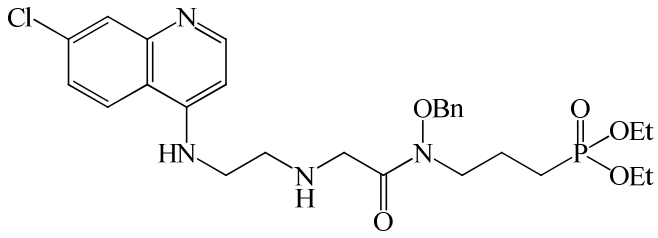

In 10 ml MeOH, 0.27 g (0.58 mmol) of **2.15** and 0.28 g (1.27 mmol) of **3.5** were dissolved and stirred at room temperature overnight. The yellow solution was concentrated and redissolved in H_2O (20 ml). The dissolved solution was extracted three times with EtOAc (10ml) and the combined fraction washed with brine (5ml). The organic phase was dried over Na_2SO_4 and concentrated under vacuum. The crude product was purified over a sephadex column (10 g) eluting with MeOH and the obtained fraction was further purified over 10 g of silica gel column chromatography eluting with MeOH to afford **3.8** (0.15g; 48%).

^{1}H NMR (400 MHz, $CDCl_3$) δ 8.43 (d, *J* = 5.30 Hz, 1H, -N-C=CH-CH=); 7.87 (s, 1H, =N-C=CH-C-Cl); 7.85 (s, 1C, Cl-C=CH-CH=); 7.30 (m, 6H, Cl-C=CH-CH= and Ar-H); 6.34 (s, 1H, Quinoline-NH-); 6.27 (d, *J* = 5.36 Hz, 1H, -N-C=CH-CH=); 4.75 (s, 2H, N-O-CH_2-Ph); 4.04 (m, 4H, P(O)-CH_2); 3.74 (t, *J* = 6.15 Hz, 2H, P-CH_2-CH_2-CH_2);3.44 (s, 2H, C(O)-CH_2); 3.21 (t, *J* = 4.86 Hz, 2H, -NH-CH_2-CH_2-N-quinoline); 2.84 (t, *J* = 4.86 Hz, 2H, -NH-CH_2-CH_2-NH-quinoline); 1.95 (m, 2H, P-CH_2-CH_2); 1.71 (m, 2H, P-CH_2); 1.26 (t, *J* = 7.01 Hz, 6H, P(O)-CH_2-CH_3) ppm. **^{13}C NMR** (100 MHz, $CDCl_3$) δ 173.6 (s, C=O); 151.8 (s, -NH-C=CH-CH=); 150.0 (s, -NH-C=); 148.9 (s, =N-C=C-); 134.6 (s, Cl-C=C-); 133.7 (s, N-O-CH_2-C=CH); 129.3 (s, 2 x CH, N-O-CH_2-C=CH-CH=); 129.2 (s, N-O-CH_2-C=CH-CH=CH); 128.7 (s, 2 x CH, N-O-CH_2-C=CH-); 128.2 (s, =N-C=CH-C-Cl);125.0 (s, Cl-C=CH-CH); 121.9 (s, Cl-C=CH-CH=); 117.3 (s, Cl-C=CH-CH=C-); 98.7 (s, -NH-C=CH-CH=); 76.2 (s, N-O-CH_2-Ph); 61.6 (d, *J* = 6.55 Hz, 2 x CH_2, P(O)-CH_2); 49.2 (s, C(O)CH_2); 47.4 (s, -NH-CH_2-CH_2-NH-quinoline); 45.8 (s, P-CH_2-CH_2-CH_2); 42.3 (s, -NH-CH_2-CH_2-NH-quinoline);

22.9(d, *J* = 142.75 Hz, P-$\underline{C}H_2$);20.1 (s, P-$CH_2\underline{C}H_2$);16.3 (d, *J* = 5.95 Hz, 2 x CH_3, P(O)-CH_2-$\underline{C}H_3$) ppm.

Mass (ESI-MS): Calculated for $C_{27}H_{36}ClN_4O_5P$ $[M]^+$: 563.2190, Found: 563.2186

IR: ν_{max} 3316, 2981, 1658 (C=O), 1234 (P=O), 960; **UV**: λ_{max} 216.83 nm

Diethyl 3-(N-(benzyloxy)-3-(2-(7-chloroquinolin-4-ylamino)ethylamino)propanamido)propylphosphonate (3.9)

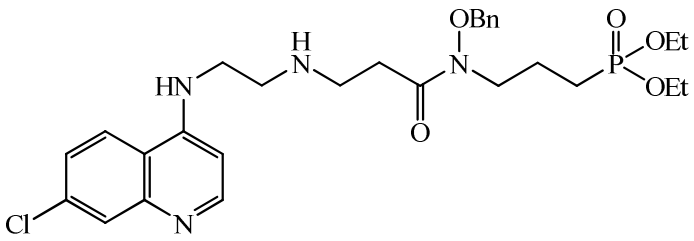

In 10 ml MeOH, 0.11 g (0.23 mmol) of **2.16** and 0.10 g (0.46 mmol) of **3.5** were dissolved and stirred at room temperature overnight. The crude product was concentrated under reduced pressure then re-suspended in $CHCl_3$ and 0.2 ml of MeOH was added. The solution was placed on ice for 10 minutes and the supernatant was separated from the precipitated excess **3.5**. Reverse phase HPLC with 20:80 H_2O: MeOH afforded pure, clear, light yellow **3.9** (0.10 g; 79%).

See Table 2.1 for **^{1}H NMR** (400 MHz, $CDCl_3$) and **^{13}C NMR** (100 MHz, $CDCl_3$) assignments.

Mass (ESI-MS): Calculated for $C_{28}H_{38}ClN_4O_5P$ $[M]^+$: 577.2347, Found: 577.2339

IR: ν_{max} 3321, 2981, 1650 (C=O), 1235 (P=O), 1023; **UV**: λ_{max}216.23 nm

2-(Benzyloxy(3-(diethoxyphosphoryl)propyl)amino)-2-oxoethyl pyrazine-2-carboxylate (3.15)

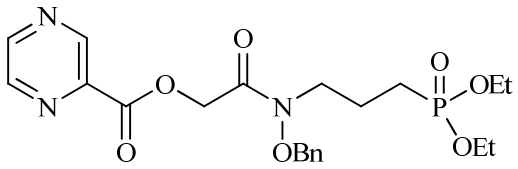

In a flame dried round bottom flask, pyrazinoic acid (**3.16**, 0.06 g; 0.48 mmol) was dissolved in 10 ml acetonitrile. Et_3N (0.07 ml; 0.48 mmol) was added to the mixture and temperature was allowed to rise to reflux. Compound **2.17** (0.20 g; 0.48 mmol) was introduced into the solution and refluxed for six hours. The solution was cooled to room temperature and then concentrated under reduced pressure. The crude product was re-dissolved in 30 ml $CHCl_3$ and washed twice with 10 ml 5% $NaHCO_3$ solution and once with 10 ml H_2O and brine. The organic phase was dried over anhydrous $MgSO_4$ and concentrated *in vacuo* to give pure 0.21 g **3.15** (79%).

^{1}H NMR (400 MHz, $CDCl_3$) δ 9.32 (s, 1H, N-C<u>H</u>-C(C=O)); 8.75 (br s, 1H, N-CH-C(C=O)-N-CH-C<u>H</u>); 8.71 (s, 1H, N-CH-C(C=O)-N-C<u>H</u>); 7.39 (s, 5H, N-O-CH_2-Ph-<u>H</u>); 5.01 (s, 2H, N-C(O)-C<u>H_2</u>-O-C(O-); 4.90 (s, 2H, N-O-C<u>H_2</u>-Ph); 4.05 (m, 4H, P(O)-C<u>H_2</u>; 3.74 (t, J = 6.8 Hz, 2H, P-CH_2-CH_2-C<u>H_2</u>); 1.95 (m, 4H; P-CH_2-C<u>H_2</u>); 1.72(m, 2H, P-C<u>H_2</u>); 1.29 (t, J = 7.0 Hz, 6H, P(O)-CH_2-C<u>H_3</u>) ppm. **^{13}C NMR** (100 MHz, $CDCl_3$) δ 167.6 (s, N-C(O)-CH_2-O-<u>C</u>(O)-); 163.5 (s, N-<u>C</u>(O)-CH_2-O-C(O)-); 147.9 (s, N-CH-C(C=O)-N-<u>C</u>H); 146.5 (s, N-CH-C(C=O)-N-CH-<u>C</u>H); 144.4 (s, N-<u>C</u>H-C(C=O)); 133.7 (s, N-O-CH_2-<u>C</u>=CH-); 129.4 (s, 2 x CH, N-O-CH_2-C=CH-<u>C</u>H= and N-O-CH_2-C=CH-CH=<u>C</u>H); 128.9 (s, 2 x CH, N-O-CH_2-C=<u>C</u>H-); 76.7 (s, N-O-<u>C</u>H_2-Ph); 62.6 (s, N-C(O)-<u>C</u>H_2-O-C(O-); 61.6 (d, J = 6.5 Hz, 2 x CH_2, P(O)-<u>C</u>H_2); 46.0 (d, J = 19.1 Hz, P-CH_2-CH_2-<u>C</u>H2); 22.8 (d, J = 142.7 Hz, P<u>C</u>H_2); 20.0 (d, J = 4.7 Hz,P-CH_2-<u>C</u>H_2); 16.39 (d, J = 6.0 Hz, 2 x CH_3, P(O)-CH_2-<u>C</u>H_3) ppm.

Mass (ESI-MS): Calculated for $C_{21}H_{28}N_3O_7P$ $[M]^+$: 466.1743, Found: 466.1736

IR: ν_{max} 3451, 2982, 1679 (C=O), 1237 (P=O); **UV**: λ_{max} 209.00 nm

Diethyl 3-(N-(benzyloxy)benzamido)propylphosphonate (3.19)

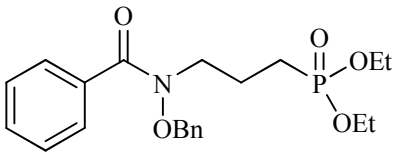

A solution of **2.4** (0.20 g; 0.66 mmol) in CH_2Cl_2(20 ml) was treated with Et_3N (0.11 ml; 0.79 mmol) at room temperature. The mixture was stirred for 1.5 h, and benzoyl chloride (0.1 ml; 0.79 mmol) was added dropwise and stirred for another 2.5 h. The mixture was diluted with CH_2Cl_2 (10 ml) and washed with water (20 ml), saturated $NaHCO_3$ solution (20 ml), and finally with saturated brine solution (5 ml). The organic layer was separated and dried over anhydrous $MgSO_4$. The concentrated product was purified by silica gel (10 g) column chromatography first eluting with EtOAc (50 ml), then MeOH/EtOAc (1:9, 50 ml) to give 0.22 g (81%) pure **3.19** as oil.

^{1}H NMR (600 MHz, $CDCl_3$) δ 7.64 (d, *J* = 7.3 Hz, 2H, 2 x NC(O)-C-C<u>H</u>), 7.47 (m, 1H, N-C(O)-C-CH-CH-C<u>H</u>), 7.40 (m, 2H, 2 x N-C(O)-C-CH-C<u>H</u>), 7.29 (m, 3H, N-O-CH_2-Ph-<u>H</u>), 7.06 (brs, 2H, N-O-CH_2-Ph-<u>H</u>)), 4.64 (s, 2H, N-O-C<u>H$_2$</u>-Ph), 4.08 (m, 4H, P(O)-C<u>H$_2$</u>), 3.74 (t, *J* = 6.8 Hz, 2H, P-CH_2-CH_2-C<u>H$_2$</u>), 2.05 (m, 2H; P-CH_2-C<u>H$_2$</u>), 1.81 (m, 2H, P-C<u>H$_2$</u>), 1.30 (t, *J* = 7.1 Hz, 6H, P(O)-CH_2-C<u>H$_3$</u>). **^{13}C NMR** (151 MHz, $CDCl_3$) δ 170.0 (s, C=O), 134.2 (s, N-O-CH_2-<u>C</u>=CH-), 133.8 (s, N-C(O)-<u>C</u>-CH), 130.4 (s, Ar-C), 129.3 (s, 2 x Ar-C), 128.7 (s, Ar-C), 128.3 (s, 2 x Ar-C), 128.1 (s, Ar-C), 127.9 (s, Ar-C), 76.3 (s, N-O-<u>C</u>H_2-Ph), 61.5 (d, *J* = 6.5 Hz 2 x CH_2, P(O)-<u>C</u>H_2), 46.9 (s, P-CH_2-CH_2-<u>C</u>H_2), 22.8 (d, *J* = 142.8 Hz, P<u>C</u>H_2), 20.4 (d, *J* = 4.6 Hz, P-CH_2-<u>C</u>H_2), 16.3 (d, *J* = 6.0 Hz, 2 x CH_3, P(O)-CH_2-<u>C</u>H_3).

Mass (ESI-MS): Calculated for $C_{21}H_{28}NO_5P$ $[M]^+$: 406.1774, Found: 406.1783

IR: ν_{max} 3454, 2981, 1638 (C=O), 1239 (P=O); **UV**: λ_{max} 204.80 nm

Diethyl 3-(N-hydroxybenzamido)propylphosphonate (3.20)

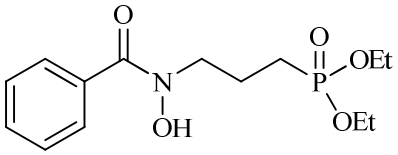

Compound **3.19** (0.12 g) was dissolved in 20 ml MeOH. Pd/C (0.03 g) was added to the solution and hydrogen gas was introduced to the mixture by means of a balloon to generate a positive pressure. The suspension was stirred for two hours at room temperature after which it was filtered through celite. The filtrate was concentrated under reduced pressure to give violet coloured oil **3.20** (0.09 g; 98%).

^{1}H NMR (400 MHz, $CDCl_3$) δ 7.54 (br s, 2H, N-O-CH_2-Ph-H), 7.31 (m, 3H, N-O-CH_2-Ph-H), 3.97 (m, 4H, 4H, P(O)-CH_2), 3.71 (br s, 2H, P-CH_2-CH_2-CH_2), 1.92 (m, P-CH_2-CH_2), 1.73 (m, 2H, P-CH_2), 1.21 (t, *J* = 7.0 Hz, 6H, P(O)-CH_2-CH_3).

Mass (ESI-MS): Calculated for $C_{14}H_{22}NO_5P$ $[M]^+$: 316.1317, Found: 316.1314

IR: ν_{max} 3141, 2982, 1614 (C=O), 1280 (P=O), 1016; **UV**: λ_{max} 201.15 nm

CHAPTER 4

4. *IN SILICO* AND IN VITRO ASSESSMENT OF HALOGENATED FR900098 ANALOGUES AS DXR INHIBITORS

4.1 INTRODUCTION

1-Deoxy-D-xylulose-5-phosphate reductoisomerase (DXR) plays a major role in the mevalonate independent biosynthesis of isoprenoid units isopentenyl pyrophosphate (IPP) and dimethylallyl pyrophosphate (DMAPP) of some bacteria, higher plants and *P. falciparum* as discussed in chapter 1. DXR catalyzes the first committed step of the pathway. Due to the absence of the pathway in humans and its necessity for survival of the plasmodium parasite, the enzymes involved are good targets for antiplasmodial drug development. We were unable to confirm if the antiplasmodial activity of the halogenated fosmidomycin analogues reported in chapter 2 was due to DXR inhibition. This part of the study thus explores the direct effect of these halogenated FR900098 analogues on DXR in an enzyme inhibition assay. Here we also report the affinity of the compounds to DXR through *in silico* studies. The study examined the possibility of the phosphonic acid chloroquine-fosmidomycin hybrids **3.3** and **3.4** binding to the DXR enzyme in the absence of NADPH.

There has been an increased interest in the development of inhibitors of DXR since the discovery of the mevalonate-independent pathway and its inhibition by fosmidomycin in *P. falciparum*.[73] Characterization of DXR from different organisms has been successful and has led to development of other active inhibitors from the lead compounds fosmidomycin and FR900098.

The ability to over-express recombinant proteins, isolate and purify them for inhibition studies is essential in drug development. Often the target recombinant protein is expressed in a host such as *E.coli*. *E. coli* is favoured mostly because of its rapid growth rate, simple genetics, ease of handling and low cost as it gives high yield per unit biomass. Recombinant DXR from various organisms have been successfully over expressed in *E. coli* to study the kinetics of the enzyme as well as perform inhibition test for inhibitor lead compounds. While it would have been ideal to conduct the inhibition test discussed in chapter 4 on *Pf*DXR, the test was carried out on *Ec*DXR. Although some research groups have been able to over

express and purify of *Pf*DXR in *E. coli*,[73, 88] this proved difficult during the course of this study. It has been reported that plasmodium genes exhibit long clusters of codons which are rare in *E. coli* and consequently lead to problems in protein translation which prevent successful expression of plasmodial recombinant protein in *E. coli.*[159] It has been reported that the catalytic domain of *Ec*DXR and *Pf*DXR are 36% identical (145 amino acid residues) and 54% similar (216 amino acid residues). This represents the vast majority of the residues involved in substrate/inhibitor, NADPH binding and divalent metal ion coordination.[160] As a result either one of the homologues can be used as a model for the inhibition studies to discover lead compounds that are active against the enzyme.

Solving the crystal structures of DXR has improved the understanding of the catalytic site of the enzyme and has made it possible to conduct *in silico* studies of potential inhibitors which in turn have improved the rate at which active inhibitors are discovered. *In silico* studies provide a means of screening thousands of compounds in a short space of time by computationally simulating binding of ligands to the crystal structure of a target receptor or protein. Apart from being quick, *in silico* studies helps to minimize waste of resources required in expensive lab work or high-throughput screening and clinical trials to test each compound which usually results in less than a 1% hit rate. The docking studies is also used to understand the binding or the structure activity relationship between ligands and receptors. This study employ the use of molecular modeling to better understand the interaction between the halogenated fosmidomycin analogues and the DXR enzyme as well as the chloroquine-fosmidomycin hybrid with the enzyme.

4.1.1 **Short review of crystallographic and modeling studies of DXR**

The *Pf*DXR is essentially very similar in structure to the *Ec*DXR discussed in section 1.6.3. In its active form *Pf*DXR is a homodimer which consists of amino acid residues from Lys75 to Ser488. Each monomer has a molecular weight of approximately 47kDa. The monomer consists of the N-terminal domain, which binds NADPH in a similar mode to *Ec*DXR and is comprised of residues 77 to 230 forming the biggest of the three domains. The catalytic domain comprises of residues 231 to 369 and the small C-terminal domain extends over

residues 396 to 486. The lid which closes upon substrate/inhibition binding spans the length of amino acid residues 291 to 299.[88]

The second step in the mevalonate independent pathway of isoprenoid synthesis involved the intramolecular rearrangement and reduction of the substrate 1-deoxy-D-xylulose 5-phosphate (DOXP) to 2-*C*-methyl –D-erythritol 4-phosphate (MEP) by DXR. The reaction is dependent on the presence of divalent metal ion Mn^{2+}, Co^{2+} or Mg^{2+} and NADPH cofactors. Each of the three divalent metal ions have been shown to activate DXR and although initial studies have shown Mn^{2+} to be the most effective[161], Koppisch and co-worker found all three to be equally effective in *E. coli*.[162] Based on the fact that Mg^{2+} is more abundant in cells as it has been found in *Synechocystis* sp. PCC6803,[163]*M. tuberculosis*,[164]and *E. coli*,[162] it is suggested to be the more relevant cofactor for DXR activity *in vivo*.

Over the past decade, a number of crystal structures of DXR has been solved and reported from *E. coli*,[89-94] *M. tuberculosis*,[165, 166] *Zymomonas mobilis*,[167] *Thermotogamaritime*,[168] and very recently the first report on *P. falciparum*.[88] The crystal structures were solved to provide a better understanding of the catalytic activity of the enzyme in order to be able to rationally design inhibitors as potential antimalarial drugs. The structures were reported as apo enzymes and in complexes. The apo form of *Ec*DXR was first reported by Reuter and co-worker (pdb code: 1K5H).[90] Since then many complexes of the enzyme have been reported by various groups. These include *Ec*DXR with sulphate ion and NADPH (1JVS),[92] with Mn^{2+} and fosmidomycin (1ONP),[91] with sulphate and bisphosphonate ions (1T1R and 1T1S),[93] with DOXP and NADPH(1Q0Q) and with NADPH and fosmidomycin (1Q0L).[89] Yajima *et al.*[94] reported the complexed structure of *Ec*DXR with NADPH, Mg^{2+} and fosmidomycin (2EGH), the only study that has reported the full cofactors for *Ec*DXR. These quaternary structures of *Ec*DXR while overall very similar, showed slight differences to each other particularly in the flexible loop, which is completely disordered in the apo enzyme but ordered and in contact with fosmidomycin in the complex structure that includes the NADPH, Mg^{2+} and the inhibitor. Slight differences in the orientation of the catalytic centre was also observed when 1Q0L, 1ONP and 2EGH were compared, which reflects the structural flexibility of the DXR conformation.[94] Umeda and co-workers[88] solved the crystal structure of *Pf*DXR and reported the enzyme in complex with fosmidomycin, Mg^{2+} and NADPH (3AU9) and also in complex

with Mg^{2+}, NADPH and FR900098 (3AUA). This was the first time DXR has been reported in complex with FR900098 which is more potent against *Pf*DXR than fosmidomycin.

4.1.2 **Approach and specific objectives of the DXR inhibition assay**

Many of the halogenated fosmidomycin derivatives synthesized and reported in chapter 2 exhibited good antiplasmodial activity against CQS and CQR strains of *P. falciparum*. One of the observations made however was that while the protected halogenated compounds **2.4**, **2.15**, **2.17** and **2.19 – 2.21** were even more active than FR900098, the protected non-halogenated FR900098 analogues **2.12** and **2.18** were inactive against the parasite. This was intriguing as the conditions under which the assay was carried indicated hydrolysis of ester protected compounds[110] possibly by non-specific esterases. No report was found on whether *P. falciparum* possess debenzylating enzymes and as a result cannot be confirmed that the protected compounds had been hydrolysed to hydroxamic acid which is necessary for chelation of the metal at DXR active site. While this could explain why **2.12** was inactive, it does not explain why **2.18** was inactive as it is not protected at the hydroxamate end. It was considered that the halogens are either solely responsible for the activity of the halogenated analogues at the enzyme's active site or they have alternative targets in the parasite. In order to investigate this theory, the direct effects of the compounds including the de-protected analogues **2.1 – 2.3** and **2.38** were tested in a preliminary *E. coli* DXR inhibition assay. *Ec*DXR was used for the assay due to the ease with which recombinant *Ec*DXR is over expressed and purified while purification of *Pf*DXR is proved to be more difficult. However due to the similarities between the homologues, *Ec*DXR is expected to be a good model of *Pf*DXR and the result of the inhibition would be useful in making a informed conclusions about the binding of the compounds to the plasmodium DXR.

While many *in silico* studies are geared towards discovering lead compounds that can be synthesized and then tested for activity, in this project the *in silico* study served to explain the binding affinity of the active halogenated fosmidomycin analogues to DXR. The docking studies further helped to compare the affinity of the compounds for *Ec*DXR and *Pf*DXR and consolidate the result obtained from the inhibition assay. The halogenated fosmidomycin analogues as well as fosmidomycin (**1.46**) and FR900098 (**1.45**) were docked into the crystal

structure of *Ec*DXR (pdb code: 2EGH) and *Pf* DXR (pdb code: 3AUA) obtained from the Protein Data Bank.

The aim of these studies were thus to determine the effect of the halogenated fosmidomycin analogues on *Ec*DXR in an enzyme inhibition assay and to determine the binding energies of the active compounds to both the plasmodium and the bacterium DXR enzyme in an *in silico* study. As such the specific objectives of these studies included:

1. Conducting inhibition studies of halogenated FR900098 analogues and
2. Conducting *in silico* studies of the halogenated FR900098 derivatives on both *Pf*DXR and *Ec*DXR.

4.2 RESULTS AND DISCUSSION

4.2.1 *Ec*DXR assay of halogenated fosmidomycin analogues

DXR inhibition assay was developed by Kuzuyama *et al*. (1998)[169] and had been widely used in screening potential inhibitors. The assay has been used successfully for testing of inhibitors on both recombinant *Ec*DXR and *Pf*DXR. For the purpose of this study, recombinant *E. coli* DXR was over expressed, produced in competent *E. coli* cells and purified. Inhibition of the enzyme was assessed based on the consumption of NADPH which is necessary for reduction step in the conversion of DOXP to MEP. The depletion of NADPH was monitored by spectrophotometric measurement of the optical density of the reaction solution over 10 minutes at 340nm. The enzyme was initially pre-incubated with the inhibitor for five minutes at 37^{o}C. The reaction was initiated by addition of the pre-incubated enzyme-inhibitor solution to a similarly incubated solution of $MnCl_2$, Tris-HCl, NADPH, DOXP and ddH_2O in 1 well of a 96-well UV microtitre plate. Pre-incubation was carried out because fosmidomycin, the known inhibitor of this enzyme is a slow, tight-binding inhibitor and the halogenated FR900098 analogues were expected to bind the same way. Pre-incubation of DXR with fosmidomycin for five minutes was found to be long enough to establish full binding of the enzyme to fosmidomycin without saturating it.[162]

A preliminary inhibition test of compounds **2.1 – 2.3**, **2.8**, **2.9**, **2.11**, **2.12**, **2.18 – 2.24** and **2.38** against *Ec*DXR at 5µM concentration was conducted with FR900098 (**1.45**) as a positive control. Five other controls were employed in the experiment. This included the assay in the absence of NADPH, $MnCl_2$, substrate, inhibitor and the DXR enzyme. The assay was blanked against the control lacking the DXR enzyme. The rate of activity of the enzyme in the presence of the FR900098 analogues was determined as the slope of the initial linear stage of the reaction and expressed as a percentage of the rate of activity of the enzyme in the absence of an inhibitor (Equation 4.1; Table 4.1)

$$\%\, rate = \frac{rate\ inhibitor}{rate\ no\ inhibitor} * 100$$ ----------Equation 4.1

Table 4.1. Relative percentage inhibition of FR900098 analogues on *Ec*DXR at 5 µM concentration

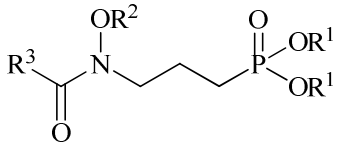

Compound	R^1	R^2	R^3	Relative rate (%)[a]
2.15	Et	Bn	$-CH_2I$	88.7
2.16	Et	Bn	$-CH_2CH_2I$	103.4
2.17	Et	Bn	$-CH_2Br$	111.3
2.1	H	H	$-CH_2Cl$	38.5
2.2	H	H	$-CH_2CH_2Cl$	28.5
2.3	H	H	$-CH_2CH_2CH_2Cl$	92.3
2.8	Et	Bn	$-CH_2Cl$	101.7
2.9	Et	Bn	$-CH_2CH_2Cl$	90.6
2.11	Et	Bn	$-CH_2CH_2CH_2Cl$	102.3
2.12	Et	Bn	$-CH_3$	83.8
2.18	Et	H	$-CH_3$	103.4
2.19	Et	H	$-CH_2Cl$	88.7
2.20	Et	H	$-CH_2Br$	87.0
2.21	Et	H	$-CH_2I$	99.1
2.22	Et	H	$-CH_2CH_2Cl$	100
2.23	Et	H	$-CH_2CH_3$	105.7
2.24	Et	H	$-CH_2CH_2CH_2Cl$	100.4
2.38	H	H	$-CH_2CH_3$	77.2
FR900098 (1.45)	H	H	$-CH_3$	24.7

[a]Relative to uninhibited reaction (i.e. no inhibitor = 100%)

As shown in Table 4.1, FR900098 (**1.45**) clearly showed the best inhibition of *Ec*DXR activity to 24.7% at 5 µM concentration. This was followed closely by phosphonic acids **2.2** (28.5%) and **2.1** (38.5%). This shows the need for a free phosphonic acid in order for the compound to bind and inhibit the enzyme. In contrast, some of the bulky protected analogues such as **2.15** and **2.12** showed a small reduction in the activity of the enzyme to 88.7 and 83.8% respectively. This could be an indication of possible displacement of NADPH from the active site but due to the protected hydroxamate group it was unable to chelate metals or bind strongly enough to significantly inhibit the enzyme.

Interestingly, the propyl phosphonic acid **2.2** showed a stronger inhibition of *Ec*DXR than the acetyl phosphonic acid **2.1**. This is contrary to the antiplasmodial result which showed the shorter chained **21** to be more active. The result observed for the enzyme inhibition could possibly be due to competitive displacement of the smaller compound **2.1** from the active site of the enzyme by the substrate. The chlorobutyryl phosphonic acid **2.3** as expected did not show any appreciable inhibition of the enzyme reducing the activity to 92.3%. This is likely because the chlorobutyryl side chain is long and unable to fit into the hydroxamic acid binding pocket of the enzyme.

The chlorinated phosphonic acid **2.2** showed superior inhibition of *Ec*DXR over its unchlorinated analogue **2.38** (77.2%) indicating that the presence of the chlorine atom contributes to its DXR inhibition activity. Conversely, the effect of chlorine appears to be secondary to the effect of lengthening the acyl side chain. This is observed with the chlorinated phosphonic acid **2.3** only reducing the activity of DXR to 92.3% while the unchlorinated propyl phosphonic acid reduced the activity to 77.2%. The observation is further supported by the fact that FR900098 (**1.45**) showed the highest inhibition despite not having any chlorine atom in its structure. Although the result indicate the acetyl chain to be the optimum acyl side chain of the FR900098 analogues, it does not preclude the possibility that the enzyme might be able to accommodate larger groups in the absence of NADPH from the site of action.

Phosphonic acids **2.1** and **2.2** showed higher enzyme inhibition but lower antiplasmodial activity than their protected analogues **2.8** and **2.9** respectively. This signifies the possibility that the protected analogues might have been better absorbed by the *Plasmodium* and then hydrolyzed to the respective phosphonic acids. It is quite possible the unprotected compounds **2.8** and **2.9** could have other targets once absorbed into the parasite especially since they carry a possibly reactive chlorine atom.

The enzyme inhibition assay showed DXR activity increase when some of the halogenated fosmidomycin analogues such as **2.17** was tested. It is not impossible that these compounds potentiate or induce the enzyme activity. However, this will contradict the antiplasmodial result especially for **2.17** which showed potent activity against the parasite. Alternatively, if

these compounds induce DXR their antiplasmodial activity would then be attributed to targeting of other proteins or enzyme in the parasite. This will most probably possibly be due to the presence of non-selective reactive halogens that they carry.

This preliminary experimental result shows a high potential for the halogenated phosphonic acid analogues of FR900098 especially the chloroacetyl and chloropropyl analogues to inhibit *Ec*DXR. Further investigations on the compounds to determine their IC_{50}, cytotoxicity and particularly their effect on *Pf*DXR are thus recommended.

4.2.1 *In silico* studies of halogenated FR900098 analogues

In silico studies of the halogenated FR900098 analogues were conducted for two reasons: 1) To be able to relate the antiplasmodial result to the DXR assay conducted on *E. coli* DXR and 2) to investigate the binding affinity of these compounds to both *E. coli* (pdb code: 2EGH) and *P. falciparum* DXR (pdb code: 3AUA) enzymes. The docking was carried out on both DXR enzymes of *P. falciparum* and *E. coli* obtained from the protein data bank. The docking was carried out on the two enzymes in order to reconcile the result of the antiplasmodial activity with the inhibition assay conducted on *Ec*DXR. Although DXR from the two organisms are similar, studies have shown that some compounds bind better to one than the other, an example been FR900098 which inhibits *Pf*DXR better than *Ec*DXR while fosmidomycin exhibit better inhibition towards *Ec*DXR than *Pf*DXR.

E. coli DXR in complex with Mg^{2+}, Fosmidomycin and NADPH (pdb code: 2EGH) and *P. falciparum* DXR (pdb code: 3AUA) in complex with Mg^{2+}, FR900098 and NADPH were obtained from the protein data bank. The enzymes were obtained as dimers and one subunit (subunit A) was removed from the enzymes using Discovery Studio Visualizer 3.0[170] to allow for easier docking and analysis of the docking result. The inhibitors were also removed from the respective crystal structures to leave the catalytic site open for the halogenated analogues to bind to the enzymes. The docking was conducted on AutoDock 4.2.[171] Preparation of the enzymes for docking involved removal of water molecules from the enzyme, addition of Gastieger charges and spreading non-integral charges across the entire surface of the enzyme. A check for missing atoms was conducted and all the missing atoms were replaced. All

hydrogen atoms were added and non-polar hydrogens were merged and all possible torsions allowed. Residues of the catalytic centres and those that complexed with the hydroxamic acid group were made flexible for the binding.

In a living system, DXR exhibit flexibility that allows it to change conformation as required especially after binding the substrate or inhibitor. In order to emulate the system in a living organism, some residues of the DXR enzymes were made flexible for the docking. Residues Ser185, Ser221, Lys227, Asp149, Glu151 and Glu230 were selected as flexible residues for the *Ec*DXR docking as these residues were reported to be necessary for the binding of fosmidomycin to the enzyme.[94] The more residues made flexible, the closer the experiment to a biological system. However the drawback to having many flexible residues is that it makes it more difficult to reproduce the same docking result when repeated. The residues that bind the inhibitor in *Pf*DXR include Ser270, Asn311, His293, Asp231 and Glu315, which were made flexible for the docking of 3AUA to the halogenated FR900098 analogues.[88]

The divalent metal (Mg^{2+}) was assigned a charge of +2.0 as AutoDock automatically assigns a charge of 0.0 to the metal. Although many reports involving the docking of DXR to inhibitors have paid little attention to the metal ion, Bodil and colleagues highlighted the importance of having the charged divalent metal ion present in the docking crystal.[118] The absence of the metal ion in inhibition assays of DXR has also shown no activity of the enzyme indicating its necessity for inhibition. The fact that DXR is inactive in the absence of a divalent metal ion also signifies the necessity of the metal being incorporated in the experiment.

After selecting the flexible residues, a grid box was created around the active site of the remaining rigid structure of DXR. Grid dimensions of 62, 52, 56 along the x, z, y axis respectively were used for 2EGH while 58, 60 and 58 were used along the same dimensions for the *Pf*DXR 3AUA. All possible atoms in the ligand including Cl, Br and I were mapped for docking using AutoDock 4.2.

Preparation of the ligands **2.1 – 2.3**, **2.8 – 2.12**, **2.15 – 2.24** and **2.38** prior to docking into the enzymes involved sketching the compounds using ChemBioDraw Ultra 11.0.1.[172] A random

rotor search for a global minimum conformation was conducted for each ligand and the best conformer was geometrically optimized using Avogadro (version 1.0.3).[173] Gasteiger charges were added with AutoDock tools, and all non-integral charges were spread over the entire molecule. Docking of the compounds was conducted on AutoDock 4.2 which makes use of genetic algorithm to search for possible orientation and conformation of the ligands at the defined active site of the enzyme. All active and rotatable bonds in the ligands were made rotatable except for the amide bonds which were made non-rotatable according to the defaults of AutoDock.

The dockings were carried out using the Lamarckian algorithm to create a population of 150 individuals with 2500000 maximum number of evaluations in 100 GA runs. Although some researchers have generated 10 conformations to investigate binding of ligands to proteins, generating 100 conformations increases the chance of obtaining conformations closer to the conformation that the compound would adopt in a biological system.

The docking conformations which were typically docked at 2.0 Å rmsd were arranged in clusters from lowest to highest energy. FR900098 (**1.45**) and fosmidomycin (**1.46**) were also docked into the active sites of both the 2EGH and the 3AUA crystal structures to validate the docking position of the compound and ensure that the parameters set for the docking of the FR900098 derivatives were appropriate for the docking. Initial docking of FR900098 (**1.45**) into the modified 3AUA gave complexes that had FR900098 orientated in the reverse direction to the original crystal structure-complex obtained from the protein data bank (Figure 4.1). That is, the phosphonate region was orientated towards the divalent metal ion. While it is not impossible for the phosphonate moiety to chelate metals, several complexes of DXR with inhibitors have consistently shown that the hydroxamic acid present in the inhibitors is responsible for metal chelation and that the phosphonate has its own binding pocket at the active site of the enzyme. The change in orientation of the FR900098 was deemed to have occurred based on the higher negative charge of the phosphonate moiety as compared to the hydroxamic acid moiety which attracts the positive charge on the metal ion. Decreasing the charge on the Mg^{2+} ion did not re-orientate the compounds. Consequently Mg^{2+} was re-assigned a charge of +2.00 and the hydroxamic acid moieties as well as the phosphonate moiety were each assigned a charge of -1.00 on the ligand (FR900098). This gave docking

results in which clusters of docked confirmations showed hydroxamic acid component orientated towards the Mg^{2+} ion as opposed to the phosphonate. These charges were thus used for the docking of all the free phosphonic acid ligands i.e. **2.1 – 2.3** and **2.38**, fosmidomycin (**1.46**) and FR90098 (**1.47**). The best docked conformation was selected based on the docking energy, visual examination of how close in orientation it is to the FR900098 that came with the crystal structure, size of the cluster and the hydrogen bond network around the ligand.

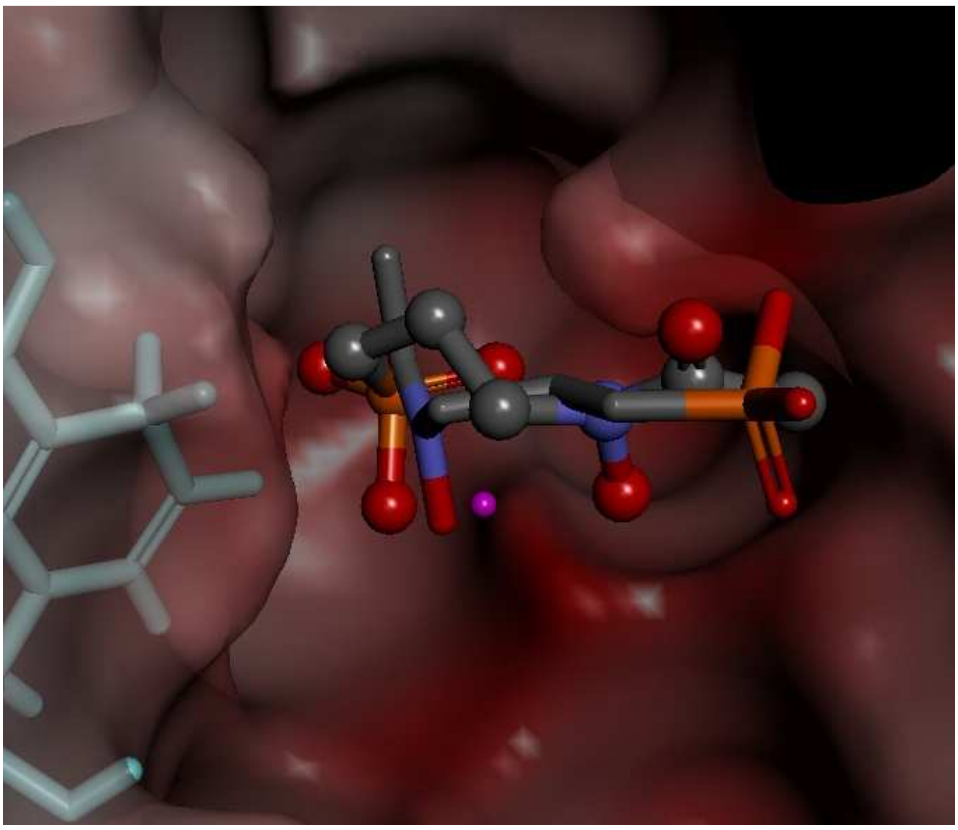

Figure 4.1. Crystal FR900098 and the reverse docked conformation of FR900098 at the *Pf*DXR active site (3AUA)

Initial docking of FR900098 prior to assigning the phosphonate and hydroxamate group a charge of -1.00 each. The figure shows reverse binding of the ligand in the active site pocket of the enzyme. The surface at 1.4 Å is coloured by interpolated charges. Docked fosmidomycin is shown as ball and stick coloured by element,crystal fosmidomycin as stick coloured by elements, NADPH as stick coloured in light blue and Mg^{2+}as pink sphere.

Fosmidomycin was docked into 2EGH for validation. The best conformation selected had a binding energy of -12.26 Kcal/mol to DXR (2EGH). Although this was not the lowest energy conformation (-15.57 kcal/mol) in the cluster, it showed the best orientation to fosmidomycin

and had similar hydrogen bond networks with the active site residues of the enzyme as the original fosmidomycin to which it was complexed. It was also part of the largest cluster of docked conformations which had 45 conformations as opposed to the lowest energy cluster which only contained 5 conformations, an indication that this group of conformation is favoured. The fact that the lowest energy cluster (cluster 1) has fewer conformers than some of the other clusters indicates that although the binding energy is low, the conformations are not the most favourable. The original complexed fosmidomycin showed hydrogen bonding to residues Ser185, Asn226, Lys227 with the phosphonate component, and to residues Asn226, Glu151, Glu230 with the hydroxamic moiety. This was mimicked by the docked fosmidomycin which showed hydrogen bonding of the phosphonate oxygens to Lys227 and Asn226 and the hydroxamate oxygen to Lys214, Ser150, Asp149 and Glu230 (Figure 4.2). This validates and confirms that the *in silico* study is able to mimic the binding of the inhibitor to DXR under the conditions and parameters used on the AutoDock. Based on this, the docked conformations of the halogenated FR900098 analogues were also analyzed.

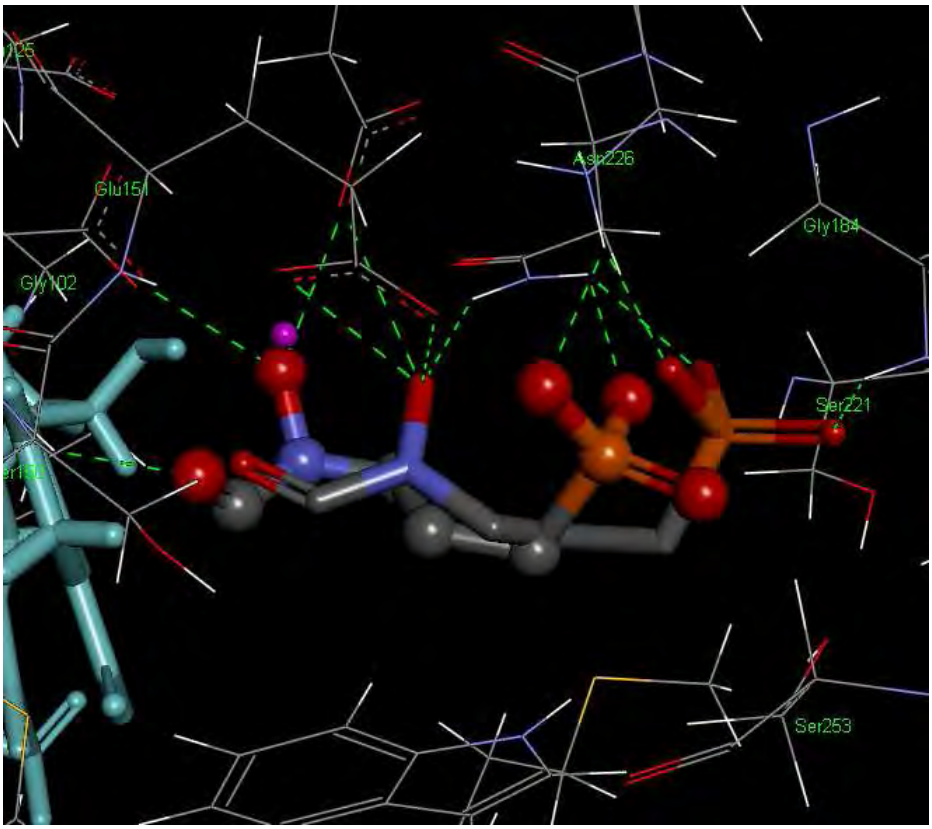

Figure 4.2. Crystal and Docked fosmidomycin at the active site of *Ec*DXR (2EGH)

Showing docked fosmidomycin correctly orientated with crystal fosmidomycin and binding to the same active site residues. Docked fosmidomycin is represented as ball and stick and coloured by element, crystal fosmidomycin as stick coloured by elements, NADPH as stick coloured in light blue and Mg^{2+}as pink sphere.

All the free phosphonic acid FR900098 analogues that were docked in this study were assigned a charge of -1.00 at the phosphonate and hydroxamate ends while the Mg^{2+} ion in the enzymes were assigned a charge +2.00. Gastieger charges were assigned to the protected phosphonates with AutoDock tools and all non-integral charged were spread over the molecules. The negative charges on the phosphonate moiety of the protected derivatives were expected to be much less than that of the free phosphonic acids and thus the attraction between the phosphonate and the divalent metal ion would be reduced such that the hydroxamic acid would have greater attraction for the ion. As such AutoDock was allowed to assign charges on the atoms of the protected analogues. Compounds **2.1 – 2.3**, **2.8 – 2.12**, **2.15 – 2.24** and **2.38** were docked into both *Ec*DXR and *Pf*DXR. Table 4.2 shows the binding energy of the best conformations of each compound after visual assessment at the active site and orientation relative to the original crystal inhibitor, the clusters according to the binding energy and the hydrogen bond network of the inhibitors with the enzyme. Binding energy is the difference between the ligand-receptor complex energy and the sum of the individual energies of the receptor and the ligand. This is automatically calculated on AutoDock 4.2.

Table 4.2. Binding energies and H-bonds of docked FR900098 analogues

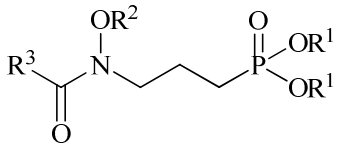

				2EGH		3AUA		*Ec*DXR assay
Comp	**R^1**	**R^2**	**R^3**	**BE (kcal/mol)**	**# H-bond**	**BE (kcal/mol)**	**# H-bond**	**Relative rate (%)**
2.15	Et	Bn	$-CH_2I$	-3.59	3	-3.25	3	88.7
2.16	Et	Bn	$-CH_2CH_2I$	-6.11	1	-3.14	3	103.4
2.10	Et	Bn	$-CH=CH_2$	-6.49	3	-2.75	2	
2.17	Et	Bn	$-CH_2Br$	-5.92	2	-3.36	3	111.3
2.1	H	H	$-CH_2Cl$	-13.68	8	-14.65	5	38.5
2.2	H	H	$-CH_2CH_2Cl$	-11.90	4	-11.33	1	28.5
2.3	H	H	$-CH_2CH_2CH_2Cl$	-11.80	4	-7.65	4	92.3
2.8	Et	Bn	$-CH_2Cl$	-3.62	1	-3.00	2	101.7
2.9	Et	Bn	$-CH_2CH_2Cl$	-7.04	1	-3.63	3	90.6
2.11	Et	Bn	$-CH_2CH_2CH_2Cl$	ND[b]	-	-2.94	3	102.3
2.12	Et	Bn	$-CH_3$	-3.86	6	-3.28	3	83.8
2.18	Et	H	$-CH_3$	-3.94	3	-1.79	5	103.4
2.19	Et	H	$-CH_2Cl$	-11.72	5	-3.59	3	88.7
2.20	Et	H	$-CH_2Br$	-13.09	7	-3.33	4	87.0
2.21	Et	H	$-CH_2I$	-12.02	10	-3.24	4	99.1
2.22	Et	H	$-CH_2CH_2Cl$	-12.11	5	-10.93	7	100
2.23	Et	H	$-CH_2CH_3$	-11.75	6	-3.56	4	105.7
2.24	Et	H	$-CH_2CH_2CH_2Cl$	-11.15	5	-2.03	4	100.4
2.38	H	H	$-CH_2CH_3$	-10.75	9	-12.08	7	77.2
FR900098 (1.45)	H	H	$-CH_3$	-12.36	5	-14.62	5	24.7
Fosmidomycin(1.46)	H	H	H	-12.26	6	-14.47	6	

[b]No docking occurred

From Table 4.2, it is clear that the unprotected phosphonic acids (**2.1 – 2.3** and **2.38**) as well as FR90098 (**1.45**) and fosmidomycin (**1.46**) binds with less energy than the protected analogues to both *Ec*DXR and *Pf*DXR. Interestingly, compounds **2.18 – 2.24** showed similar binding affinity for *Ec*DXR as the phosphonic acid where it was reasoned that the absence of a free phosphonic acid will diminish binding. These results suggest that perhaps the *Ec*DXR harbors enough space to fit the phosphonate ethyl esters of the halogenated FR90098 analogues.

The docking result also showed that the binding affinity of FR900098 derivatives to DXR decreases with increasing length of the side chain, which is consistent with the result of the antiplasmodial test. From the phosphonic acid series **2.1 – 2.3** and **2.38** the derivative with chloroacetyl side chain (**2.1**) had the lowest binding energy of -14.65 kcal/mol while the chlorobutyryl side chain derivative had the highest binding energy of -7.65 kcal/mol (Table 4.2) when docked into *Pf*DXR (3AUA) active site. This trend was however not clear with the ester protected analogues as they did not dock into the active site of the enzyme, which is attributed to their bulky sizes. Compound **2.1** exhibited the best inhibition of both 3AUA and 2EGH even when compared with fosmidomycin and FR900098. Where fosmidomycin and FR900098 had six H-bonds and five H-bonds respectively to the active site residues in 2EGH, **2.1** had eight H-bonds. Its phosphonate oxygen atoms were bound to Ser185, Asn210, Trp211 and Ser 253 while its hydroxamate moiety had H-bond interaction with Glu151, Asn226 and Glu230 (Figure 4.3) all of which with the exception of Asn210 and Ser253 are active site residues of *Ec*DXR.[94]At the *Pf*DXR active site, the phosphonate group of **2.1** had H-bond interaction with Gly271 and the active site residue Asn311 while its hydroxamate oxygens formed a H-bond network with residues Glu315 and Glu233. These H-bond interactions and the low binding energy of compound **2.1** to both DXR enzymes confirm the inhibition superiority of the compound to fosmidomycin and FR900098. This is supported by the antiplasmodial test which showed its protected and partially protected analogues **2.8** and **2.19** respectively (envisaged to hydrolyze to **2.1**) to have higher antiplasmodial activity than FR900098 and its protected and partially protected analogues **2.12** and **2.18** respectively. In light of this observation the possibility exists that the lower assay inhibition of *Ec*DXR by **2.1** as compared to FR900098 (Table 4.1) occurred over time and could be greater than that of FR900098, but is displaced from DXR more quickly. This reiterates the importance of

evaluating the enzyme inhibition from the moment the reaction is initiated. The molecular modeling being a static state, cannot explain how long the inhibitor would remain bound to the enzyme or if it will be displaced by another inhibitor or substrate of the enzyme but it does suggest that that **2.1** binds more strongly to DXR than FR900098.

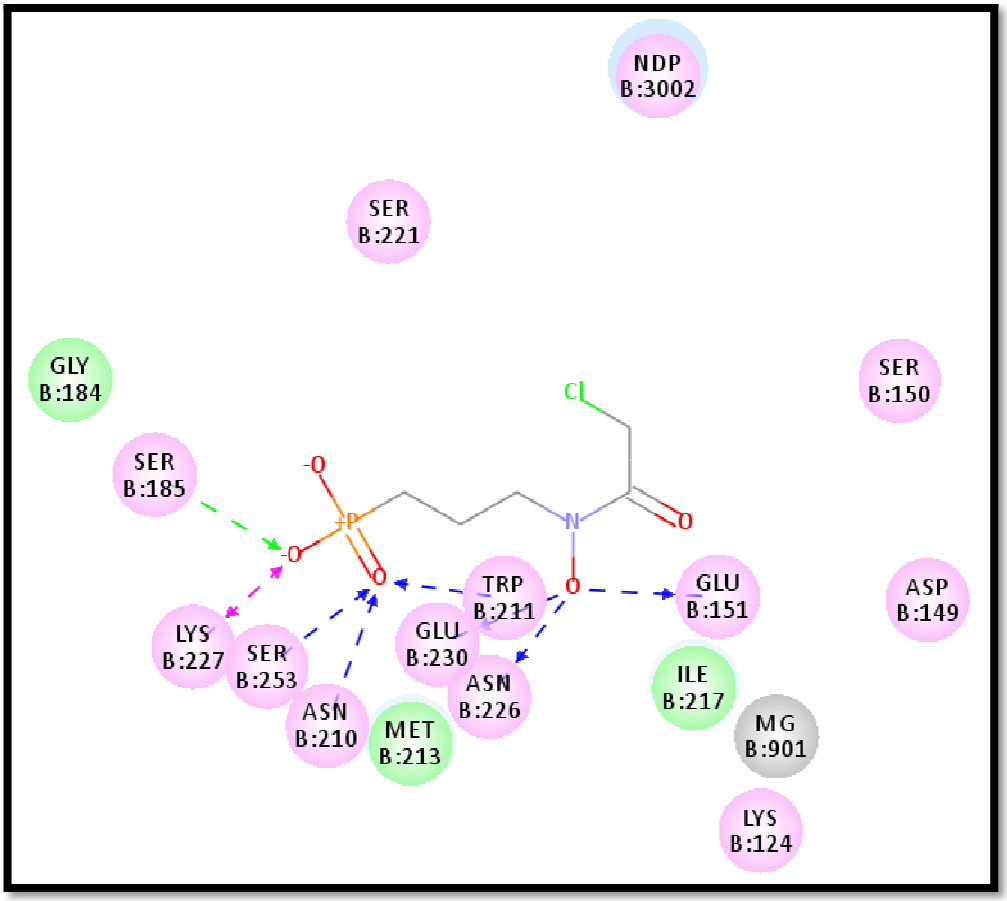

Figure 4.3. 2D visualization of the docked conformation of **2.1** into *Ec*DXR

Docked conformation of **2.1** showing residues involved in H-bond (pink circles) and Van der Waal interaction (Green circle). Dashed blue arrows represent H-bond interaction with amino acid side chain, green dashed arrow represent H-bond interaction with main chain amino acid and pink double headed arrow represent charge interaction between the amino acid and the ligand.

With the exception of one conformation of the 100 docks of **2.22**, all protected and partially protected derivatives of FR900098 did not bind at the active site where FR900098 was originally removed from 3AUA. Conversely, a significant number of the 100 conformations from each of the phosphonic acids formed a cluster and were docked and orientated at the active site as the original FR900098. Since the same grid and parameter were used to dock the ligands, the result supports the knowledge that bulky compounds such as the protected

analogues might be unable to fit into the active site pocket of the enzyme. The inhibition assay (Table 4.1) also supports this result as the protected compound showed no significant activity on the DXR enzyme. An example of the cluster of FR900098 and protected FR900098 (**2.12**) docked into 3AUA is shown in Figure 4.4 A and B respectively. This clearly shows the docked conformations of **2.12** outside the active site of the enzyme and although FR900098 also showed some clusters outside the active site pocket, several of the conformations were bound at the active site pocket.

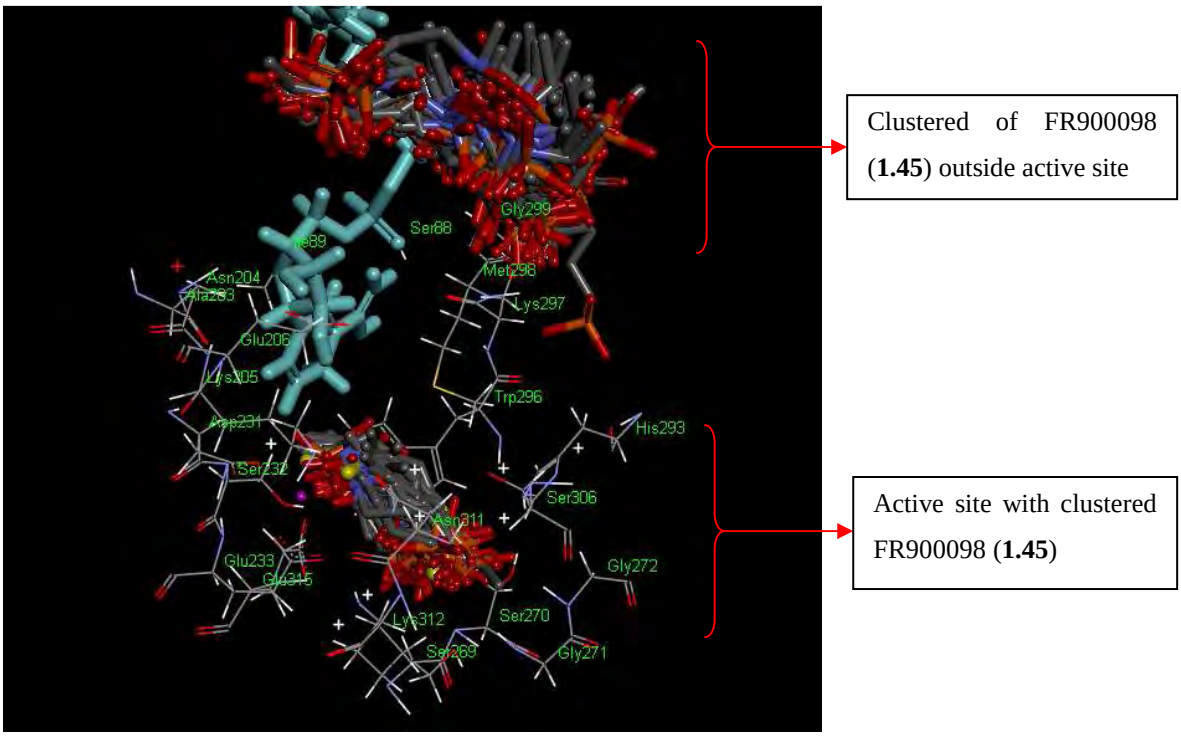

A

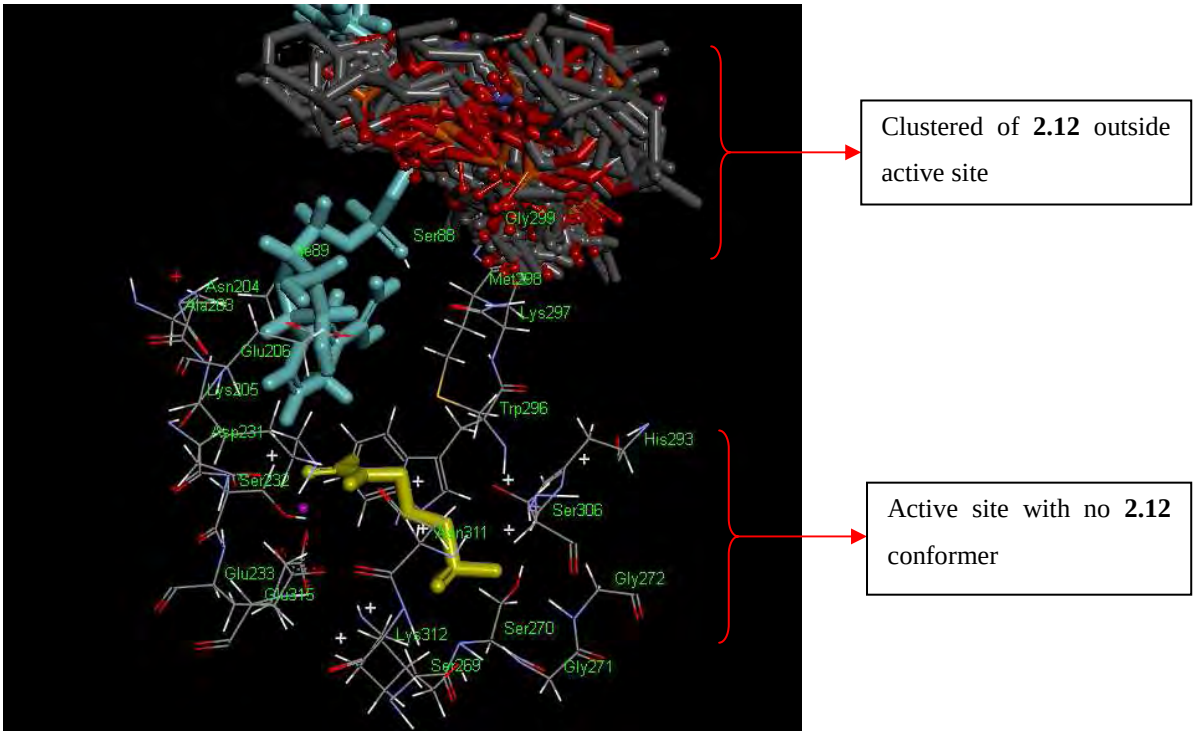

B

Figure 4.4. Docked conformation clusters of FR900098 (**1.45**, A) and **2.12** (B)

Clusters are shown in sticks coloured by atoms, protein residues as wireframe coloured by atom, NADPH as sticks coloured in light blue, Mg^{2+} as a pink sphere and original crystal FR900098 coloured in yellow.

Hydrogen bonding between the inhibitors and the enzyme, particularly at the active site plays a role in indicating the level of inhibition exhibited by an inhibitor. This is proved by the number of hydrogen bonds observed for the different categories of the FR900098 derivatives tested. The protected compounds **2.8 – 2.12, 2.15** and **2.17** showed the least number of hydrogen bonds with the enzymes. This is not surprising since the protective groups on the compounds rendered the active sites unavailable for interaction. The protective groups also render the compounds more bulky and unable to fit into the active site pocket where they could interact with the active site residues. Figure 4.5 and 4.6 representing the partially protected and fully chloroacetyl analogues **2.8** and **2.9** respectively, showed less H-bond when compared to the free phosphonic acid compound **2.1** (Figure 4.3). The number of H-bonds clearly decreased with increased protection of the pharmacophores in the compounds.

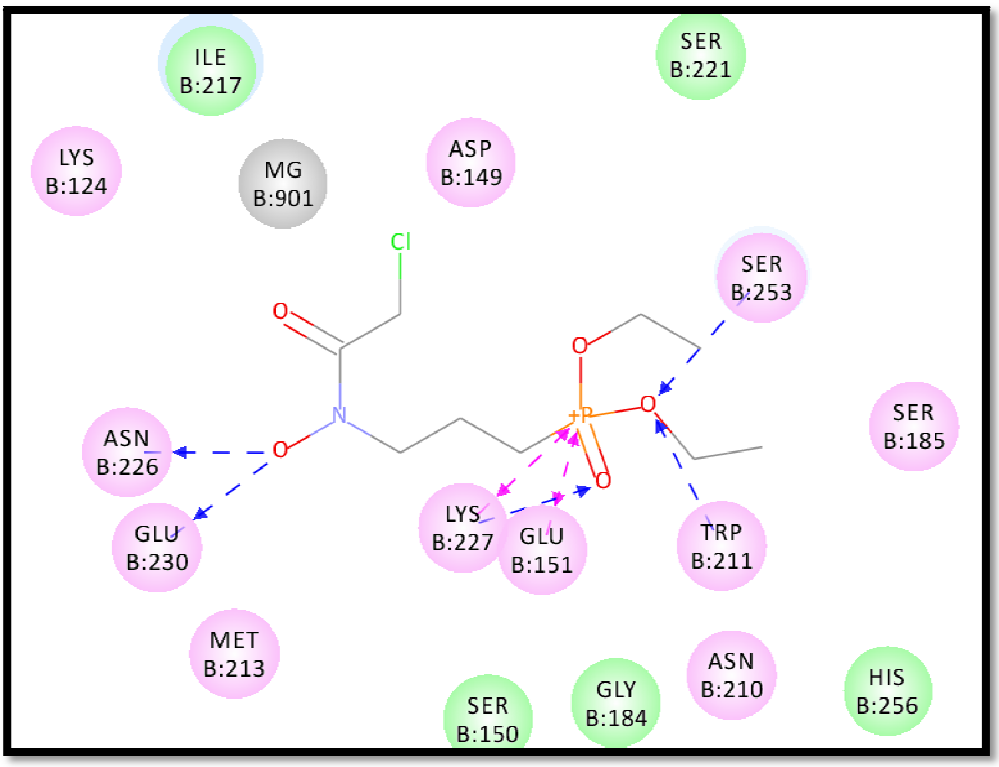

Figure 4.5. 2D visualization of the docked conformation of **2.1** into *Ec*DXR

Docked conformation of **2.8** showing residues involved in H-bond (pink circles) and Van der Waal interaction (Green circle), and the Mg^{2+} ion (Grey circle). Dashed blue arrows represent H-bond interaction with amino acid side chain and pink double headed arrow represent charge interaction between the amino acid and the ligand.

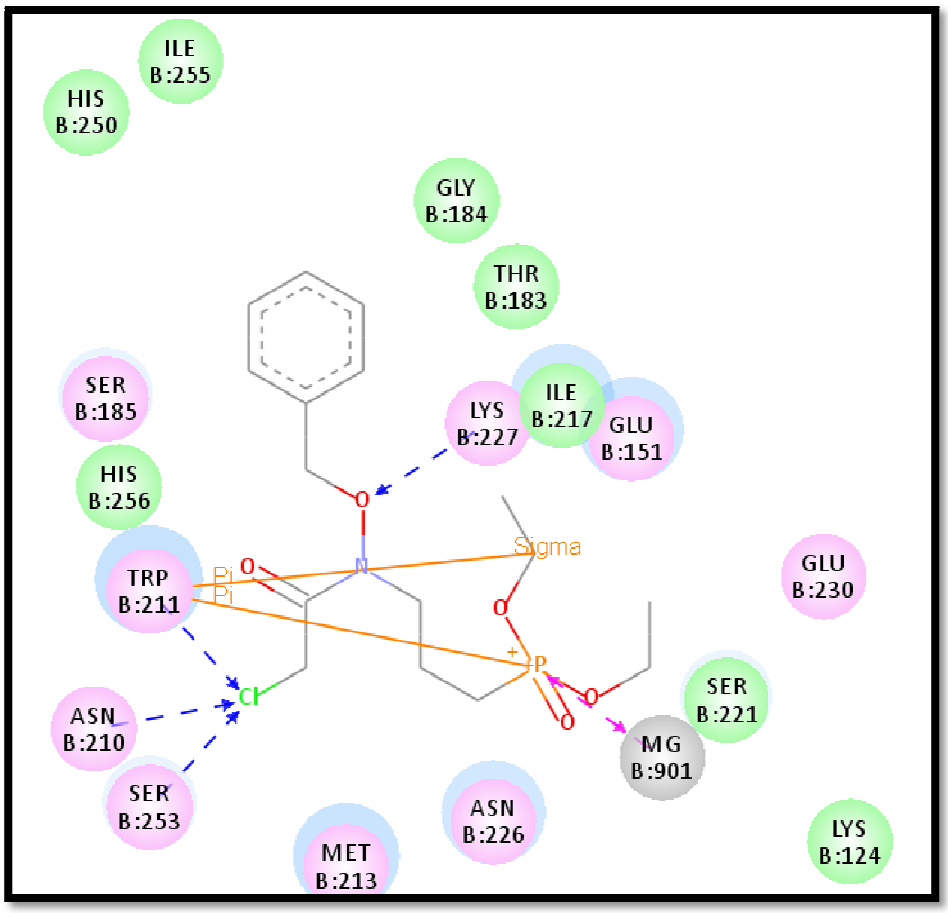

Figure 4.6. 2D visualization of the docked conformation of **2.1** into *Ec*DXR

Docked conformation of **2.9** showing residues involved in H-bond (pink circles) and Van der Waal interaction (Green circle), and the Mg^{2+} ion (Grey circle). Dashed blue arrows represent H-bond interaction with amino acid side chain, pink double headed arrow represent charge interaction and the orange line shows Pi interactions between the amino acid and the ligand.

One very interesting observation was the high binding affinity of the protected chloropropyl analogues as compared to the protected chloroacetyl analogues. This is contrary to what is observed in the antiplasmodial activity and the unprotected analogues of the compounds where there is reduced activity with the longer side chain. Of the series of protected compounds, **2.22** and **2.9** showed less binding energy (greater binding) to 2EGH and 3AUA than **2.19** and **2.8**. Combined with the fact that **2.2** gave the best *in vitro* inhibition of *Ec*DXR when compared with the other FR900098 analogues (Table 4.1), there appears to be a high level of inhibition with the chloropropyl analogues is worth investigating. It would appear that the presence of chlorine atom in the compound is responsible for the observed antiplasmodial and DXR inhibition activities since the non-halogenated analogue of the

compound (**2.38**) did not show the same activity. Unfortunately the protected and unprotected analogues **2.9**, **2.22** and **2.2** did not show any significant antiplasmodial activity. This is suspected to be a delivery problem where the compound is unable to reach its site of action i.e. the DXR active site. Compound **2.2** would therefore make a good lead compound for investigation to determine how to ensure that the drug gets to the site of action where it can bind to DXR.

The *in silico* studies did not reveal any significant difference in the binding of compounds carrying different halogens. No major difference was observed between the binding energies of compounds **2.19**, **2.20** and **2.21** and between compounds **2.8**, **2.15** and **2.17**. This further confirms the observation made from the antiplasmodial test where compounds with different halogens did not show any significant difference in their antiplasmodial activity (Table 2.5). This can be interpreted to mean that the type of halogen present in compound have no effect on the binding of the compounds to DXR although the presence of a halogen promotes the inhibition property of the compounds. The effect of the presence of chlorine is observed with the chloropropyl analogue **2.2** and the chloroacetyl analogue **2.1** which showed better binding affinity for both *Ec*DXR and *Pf*DXR than the unchlorinated propyl (**2.38**) and acetyl (FR900098 (**1.45**)) analogues respectively.

The phosphonic acids **2.1 – 2.3** and **2.38** as well as FR900098 (**1.45**) and fosmidomycin (**1.46**) showed slightly higher affinity for *Pf*DXR than *Ec*DXR. However, apart from the partially deprotected compounds which showed significantly higher preference for 2EGH than 3AUA, binding of the analogues to the two enzymes showed similar trends and are thus comparable i.e. no significant difference was observed in the binding of the compounds to both enzymes. Thus the enzyme assay inhibition result can be expected to be similar to what would be obtained had *Pf*DXR been used for the assay.

From the series of compounds docked, compound **2.1** showed the best (strongest) binding to both *Ec*DXR and *Pf*DXR even when compared with fosmidomycin and FR90098. However while this compound showed good antiplasmodial and DXR inhibition property, it was not as active as fosmidomycin and FR900098 in the enzyme inhibition assays. Its ester-protected analogue **2.19**, though cannot inhibit the enzyme or bind to the enzyme as indicated by the

docking, has antiplasmodial activity superior to FR900098 (**1.45**) which indicates that if absorbed appropriately the chlorinated FR900098 derivative has the potential to highly inhibit DXR once the protective groups have been removed after absorption into the parasite.

4.2.2 *In silico* studies of chloroquine-fosmidomycin hybrids 3.3 and 3.4

Many studies focused on developing inhibitors against DXR rightly take into consideration the small pocket into which such inhibitors must fit in order to inhibit the enzyme. We postulated that bulky inhibitors could fit into this pocket if NADPH is removed or displaced. The chloroquine-fosmidomycin hybrids **3.3** and **3.4** designed and discussed in chapter 3 were considered good candidates to displace NADPH from binding to DXR. To test this hypothesis, the hybrids **3.3** and **3.4** were prepared and docked into the active sites of *Pf*DXR (PDB code: 3AUA) and *Ec*DXR (PDB code: 2EGH) after removing NADPH and inhibitors from the sites.

The experiment was conducted on AutoDock 4.2 using the Lamarckian algorithm to create a population of 150 individuals with 2500000 maximum number of evaluations in 10 GA runs. As this was an experiment to determine the feasibility of the hybrids binding to DXR, 10 GA runs were considered sufficient. The docked conformations were assessed based on their binding energy and the number of hydrogen bonds formed with the enzyme amino acid residues.

Table 4.3. Binding energies and H-bonds of docked chloroquine-fosmidomycin hybrids **3.3** and **3.4**

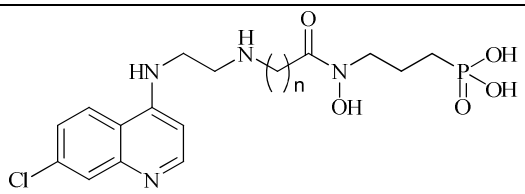

		2EGH		3AUA	
Compound	**n**	**BE (Kcal/mol)**	**# H-bonds**	**BE (Kcal/mol)**	**# H-bonds**
3.3	1	-10.72	4	-3.75	3
3.4	2	-3.72	3	-3.23	5
NADPH		ND	6	ND	10

Analysis of the docking result of hybrids **3.3** and **3.4** showed that both hybrids required less energy to bind to *Ec*DXR than *Pf*DXR i.e. the hybrids have more affinity for the *Ec*DXR. The acetyl linked hybrid **3.3** binds with the least energy (-10.72 Kcal/mol) to *Ec*DXR as compared to the propyl linked hybrid **3.4**. This supports the antiplasmodial activity of their protected derivatives which showed the acetyl linked hybrid **3.8** to be more active than the propyl linked hybrid **3.9** (Chapter 3, Table 3.2) indicating the important role of the linker. Hybrid **3.3** showed four hydrogen bonds to the active site residues Lys124, Asn226, Asp149 and Glu230 of the *Ec*DXR (Figure 4.7). Although this is less than the number of hydrogen bond interaction of NADPH with the same enzyme (6 H-bonds), it shows that there is a possibility for the compound to bind to *Ec*DXR. Hybrid **3.3** orientate such that it spans the space between the fosmidomycin (**1.46**) and NADPH binding site with its hydroxamate end towards the Mg^{2+} metal ion and overlapping towards the NADPH binding site. This indicates a potential of the hybrid to displace or prevent the optimum binding of NADPH to the enzyme.

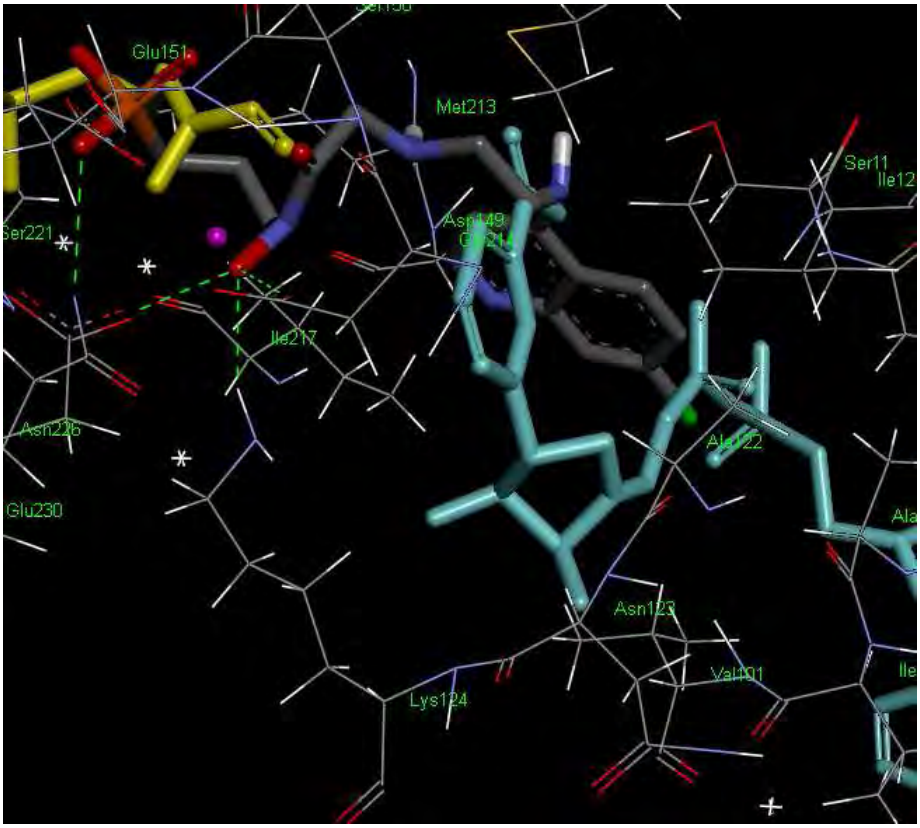

Figure 4.7. Docked conformation of protected chloroquine-fosmidomycin hybrid **3.3** in 2EGH

Showing hybrid **3.3** docked between fosmidomycin (**1.46**) and NADPH binding sites and overlapping into the NADPH binding site. Hybrid **3.3** is represented as stick coloured by element, fosmidomycin as stick coloured in yellow, NADPH as stick coloured in light blue,Mg^{2+}as pink sphere and hydrogen bonds as broken green lines.

Unfortunately both hybrids **3.3** and **3.4** showed considerably less hydrogen bonds to the enzyme residues as compared to NADPH and coupled with the generally high binding energy for *Pf*DXR they might not exhibit good inhibition of the DXR enzymes. It should be noted however, that the crystal structures 3AUA and 2EGH were obtained with NADPH and inhibitors already docked into the active sites. This means that the enzyme had already rearranged into a particular conformation upon binding of the inhibitors. Since there is limited flexibility during docking it is possible that the compounds could not conform to the more rigid structure and hence could not attain optimum binding or interaction with the enzyme. In a biological system, the enzymes would be more flexible and might be able to adjust their conformation to better fit the hybrids.

4.3 EXPERIMENTAL

4.3.1 Expression and purification of *E. coli* DXR

The expression and purification of *E. coli* was carried out by Nicodemus Mautsa at the Rhodes University Centre for Chemico- and Biomedicinal Research using an established method developed by Kuzuyama *et al*. (1998).[169] In summary, competent *E. coli* XL1 Blue cells were transformed with *E. coli* DXR plasmid construct. The transformed cells were incubated in 2xYT broth until the mid-logarithmic growth was reached after which isopropyl β-D-1-thiogalactopyranoside (IPTG) was added to the culture to induce over expression of the DXR gene and hence over production of the enzyme. The cells were harvested and treated with lysozyme. Sonication of the cells allowed the release of DXR from the bacterial cells and removal of the cell debris was achieved by centrifugation. Purification of DXR was achieved by agitation of the lysate with nickel charged resins to adsorb the protein unto the resins. Pure DXR was obtained by displacement of the enzyme from the resins by washing with native elution buffer which was made up of 20mM Tris-HCl, 300mM NaCl and 1M imidazole at pH 8.0.

4.3.2 *In vitro Ec*DXR inhibition assay

The inhibition assay was conducted by Nicodemus Maustsa at the Centre for Chemico- and Biomedicinal Research, Rhodes University. The assay was conducted in 96-well UV microtitre plates. The reaction mixture was made up of 100mM Tris-HCl, 1mM $MnCl_2$, 0.3 mM NADPH and 0.3mM DOXP to a volume of 100 µl in ddH_2O. Negative controls or blanks which included mixture lacking 1) DOXP, 2) $MnCl_2$, 3) DXR and 4) NADPH were prepared and tested to determine activity of the enzyme. The enzyme was pre-incubated with equal volumes of inhibitor and in case of the blanks with ddH_2O for five minutes at 37^oC before initiating the reaction. The reactions were initiated by introduction of 100 µl of the pre-incubated enzyme-inhibitor solution into the reaction mixture to make a total of 200 µl and 5 µM concentration of inhibitor in each case. The reaction which involved the consumption of NADPH to give NADP at 37^oC was monitored on a PowerWave

spectrophotometer by measuring the UV absorbance of the reaction mixture at 340nm over 10 minutes.

4.3.3 *In silico Ec*DXR inhibition assay

Preparation of Ligands for docking

Structures of ligands **2.1 – 2.3**, **2.8 – 2.12**, **2.15 – 2.24**, **3.3** and **3.4** were sketched in chemDraw Ultra 11.0.1 with the phosphonic acids deprotonated. A random rotor search was conducted on Avogadro 1.0.3 to obtain the *in vacuo* global minimum conformer for each ligand. The lowest energy conformer of the 100 conformations generated for each lignad was further optimized geometrically and saved as pdb files.

Flexible docking of FR900098 analogues to EcDXR and PfDXR

The X-ray crystal structures of *Ec*DXR (PDB code: 2EGH) and *Pf*DXR (PDB code: 3AUA) were obtained from the Protein Data Bank. On AutoDock 4.2, missing atoms from the proteins were repaired and water molecules were removed from the proteins. Gastieger charges were added, all non-polar hydrogens were merged and residual charges were spread over the protein. Active site residues Ser185, Ser221, Lys227, Asp149, Glu151 and Glu230 from 2EGH and Ser270, Asn311, His293, Asp231 and Glu315 from 3AUA were defined as flexible residues. In the remaining rigid protein structure Mg^{2+} was manually assigned a charge of +2.00. The prepared geometry optimized ligands were imported into AutoDock 4.2 where the Gastiger charges were added and non-polar hydrogens were merged. All possible torsions were allowed and the amide bonds were by default made non-rotatable. Maps of all possible atoms involved in the ligand-receptor interaction were created and a grid box was placed at the active site to localize the site to which the ligands would dock. A grid box of 62, 52, 56 units dimension along the x, z, y axis respectively and a grid point of 0.375 Å were used for 2EGH. The box was offset from center by -1.694, 0.944 and 1.472 at the x, y and z axis respectively. On 3AUA, the grid box had dimensions of 58, 60 and 58units along the x, y and z axis and were offset from the centre by 4.333, -1.083 and 2.500 Å respectively. A grid point spacing of 0.375 Å was maintained. A Lamarckian genetic algorithm was

employed for the docking simulation in AutoDock 4.2. The default genetic algorithm parameters on AutoDock 4.2 was used except the number of GA runs which was increased to 100. That is, a population size of 150 allowing for a maximum of 2 500 000 energy evaluations and 27 000 generation was used for the docking. The 100 conformers generated for each ligand after the docking were clustered at 2.0 rmsd.

The docked conformations were visualized on Discovery Studio Visualizer 3.0. The docked conformers were assessed based on the numbers in the clusters, the binding energy, the number of hydrogen bonds with the protein residues and visual assessment of the orientation of the conformers at the active site of the enzyme.

CHAPTER 5

5. SUMMARY AND CONCLUSIONS

The aim of the study was to design and synthesize FR900098 analogues with improved antiplasmodial and lipophilic properties. This was to be achieved through the synthesis of halogenated fosmidomycin analogs and hybrid compounds.. Although both sets of compounds were successfully synthesised, synthetic challenges prevented the full exploration of the synthetic molecules.

The series of synthesized halogenated FR900098 analogues investigated the effect of varying acyl side chain length, different halogens and effect of protection groups on the pharmacophore of the compounds. The phosphonate esters of the halogenated FR900098 analogues showed higher antiplasmodial activity than their free phosphonic acid analogues. The antiplasmodial activity decreased with increasing length of the acyl side chain with the halogenated acetyl analogues **2.8**, **2.15**, **2.17** and **2.19 – 2.21** showing the best activity. No significant difference was observed in the antiplasmodial activity when the compound was substituted with different halogens. However, the presence of the halogens increased their potency when compared with their non-halogenated analogues.

Two protected chloroquinoline-fosmidomycin hybrids **3.8** and **3.9** were successfully synthesized, differentiated by the length of the linker between the quinoline and the fosmidomycin components. The two components of the hybrids were covalently linked through their side chains having synthesized each component separately. The study revealed the chloroquinoline-fosmidomycin hybrids as potent antiplasmodial agents against both the D10 and FCR-3 strains of *P. falciparum*. The acetyl linked hybrid **3.8** was four times more potent than the propionyl linked hybrid **3.9** on the Gambian FCR-3*P. falciparum* strain. It is however suspected that the activity of the hybrids was due more to the quinoline moiety than the fosmidomycin moiety since other hybrids of fosmidomycin such as the pyrazinoic acid-fosmidomycin hybrid showed no antiplasmodial activity.

Preliminary enzyme inhibition studies of the halogenated FR900098 analogues were conducted on recombinant *E. coli* DXR. The phosphonic acids as opposed to the phosphonate esters showed the best inhibition of the enzyme. Here the chloropropionyl analogue **2.2**

demonstrated the best inhibition of DXR followed by the chloroacetyl derivative **2.1**, reducing the activity of the enzyme to 28.5% and 38.5% respectively. FR900098 however showed better inhibition of *Ec*DXR than derivatives **2.1** and **2.2**. However both **2.1** and **2.2** are provide good lead compounds for further modifications and development as antiplasmodial agents.

Molecular modelling of the halogenated fosmidomycin analogues into crystal structures of *E. coli* and *P. falciparum* DXR was conducted to investigate the binding potential and interaction of the compounds with the enzymes. The phosphonic acids **2.1 – 2.3** and **2.38** exhibited the lowest binding energies comparable to fosmidomycin and FR900098. The phosphonate esters showed minimal to moderate binding probably due to their bulky structure which prevented optimum fitting into DXR active site. This corroborates the result of the enzyme inhibition assay and confirms the need for free phosphonic acids to bind at DXR active site.

Phosphonic acid hybrids **3.3** and **3.4** were docked into *Ec*DXR and *Pf*DXR lacking NADPH, to explore their potential to fit into the active site and possibly displace NADPH. The acetyl linked hybrid **3.3** showed more promising interactions to both enzymes indicating that the linker between the quinoline and fosmidomycin moieties is important for efficient binding. Although the binding energy of the hybrids were much higher than FR900098 or the halogenated FR900098 derivatives, the hybrids bind such that it aligns itself in the space between FR900098 and the NADPH binding site. The possibility therefore exist that the hybrids might be able to compete with NADPH for binding to DXR.

Overall the halogenated acetyl FR900098 analogues and the acetyl linked hybrid are a very promising group of compounds that could be valuable for further development as antimalarial drugs. Based on the enzyme inhibition assay and the *in silico* study result, the chloropropionyl phosphonic acid **2.3**, which also exhibited intriguing inhibition and binding to DXR will be worth investigating further as a lead compound for antiplasmodial drug development.

5.1 RECOMMENDATIONS

The scope of the present study was centered on the synthesis of the halogenated fosmidomycin derivatives and the chloroquinoline-fosmidomycin hybrids. As such the biological activity of the synthesized compounds has not been fully explored. Further assessment of their enzyme inhibition and the nature of inhibition especially on *Pf*DXR is recommended.

The reactive nature of halogens potentiates the halogenated FR90098 analogues to undergo non-specific reactions. For this reason it is imperative and recommended that future studies on the group of compounds include full cytotoxicity studies to determine their selectivity for the malaria parasite.

Further studies into developing synthetic methods for the preparation of fully deprotected hybrids are important in confirming both the binding to DXR and haematin detoxification. The molecular docking studies of the hybrids support the idea of designing new DXR inhibitors by exploring the NADPH binding pocket.

Reference List

1. World Health Organization. World Malaria Report 2010. 2010. Geneva, Switzerland.
2. Burger, E. T. Preparing adult patients for international travel. *Nurse Pract.* **2001,** *26*, 13-23.
3. Ridley, R. G. Perspectives: Biomedicine - Planting the seeds of new antimalarial drugs. *Science* **1999,** *285*, 1502-1503.
4. Collins, W. E. *Plasmodium knowlesi*: A Malaria Parasite of Monkeys and Humans. *Annual Reviews of Entomology* **2012,** *57*, 107-121.
5. Williams, D. A.; Lemke, T. L. *Foye's principles of medicinal chemistry*; Lippincott Williams & Wilkins: Philadelphia, 2002; pp 867-910.
6. Beers, M. H.; Berkow, R.; Merck, R. L. *The Merck manual of diagnosis and therapy*; Merck Research Laboratories: Whitehouse Station, N.J, 1999; pp 1241-1242.
7. Wirth, D. F. The parasite genome: Biological revelations. *Nature* **2002,** *419*, 495-496.
8. Greenwood, B. M.; Fidock, D. A.; Kyle, D. E.; Kappe, S. H. I.; Alonso, P. L.; Collins, F. H.; Duffy, P. E. Malaria: progress, perils, and prospects for eradication. *The Journal of Clinical Investiation* **2008,** *118*, 1266-1276.
9. Katzung, B. G. *Basic & clinical pharmacology*; Lange Medical Books/McGraw Hill: New York, 2004; pp 852-875.
10. Daneshvar, C.; Davis, T. M. E.; Cox-Singh, J.; Rafa'ee, M.; Zakaria, S. K.; Divis, P. C. S.; Singh, B. Clinical and parasitological response to oral chloroquine and primaquine in uncomplicated human *Plasmodium knowlesi* infections. *Malaria Journal* **2010,** *9*, 238.
11. Cui, L. W.; Su, X. Z. Discovery, mechanisms of action and combination therapy of artemisinin. *Expert Review of Anti-Infective Therapy* **2009,** *7*, 999-1013.
12. Klayman, D. L. Qinghaosu (artemisinin): an antimalarial drug from China. *Science* **1985,** *228*, 1049-1055.
13. White, N. J. Drug treatment and prevention of malaria. *European Journal of Clinical Pharmacology* **1988,** *34*, 1-14.
14. Wainwright, M.; Amaral, L. Review: The phenothiazinium chromophore and the evolution of antimalarial drugs. *Tropical Medicine & International Health* **2005,** *10*, 501-511.
15. Schulemann, W. Synthetic Anti-Malarial Preparations. *Proceedings of the Royal Society of Medicine* **1932,** *25*, 897-905.
16. Elderfield, R. C.; Gensler, W. J.; Bembry, T. H.; Brody, F.; Wiederhold, L.; Newman, B. Aminoalkylamino Derivatives of 8-Aminoquinoline1. *Journal of the American Chemical Society* **1946,** *68*, 1568-1569.

17. Elderfield, R. C.; Mertel, H. E.; Mitch, R. T.; Wempen, I. M.; Werble, E. Synthesis of Primaquine and Certain of its Analogs1. *Journal of the American Chemical Society* **1955,** *77*, 4816-4819.
18. Vennerstrom, J. L.; Nuzum, E. O.; Miller, R. E.; Dorn, A.; Gerena, L.; Dande, P. A.; Ellis, W. Y.; Ridley, R. G.; Milhous, W. K. 8-Aminoquinolines Active against Blood Stage *Plasmodium falciparum* In Vitro Inhibit Hematin Polymerization. *Antimicrobial Agents and Chemotherapy* **1999,** *43*, 598-602.
19. Peters, W. The evolution of tafenoquine - antimalarial for a new millennium? *Journal of the Royal Society of Medicine* **1999,** *92*, 345-352.
20. Hemmi, K.; Takeno, H.; Hashimoto, M.; Kamiya, T. Studies on Phosphonic Acid Antibiotics .3. Structure and Synthesis of 3-(N-Acetyl-N-Hydroxyamino)Propylphosphonic Acid (Fr-900098) and 3-(N-Acetyl-N-Hydroxyamino)-2(R)-Hydroxypropylphosphonic Acid (Fr-33289). *Chemical & Pharmaceutical Bulletin* **1981,** *29*, 646-650.
21. Brueckner, R. P.; Coster, T.; Wesche, D. L.; Shmuklarsky, M.; Schuster, B. G. Prophylaxis of *Plasmodium falciparum* infection in a human challenge model with WR 238605, a new 8-aminoquinoline antimalarial. *Antimicrobial Agents and Chemotherapy* **1998,** *42*, 1293-1294.
22. Brueckner, R. P.; Lasseter, K. C.; Lin, E. T.; Schuster, B. G. First-time-in-humans safety and pharmacokinetics of WR 238605, a new antimalarial. *The American Journal of Tropical Medicine and Hygiene* **1998,** *58*, 645-649.
23. Covell, G.; Coatney, G. R.; Field, J. W.; Singh, J. Chemotherapy of Malaria. 27, 1-122. 1955. Geneva. World Health Organization Monograph Series.
24. Meshnick, S. R.; Dobson, M. J. The History of Antimalarial Drugs. In *Antimalarial chemotherapy: mechanisms of action, resistance, and new directions in drug discovery*; Rosenthal, P. J. Ed.; Humana Press Inc: Totowa, New Jersey, 2001; pp 15-25.
25. Churchill, F. C.; Patchen, L. C.; Campbell, C.; Schwartz, I. K.; Nguyen-Dinh, P.; Dickinson, C. M. Amodiaquine as a prodrug: Importance of metabolite(s) in the antimalarial effect of amodiaquine in humans. *Life Sciences* **1985,** *36*, 53-62.
26. Brasseur, P.; Guiguemde, R.; Diallo, S.; Guiyedi, V.; Kombila, M.; Ringwald, P.; Olliaro, P. Amodiaquine remains effective for treating uncomplicated malaria in West and Central Africa. *Transactions of the Royal Society of Tropical Medicine and Hygiene* **2011,** *93*, 645-650.

27. Egan, T. J.; Hunter, R.; Kaschula, C. H.; Marques, H. M.; Misplon, A.; Walden, J. Structure-Function Relationships in Aminoquinolines: Effect of Amino and Chloro Groups on Quinoline-Hematin Complex Formation, Inhibition of β-Hematin Formation, and Antiplasmodial Activity. *Journal of Medicinal Chemistry* **1999,** *43*, 283-291.
28. Kaschula, C. H.; Egan, T. J.; Hunter, R.; Basilico, N.; Parapini, S.; Taramelli, D.; Pasini, E.; Monti, D. StructureΓêÆActivity Relationships in 4-Aminoquinoline Antiplasmodials. The Role of the Group at the 7-Position. *Journal of Medicinal Chemistry* **2002,** *45*, 3531-3539.
29. Croft, A. M. Developing safe antimalaria drugs: Key lessons from mefloquine and halofantrine. *The International Journal of Risk and Safety in Medicine* **2007,** *19*, 153-161.
30. Mbai, M.; Rajamani, S.; January, C. T. The anti-malarial drug halofantrine and its metabolite N-desbutylhalofantrine block HERG potassium channels. *Cardiovascular Research* **2002,** *55*, 799-805.
31. Fitch, C. D. Ferriprotoporphyrin IX, phospholipids, and the antimalarial actions of quinoline drugs. *Life Sciences* **2004,** *74*, 1957-1972.
32. Wong, R. P. M.; Salman, S.; Ilett, K. F.; Siba, P. M.; Mueller, I.; Davis, T. M. E. Desbutyl-Lumefantrine Is a Metabolite of Lumefantrine with Potent In Vitro Antimalarial Activity That May Influence Artemether-Lumefantrine Treatment Outcome. *Antimicrobial Agents and Chemotherapy* **2011,** *55*, 1194-1198.
33. Koepf-Maier, P.; Koepf, H. Non-platinum group metal antitumor agents. History, current status, and perspectives. *Chemical Reviews* **1987,** *87*, 1137-1152.
34. Biot, C.; Glorian, G.; Maciejewski, L. A.; Brocard, J. S.; Domarle, O.; Blampain, G.; Millet, P.; Georges, A. J.; Abessolo, H.; Dive, D.; Lebibi, J. Synthesis and Antimalarial Activity in Vitro and in Vivo of a New FerroceneΓêÆChloroquine Analogue. *Journal of Medicinal Chemistry* **1997,** *40*, 3715-3718.
35. Domarle, O.; Blampain, G.; Agnaniet, H.; Nzadiyabi, T.; Lebibi, J.; Brocard, J.; Maciejewski, L.; Biot, C.; Georges, A. J.; Millet, P. In Vitro Antimalarial Activity of a New Organometallic Analog, Ferrocene-Chloroquine. *Antimicrobial Agents and Chemotherapy* **1998,** *42*, 540-544.
36. Dubar, F.; khalife, J.; Brocard, J.; Dive, D.; Biot, C. Ferroquine, an Ingenious Antimalarial Drug –Thoughts on the Mechanism of Action. *Molecules* **2008,** *13*, 2900-2907.
37. Nzila, A. The past, present and future of antifolates in the treatment of Plasmodium falciparum infection. *Journal of Antimicrobial Chemotherapy* **2006,** *57*, 1043-1054.

38. Hitchings, G. H.; Elion, G. B.; Falco, E. A.; Russell, P. B.; Sherwood, M. B.; Vanderwerff, H. Antagonists of Nucleic Acid Derivatives. *Journal of Biological Chemistry* **1950,** *183*, 1-9.
39. Falco, E. A.; Goodwin, L. G.; Hitchings, G. H.; Rollo, I. M.; Russell, P. B. 2:4-Diaminopyrimidines—a new series of antimalarials. *British Journal of Pharmacology* **1951,** *6*, 185-200.
40. Wolf, R.; Tuzun, B.; Tuzun, Y. Dapsone: unapproved uses or indications. *Clinics in Dermatology* **2001,** *18*, 37-53.
41. Nzila, A. Inhibitors of de novo folat enzymes in Plasmodium falciparum. *Drug Discovery Today* **2006,** *11*, 939-944.
42. Gregson, A.; Plowe, C. V. Mechanisms of Resistance of Malaria Parasites to Antifolates. *Pharmacological Reviews* **2005,** *57*, 117-145.
43. Schmid, G.; Hofheinz, W. Total synthesis of qinghaosu. *Journal of the American Chemical Society* **1983,** *105*, 624-625.
44. Patrick S., C. Making artemisinin. *Phytochemistry* **2008,** *69*, 2881-2885.
45. Li, Y.; Wu, Y. L. An over four millennium story behind qinghaosu (Artemisinin) - A fantastic antimalarial drug from a traditional Chinese herb. *Current Medicinal Chemistry* **2003,** *10*, 2197-2230.
46. van Agtmael, M. A.; Eggelte, T. A.; van Boxtel, C. J. Artemisinin drugs in the treatment of malaria: from medicinal herb to registered medication. *Trends in Pharmacological Sciences* **1999,** *20*, 199-205.
47. Chaturvedi, D.; Goswami, A.; Pratim Saikia, P.; Barua, N. C.; Rao, P. G. Artemisinin and its derivatives: a novel class of anti-malarial and anti-cancer agents. *Chemical Society Reviews* **2010,** *39*, 435-454.
48. Dondorp, A. M.; Nosten, F.; Yi, P.; Das, D.; Phyo, A. P.; Tarning, J.; Lwin, K. M.; Ariey, F.; Hanpithakpong, W.; Lee, S. J.; Ringwald, P.; Silamut, K.; Imwong, M.; Chotivanich, K.; Lim, P.; Herdman, T.; An, S. S.; Yeung, S.; Singhasivanon, P.; Day, N. P. J.; Lindegardh, N.; Socheat, D.; White, N. J. Artemisinin Resistance in Plasmodium falciparum Malaria. *New England Journal of Medicine* **2009,** *361*, 455-467.
49. Jones, K. L.; Donegan, S.; Lalloo, D. G. Artesunate versus quinine for treating severe malaria. *Cochrane Database of Systematic Reviews* **2007**.
50. Walsh, J. J.; Coughlana, D.; Heneghan, N.; Gaynor, C.; Bell, A. A novel artemisinin-quinine hybrid with potent antimalarial activity. *Bioorganic & Medicinal Chemistry Letters* **2007,** *17*, 3599-3602.

51. Paik, I. H.; Xie, S.; Shapiro, T. A.; Labonte, T.; Narducci Sarjeant, A. A.; Baege, A. C.; Posner, G. H. Second Generation, Orally Active, Antimalarial, Artemisinin-Derived Trioxane Dimers with High Stability, Efficacy, and Anticancer Activity. *Journal of Medicinal Chemistry* **2006,** *49*, 2731-2734.
52. O'Neill, P. M.; Searle, N. L.; Kan, K. W.; Storr, R. C.; Maggs, J. L.; Ward, S. A.; Raynes, K.; Park, B. K. Novel, Potent, Semisynthetic Antimalarial Carba Analogues of the First-Generation 1,2,4-Trioxane Artemether. *Journal of Medicinal Chemistry* **1999,** *42*, 5487-5493.
53. Vennerstrom, J. L.; Arbe-Barnes, S.; Brun, R.; Charman, S. A.; Chiu, F. C. K.; Chollet, J.; Dong, Y.; Dorn, A.; Hunziker, D.; Matile, H.; McIntosh, K.; Padmanilayam, M.; Santo Tomas, J.; Scheurer, C.; Scorneaux, B.; Tang, Y.; Urwyler, H.; Wittlin, S.; Charman, W. N. Identification of an antimalarial synthetic trioxolane drug development candidate. *Nature* **2004,** *430*, 900-904.
54. Charman, S. A.; Arbe-Barnes, S.; Bathurst, I. C.; Brun, R.; Campbell, M.; Charman, W. N.; Chiu, F. C. K.; Chollet, J.; Craft, J. C.; Creek, D. J.; Dong, Y.; Matile, H.; Maurer, M.; Morizzi, J.; Nguyen, T.; Papastogiannidis, P.; Scheurer, C.; Shackleford, D. M.; Sriraghavan, K.; Stingelin, L.; Tang, Y.; Urwyler, H.; Wang, X.; White, K. L.; Wittlin, S.; Zhou, L.; Vennerstrom, J. L. Synthetic ozonide drug candidate OZ439 offers new hope for a single-dose cure of uncomplicated malaria. *Proceedings of the National Academy of Sciences* **2011,** *108*, 4400-4405.
55. P.A., W. Chemotherapy for Falciparum Malaria: The Armoury, the Problems and the Prospects. *Parasitology Today* **2000,** *16*, 146-153.
56. White, N. J. Drug resistance in malaria. *British Medical Bulletin* **1998,** *54*, 703-715.
57. Sidhu, A. B. S.; Verdier-Pinard, D.; Fidock, D. A. Chloroquine Resistance in *Plasmodium falciparum* Malaria Parasites Conferred by pfcrt Mutations. *Science* **2002,** *298*, 210-213.
58. Sanchez, C. P.; Stein, W. D.; Lanzer, M. Is PfCRT a channel or a carrier? Two competing models explaining chloroquine resistance in *Plasmodium falciparum*. *Trends in Parasitology* **2007,** *23*, 332-339.
59. Naudé, B.; Brzostowski, J. A.; Kimmel, A. R.; Wellems, T. E. *Dictyostelium discoideum* Expresses a Malaria Chloroquine Resistance Mechanism upon Transfection with Mutant, but Not Wild-type, *Plasmodium falciparum* Transporter PfCRT. *Journal of Biological Chemistry* **2005,** *280*, 25596-25603.
60. Martiney, J. A.; Cerami, A.; Slater, A. F. G. Verapamil Reversal of Chloroquine Resistance in the Malaria Parasite *Plasmodium falciparum* Is Specific for Resistant Parasites and

Independent of the Weak Base Effect. *Journal of Biological Chemistry* **1995,** *270*, 22393-22398.

61. Yuvaniyama, J.; Chitnumsub, P.; Kamchonwongpaisan, S.; Vanichtanankul, J.; Sirawaraporn, W.; Taylor, P.; Walkinshaw, M. D.; Yuthavong, Y. Insights into antifolate resistance from malarial DHFR-TS structures. *Nature Structural & Molecular Biology* **2003,** *10*, 357-365.
62. Kublin, J. G.; Dzinjalamala, F. K.; Kamwendo, D. D.; Malkin, E. M.; Cortese, J. F.; Martino, L. M.; Mukadam, R. A. G.; Rogerson, S. J.; Lescano, A. G.; Molyneux, M. E.; Winstanley, P. A.; Chimpeni, P.; Taylor, T. E.; Plowe, C. V. Molecular Markers for Failure of Sulfadoxine-Pyrimethamine and Chlorproguanil-Dapsone Treatment of Plasmodium falciparum Malaria. *Journal of Infectious Diseases* **2002,** *185*, 380-388.
63. Jambou, R.; Legrand, E.; Niang, M.; Khim, N.; Lim, P.; Volney, B.; Ekala, M. T.; Bouchier, C.; Esterre, P.; Fandeur, T.; Mercereau-Puijalon, O. Resistance of *Plasmodium falciparum* field isolates to in-vitro artemether and point mutations of the SERCA-type PfATPase6. *The Lancet* **2005,** *366*, 1960-1963.
64. Rosenthal, P. J. Antimalarial drug discovery: old and new approaches. *Journal of Experimental Biology* **2003,** *206*, 3735-3744.
65. Grellier, P.; Depoix, D.; Schrevel, J.; Florent, I. Discovery of new targets for antimalarial chemotherapy. *Parasite-Journal de la Societe Francaise de Parasitologie* **2008,** *15*, 219-225.
66. Sahu, N. K.; Sahu, S.; Kohli, D. V. Novel Molecular Targets for Antimalarial Drug Development. *Chemical Biology & Drug Design* **2008,** *71*, 287-297.
67. Ralph, S. A.; D'Ombrain, M. C.; McFadden, G. I. The apicoplast as an antimalarial drug target. *Drug Resistance Updates* **2001,** *4*, 145-151.
68. Botté, C. Y.; Dubar, F.; McFadden, G. I.; Maréchal, E.; Biot, C. *Plasmodium falciparum* Apicoplast Drugs: Targets or Off-Targets? *Chemical Reviews* **2011,** *112*, 1269-1283.
69. Fidock, D. A.; Rosenthal, P. J.; Croft, S. L.; Brun, R.; Nwaka, S. Antimalarial drug discovery: efficacy models for compound screening. *Nature Reviews Drug Discovery* **2004,** *3*, 509-520.
70. Weissig, V.; Vetro-Widenhouse, T. S.; Rowe, T. C. Topoisomerase II Inhibitors Induce Cleavage of Nuclear and 35-kb Plastid DNAs in the Malarial Parasite *Plasmodium falciparum*. *DNA and Cell Biology* **1997,** *16*, 1483-1492.
71. Waller, R. F.; Keeling, P. J.; Donald, R. G. K.; Striepen, B.; Handman, E.; Lang-Unnasch, N.; Cowman, A. F.; Besra, G. S.; Roos, D. S.; McFadden, G. I. Nuclear-encoded proteins

target to the plastid in *Toxoplasma gondii* and *Plasmodium falciparum*. *Proceedings of the National Academy of Sciences* **1998,** *95*, 12352-12357.

72. Surolia, N.; Surolia, A. Triclosan offers protection against blood stages of malaria by inhibiting enoyl-ACP reductase of *Plasmodium falciparum*. *Nature Medicine* **2001,** *7*, 167-173.
73. Jomaa, H.; Wiesner, J.; Sanderbrand, S.; Altincicek, B.; Weidemeyer, C.; Hintz, M.; Türbachova, I.; Eberl, M.; Zeidler, J.; Lichtenthaler, H. K.; Soldati, D.; Beck, E. Inhibitors of the Nonmevalonate Pathway of Isoprenoid Biosynthesis as Antimalarial Drugs. *Science* **1999,** *285*, 1573-1576.
74. Yeh, E.; DeRisi, J. L. Chemical Rescue of Malaria Parasites Lacking an Apicoplast Defines Organelle Function in Blood-Stage *Plasmodium falciparum*. *PLoS Biology* **2011,** *9*, e1001138.
75. Rodriguez-Concepcion, M.; Campos, N.; Lois Luisa Maria; Maldonado, C.; Hoeffler, J. F.; Grosdemange-Billiard, C.; Rohmer, M.; Boronat, A. Genetic evidence of branching in the isoprenoid pathway for the production of isopentenyl diphosphate and dimethylallyl diphosphate in *Escherichia coli*. *FEBS Letters* **2000,** *473*, 328-332.
76. Rohmer, M.; Knani, M.; Simonin, P.; Sutter, B.; Sahm, H. Isoprenoid Biosynthesis in Bacteria - A Novel Pathway for the Early Steps Leading to Isopentenyl Diphosphate. *Biochemical Journal* **1993,** *295*, 517-524.
77. Disch, A.; Schwender, J.; Müller, C.; Lichtenthaler, H. K.; Rohmer, M. Distribution of the mevalonate and glyceraldehyde phosphate/pyruvate pathways for isoprenoid biosynthesis in unicellular algae and the cyanobacterium *Synechocystis PCC* 6714. *Biochemical Journal* **1998,** *333*, 381-388.
78. Hunter, W. N. The Non-mevalonate Pathway of Isoprenoid Precursor Biosynthesis. *Journal of Biological Chemistry* **2007,** *282*, 21573-21577.
79. Lois, L. M.; Campos, N.; Putra, S. R.; Danielsen, K.; Rohmer, M.; Boronat, A. Cloning and characterization of a gene from Escherichia coli encoding a transketolase-like enzyme that catalyzes the synthesis of d-1-deoxyxylulose 5-phosphate, a common precursor for isoprenoid, thiamin, and pyridoxol biosynthesis. *Proceedings of the National Academy of Sciences* **1998,** *95*, 2105-2110.
80. Kuzuyama, T.; Shimizu, T.; Takahashi, S.; Seto, H. Fosmidomycin, a specific inhibitor of 1-deoxy--xylulose 5-phosphate reductoisomerase in the nonmevalonate pathway for terpenoid biosynthesis. *Tetrahedron Letters* **1998,** *39*, 7913-7916.
81. Borrmann, S.; Issifou, S.; Esser, G.; Adegnika, A. A.; Ramharter, M.; Matsiegui, P. B.; Oyakhirome, S.; Mboumba, D. n. P. M.; Missinou, M. A.; Kun, J. F. J.; Jomaa, H.;

Kremsner, P. G. Fosmidomycin-Clindamycin for the Treatment of *Plasmodium falciparum* Malaria. *Journal of Infectious Diseases* **2004,** *190*, 1534-1540.

82. Dhiman, R. K.; Schaeffer, M. L.; Bailey, A. M.; Testa, C. A.; Scherman, H.; Crick, D. C. 1-Deoxy-D-Xylulose 5-Phosphate Reductoisomerase (IspC) from Mycobacterium tuberculosis: towards Understanding Mycobacterial Resistance to Fosmidomycin. *The Journal of Bacteriology* **2005,** *187*, 8395-8402.
83. Cassera, M. B.; Gozzo, F. C.; D'Alexandri, F. L.; Merino, E. F.; del Portillo, H. A.; Peres, V. J.; Almeida, I. C.; Eberlin, M. N.; Wunderlich, G.; Wiesner, J.; Jomaa, H.; Kimura, E. A.; Katzin, A. M. The Methylerythritol Phosphate Pathway Is Functionally Active in All Intraerythrocytic Stages of *Plasmodium falciparum*. *Journal of Biological Chemistry* **2004,** *279*, 51749-51759.
84. Cassera, M. B.; Merino, E. F.; Peres, V. J.; Kimura, E. A.; Wunderlich, G.; Katzin, A. M. Effect of fosmidomycin on metabolic and transcript profiles of the methylerythritol phosphate pathway in *Plasmodium falciparum*. *Memórias do Instituto Oswaldo Cruz* **2007,** *102*, 377-384.
85. Dharia, N.; Sidhu, A.; Cassera, M.; Westenberger, S.; Bopp, S.; Eastman, R.; Plouffe, D.; Batalov, S.; Park, D.; Volkman, S.; Wirth, D.; Zhou, Y.; Fidock, D.; Winzeler, E. Use of high-density tiling microarrays to identify mutations globally and elucidate mechanisms of drug resistance in *Plasmodium falciparum*. *Genome Biology* **2009,** *10*, R21.
86. Odom, A. R.; Van Voorhis, W. C. Functional genetic analysis of the Plasmodium falciparum deoxyxylulose 5-phosphate reductoisomerase gene. *Molecular and Biochemical Parasitology* **2010,** *170*, 108-111.
87. Zhang, B.; Watts, K. M.; Hodge, D.; Kemp, L. M.; Hunstad, D. A.; Hicks, L. M.; Odom, A. R. A Second Target of the Antimalarial and Antibacterial Agent Fosmidomycin Revealed by Cellular Metabolic Profiling. *Biochemistry* **2011,** *50*, 3570-3577.
88. Umeda, T.; Tanaka, N.; Kusakabe, Y.; Nakanishi, M.; Kitade, Y.; Nakamura, K. T. Molecular basis of fosmidomycin's action on the human malaria parasite *Plasmodium falciparum*. *Science Report* **2011,** *1*.
89. Mac Sweeney, A.; Lange, R.; Fernandes, R. P. M.; Schulz, H.; Dale, G. E.; Douangamath, A.; Proteau, P. J.; Oefner, C. The Crystal Structure of *E.coli* 1-Deoxy-d-xylulose-5-phosphate Reductoisomerase in a Ternary Complex with the Antimalarial Compound Fosmidomycin and NADPH Reveals a Tight-binding Closed Enzyme Conformation. *Journal of Molecular Biology* **2005,** *345*, 115-127.

90. Reuter, K.; Sanderbrand, S.; Jomaa, H.; Wiesner, J.; Steinbrecher, I.; Beck, E.; Hintz, M.; Klebe, G.; Stubbs, M. T. Crystal Structure of 1-Deoxy-d-xylulose-5-phosphate Reductoisomerase, a Crucial Enzyme in the Non-mevalonate Pathway of Isoprenoid Biosynthesis. *Journal of Biological Chemistry* **2002,** *277*, 5378-5384.
91. Steinbacher, S.; Kaiser, J.; Eisenreich, W.; Huber, R.; Bacher, A.; Rohdich, F. Structural Basis of Fosmidomycin Action Revealed by the Complex with 2-C-Methyl-d-erythritol 4-phosphate Synthase (IspC). *Journal of Biological Chemistry* **2003,** *278*, 18401-18407.
92. Yajima, S.; Nonaka, T.; Kuzuyama, T.; Seto, H.; Ohsawa, K. Crystal structure of 1-deoxy-D-xylulose 5-phosphate reductoisomerase complexed with cofactors: Implications of a flexible loop movement upon substrate binding. *Journal of Biochemistry* **2002,** *131*, 313-317.
93. Yajima, S.; Hara, K.; Sanders, J. M.; Yin, F.; Ohsawa, K.; Wiesner, J.; Jomaa, H.; Oldfield, E. Crystallographic Structures of Two Bisphosphonate:1-Deoxyxylulose-5-Phosphate Reductoisomerase Complexes. *Journal of the American Chemical Society* **2004,** *126*, 10824-10825.
94. Yajima, S.; Hara, K.; Iino, D.; Sasaki, Y.; Kuzuyama, T.; Ohsawa, K.; Seto, H. Structure of 1-deoxy-d-xylulose 5-phosphate reductoisomerase in a quaternary complex with a magnesium ion, NADPH and the antimalarial drug fosmidomycin. *Acta Crystallographica Section F* **2007,** *63*, 466-470.
95. Hoeffler, J. F.; Tritsch, D.; Grosdemange-Billiard, C.; Rohmer, M. Isoprenoid biosynthesis via the methylerythritol phosphate pathway. *European Journal of Biochemistry* **2002,** *269*, 4446-4457.
96. Wong, U.; Cox, R. J. The Chemical Mechanism of D-1-Deoxyxylulose-5-phosphate Reductoisomerase from Escherichia coli. *Angewandte Chemie International Edition* **2007,** *46*, 4926-4929.
97. Munos, J. W.; Pu, X.; Mansoorabadi, S. O.; Kim, H. J.; Liu, H. w. A Secondary Kinetic Isotope Effect Study of the 1-Deoxy-d-xylulose-5-phosphate Reductoisomerase-Catalyzed Reaction: Evidence for a Retroaldol-Aldol Rearrangement. *Journal of the American Chemical Society* **2009,** *131*, 2048-2049.
98. Fox, D. T.; Poulter, C. D. Mechanistic Studies with 2-C-Methyl-d-erythritol 4-Phosphate Synthase from Escherichia coli. *Biochemistry* **2005,** *44*, 8360-8368.
99. Proteau, P. J. 1-Deoxy-D-xylulose 5-phosphate reductoisomerase: an overview. *Bioorganic Chemistry* **2004,** *32*, 483-493.

100. Okuhara, M.; Kuroda, Y.; Goto, T.; Okamoto, M.; Terano, H.; Kohsaka, M.; Aoki, H.; Imanaka, H. Studies on New Phosphonic Acid Antibiotics .1. FR-900098, Isolation and Characterization. *Journal of Antibiotics* **1980,** *33*, 13-17.

101. Kamiya, T.; Hemmi, K.; Takeno, H.; Hashimoto, M. Studies on phosphonic acid antibiotics. I. Structure and synthesis of 3-(n-acetyl-n-hydroxyamino)propylphosphonic acid (FR-900098) and its n-formyl analogue (FR-31564). *Tetrahedron Letters* **1980,** *21*, 95-98.

102. Okuhara, M.; Kuroda, Y.; Goto, T.; Okamoto, M.; Terano, H.; Kohsaka, M.; Aoki, H.; Imanaka, H. Studies on New Phosphonic Acid Antibiotics .3. Isolation and Characterization of Fr-31564, Fr-32863 and Fr-33289. *Journal of Antibiotics* **1980,** *33*, 24-28.

103. Shigi, Y. Inhibition of bacterial isoprenoid synthesis by fosmidomycin, a phosphonic acid-containing antibiotic. *Journal of Antimicrobial Chemotherapy* **1989,** *24*, 131-145.

104. Devreux, V.; Wiesner, J.; Jomaa, H.; Rozenski, J.; Van der Eycken, J.; Van Calenbergh, S. Divergent strategy for the synthesis of alpha-aryl-substituted fosmidomycin analogues. *Journal of Organic Chemistry* **2007,** *72*, 3783-3789.

105. Tsuchiya, T.; Ishibashi, K.; Terakawa, M.; Nishiyama, M.; Itoh, N.; Noguchi, H. Pharmacokinetics and Metabolism of Fosmidomycin, A New Phosphonic Acid, in Rats and Dogs. *European Journal of Drug Metabolism and Pharmacokinetics* **1982,** *7*, 59-64.

106. Kuemmerle, H. P.; Murakawa, T.; Soneoka, K.; Konishi, T. Fosmidomycin - A New Phosphonic Acid Antibiotic .1. Phase-1 Tolerance Studies. *International Journal of Clinical Pharmacology and Therapeutics* **1985,** *23*, 515-520.

107. Haemers, T.; Wiesner, J.; Poecke, S. V.; Goeman, J.; Henschker, D.; Beck, E.; Jomaa, H.; Calenbergh, S. V. Synthesis of α-substituted fosmidomycin analogues as highly potent *Plasmodium falciparum* growth inhibitors. *Bioorganic & Medicinal Chemistry Letters* **2006,** *16*, 1888-1891.

108. Ortmann, R.; Wiesner, J.; Reichenberg, A.; Henschker, D.; Beck, E.; Jomaa, H.; Schlitzer, M. Alkoxycarbonyloxyethyl Ester Prodrugs of FR900098 with Improved In Vivo Antimalarial Activity. *Archiv der Pharmazie* **2005,** *338*, 305-314.

109. Reichenberg, A.; Wiesner, J.; Weidemeyer, C.; Dreiseidler, E.; Sanderbrand, S.; Altincicek, B.; Beck, E.; Schlitzer, M.; Jomaa, H. Diaryl ester prodrugs of FR900098 with improved in vivo antimalarial activity. *Bioorganic & Medicinal Chemistry Letters* **2001,** *11*, 833-835.

110. Wiesner, J.; Ortmann, R.; Jomaa, H.; Schlitzer, M. Double Ester Prodrugs of FR900098 Display Enhanced *In-Vitro* Antimalarial Activity. *Archiv der Pharmazie* **2007,** *340*, 667-669.

111. Woo, Y. H.; Fernandes, R. P. M.; Proteau, P. J. Evaluation of fosmidomycin analogs as inhibitors of the *Synechocystis sp.* PCC6803 1-deoxy-d-xylulose 5-phosphate reductoisomerase. *Bioorganic & Medicinal Chemistry* **2006,** *14*, 2375-2385.

112. Kuntz, L.; Tritsch, D.; Grosdemange-Billiard, C.; Hemmerlin, A.; Willem, A.; Bacht, T. J.; Rohmer, M. Isoprenoid biosynthesis as a target for antibacterial and antiparasitic drugs: phosphonohydroxamic acids as inhibitors of deoxyxylulose phosphate reducto-isomerase. *Biochemical Journal* **2005,** *386*, 127-135.

113. Courtois, M.; Mincheva, Z.; Andreu, F.; Rideau, M.; Viaud-Massuard, M. C. Synthesis and biological evaluation with plant cells of new fosmidomycin analogues containing a benzoxazolone or oxazolopyridinone ring. *Journal of Enzyme Inhibition and Medicinal Chemistry* **2004,** *19*, 559-565.

114. Mincheva, Z.; Courtois, M.; Andreu, F.; Rideau, M.; Viaud-Massuard, M. C. Fosmidomycin analogues as inhibitors of monoterpenoid indole alkaloid production in *Catharanthus roseus* cells. *Phytochemistry* **2005,** *66*, 1797-1803.

115. Ortmann, R.; Wiesner, J.; Silber, K.; Klebe, G.; Jomaa, H.; Schlitzer, M. Novel deoxyxylulosephosphate-reductoisomerase inhibitors: Fosmidomycin derivatives with spacious acyl residues. *Archiv der Pharmazie* **2007,** *340*, 483-490.

116. Hemmi, K.; Takeno, H.; Hashimoto, M.; Kamiya, T. Studies on phosphonic acid antibiotics. IV. Synthesis and antibacterial activity of analogs of 3-(N-acetyl-N-hydroxyamino)-propylphosphonic acid (FR-900098). *Chemical and Pharmaceutical Bulletin* **1982,** *30*, 111-118.

117. Zingle, C.; Kuntz, L.; Tritsch, D.; Grosdemange-Billiard, C.; Rohmer, M. Isoprenoid Biosynthesis via the Methylerythritol Phosphate Pathway: Structural Variations around Phosphonate Anchor and Spacer of Fosmidomycin, a Potent Inhibitor of Deoxyxylulose Phosphate Reductoisomerase. *The Journal of Organic Chemistry* **2010,** *75*, 3203-3207.

118. Bodill, T.; Conibear, A. C.; Blatch, G. L.; Lobb, K. A.; Kaye, P. T. Synthesis and evaluation of phosphonated N-heteroarylcarboxamides as DOXP-reductoisomerase (DXR) inhibitors. *Bioorganic & Medicinal Chemistry* **2011,** *19*, 1321-1327.

119. Haemers, T.; Wiesner, J.; Gießmann, D.; Verbrugghen, T.; Hillaert, U.; Ortmann, R.; Jomaa, H.; Link, A.; Schlitzer, M.; Van Calenbergh, S. Synthesis of β- and γ-oxa isosteres of

fosmidomycin and FR900098 as antimalarial candidates. *Bioorganic & Medicinal Chemistry* **2008,** *16*, 3361-3371.

120. Kurz, T.; Schluter, K.; Kaula, U.; Bergmann, B.; Walter, R. D.; Geffken, D. Synthesis and antimalarial activity of chain substituted pivaloyloxymethyl ester analogues of Fosmidomycin and FR900098. *Bioorganic & Medicinal Chemistry* **2006,** *14*, 5121-5135.
121. Verbrugghen, T.; Cos, P.; Maes, L.; Van Calenbergh, S. Synthesis and Evaluation of α-Halogenated Analogues of 3-(Acetylhydroxyamino)propylphosphonic Acid (FR900098) as Antimalarials. *Journal of Medicinal Chemistry* **2010,** *53*, 5342-5346.
122. Silber, K.; Heidler, P.; Kurz, T.; Klebe, G. AFMoC Enhances Predictivity of 3D QSAR:ΓÇë A Case Study with DOXP-reductoisomerase. *Journal of Medicinal Chemistry* **2005,** *48*, 3547-3563.
123. Jeschke, P. The unique role of halogen substituents in the design of modern agrochemicals. *Pest Management Science* **2010,** *66*, 10-27.
124. Michaelis, A.; Kaehne, R. Ueber das Verhalten der Jodalkyle gegen die sogen. Phosphorigsäureester oder O-Phosphine. *Ber. Dtsch. Chem. Ges.* **1898,** *31*, 1048-1055.
125. Arbuzov, A. E. *J. Russ. Phys. Chem. Soc.* **1906,** *38*, 687.
126. Arbuzov, A. E. *Chem. Zentr.* **1906,** *II*, 1639.
127. Crofts, P. C. Compounds containing carbon-phosphorus bonds. *Quarterly Reviews of the Chemical Society* **1958,** *12*, 341-366.
128. Cohen, R. J.; Fox, D. L.; Eubank, J. F.; Salvatore, R. N. Mild and efficient Cs2CO3-promoted synthesis of phosphonates. *Tetrahedron Letters* **2003,** *44*, 8617-8621.
129. Exner, J. H.; Steiner, E. C. Solvation and ion pairing of alkali-metal alkoxides in dimethyl sulfoxide. Conductometric studies. *Journal of the American Chemical Society* **1974,** *96*, 1782-1787.
130. Devreux, V.; Wiesner, J.; Jomaa, H.; Van der Eycken, J.; Van Calenbergh, S. Synthesis and evaluation of α-, β-unsaturated [alpha]-aryl-substituted fosmidomycin analogues as DXR inhibitors. *Bioorganic & Medicinal Chemistry Letters* **2007,** *17*, 4920-4923.
131. Isowa, Y.; Takashima, T.; Ohmori, M.; Kurita, H.; Sato, M.; Mori, k. Synthesis of N^{δ}-Hydroxyornithine. *Bulletin of the Chemical Society of Japan* **1972,** *45*, 1461-1464.
132. Ortmann, R.; Wiesner, J.; Reichenberg, A.; Henschker, D.; Beck, E.; Jomaa, H.; Schlitzer, M. Acyloxyalkyl ester prodrugs of FR900098 with improved *in vivo* anti-malarial activity. *Bioorganic & Medicinal Chemistry Letters* **2003,** *13*, 2163-2166.

133. Kurz, T.; Geffken, D.; Wackendorff, C. Carboxylic acid analogues of fosmidomycin. *Zeitschrift fur Naturforschung Section B-A Journal of Chemical Sciences* **2003,** *58*, 457-461.

134. Schlüter, K.; Walter, R. D.; Bergmann, B.; Kurz, T. Arylmethyl substituted derivatives of Fosmidomycin: Synthesis and antimalarial activity. *European Journal of Medicinal Chemistry* **2006,** *41*, 1385-1397.

135. Gebhardt, P.; Crumbliss, A.; Miller, M.; Möllmann, U. Synthesis and biological activity of saccharide based lipophilic siderophore mimetics as potential growth promoters for mycobacteria. *BioMetals* **2008,** *21*, 41-51.

136. Karplus, M. Contact Electron-Spin Coupling of Nuclear Magnetic Moments. *Journal of Chemical Physics* **1959,** *30*, 11-15.

137. Karplus, M. Vicinal Proton Coupling in Nuclear Magnetic Resonance. *Journal of the American Chemical Society* **1963,** *85*, 2870-2871.

138. Trager, W.; Jensen, J. B. Human Malaria Parasites in Continuous Culture. *Science* **1976,** *193*, 673-675.

139. van Zyl, R. L.; Viljoen, A. M. In vitro activity of Aloe extracts against *Plasmodium falciparum*. *South African Journal of Botany* **2002,** *68*, 106-110.

140. Kumar, G. D. K.; Saenz, D.; Lokesh, G. L.; Amarnath N. Microwave-assisted cleavage of phosphate, phosphonate and phosphoramide esters. *Tetrahedron Letters* **2006,** *47*, 6281-6284.

141. Devreux, V.; Wiesner, J.; Goeman, J. L.; Van der Eycken, J.; Jomaa, H.; Van Calenbergh, S. Synthesis and Biological Evaluation of Cyclopropyl Analogues of Fosmidomycin as Potent *Plasmodium falciparum* Growth Inhibitors. *Journal of Medicinal Chemistry* **2006,** *49*, 2656-2660.

142. Lambros, C.; Vanderberg, J. P. Synchronization of Plasmodium falciparum Erythrocytic Stages in Culture. *The Journal of Parasitology* **1979,** *65*, 418-420.

143. Desjardins, R. E.; Canfield, C. J.; Haynes, J. D.; Chulay, J. D. Quantitative Assessment of Anti-Malarial Activity Invitro by A Semiautomated Microdilution Technique. *Antimicrobial Agents and Chemotherapy* **1979,** *16*, 710-718.

144. Makler, M. T.; Ries, J. M.; Williams, J. A.; Bancroft, J. E.; Piper, R. C.; Gibbins, B. L.; Hinrichs, D. J. Parasite Lactate Dehydrogenase as an Assay for *Plasmodium falciparum* Drug Sensitivity. *The American Journal of Tropical Medicine and Hygiene* **1993,** *48*, 739-741.

145. Casey, M.; Lonard, J.; Lygo, B. *Advanced practical organic chemistry*; Blackie: Glasgow, 1990.

146. Ortmann, R.; Schlitzer, M. An Inexpensive Procedure for Reductive Aminations Using Dimethylamineborane on Millimolar and Molar Scale. *Synthesis-Stuttgart* **2009,** 1757-1759.

147. Fokin, A. A.; Yurchenko, A. G.; Rodionov, V. N.; Gunchenko, P. A.; Yurchenko, R. I.; Reichenberg, A.; Wiesner, J.; Hintz, M.; Jomaa, H.; Schreiner, P. R. Synthesis of the Antimalarial Drug FR900098 Utilizing the Nitroso-Ene Reaction. *Organic Letters* **2007,** *9*, 4379-4382.

148. Muregi, F. W.; Ishih, A. Next-generation antimalarial drugs: hybrid molecules as a new strategy in drug design. *Drug Development Research* **2010,** *71*, 20-32.

149. Burgess, S. J.; Selzer, A.; Kelly, J. X.; Smilkstein, M. J.; Riscoe, M. K.; Peyton, D. H. A Chloroquine-like Molecule Designed to Reverse Resistance in Plasmodium falciparum. *Journal of Medicinal Chemistry* **2006,** *49*, 5623-5625.

150. Martin, S. K.; Oduola, A. M. J.; Milhous, W. K. Reversal of Chloroquine Resistance in *Plasmodium falciparum* by Verapamil. *Science* **1987,** *235*, 899-901.

151. Miki, A.; Tanabe, K.; Nakayama, T.; Kiryon, C.; Ohsawa, K. *Plasmodium chabaudi*: Association of reversal of chloroquine resistance with increased accumulation of chloroquine in resistant parasites. *Experimental Parasitology* **1992,** *74*, 134-142.

152. Basco, L. K.; Lebras, J. In-Vitro Reversal of Chloroquine Resistance with Chlorpheniramine Against African Isolates of *Plasmodium falciparum*. *Japanese Journal of Medical Science & Biology* **1994,** *47*, 59-63.

153. Natarajan, J. K.; Alumasa, J. N.; Yearick, K.; Ekoue-Kovi, K. A.; Casabianca, L. B.; de Dios, A. C.; Wolf, C.; Roepe, P. D. 4-N-, 4-S-, and 4-O-Chloroquine Analogues: Influence of Side Chain Length and Quinolyl Nitrogen pKa on Activity vs Chloroquine Resistant Malaria. *Journal of Medicinal Chemistry* **2008,** *51*, 3466-3479.

154. Czech, B. P.; Bartsch, R. A. Effect of amines on O-benzyl group hydrogenolysis. *The Journal of Organic Chemistry* **1984,** *49*, 4076-4078.

155. Feng, T. S.; Guantai, E. M.; Nell, M. J.; van Rensburg, C. E. J.; Hoppe, H. C.; Chibale, K. Antiplasmodial and antitumor activity of dihydroartemisinin analogs derived via the aza-Michael addition reaction. *Bioorganic & Medicinal Chemistry Letters* **2011,** *21*, 2882-2886.

156. Brown, A.; Parish, T. Dxr is essential in *Mycobacterium tuberculosis* and fosmidomycin resistance is due to a lack of uptake. *BMC Microbiology* **2008,** *8*, 78.

157. Scorpio, A.; Lindholm-Levy, P.; Heifets, L.; Gilman, R.; Siddiqi, S.; Cynamon, M.; Zhang, Y. Characterization of pncA mutations in pyrazinamide-resistant Mycobacterium tuberculosis. *Antimicrobial Agents and Chemotherapy* **1997,** *41*, 540-543.

158. Rojas, F. A.; Kouznetsov, V. V. Property-based design and synthesis of new chloroquine hybrids via simple incorporation of 2-imino-thiazolidin-4-one or 1H-pyrrol-2, 5-dione fragments on the 4-amino-7-chloroquinoline side chain. *Journal of the Brazilian Chemical Society* **2011,** *22*, 1774-1781.

159. Ahuja, S.; Ahuja, S.; Chen, Q. J.; Wahlgren, M. Prediction of solubility on recombinant expression of *Plasmodium falciparum* erythrocyte membrane protein I domains in Escherichia coli. *Malaria Journal* **2006,** *5*.

160. Kaiser, J.; Yassin, M.; Prakash, S.; Safi, N.; Agami, M.; Lauw, S.; Ostrozhenkova, E.; Bacher, A.; Rohdich, F.; Eisenreich, W.; Safi, J.; Golan-Goldhirsh, A. Anti-malarial drug targets: Screening for inhibitors of 2C-methyl-d-erythritol 4-phosphate synthase (IspC protein) in Mediterranean plants. *Phytomedicine* **2007,** *14*, 242-249.

161. Takahashi, S.; Kuzuyama, T.; Watanabe, H.; Seto, H. A 1-deoxy-d-xylulose 5-phosphate reductoisomerase catalyzing the formation of 2-C-methyl-d-erythritol 4-phosphate in an alternative nonmevalonate pathway for terpenoid biosynthesis. *Proceedings of the National Academy of Sciences* **1998,** *95*, 9879-9884.

162. Koppisch, A. T.; Fox, D. T.; Blagg, B. S. J.; Poulter, C. D. E. coli MEP Synthase: Steady-State Kinetic Analysis and Substrate Binding. *Biochemistry* **2002,** *41*, 236-243.

163. Yin, X.; Proteau, P. J. Characterization of native and histidine-tagged deoxyxylulose 5-phosphate reductoisomerase from the cyanobacterium *Synechocystis sp*. PCC6803. *Biochimica et Biophysica Acta (BBA) - Proteins & Proteomics* **2003,** *1652*, 75-81.

164. Argyrou, A.; Blanchard, J. S. Kinetic and Chemical Mechanism of Mycobacterium tuberculosis 1-Deoxy-d-xylulose-5-phosphate Isomeroreductase. *Biochemistry* **2004,** *43*, 4375-4384.

165. Henriksson, L. M.; Unge, T.; Carlsson, J.; Åqvist, J.; Mowbray, S. L.; Jones, T. A. Structures of Mycobacterium tuberculosis 1-Deoxy-D-xylulose-5-phosphate Reductoisomerase Provide New Insights into Catalysis. *Journal of Biological Chemistry* **2007,** *282*, 19905-19916.

166. Henriksson, L. M.; Bjorkelid, C.; Mowbray, S. L.; Unge, T. The 1.9 A resolution structure of *Mycobacterium tuberculosis* 1-deoxy-D-xylulose 5-phosphate reductoisomerase, a potential drug target. *Acta Crystallographica Section D-Biological Crystallography* **2006,** *62*, 807-813.

167. Ricagno, S.; Grolle, S.; Bringer-Meyer, S.; Sahm, H.; Lindqvist, Y.; Schneider, G. Crystal structure of 1-deoxy-d-xylulose-5-phosphate reductoisomerase from Zymomonas mobilis at 1.9-+à resolution. *Biochimica et Biophysica Acta (BBA) - Proteins & Proteomics* **2004,** *1698*, 37-44.

168. Takenoya, M.; Ohtaki, A.; Noguchi, K.; Endo, K.; Sasaki, Y.; Ohsawa, K.; Yajima, S.; Yohda, M. Crystal structure of 1-deoxy-d-xylulose 5-phosphate reductoisomerase from the hyperthermophile *Thermotoga maritima* for insights into the coordination of conformational changes and an inhibitor binding. *Journal of Structural Biology* **2010,** *170*, 532-539.

169. Kuzuyama, T.; Takahashi, S.; Watanabe, H.; Seto, H. Direct formation of 2-C-methyl-d-erythritol 4-phosphate from 1-deoxy-d-xylulose 5-phosphate by 1-deoxy-d-xylulose 5-phosphate reductoisomerase, a new enzyme in the non-mevalonate pathway to isopentenyl diphosphate. *Tetrahedron Letters* **1998,** *39*, 4509-4512.

170. Discovery Studio Visualizer. [3.0]. 2010. Accelrys Software Inc.

171. Morris, G. M.; Goodsell, D. S.; Halliday, R. S.; Huey, R.; Hart, W. E.; Belew, R. K.; Olson, A. J. Automated docking using a Lamarckian genetic algorithm and an empirical binding free energy function. *Journal of Computational Chemistry* **1998,** *19*, 1639-1662.

172. ChemBioDraw Ultra. [11.0.1]. 2007. CambridgeSoft.

173. Avogadro: open-source molecular builder and visualization tool. [1.0.3]. 2011. OpenMolecules.net.